Impact of *Plasmodium falciparum* Infection on Host Red Blood Cell Eryptosis: Exploring Host-Directed Opportunities

Coralie Boulet, MSc

A thesis submitted for the degree of
Doctor of Philosophy
in total fulfilment of the requirements for that degree

School of Life Sciences
College of Science, Health and Engineering
La Trobe University
Victoria, Australia

October 2020

Statement of Authorship

This thesis includes work by the author that has been published or submitted for publication as described in the text. Except where reference is made in the text of the thesis, this thesis contains no other material published elsewhere or extracted in whole or in part from a thesis accepted for the award of any other degree or diploma. No other person's work has been used without due acknowledgment in the main text of the thesis. This thesis has not been submitted for the award of any degree or diploma in any other tertiary institution.

Chapter 2 is comprised of a publication in the journal Frontiers in Cellular and Infection Microbiology. Frontiers Copyright Statement can be found on their website.

Chapter 4A is comprised of an article currently under revision at the journal Frontiers in Cellular and Infection Microbiology. Frontiers Copyright Statement can be found on their website.

This work was supported by an Australian Government Research Training Program Scholarship.

All research procedures reported in this thesis were approved by the relevant Ethics Committee.

Coralie Boulet
Monday 5th October 2020

Acknowledgements

I would like to start by acknowledging that this project was conducted on the stolen lands of the Wurundjeri people of the Kulin nation. I would like to pay my respect to Elders, past, present and emerging, and to extend this respect to all First Nations people.

I would like to thank Dr Teresa Carvalho for being such an amazing supervisor, mentor and inspiration. This PhD project would not have been the same without her guidance, her constant enthusiasm about new ideas and her incredible support. I will be forever thankful to have been able to grow as a scientist with such a smart, successful and inspirational role-model.

I would also like to acknowledge my fantastic co-supervisor, Prof Chritian Doerig for his support and ideas, as well as the other members of my PhD panel: A/Prof Karla Helbig for being an outstanding chair, Dr Delphine Merino and Prof Patrick Humbert for their precious insights and feedback on my project.

I would like to extend my thanks to the crucial collaborators, without whom this project would not be complete. For all the mass spectrometry experiments, a huge thanks to A/Prof Darren Creek, Dr Ghizal Siddiqui and all the Creek lab members. I have really enjoyed working with Ghizal, who has also been a great mentor to me for quite a few years. For the work with extracellular vesicles, I am extremely thankful to Dr Neta Regev-Rudzki who hosted me in her lab to learn the purification techniques. I am very proud that Teresa trusted me with the mission of bringing back this skill to La Trobe University. In the Weizmann Institute, a particular thanks to Dr Elya Dekel and Hila Ben Ami for their supervision and support.

During this 3.5-year adventure, I was extremely lucky to have been surrounded by such a fun team too: Mary, Jose, Taylah, Derek, Manon, Lars and Liana, and all the other students who came by our lab. Thanks for being supportive, patient, for making me laugh when I needed it and for the numerous coffee breaks. A particular thanks to Taylah who I have worked closely with and who has been such a bright and delightful co-worker. This positive and vibrant environment extends to the PAM department, in particular to the PAM HDR Society and its members. Shout-out as well to Aurelie and Manon for helping me through the thesis writing under COVID-19 lock-down.

I was also lucky to have been mentored by Dr Krystal Evans throughout my last year. She provided me with more advice than I can count, boosted my confidence and taught me a lot in how to navigate and plan my career.

The ASP has also been a great support throughout my PhD. The CiP course 2017 holds a very special place in my memories, so a big thanks to Prof Alex Maier, to all the participants (in particular Bec, Kat and Maddy) and the lecturers.

Besides ‘sciencing’ in the lab, there are two communities that I am very thankful for, as they supported my mental health, in two very different ways. First, the latin dance community: thanks for all the social dances and the online classes during COVID-19 lock-down. Secondly, to the environmental activists, in particular Extinction Rebellion, a huge thanks for all the work you are doing and for providing me with a shred of optimism for the future.

Although I could not see them or talk to them as often as I wished to, to all my awesome friends from overseas: thanks for your support, thanks for visiting me, thanks for being present even at such a long distance.

And of course, the biggest thanks to my family and my partner. To my parents, Micheline and Jean-Yves, who helped me become the person that I am today and who continued to support me even at the other side of the world: merci. And the same goes to Louis, Elsa and Sylvain: thanks for being present, supportive and keeping in touch. This extends to my partner’s family too, especially Sylvie and Jean-Marie. And Nicolas, thanks for being my rock throughout our journey together, thanks for taking a huge leap-of-faith in coming to Australia with me. We are having the best adventures together! Je vous aime tou-te-s de tout mon coeur.

Finally, I would like to dedicate this thesis to Matthew Lennon-Smith, an awesome friend, a fantastic soul who has been working hard to make this world a better place. He left us way too early. We miss you every day.

“Quand tu regarderas le ciel, la nuit, puisque j’habiterai dans l’une d’elles, puisque je rirai dans l’une d’elles, alors ce sera pour toi comme si riaient toutes les étoiles. Tu auras, toi, des étoiles qui savent rire !”

Le Petit Prince (1943), Antoine de Saint-Exupery

Experimental support and collaborations

This PhD project was supervised by Dr Teresa Carvalho (La Trobe University) and Prof Christian Doerig (RMIT).

All the experiments were designed in conjunction with Dr Teresa Carvalho.

In Chapter 1, Chapter 4B and Chapter 8, figures 1.3, 1.5, 4.6, 8.1 and 8.2 were designed on BioRender (https://biorender.com/).

In Chapters 4, Chapter 5, and Chapter 6, the time-course experiments (analysis of eryptosis hallmarks over time) were conducted with Taylah Gaynor (Carvalho lab, 2019); I performed the data analysis.

In Chapter 5, the mass spectrometry peptide library was prepared with Dr Ghizal Siddiqui (Creek Laboratory, at Monash Institute for Pharmaceutical Sciences). I prepared the cell cultures and the protein samples, we performed the peptide preparation together, she performed the acquisition and data analysis. The resulting proteomic and phosphoproteomic libraries are attached to this thesis (Excel files "Boulet-2020-proteinGroups_proteome" and "Boulet-2020-proteinGroups_phospho").

In Chapter 6, Taylah Gaynor performed the IC_{50} for the compounds WEHI-539, A-1155463 and A-1331852. Regarding the localisation of BCL-x_L by Western Blot, although I have repeated this experiment during my PhD, the Western Blot shown (Figure 6.6A) was performed during my master's degree (Monash University). The immunofluorescence assay (IFA) was done by Dr Teresa Carvalho (Figure 6.6B). Regarding the BCL-x_L Immuno-Precipitation (IP): I prepared the cultures and protein samples, I did the Western Blots, Dr Ghizal Siddiqui (Creek Laboratory) prepared the peptide samples, performed the mass spectrometry acquisition and first analysis; the final analysis of these proteomic data was done by me under Dr Siddiqui's guidance.

In Chapter 7, the Transmission Electron Microscopy was performed under the guidance of Dr. Julian Ratcliffe (Bioimaging platform, La Trobe University).

Communications

- **Publications**

Published:

Boulet C, Doerig CD and Carvalho TG (2018) *Manipulating Eryptosis of Human Red Blood Cells: A Novel Antimalarial Strategy?* Front. Cell. Infect. Microbiol. 8:419. doi: 10.3389/fcimb.2018.00419
Chapter 2 of this thesis.

Boulet C, Egan SL, Jones L, Jonsdottir TK, Power ML, Ralph SA, Tran L, White MAF (2020) *Parasitravaganza 2020: insights into a virtual parasitology conference.* Trends In Parasitol.
Available at: https://www.cell.com/trends/parasitology/fulltext/S1471-4922(20)30252-X

Under revision:

Boulet C, Gaynor TL and Carvalho TG. *Previously described eryptosis inducers impair Plasmodium falciparum growth via an eryptosis-independent mechanism.* Font. Cell. Infect. Microbiol. (Nov-2020)
Chapter 4A of this thesis.

- **Conferences**

Parasitravaganza Online Conference (Aug-20)
- Co-organiser
- Session chair
Online

Molecular Approaches to Malaria – international conference (Feb-2020)
- Poster presentation
Lorne, Australia

Physiology Anatomy Microbiology (PAM) Research Symposium (Dec-19)
- Speed talk: *Highly Commended*
- Poster presentation
Melbourne, Australia

Malaria in Melbourne (Oct-19)
- Poster presentation
Melbourne, Australia

Red blood cell workshop (Sep-19)
- Invited speaker
Melbourne, Australia

Australian Society for Parasitology (ASP) Annual Conference (Jul-19)
- Poster presentation
- Speed talk
Adelaide, Australia

PAM Research Symposium (Dec-18)
- Co-organiser
Melbourne, Australia

Victoria Immunity and Infection Network (VIIN) Young Investigator Symposium (Oct-18)
- Speed talk
Melbourne, Australia

First Malaria World Congress – international conference (Jul-18)
- Poster presentation
Melbourne, Australia

Malaria in Melbourne (Oct-17)
- Poster presentation
- Session chair
Melbourne, Australia

- **Outreach**

National Science Week (Aug-20)
Organisation and creation of short videos to explain our laboratory research to the wider public available on social media. In conjunction with the Australian Society for Parasitology.

Microbiology outreach program (Oct-18)
Founding member of the program. Supervision of high-school students for four modules in the laboratory (La Trobe University). Presentation of one of the module.

- **Science Communication**

Radio communication (Jul-20)
Invited on the radio RRR for its science show Einstein A Go Go (hosted by Dr Shane Huntington), available here.

3 Minute Thesis competition 2020
- La Trobe University finalist

3 Minute Thesis competition 2019
- 2nd prize School of Life Sciences (La Trobe University)

Visualise Your Thesis competition (Aug-18)

- 1st prize La Trobe University. Entry available here.

- **Teaching & Training**

Teaching (2018 & 2019)
Demonstrator for the 2nd year Microbiology practical classes (La Trobe University)

International Collaboration (Nov-18)
Visit to the Regev-Rudzki laboratory, Weizman Institute (Israel) to work on Extracellular Vesicles (EVs) purification (RFA grant funding, La Trobe University 2018)

Concept in Parasitology Course (Dec-17)
An intensive two-weeks parasitology course organised by the ASP.

- **Climate specific initiatives**

Climate initiatives within the ASP (2019-2020)
During the ASP Annual Conference, I presented ideas for climate actions to the Annual General Meeting. The outcomes include:
- the ASP declared a climate and ecological emergency
- the ASP supported the climate strikes
- I designed an outreach flyer on the impact of the climate crisis on parasitic diseases
- the creation of a subcommittee to design a plan of action following the emergency declaration

Science Communication within Extinction Rebellion (2019-2020)
Presentation of the "Introductory Talk" within Extinction Rebellion: covering the science of the climate and ecological crises.

Abstract

Malaria is a life-threatening disease, affecting over 200 million people every year. Resistance to all antimalarial drugs has emerged and an efficient vaccine is yet to be developed, creating an urgent need for new antimalarial treatments. Host-targeted therapies are a novel strategy, whereby factors from the host cell are targeted, rather than the malaria parasite. Host cell death pathways appear as a particularly attractive target, because many intracellular pathogens (including malaria parasites) manipulate these pathways for their own survival.

Eryptosis, the programmed cell death of erythrocytes, displays hallmarks that resemble those of apoptosis in nucleated cells, including exposure of phosphatidylserine on the cell surface. Although many compounds have been described to induce or inhibit eryptosis, its molecular pathways remain to be elucidated.

In this thesis, I investigated the relationship between the malaria parasite, *Plasmodium falciparum*, and its host cell eryptosis. First, I established a methodology to study eryptosis within a *P. falciparum in vitro* culture. I discovered that only the mature stages of the parasite induce eryptosis of their host cell, suggesting that the parasite suppresses eryptosis during its early erythrocytic stages. Surprisingly, bystander non-infected erythrocytes present within a *P. falciparum* culture also showed increased levels of eryptosis. I identified that this bystander effect was due to parasite secreted factors. Finally, I discovered that the erythrocyte proteins BCL-x_L and Raf kinase, mediators of apoptosis in nucleated cells, play an important role in parasite survival. Importantly, I identified that clinically approved drugs targeting these human proteins display antiparasitic activity.

Overall, this work opens exciting perspectives for host-targeted antimalarial intervention. Such strategies would significantly reduce the risk of drug resistance, while enabling repurposing of existing drugs targeting cell death proteins, many of which are clinically available in the context of cancer chemotherapy.

Contents

List of Tables

List of Figures

Chapter 1

Introduction

1.1 Malaria

1.1.1 Malaria impact

Malaria is a life-threatening disease transmitted to humans by female *Anopheles* mosquitoes. It is caused by unicellular eukaryotic parasites of the *Plasmodium* genus, within the Apicomplexan phylum. In humans, malaria can be caused by at least five *Plasmodium* species: *P. falciparum*, *P. vivax*, *P. ovale*, *P. malariae* and *P. knowlesi*. *Plasmodium falciparum* is the most prevalent (99.7% of the cases in the World Health Organization (WHO) African Region) and the most virulent species in humans [1]. For these reasons, *Plasmodium falciparum* is the focus of this project. Malaria is prevalent in many countries around the globe, particularly in tropical regions where *Anopheles* mosquitoes are present, as shown in Figure 1.1. Malaria predominantly affects the African continent where 93% of the global malaria cases and 94% of the malaria deaths occur [1]. In 2018, more than 200 million cases and nearly half a million deaths were reported, affecting primarily children under the age of five, who accounted for 67% of all malaria deaths [1]. Besides the morbidity and mortality caused by the disease, malaria strongly impacts the socio-economical development of endemic countries [2]. For all these reasons, the World Health Organization has targeted the global elimination of malaria by 2030. However, this elimination goal is currently facing major challenges.

1.1.2 Major challenges preventing malaria elimination

Malaria control and, ultimately, global malaria elimination, is an ambitious goal that faces multiple challenges, including insufficient funding, insecticide resistance, the lack of a vaccine, the climate crisis, parasitic mutations hindering their detection and drug resistance.

Indeed, although substantial funding has been invested to fight malaria over the last decade (*e.g.* US$ 2.7 billion in 2018), the WHO estimates that double the amount that is currently spent is needed to meet the 2030 elimination goals [1].

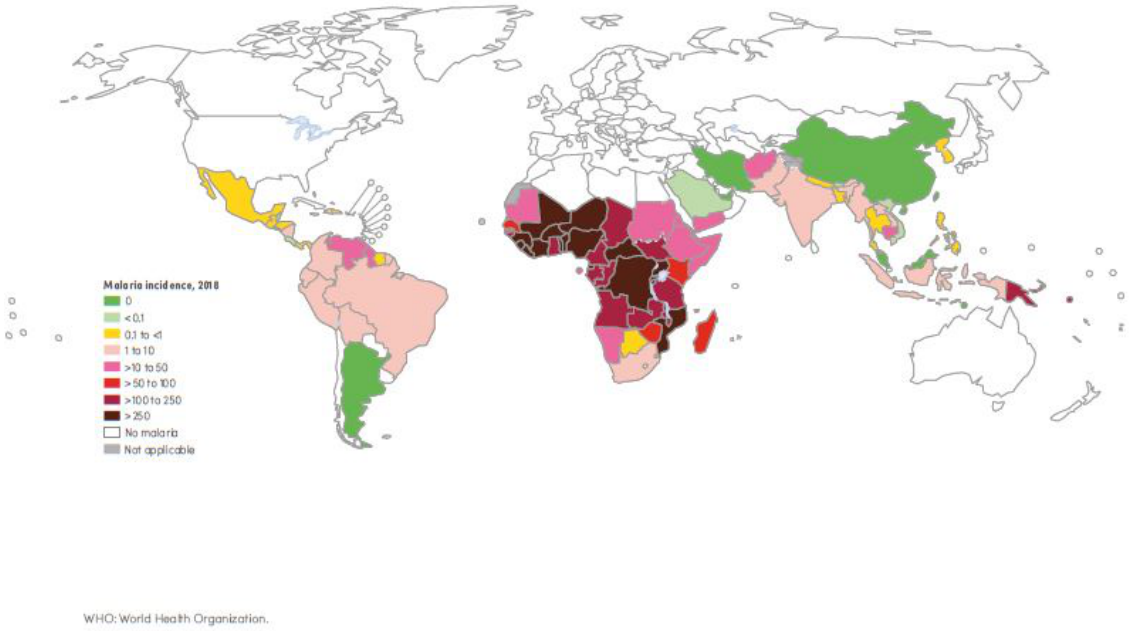

Figure 1.1: Map of malaria case incidence rate (cases per 1000 population at risk) by country, 2018 Source: World Health Organization (WHO) estimates [1].

Historically, vector control has been the most efficient approach to combat the disease, in particular, with the use of Indoor Residual Spraying (IRS) and the massive distribution of Insecticide Treated bed Nets (ITN). The latter was estimated to have contributed to a two-thirds drop of cases worldwide between 2000 and 2015 [3]. However, increasing mosquito resistance to available insecticides has been observed [1], putting at risk the success of such interventions in the long term.

Besides vector control, the research for an antimalaria-vaccine is ongoing. However, malaria parasites are extremely complex organisms, due in part to their multiple stages and use of antigenic variation mechanisms. In particular, the immunity developed by malaria patients allows to control disease severity, but individuals remain infectious. Therefore, the development of a malaria vaccine that would confer sterile immunity has been the focus of intense research for decades. Although the first proof of principle in human immunization using attenuated sporozoites was published in 1975 [4], the most advanced antimalarial vaccine, the RTS,S vaccine, only recently entered large-scale Phase III clinical trials [5]. RTS,S targets the liver stages of malaria, and although it will be a much needed tool for malaria control, its efficacy is somewhat disappointing: reduction of 36% of severe malaria in children aged 5-17 months [5] and a relatively short-lived protection (up to 4 years) [6].

The ongoing climate and ecological crises bring further obstacles to the fight against malaria. First, the distribution of mosquitoes is changing due to global heating: some areas will soon be too hot for mosquitoes (and likely humans) to thrive, while other areas, previously unaf-

fected by malaria, may see a migration of mosquitoes [7, 8]. The Intergovernmental Panel on Climate Change (IPCC) predicts that poverty and conflicts will rise due to the climate crisis, with increasing warming leading to intensifying severities of both poverty and conflicts [9]. This might in turn lead to an increase in infectious diseases, as "poverty creates conditions that favour the spread of infectious diseases and prevents affected populations from obtaining adequate access to prevention and care" [10]. Further, with increasing global temperatures, the intensity and frequency of extreme weather events will rise [9], leading to more frequent flooding, which provides ideal mosquito breading conditions, as demonstrated by the spike in malaria cases following the Cyclone Idai in Mozambique in 2019 [11]. Lastly, hundreds of millions of people will be forced to migrate due to the climate crisis. A large proportion of these population displacements is stemming from high-parasitic disease burdened areas [12], therefore threatening to further spread such diseases to areas previously non-endemic for malaria.

Another increasing worry is the spread of the deletion of the *pfhrp2/3* genes (pfhrp: *Plasmodium falciparum* histidine rich protein) within large numbers of parasite genotypes. This is important because, one of the key tools used to diagnose malaria are Rapid Diagnostic Tests (RDTs) that detect the presence of PfHRP2/3 antigens in a patient blood sample. Deletions of these genes therefore render the parasite undetectable by such tests. The prevalence of these deletions can reach 80% in symptomatic patients in certain countries [1]. Other antigens are currently being investigated to create much needed novel RDTs.

Finally, one of the most complex and serious threat to malaria control and malaria elimination is the systematic emergence of drug resistant parasites, against available antimalarial drugs. In particular, drug resistance is emerging against the front-line treatment: Artemisinin-Combination Therapy (ACT) [13]. Antimalarial drug resistance is particularly relevant for the work undertaken in this thesis and is therefore detailed below.

1.1.3 History of antimalarial treatments and the emergence of drug resistance

Malaria is among the oldest disease and *Plasmodium* parasites have infected humans for millennia: in Egypt, *P. falciparum* was detected in mummies dated from 3,200 BC [14]; in Greece, Homer mentions malaria in *The Iliad* (750 BC); in China, the canon of medicine, the Nei Ching, identified malaria-like symptoms and links between fevers and enlarged spleen in 270 BC [15]. Therefore, herbal medicine has been used as antimalarial treatments for millenia. Quinine is the active compound from the bitter bark, or cinchona bark, a tree native to South America that has historically been used by native peoples [15]. Upon isolation of quinine in 1820, it became a drug used globally to treat intermittent fevers, and is still used to date to treat malaria, despite sporadic resistance occurrence [15]. During the 20^{th} century, considerable research in malaria treatments was conducted, particularly after World War I and II, due to the great toll malaria had on various troops (quinine production

being dominated by a handful of countries) [15]. From the 1950's onwards, chloroquine and its derivatives have been especially key in the fight against malaria [15]. However, resistant parasites emerged a mere decade after its widespread distribution (Figure 1.2): resistance emerged independently in the Greater Mekong region, Papua New Guinea and South America [16, 17, 18]. Chloroquine resistance later spread from Asia to Africa in the early 1980's [19]. Other antimalarial drugs were introduced, such as sulfadoxine-pyrimethamine and mefloquine, but resistance also quickly emerged in South East Asia (Figure 1.2, [20]).

Similar to quinine and the South American cinchona bark, artemisinin is a compound originally used in Chinese traditional medicine. The sweet wormwood (*Artemisia annua* or qing-hao) has been used for over 2,000 years in China to treat fevers and malaria [21]. Artemisinin was successfully isolated in 1971, and Prof Youyou Tu received a Nobel Prize in 2015 for this discovery [22]. Artemisinin is, along with its derivatives, currently the front-line treatment, in combination with another antimalarial drug (partner drug) with a longer half-life, such as lumefantrine, amodiaquine or mefloquine [23]. This artemisinin-based combination therapy (ACT) is meant to reduce the spread of resistance both to artemisinin and the partner drug. However, partial resistance to artemisinin is now also observed in South East Asia, where parasites tolerate the drug for extended periods of time [13]. Worryingly, parasites carrying the mutation responsible for such tolerance to the drug (namely *pfkelch13* R561H mutation) have recently been identified on the African continent (in Rwanda) for the first time [24].

Although artemisinin is, so far, still effective at killing *Plasmodium* parasites, we urgently need new antimalarial treatment options before full resistance emerges.

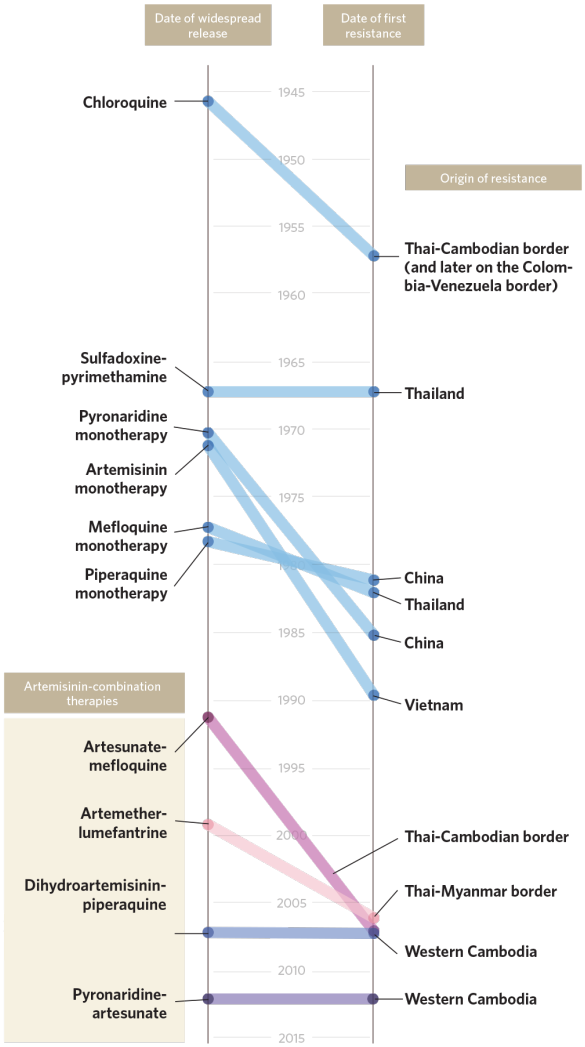

Figure 1.2: Antimalarial drugs and the emergence of drug resistance. Date of widespread release of antimalarial drugs and dates and origin of drug resistance emergence (Figure from Slivinski - *The Scientist* (2019) [20]).

1.1.4 *Plasmodium falciparum* life cycle in humans

P. falciparum has a complex lifecycle, involving two hosts: humans and mosquitoes (Figure 1.3). The infection of the human host begins with the blood meal of an infected female *Anopheles* mosquito. During a blood meal, mosquitoes inject saliva containing anticoagulants, vasodilators and, in the case of infected mosquitoes, parasites, in the form of sporozoites [25]. From the skin, the sporozoites navigate to the blood stream, attain the liver within a few hours and establish an infection inside hepatocytes. Each parasite undergoes a series of cell division, or schizogony, within a parasitophorous vacuole, giving rise to tens of thousands of merozoites [26]. Merozoite-containing vesicles, called merosomes, bud out in the blood stream, where they burst and release free merozoites, now able to invade mature red blood cells (RBC), or erythrocytes. Up until this stage, the malaria infection is asymptomatic.

Merozoites quickly invade RBCs (in less than 2 min) and undergo asexual schizogony, a cycle of replication that lasts 48h. The invasion relies on multiple receptor-ligand interactions, induces a short calcium (Ca^{2+}) influx into the host cell [27] and leads to a parasitic actin-myosin motor pulling the parasite into the RBC, creating the parasitophorous vacuole in the process [28]. During the first 24h inside the RBC, the parasite is in a ring stage (so called due to its appearance under the microscope, a thin central area containing few structures appearing transparent [29]). During the ring stage, the parasite begins to modify its environment for successful growth by engulfing the host cell haemoglobin into its food vacuole compartment. During the next 20h, the parasite matures into a trophozoite. At the trophozoite stage, the parasite is significantly bigger and has extensively modified its host RBC [30]. *P. falciparum* establishes Maurer's clefts in the RBC cytosol, structures that enable trafficking of hundreds of proteins to the RBC, in particular, to the RBC plasma membrane. This major remodelling of the RBC membrane and its pathogenicity consequences are further described below. Trophozoites also generate Novel Permeability Pathways (NPP), channels at the RBC plasma membrane, that allow for increased import of nutrients and export of waste [31]. Further, the continuous digestion of haemoglobin within the food vacuole leads to the production of hemozoin, or "malaria pigment", the result of the detoxification of the heme component of hemoglobin [32]. Finally, during the last 4h of intraerythrocytic development, DNA replication occurs, and the parasite develops into a multi-nucleated schizont [33]. Each schizont contains ∼30 newly formed merozoites that are released in the blood circulation and re-invade healthy erythrocytes, hence continuing the infection.

A minority of the newly formed merozoites commit to sexual differentiation to become either female or male gametocytes (over 8-12 days), the stage that is transmitted to mosquitoes and allows the continuation of the *Plasmodium* life cycle [34].

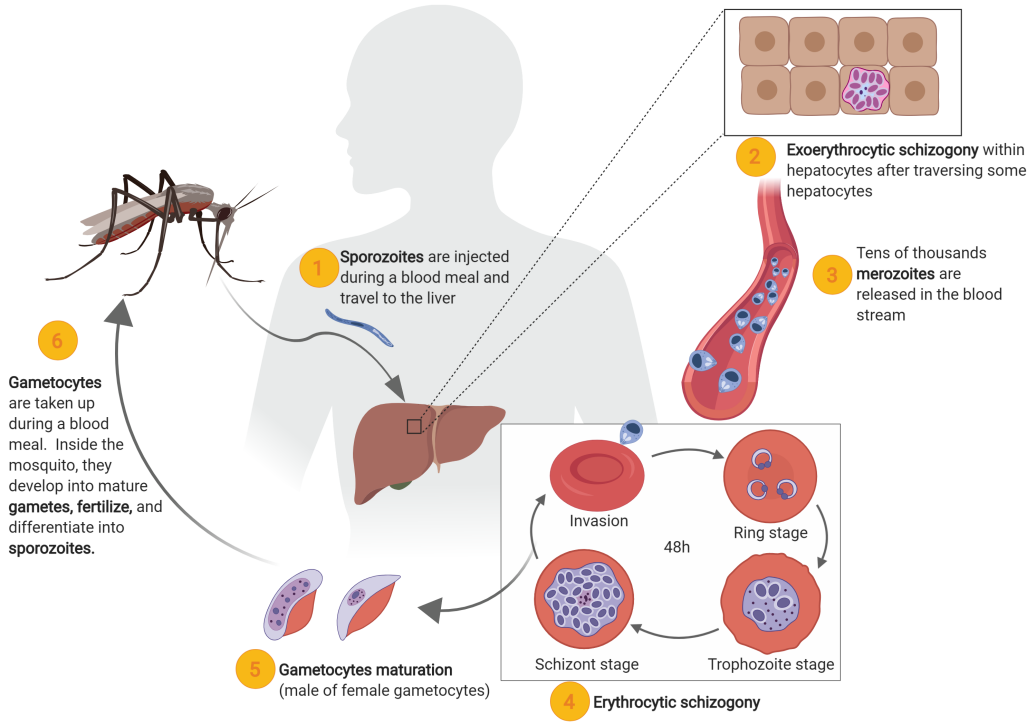

Figure 1.3: ***Plasmodium falciparum*** **life cycle in humans. (1)** A malaria infection in humans starts with the blood meal of an infected female *Anopheles* mosquito, which injects sporozoites in the skin. **(2)** These sporozoites travel through the blood stream to the liver, where they invade hepatocytes. **(3)** After several replication cycles in hepatocytes, thousands of merozoites are released in the blood stream, and invade mature red blood cells (RBCs), where the erythrocytic asexual replication, or schizogony, takes place **(4)**: every merozoite becomes an intraerythrocytic ring stage, which matures into a trophozoite stage, and further into a multinucleated schizont stage. Mature schizonts burst and release 8 to 32 new merozoites in the blood circulation. It is the erythrocytic stage that gives rise to disease symptoms, whereas the pre-erythrocytic stages are asymptomatic. **(5)** Occasionally, intraerythrocytic parasites can develop into female or male gametocytes, **(6)** that are taken up and fertilise within an *Anopheles* mosquito.

1.1.5 Pathogenesis of *P. falciparum* infections

Most malaria cases occur as uncomplicated malaria, either asymptomatic, or with relatively mild and non-specific symptoms, such as fever and fatigue [35]. If left untreated however, symptoms can reoccur in successive waves: symptoms increase with parasitemia and repeated lysis of infected RBCs, until parasitemia is controlled to low levels, reducing symptoms. However, when patients cannot control the infection, in particular in the case of young children, malaria can evolve into a severe disease, which can be lethal. Some of the most common complications of severe malaria include organ failure, cerebral malaria, respiratory distress and severe anaemia [35].

P. falciparum is responsible for a vast majority of severe malaria cases and malaria-related deaths, because of its ability to exponentially grow, sequester and escape immune clearance. Indeed, the repeated 48h-cycles of RBC rupture and reinvasion can lead to hyperparasitemia (defined as more than 4% of RBCs being infected [23]), which is associated with severity and poor prognosis. The metabolic activity of the parasites can lead to acidosis and tissue hypoxia, ultimately resulting in respiratory distress [36].

One of the factors that allows *P. falciparum* growth is its ability to escape splenic and immunity clearance. Indeed, mature parasites expose proteins on the surface of the RBC, such as *P. falciparum* erythrocyte membrane protein 1 (PfEMP1) on protruding structures called knobs [37, 38]. These exposed ligands bind to host receptors on the surface of (i) endothelial cells, resulting in tissue sequestration of the infected red blood cells (iRBCs) [39], and (ii) surrounding uninfected RBCs (uRBCs), resulting in rosetting [40]. Sequestration and rosetting are protective strategies developed by the parasite to avoid clearance by the spleen and to avoid being recognised by the host immune system. Both sequestration and rosetting are also responsible for obstruction of the blood flow in the microvasculature, potentially leading to organ failure [41]. In particular, sequestration of iRBCs in the brain microvasculature can lead to a severe form of malaria disease known as cerebral malaria, which often results in coma and can be fatal [42].

Another severe form of malaria disease is known as severe anaemia [43]. Anaemia is classified as mild, moderate or severe, depending on total haemoglobin levels present in the blood (typically <11g/dL, <10g/dL and <7g/dL respectively for children under the age of five [44]). During an acute malaria infection, anaemia develops quickly in symptomatic patients, and only begins to resolve several weeks after treatment. The severity of anaemia is correlated to the severity and duration of the disease before treatment is initiated [43]. In particular, mortality due to malaria dramatically increases when haemoglobin levels drop below 3g/dL [45].

Although the repeated bursting of iRBCs every 48h contributes to the depletion of erythrocytes, malarial anaemia cannot be explained solely by the loss of rupturing iRBCs [46]. Another explanation for malarial anaemia is a decreased effectivity of erythropoiesis, due to the host immune response as well as parasite factors (*e.g.* hemozoin or metabolites) [47]. The contribution of dyserythropoiesis to malarial anaemia is unclear, but it is believed to be somewhat minimal [48]. In fact, the key driver of malarial anaemia appears to be the significant loss of uRBCs [49]. An early mathematical model based on data from *P. falciparum*-infected patients estimated that for each iRBC, 8.5 uRBCs were cleared from circulation [48]. An experimental murine model confirmed that malarial anaemia resulted primarily from the loss of uRBCs and that this process continued even after the clearance of parasites in the blood stream [50]. The authors estimated the ratio of destruction of iRBCs vs. uRBCs to be 1:30 [50]. Finally, in a malaria macaque model, the clearance of uRBCs was estimated to account for 76% of all RBCs loss [51].

Overall, malarial anaemia is a common and severe complication: although we now understand that it is caused by the loss of uRBCs, the mechanisms responsible for the clearance of these cells are poorly understood.

1.2 Eryptosis in malarial anemia: the role of *P. falciparum* extracellular factors

1.2.1 Mechanisms of uRBCs clearance during malaria

The mechanisms underlying the clearance of bystander uninfected RBCs from circulation during a malaria infection are yet to be elucidated. Here I discuss a few possible explanations for this phenomenon, including reduced deformability of uRBCs, presence of parasites antigens on the surface of uRBCs, increased amounts of autoantibodies and increased eryptosis of uRBCs.

- **Reduced uRBC deformability enhances clearance by the spleen**

In normal conditions, erythrocytes are cleared from circulation by macrophages after their 120 days lifespan upon recognition of senescent markers in the spleen. It is thought that the reduced deformability of senescent erythrocytes marks them to be mechanically filtered by the spleen. Indeed, erythrocytes traveling through the spleen must squeeze through tight intercellular spaces, representing a quality control test for erythrocytes, to ensure that they can carry out their role effectively [52]. In the context of malaria infections, the spleen has been shown to enlarge and reorganise [53, 54]: these changes reduce splenic clearance threshold of erythrocytes, leading to accelerated clearance and shortened life span of RBCs [55, 56, 57].

It is known that iRBCs lose deformability as parasites mature. The mere presence of a foreign entity (the parasite), within the usually extremely flexible erythrocyte, accounts for a large proportion of the deformability loss [58]. But, not only do iRBCs become 'stiffer', uRBCs of *P. falciparu*m-infected patients also display decreased deformability, which correlates with anaemia [59]. In the murine model *P. yoelii,* uRBCs are stiffer, which promotes their mechanical filtration by the spleen [60]. This change in deformability of bystander RBCs was also observed in *P. falciparum in vitro* cultures, where changes cannot be attributed to the immune response or other host reactions [61]. Further, naïve erythrocytes incubated with conditioned medium from a parasite culture also showed decreased deformability [61]. In a recent follow up study, the authors suggest that these changes were partly due to a rise in intracellular cAMP levels within erythrocytes [62]. These increased cAMP levels might result in protein kinase A (PKA) activation and hence cytoskeletal proteins phosphorylation and stiffness changes.

- ***Plasmodium* factors prime uRBCs for clearance**

P. falciparum may directly be responsible for the exacerbated clearance of uRBCs. In particular, haemoglobin digestion by-products might negatively affect uRBCs viability: β-hematin (the equivalent of *Plasmodium* hemozoin) was shown to induce lysis of uRBCs and decrease their deformability [63]. Moreover, an *in vitro* study demonstrated that *P.*

falciparum Ring Surface Protein 2 (RSP2) binds to uRBCs, as well as other members of the erythropoietic lineage [64]. The binding of RSP2 was shown to prime the engulfment of these cells by macrophages, a process mediated by anti-RSP2 antibodies [64]. Similarly, the parasitophorous vacuole, released upon schizont egress, was shown to induce complement deposition and phagocytosis on bystander RBCs [65].

- **Autoantibodies increase during a malaria infection and lead to erythrophagocytosis**

During senescence, oxidative stress of the RBC leads to modification of the membrane band 3 protein, which results in its clustering [66]. Band 3 clusters are recognised by naturally occurring immunoglobulin G (IgG) antibodies, which allow for phagocytosis of these aging cells [66].

Patients with severe *falciparum* anaemia show more antibodies bound to their erythrocytes compared to asymptomatic and non-anaemic controls [67]. Further, this IgG presence on erythrocytes surface correlates with erythrophagocytosis. However, this study did not identify whether these antibodies were detecting injured RBCs or *Plasmodium* factors sticking on the uRBCs surface (as discussed above). In *P. vivax* infections, autoantibodies recognising erythrocyte proteins band 3 and spectrin were increased in anaemic patients [68].

Another autoantibody that has been associated with anaemia and shown to increase during malaria infections is anti-phosphatidylserine (PS) antibodies [69]. Note that changes in erythrocytes PS exposure will be explored thoroughly in the following paragraph. It was shown that levels of anti-PS IgM and IgG were increased in malaria infections compared to controls, and that they correlated with anaemia [70]. In non-immune volunteers infected with *P. falciparum* or *P. vivax*, it was confirmed that both anti-PS IgM and IgG levels increased over the period of infection [70].

- **PS exposure of uRBCs is responsible for their clearance by macrophages**

Erythrocytes are unique cells in the human body as they lack a mitochondrion and a nucleus, two key organelles for eukaryotic cell's apoptosis regulation. Regardless, RBCs display a particular form of programmed cell death, termed eryptosis. Eryptosis is further described and discussed in Section 1.4.4. and in Chapter 2 [71]. Although the molecular cascade is yet to be described, major hallmarks of eryptosis resemble those of apoptosis, including cell shrinkage, increased intracellular calcium levels and cell surface exposure of phosphatidylserine (PS) [72]. PS is a phospholipid actively maintained in the inner leaflet of the plasma membrane of healthy cells. Its exposure on the outer cell surface acts as an "eat-me" signal for macrophages [73].

In the context of malaria, it is well established that a larger proportion of iRBCs expose PS compared to uRBCs [74, 75, 76]. But it has also been observed that bystander RBCs

expose more PS than naïve RBCs (*i.e.* uRBCs which have never been in the presence of *Plasmodium* parasites). In a malaria murine model, it has been shown that uRBCs of *P. yoelii*-infected mice exposed more PS compared to the non-infected mice, and these PS exposure levels correlated with anaemia [77]. Further, serum from *P. falciparum* patients induced an increase in PS exposure of naïve RBCs [78]. Collectively, these findings suggest that the induction of PS exposure of uRBCs by malaria parasites is (at least partly) due to parasite soluble factors, and not (only) to cell-to-cell contact. Moreover, the induction of PS exposure could be attributed to the host immune and inflammatory response. However, the increased PS exposure of bystander RBCs has also been shown in *in vitro* cultures of *P. falciparum* (that do not contain any immune cells), therefore highlighting that the host immune response could not be the full mechanism behind the phenomenon [79, 80].

1.2.2 *P. falciparum* extracellular factors induce death of other human cell types

RBCs are not the only host cell type affected by the presence of the parasite. Viability of cardiomyocytes, erythroblasts, brain vascular endothelium and neuroglial cells were all shown to be affected by secreted factors of *P. falciparum*, either using purified toxins or conditioned media [81, 82, 83]. Candidates for the induction of cell death by *P. falciparum* include glycosyl phosphatidylinositol [81], hemozoin [82] and methemoglobin [84]. Overall, these findings highlight the importance of parasitic extracellular factors during a malaria infection, and their possible role in bystander RBCs death and malarial anaemia.

1.3 Extracellular Vesicles and their role in malaria disease

1.3.1 What are Extracellular Vesicles?

Extracellular vesicles (EVs) are "particles naturally released from the cell that are delimited by a lipid bilayer and cannot replicate" [85]. Different subtypes of EVs exist depending on the subcellular origin of the vesicle, including exosomes for endosome-derived particles (typically small, 40-120nm in diameter) and microvesicles for plasma-derived particles (typically bigger, 20-1,000nm in diameter) [85].

All eukaryotic cells secrete EVs, even the organelle-deprived erythrocytes. EVs can serve a range of cellular functions, including waste removal, antigen presentation and cell-to-cell communication, on which I will focus here. EVs can contain different types of molecules, including DNA, RNA, proteins, enzymes and lipids. Their content is usually representative of the parent cell's content, although EVs can be enriched in specific molecule types [85]. Further, EVs can be uptaken by recipient cells, which are not necessarily of the same type as the secreting cell.

1.3.2 Role of EVs in malaria

EVs numbers present in the human serum increase upon a malaria infection, and high-EV content is associated with severity of the disease, in particular in cerebral malaria [86]. These EVs are thought to be secreted by RBCs (both infected and uninfected), platelets and endothelial cells. In particular, a field study found that iRBCs produced more than ten-fold EVs compared to uRBCs (iRBC-derived EVs were recognised with the parasite protein RESA) [87]. *In vitro*, the secretion of EVs increases as the parasite matures [88, 87], and *P. falciparum* demonstrates the ability to communicate with other iRBCs via EVs. In particular, genetically modified parasites are able to exchange resistance genes through EVs, a horizontal gene transfer never observed before in *Plasmodium* [89]. iRBC-derived EVs also promote gametogenesis [89, 88]. In addition to establishing communication between parasite cells, iRBC-derived EVs also affect host cells: they modulate the inflammatory response of macrophages and neutrophils [88, 86] and miRNA contained in iRBC-derived EVs affects endothelial cells [90]. Recently, RBC-derived EVs were proposed as a drug delivery strategy to enhance antimalarial efficacy and therefore reduce side-effects [91].

Moreover, it was recently shown that iRBC-derived EVs also induce changes in naïve uRBCs, proposed to be a "preparation" before invasion [92]. Specifically, iRBC-derived EVs reduced membrane stiffness of naïve RBCs, presumably to facilitate invasion, through phosphorylation and degradation of erythrocyte cytoskeletal proteins. However, the role of EVs in eryptosis of uRBCs, and in malarial anaemia, is yet to be investigated.

1.4 Eryptosis and how *Plasmodium falciparum* interacts with its host cell death

1.4.1 Intracellular pathogens and their host cell death

Intracellular pathogens strictly require to be within a host cell to replicate. Intracellular pathogens benefit from direct access to host nutrients and intracellular machinery while avoiding direct contact with the host immunity [93, 94]. However, infected cells often recognise an invading pathogen via Pattern Recognition Receptors (PRRs) that are activated by Pathogen Associated Molecular Patterns (PAMPs) [95, 96]. Upon this recognition, infected cells might commit to apoptosis, a form of programmed cell death, in an attempt to clear the infection and protect surrounding healthy cells [97]. The intracellular pathogens can, in turn, inactivate or delay the host apoptosis response to maintain the host cell alive, and therefore achieve its own survival [98, 99, 97]. Ultimately, apoptosis can be re-activated in order to facilitate the exit of the pathogen from the host cell, a strategy adopted for instance by *Leishmania spp.* [100].

1.4.2 Programmed cell death in nucleated cells: Apoptosis

Apoptosis is an active process of cell death and is often referred to as cell "suicide". Apoptosis can be activated by an intrinsic pathway when the trigger initiates within the cell, for example when DNA damage occurs or growth factors are withdrawn; or by an extrinsic pathway upon the binding of death ligands (such as Fas Ligand (FasL) or Tumor Necrosis Factor (TNF)) to membrane receptors [101]. The intrinsic pathway is necessarily mitochondria-dependent, while the extrinsic pathway can bypass the mitochondrial signalling (Figure 1.4, [101]). Commitment to cell life or death relies on the fine balance between pro-survival and pro-apoptotic molecular signals. The proteins within the B-cell lymphoma 2 (BCL-2) family are key in the regulation of apoptosis and are further described in the following section [101].

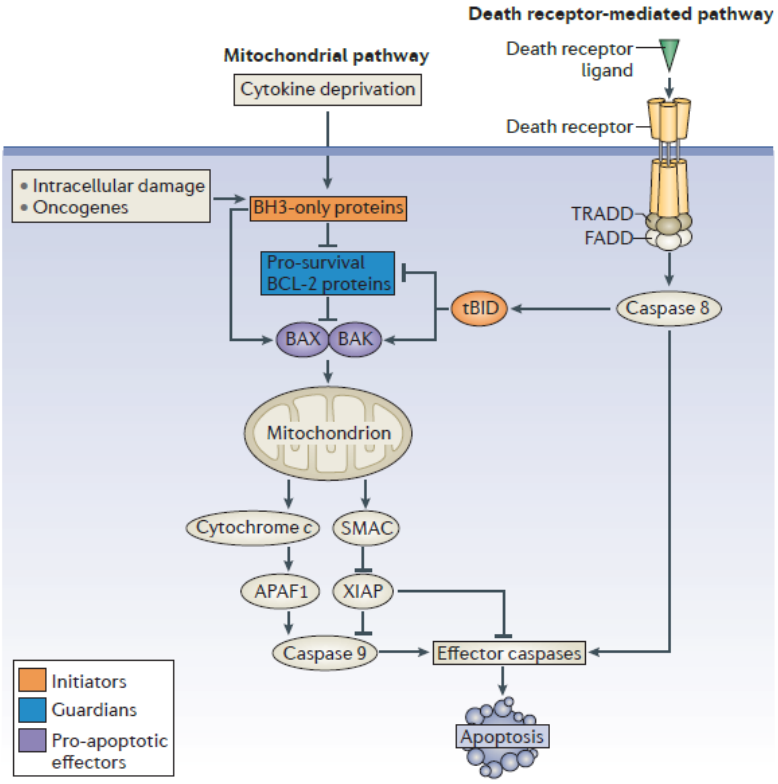

Figure 1.4: Mitochondrial apoptosis. Intrinsic apoptosis can be triggered by cytokine deprivation, intracellular damage (such as DNA damage) or oncogenes exposure. These signals will activate the "initiators": pro-apoptotic members of the BCL-2 family called BH3-only proteins. These initiators can both directly activate pro-apoptotic effectors (BAX and BAK) and inhibit their inhibitors (*i.e.* the "guardians", pro-survival BCL-2 proteins, such as BCL-x_L). BAX and BAK homodimerise and form pores in the outer membrane of the mitochondrion, releasing pro-apoptotic signals such as cytochrome c. Further signalling cascades result in the activation of effector caspases which cleave, among others, DNA and membrane proteins. Extrinsic apoptosis is triggered by binding of a death ligand to a death receptor. The downstream signalling can either require the involvement of the mitochondrion (in "type 2" cells, such as hepatocytes), or completely bypass the mitochondrion (in "type 1" cells, such as thymocytes). (Figure from Czabotar *et al.* - *Nature Reviews Molecular Cell Biology* (2014) [101])

During mitochondrial apoptosis, when pro-apoptotic signals tip the balance over pro-survival signals, the effector proteins BAK and BAX homodimerise and form pores in

the outer-membrane of the mitochondrion [102]. This releases apoptogenic factors (such as calcium and cytochrome c) that activate the caspase pathway and commits the cell to apoptosis. Effector caspases cleave numerous substrates and induce DNA fragmentation [103], membrane blebbing [104] and the exposure of the phosphatidylserine on the outer cell membrane [105]. Phosphatidylserine (PS) is a phospholipid of the cell membrane lipid bilayer and is usually present on the cytosolic side of the membrane. This asymmetry is maintained by "flippase" proteins that actively flip PS to the inner leaflet [73]. Scramblases, on the other hand, are proteins able to diffuse lipids to both directions. High cytosolic calcium content inactivates flippases while activating scramblases, leading to the rapid exposure of PS to the extracellular side of the plasma membrane [73]. Noteworthy, this is a reversible process. However, caspase-3 can irreversibly inactivate flippases and irreversibly activate scramblases by cleaving the intracellular domains of these proteins. PS-exposing cells are recognised and engulfed by macrophages which has led to PS being referred to as an "eat-me" signal [73].

1.4.3 *Plasmodium* interferes with its host cell apoptosis in hepatocytes

Before infecting RBCs, *Plasmodium spp.* develop in hepatocytes, where they undergo schizogony, giving rise to tens of thousands of merozoites over a week [35]. This extended period of extreme replication, although asymptomatic for the human host, substantially disrupts the host cell. In particular, a subset of infected hepatocytes undergo apoptosis, more so than the uninfected hepatocytes [106]. Nevertheless, the presence of the parasite seems to protect the host cell from some apoptosis stimuli, including t-butyl-hydroperoxide (tBHP), tumor necrosis factor alpha (TNFα) [107] and Fas activating antibody [106]. Moreover, apoptosis and phagocytosis of infected hepatocytes was mainly observed when the parasite was dead [107], either suggesting that the host cell was successful at 'killing' the invader by undergoing apoptosis, and/or that the parasite was dead, therefore not inhibiting apoptosis completion. The correct establishment of the parasitophorous vacuole (PV) has been found to be crucial for the success of the parasite: without it, the host cell undergoes apoptosis [106].

On the other hand, infected hepatocytes seem to be more sensitive to other apoptotic stimuli compared to non-infected cells. In particular, parasitised hepatocytes were susceptible to mitochondria-dependent apoptosis. Indeed, Kaushansky *et al.* (2013) found that the chemical inhibition of anti-apoptotic BCL-2-family proteins increased infected hepatocytes death and reduced the parasites burden [106]. Moreover, they found that the absence of pro-apoptotic BID promoted *Plasmodium* development. Overall, they concluded that infected hepatocytes may be somewhat similar to cancer cells in their "oncogene addiction", whereby cells are highly dependent on particular pathways, in this case, mitochondria-driven apoptosis.

1.4.4 Interaction between *P. falciparum* and the host cell eryptosis

Mature erythrocytes uniquely lack all cell organelles (nucleus, mitochondria, endoplasmic reticulum) and have a lifespan of 120 days, after which they undergo senescence and are cleared from circulation by the spleen [108, 109]. However, premature erythrocyte death can be triggered by various factors including oxidative stress [110], energy depletion [111], and numerous compounds [112, 113]. Eryptosis (erythrocyte apoptosis) defines the programmed cell death of erythrocytes and is characterised by PS exposure, cell shrinkage, high intracellular calcium levels and membrane blebbing - phenotypic aspects shared with apoptosis of nucleated cells [112]. However, no molecular pathways for eryptosis have been described yet. Since erythrocytes cannot synthesise *de novo* proteins, the eryptosis pathway cannot include gene regulation; instead, it must rely on post-translational modifications (such as phosphorylation), changes in molecule localisation, modifications of molecular complexes and protein degradation.

Chapter 2 of this thesis, Boulet *et al.* (2018) [71] summarises the current knowledge (and highlights the many gaps in knowledge) regarding eryptosis, the interaction between *P. falciparum* and eryptosis of its host cell, as well as the effects of eryptotic inducers on the development of *Plasmodium* both *in vitro* and *in vivo* (with murine models).

1.4.5 Host-targeted therapy: the case for targeting programmed cell death proteins

Resistance to all currently available antimalarial drugs has been detected, including resistance to the front-line treatment artemisinin [13]. Targeting host molecules that are required for *Plasmodium* development is an exciting avenue for antimalarial drug development for two main reasons [114]. First, the drug would not target a molecule under the genetic control of the parasite, therefore limiting the most straightforward pathway for drug resistance (mutation of the target molecule). Second, many drugs targeting human molecules already exist in the context of other diseases such as cancers [115, 116, 117]: some may be repurposed for antimalarial treatment therefore saving precious time and resources linked to drug development.

Within the umbrella of host-targeted therapies, targeting host cell death pathways appears as a particularly interesting approach. Indeed, as discussed above, it has been demonstrated that *P. falciparum* manipulates apoptosis in hepatocytes. A drug that would prevent *Plasmodium* from inhibiting programmed cell death should help to clear the infection. Moreover, many drugs have been developed to interfere with the apoptotic process, and in particular, to enhance apoptosis, in the context of cancer therapies [116, 117]. Indeed, cancer cells typically mutate in ways that prevent apoptosis completion. Such drugs, some already used in the clinic, some still in development, could be repurposed for infectious diseases [114].

Malaria symptoms appear during the blood stages of infection, therefore developing drugs that target erythrocytic stages is crucial. However, little is known about the molecular details of eryptosis, the programmed cell death of RBCs [72]. Even less so is known about *Plasmodium* interactions with RBC signalling pathways [71]. In the following section, we explore a protein candidate that could play a role in eryptosis: BCL-x_L.

1.5 BCL-x_L: its role in apoptosis, erythropoiesis and mature erythrocytes

1.5.1 BCL-x_L: a key anti-apoptotic regulator

Commitment to cell life or death relies on the fine balance between pro-survival and pro-apoptotic molecular signals. In the case of mitochondrial-driven apoptosis, the balance between pro- and anti-apoptotic proteins of the BCL-2 (B-cell lymphoma 2) family is crucial [101]. The BCL-2 family consists of:

- anti-apoptotic proteins: BCL-2, BCL-x_L, MCL-1 and BCL-w
- pro-apoptotic proteins:
  - BH3-only initiators (exclusively contain the BCL-2 Homology (BH) domain 3): BID, BIM, BAD, NOXA and PUMA
  - Multi-domain effectors: BAX, BAK, BOK

In healthy cells, apoptosis is naturally repressed as anti-apoptotic proteins (typically BCL-2 and BCL-x_L) bind to, and inhibit, the death effectors BAK and BAX, while scaffold protein 14-3-3 sequesters BAD (BCL2-Associated Death promoter) in the cytosol (Figure 1.5) [118]. Apoptotic signals lead to changes in BAD phosphorylation, disrupting its binding affinity with protein 14-3-3, and instead, promoting binding of BAD to BCL-x_L. Consequently, BAK and BAX are freed: they homodimerise to form pores in the outer membrane of the mitochondrion, which commits the cell to apoptosis. In summary, BCL-x_L has a pro-survival role that is strictly dependent on its binding partners: binding to effectors BAX and BAK promotes survival, while binding to BAD promotes apoptosis.

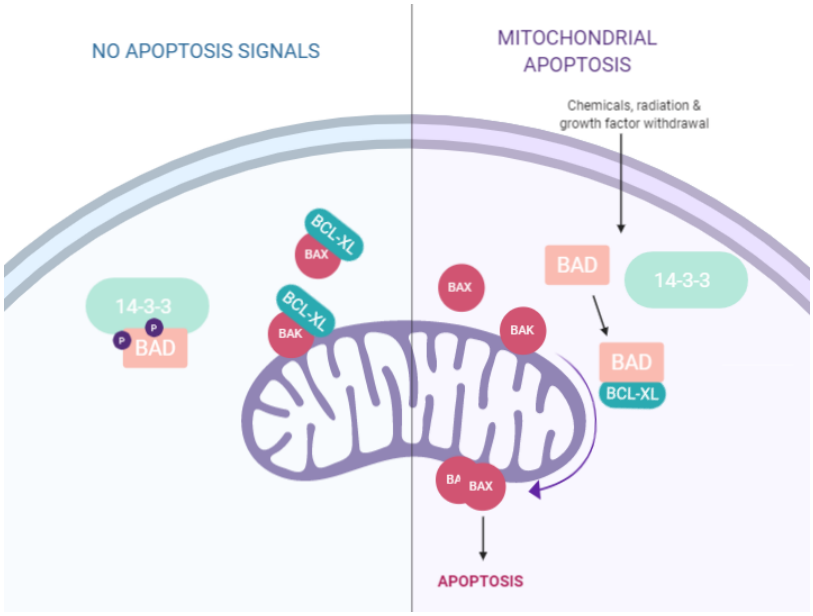

Figure 1.5: BCL-x_L during mitochondrial apoptosis. Under normal conditions, apoptosis effectors BAK and BAX are sequestered by BCL-x_L, and protein 14-3-3 sequesters BAD in the cytosol. Upon intrinsic apoptotic signals, phosphorylation of BAD disrupts its binding affinity to 14-3-3, and instead BAD binds to BCL-x_L. This liberates BAX and BAK, which dimerise and form pores in the outer membrane of the mitochondrion, committing the cell to apoptosis.

1.5.2 BCL-x_L: its role in the hematopoietic lineage and in mature erythrocytes

Mature red blood cells are produced from hematopoietic stem cells (HSC), through a multi-step expansion and differentiation process, as seen in Figure 1.6. Interestingly, besides its role in apoptosis, BCL-x_L is also required for erythropoiesis, the production of RBCs. First, BCL-x_L is highly expressed in the erythroid lineage, especially during the terminal differentiation stages [119]. Moreover, mice lacking the *bcl2-l1* gene (which gives rise to BCL-x_L or BCL-x_S in a splicing-dependent manner) die at embryonic day 13, partly because of the death of hematopoietic cells in the liver [120]. Importantly, the induced loss of BCL-x_L in adult mice results in severe anemia due to deficient erythropoiesis [121]. In particular, reticulocytes (immature red blood cells that have lost their nucleus but still contain mitochondria) undergo apoptosis when BCL-x_L is removed [121]. The importance of BCL-x_L for erythropoiesis was recently confirmed in human stem cell lineages [122]. Overall, BCL-x_L appears to be crucial in the late stages of erythropoiesis.

Platelets are another atypical cell type of the erythroid lineage: they lack a nucleus but contain mitochondria. Here again, BCL-x_L was found to be essential: BCL-x_L represents a "molecular clock", its slow degradation leading to the clearance of platelets after their 10 days lifespan [123].

In mature erythrocytes, BCL-x_L was identified by mass spectrometry in the cytoplasmic

fraction [124]. However, Walsh and colleagues (2002) identified BCL-x_L at the membrane of RBCs [125]. They also found that, in the absence of serum, inhibition of BCL-x_L with BH3-mimetics leads to PS exposure of RBCs, suggesting a pro-survival role of BCL-x_L within the eryptotic pathway, in a mitochondria-independent manner.

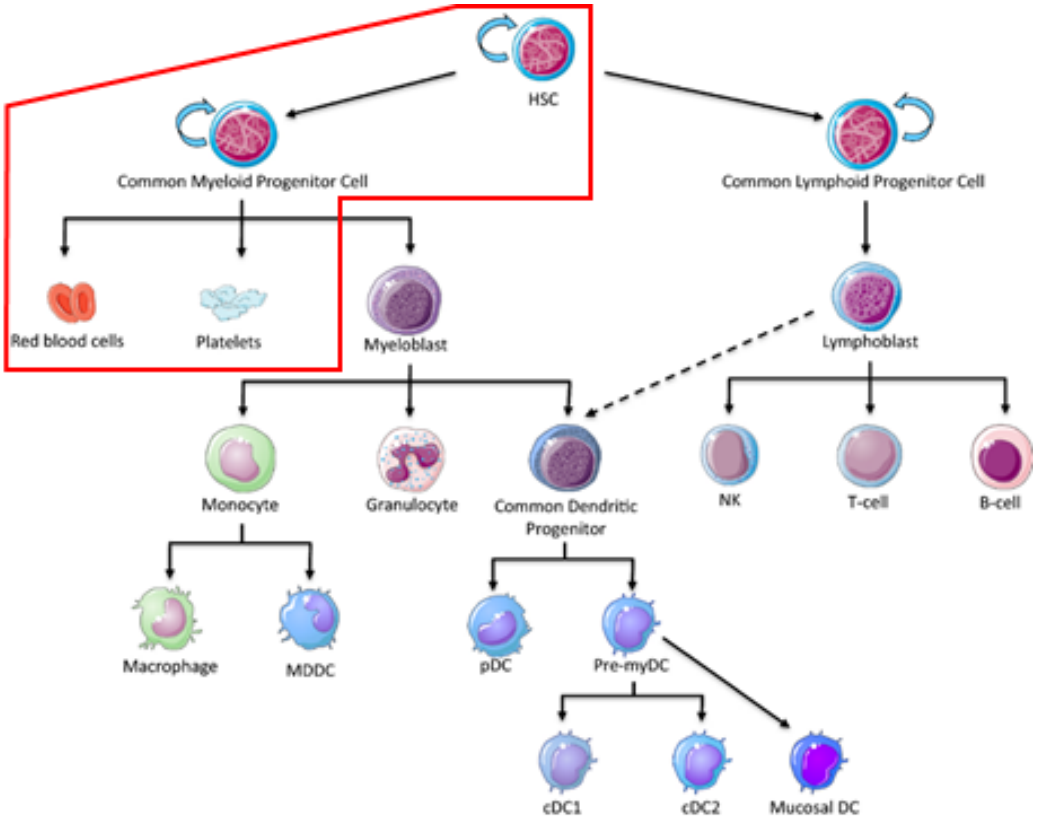

Figure 1.6: Hematopoiesis. Hematopoietic stem cells (HSC) are multipotent stem cells, giving rise to either the myeloid or the lymphoid cell lineages. Here, we focus on the erythroid lineage. Common myeloid progenitor cells can undergo erythropoiesis, ultimately producing mature red blood cells, or can differentiate to megakaryocytes, whose fragmentation results in platelets production. (Adapted from Rocamonde et al. - Retrovirology (2019) [126])

1.5.3 BCL-x_L inhibitors & drug treatments

Upregulation of pro-survival BCL-2 proteins, including BCL-x_L, is common in many cancer types [127]. Therefore, various drugs have been developed to address apoptosis dysregulation in this context. In particular, many BCL-x_L inhibitors have been developed. These inhibitors mimic BH3-only proteins, such as BAD, and bind to BCL-x_L with a high affinity, therefore freeing apoptotic effectors BAX and BAK. The first BH3-mimetic drug, ABT-737, was developed in 2005 [128], but its low solubility and bioavailability prevented it from being used in the clinic. An improved BCL-x_L inhibitor was developed in 2008 [129]: ABT-263 (Navitoclax), which is undergoing clinical trials for various cancer types [130, 131]. However, concerning side effects include thrombocytopenia, due to the loss of platelets after continuous administration of ABT-263 [132]. In order to circumvent this side effect, ABT-199 was developed to inhibit more specifically BCL-2 (*i.e.* decreased affinity towards BCL-x_L) [133]. ABT-199 is now an approved drug (FDA-approved in 2016) under the

name Venclexta, Venclyxto or Venetoclax, to treat chronic and small lymphocytic leukemia (CLL and SLL) [134, 135]. In parallel, more specific inhibitors of BCL-x_L have also been developed, including WEHI-539 [136], A-1155463 [137], and A-1331852 [138]. So far, these molecules remain research tools to investigate the role of BCL-x_L rather than potential drug candidates.

Although ABT-737 was found to reduce parasitic burden of *P. yoelii*-infected mice during the liver stages [106], the impact of BCL-x_L inhibitors, and the role of BCL-x_L, has never been investigated in the blood stages of *Plasmodium spp.*

1.6 Hypotheses & Aims

P. falciparum was shown to manipulate its host hepatocyte apoptosis during the liver stages [107, 106]. **We hypothesise that *P. falciparum* also manipulates eryptosis of its host red blood cell in order to survive**. To test this hypothesis, I aim to:

- **Aim 1**: Review the literature on eryptosis regulation and the relationship between *P. falciparum* and its host eryptosis.
- **Aim 2**: Chemical manipulation of eryptosis in *P. falciparum*-iRBCs to characterise host-parasite interactions.
- **Aim 3**: Study eryptosis of infected RBCs at different stages of the parasite.

BCL-x_L is a key regulator of apoptosis in nucleated cells and appears to also inhibit eryptosis [125]. Inhibition of BCL-x_L impairs *P. falciparum* during the liver stages [106]. **We hypothesise that BCL-x_L regulates eryptosis and that *P. falciparum* hijacks it for its survival in erythrocytes**. To test this hypothesis, I aim to:

- **Aim 4**: Investigate the role of erythrocytic BCL-x_L during infection
  - First, I will study the effect of BCL-x_L inhibitors on eryptosis hallmarks of both uninfected RBCs and infected RBCs.
  - Then, I will test the impact of BCL-x_L inhibitors on *P. falciparum* growth *in vitro*.
  - Finally, I will investigate the role of erythrocytic BCL-x_L during infection by defining its subcellular localisation and identifying its binding partners.

The main driver of malarial anaemia is the loss of bystander RBCs [48]. Although the mechanisms behind this enhanced destruction of erythrocytes is poorly understood, induction of eryptosis appears as an important contributor [49]. **We hypothesise that extracellular vesicles and/or other extracellular factors secreted by the parasite induce eryptosis of bystander RBCs**. To test this hypothesis, I aim to:

- **Aim 5**: Identify extracellular factors of *P. falciparum* which are responsible for bystander RBC death
  - First, I will test the impact of iRBC-derived EVs on eryptosis hallmarks of fresh RBCs.
  - Then, I will test the impact of conditioned media (filtered media from parasite cultures) on eryptosis hallmarks of fresh RBCs.

Chapter 2

Manipulating Eryptosis of Human Red Blood Cells: A Novel Antimalarial Strategy?

Mature erythrocytes uniquely lack all organelles (nucleus, mitochondrion, endoplasmic reticulum) and have a lifespan of 120 days, after which they undergo senescence and are cleared from the circulation by the spleen [108, 109]. However premature erythrocyte death can be triggered by various factors including oxidative stress, energy depletion and numerous compounds [139, 111, 113]. Eryptosis (erythrocyte apoptosis) defines the programmed cell death of erythrocytes and is characterised by PS exposure, cell shrinkage, high intracellular calcium levels and membrane blebbing - phenotypic aspects shared with apoptosis of nucleated cells [112].

Boulet *et al.* (2018) [71] summarizes the current knowledge (and highlights the many gaps in knowledge) regarding regarding eryptosis and its molecular regulators. This review further discusses the interaction between intracellular *P. falciparum* and eryptosis of its host cell, and the effects of eryptotic inducers on the development of *Plasmodium* both *in vitro* and *in vivo* (with murine models). Finally, this article discusses the possibility of targeting key human eryptotic molecules to specifically inhibit *P. falciparum* development in a host-directed therapy approach.

frontiers in Cellular and Infection Microbiology

REVIEW
published: 30 November 2018
doi: 10.3389/fcimb.2018.00419

Manipulating Eryptosis of Human Red Blood Cells: A Novel Antimalarial Strategy?

Coralie Boulet[1], *Christian D. Doerig*[2] *and Teresa G. Carvalho*[1]*

[1] Molecular Parasitology Laboratory, Department of Physiology, Anatomy and Microbiology, La Trobe University, Bundoora, VIC, Australia, [2] Infection and Immunity Program, Biomedicine Discovery Institute, Department of Microbiology, Monash University, Clayton, VIC, Australia

Malaria is a major global health burden, affecting over 200 million people worldwide. Resistance against all currently available antimalarial drugs is a growing threat, and represents a major and long-standing obstacle to malaria eradication. Like many intracellular pathogens, *Plasmodium* parasites manipulate host cell signaling pathways, in particular programmed cell death pathways. Interference with apoptotic pathways by malaria parasites is documented in the mosquito and human liver stages of infection, but little is known about this phenomenon in the erythrocytic stages. Although mature erythrocytes have lost all organelles, they display a form of programmed cell death termed eryptosis. Numerous features of eryptosis resemble those of nucleated cell apoptosis, including surface exposure of phosphatidylserine, cell shrinkage and membrane ruffling. Upon invasion, *Plasmodium* parasites induce significant stress to the host erythrocyte, while delaying the onset of eryptosis. Many eryptotic inducers appear to have a beneficial effect on the course of malaria infection in murine models, but major gaps remain in our understanding of the underlying molecular mechanisms. All currently available antimalarial drugs have parasite-encoded targets, which facilitates the emergence of resistance through selection of mutations that prevent drug-target binding. Identifying host cell factors that play a key role in parasite survival will provide new perspectives for host-directed anti-malarial chemotherapy. This review focuses on the interrelationship between *Plasmodium falciparum* and the eryptosis of its host erythrocyte. We summarize the current knowledge in this area, highlight the different schools of thoughts and existing gaps in knowledge, and discuss future perspectives for host-directed therapies in the context of antimalarial drug discovery.

Keywords: malaria, eryptosis, *Plasmodium*, apoptosis, programmed cell death, host-pathogen interaction, host-directed therapy

OPEN ACCESS

Edited by:
Alexis Kaushansky,
Seattle Children's Research Institute,
United States

Reviewed by:
Marisa Ponpuak,
Mahidol University, Thailand
Anat Florentin,
University of Georgia, United States

***Correspondence:**
Teresa G. Carvalho
t.carvalho@latrobe.edu.au

Specialty section:
This article was submitted to Parasite and Host, a section of the journal Frontiers in Cellular and Infection Microbiology

Received: *04 September 2018*
Accepted: *14 November 2018*
Published: *30 November 2018*

Citation:
Boulet C, Doerig CD and Carvalho TG (2018) Manipulating Eryptosis of Human Red Blood Cells: A Novel Antimalarial Strategy? Front. Cell. Infect. Microbiol. 8:419. doi: 10.3389/fcimb.2018.00419

INTRODUCTION

Malaria is a vector-borne parasitic disease that affects millions of people worldwide. It is estimated that half the world population is at risk of infection and in 2016, malaria was responsible for 200 million new cases and half a million deaths (WHO|World Malaria Report, 2017). An efficient malaria vaccine has yet to be developed, and resistance against all antimalarial drugs has been recorded, including to artemisinin (reviewed in Tilley et al., 2016), the front-line drug treatment

recommended by the World Health Organization (WHO). The path to controlling and eliminating malaria is a difficult one, and the systematic emergence of drug resistant parasites against every anti-malarial drug introduced over the last century represents a major road block (Menard and Dondorp, 2017). The encouraging decrease in malaria morbidity and mortality observed in recent decades has now been reported to be slowing down, and be reversing in parts of the world (WHO|World Malaria Report, 2017). To reach the strategic objective set by the WHO to reduce global malaria incidence and mortality by at least 90% by 2030 (WHO|Global Technical Strategy for Malaria , 2016–2030), new antimalarial drugs with a novel mode of action are urgently needed.

Malaria is caused by the unicellular apicomplexan parasite *Plasmodium*. A human infection starts when an infected *Anopheles* mosquito injects parasites (in the form of sporozoites) during a blood meal. Sporozoites circulate in the blood stream and reach the liver, where they invade hepatocytes and establish an asymptomatic infection. *Plasmodium* hepatic stages replicate by schizogony, ultimately releasing tens of thousands progeny merozoites in the blood stream. Once in the blood stream, *Plasmodium* merozoites invade red blood cells, where they proliferate by schizogony in an asexual replication cycle, known as the erythrocytic cycle (**Figure 1**). The cycle begins when an extracellular merozoite invades an erythrocyte. Once intracellular, the parasite develops into a ring stage, grows into a metabolically active trophozoite, and, following DNA replication and asynchronous nuclear divisions matures into a multi-nucleated schizont. After cytokinesis, up to 32 new merozoites egress from each schizont, lysing the host red blood cell and allowing for a new cycle to begin. Alternatively, early ring stage parasites can mature into female or male gametocytes (immature sexual stage of the parasite), which, once taken up by an *Anopheles* mosquito, complete maturation and fertilization within the mosquito's gut. The resulting oocyst produces sporozoites that travel to the salivary gland of the mosquito, allowing for further transmission of the parasite. The erythrocytic stages of infection are responsible for malaria pathogenesis, whose clinical manifestations include severe anemia, organ failure and cerebral malaria (Autino et al., 2012). Among the five *Plasmodium* species that infect humans, *P. falciparum* is the most virulent. Here, we focus on host-parasite interaction mechanisms that allow the development of *P. falciparum* inside human erythrocytes (**Figure 1**).

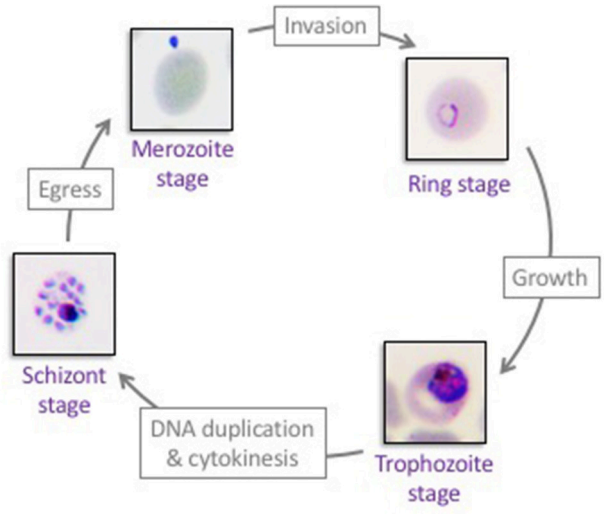

FIGURE 1 | The asexual proliferation cycle of *Plasmodium falciparum* in human erythrocytes. Extracellular merozoites invade red blood cells to establish the erythrocytic asexual cycle. Each intracellular merozoite develops into an intra-erythrocytic ring stage, matures into a trophozoite stage, and subsequently forms a multi-nucleated schizont. Forty-eight hours post-merozoite infection, 8–32 new merozoites egress from each schizont-infected erythrocyte and a new erythrocytic cycle begins. Repeated cycles of erythrocyte invasion by *Plasmodium falciparum* parasites lead to all aspects of malaria pathogenesis.

AVOIDING ANTIMALARIAL DRUG RESISTANCE BY TARGETING THE HOST CELL?

Curative antimalarials target the asexual proliferation of parasites in erythrocytes, and all antimalarial drugs developed to date directly target parasite factors. These include artemisinin (whose mechanism of action is yet to be fully understood), chloroquine (interferes with haemozoin formation, a process that detoxifies free haem released by hemoglobin digestion), atovaquone (inhibits mitochondrial respiration), proguanil/pyrimethamine (inhibits folate biosynthesis by targeting dihydrofolate reductase, PfDHFR), and various antibiotics which inhibit protein synthesis (Antony and Parija, 2016). Parasite resistance against anti-malarial drugs is a major long-standing issue, resulting in failure of many malaria eradication attempts. For instance, in 1955, the WHO launched a Global Malaria Eradication campaign, introducing Mass Drug Administration of chloroquine, the cheapest and most widely used antimalarial drug. However, in the 1960's, chloroquine resistance was reported in various South American and South-East Asian countries, and quickly spread, reaching African nations in the early 1970's (D'Alessandro and Buttiëns, 2001). Remarkably, *all* anti-malarial drugs saw resistance emerging within a couple of years of being commercialized (McClure and Day, 2014). Alarmingly, this also includes resistance against the current front-line drug, artemisinin, commonly used in combination therapies (Menard and Dondorp, 2017). Over relatively short periods of time, *Plasmodium* parasites have acquired genetic modifications, typically point mutations or copy number variations, resulting in resistance to antimalarial drugs. Such alterations have been shown to either affect the product directly targeted by the drug, or a membrane transporter, increasing the efflux of the drug to the outside environment. Such transporters are located on the plasma membrane of the parasite (e.g., multidrug resistance-associated protein, PfMRP) or on the food vacuole of the parasite (e.g., multidrug resistant protein 1, PfMDR1) (Antony and Parija, 2016).

Considering that *Plasmodium* is an obligate intracellular pathogen, and therefore relies on host cell factors to thrive, an alternative drug target strategy based on host cell factors can be envisaged. Host factors are not under the genetic control of the parasite, therefore host-directed therapy approaches bypass the most direct path to resistance, i.e., the selection of parasite genotypes encoding a mutated drug target.

For example, the host programmed cell death pathway could be targeted. Indeed, most intracellular pathogens avoid being eliminated by the immune system by "hiding" inside a host cell, while also gaining direct access to the host cell intracellular environment. Although this is highly beneficial to the pathogen, the stress induced by infection leads the host cell to trigger a cell death response or apoptosis. As a consequence, the pathogen is required to inhibit the host cell apoptotic response to ensure host cell survival until completion of its own replication cycle. In the case of *Plasmodium*, interference with host cell apoptosis has been established in the hepatic stage of infection (van de Sand et al., 2005; Kaushansky et al., 2013). However, the existence of a similar process in the erythrocytic stage of infection remains to be explored, likely because of the unique nature of the host erythrocyte cell.

RED BLOOD CELLS—A UNIQUE CELL TYPE

Maturation of erythrocyte progenitors in the bone marrow leads to the formation of enucleated reticulocytes that are released in the blood stream. Reticulocytes mature into erythrocytes, a process involving the loss of all intracellular organelles, including the nucleus, mitochondria, and endoplasmic reticulum (Lang and Föller, 2012). In the absence of *de novo* protein biosynthesis and mitochondria (which house the TCA cycle enzymes in nucleated cells), the survival and metabolism of mature erythrocytes rely exclusively on the existing pool of proteins and on glycolysis for the production of ATP (Lang and Föller, 2012). Further, a specialized function of oxygen transporter combined with a lack of organelles, have led RBCs to develop unique mechanisms of cell survival and cell death, which we outline below.

Erythrocytes Protect Themselves From Oxidative Stress

Red blood cells (RBCs) have a high haem iron content, essential for their role as oxygen and carbon dioxide transporters (Lang and Föller, 2012). For this reason, RBCs are constantly producing, and consequently exposed to, reactive oxygen species (ROS), including superoxide anion (O_2^-), hydrogen peroxide (H_2O_2) and hydroxyl radicals (OH^-) (Baynes, 2005; Cimen, 2008; Schieber and Chandel, 2014). Reactive oxygen species impose oxidative stress on the cell, due to their inherent capability to damage lipids, proteins and DNA (although the latter is irrelevant in the context of RBCs). Erythrocytes possess a number of antioxidant strategies to counteract this stress, including ROS scavengers, such as glutathione and vitamins C and E, as well as various redox enzymes such as superoxide dismutase, catalase and glutathione peroxidase (Baynes, 2005). Glutathione is a Glu-Cys-Gly tri-peptide of crucial importance to maintain the intracellular environment in a reduced state (Wu et al., 2004). The ratio between reduced glutathione (GSH) and oxidized glutathione (GSSG) is a good indicator of the cellular redox state. Glutathione is naturally most required in tissues exposed to high ROS and oxidative stress levels, such as the liver and erythrocytes (Wu et al., 2004; Lu, 2009).

How Do RBCs Die? Senescence vs. Eryptosis

Mature RBCs have a life span of ∼115 days (Franco, 2012), after which they undergo senescence, a gradual deterioration of the cell functional capacity, and clearance by the spleen. ROS accumulation has been proposed as a key life-span determinant (Hattangadi and Lodish, 2007). During this aging process, erythrocytes lose membranes through microvesiculation, become denser, intracellular enzymes display decreased activity, oxidative damages accumulate, and the membrane becomes more rigid (Lutz and Bogdanova, 2013). The Band 3 membrane protein (also called anion exchanger 1 or AE1) forms clusters (partly due to oxidation and hyperphosphorylation), that enhances deposition of complement C3 and subsequent binding of autoantibodies present in the serum, followed by clearance by macrophages (Lutz, 2004; Arese et al., 2005, p. 3; Lutz and Bogdanova, 2013). Additionally, the progressive exposure of the "eat-me" signal phosphatidylserine (PS), along with the reduced exposure of the "do-not eat-me" signal Cluster of Differentiation 47 (CD47, further discussed below), on the outside of a senescent erythrocyte further stimulate clearance by macrophages (Lutz and Bogdanova, 2013).

In addition to this type of "death by exhaustion," RBCs can undergo a form of programmed cell death throughout their lifetime. This phenomenon was first described in 2001 (Bratosin et al., 2001) and the term eryptosis was proposed in 2005 (Lang K. et al., 2005). Eryptosis shares numerous similarities with apoptosis (Bratosin et al., 2001; Lang K. et al., 2005). Both apoptosis and eryptosis share the common purpose of destruction of damaged cells without inducing an inflammatory response (i.e., absence of cell lysis). This is particularly relevant in the case of RBC death, as the release of free hemoglobin in the blood induces renal impairment and thrombosis (Tolosano et al., 1999; Buehler et al., 2012; Schaer et al., 2013). Further, eryptotic and apoptotic cells share physiological characteristics including increased intracellular calcium concentrations, cell shrinkage, exposure of phosphatidylserine on the outer cell surface and membrane ruffling and blebbing (Bratosin et al., 2001; Lang K. et al., 2005). Like apoptosis, eryptosis can be triggered by a wide range of xenobiotics some of which have been listed in **Table 1**.

Unbalanced levels of eryptosis have been proposed to play a key role in the pathology of numerous clinical disorders, including in metabolic syndrome (Zappulla, 2008), haemolytic uremic syndromes (Lang et al., 2006a), sickle-cell disease (Lang et al., 2002), thalassemia (Lang et al., 2002), and

TABLE 1 | Examples of relevant eryptosis inducers and inhibitors and their molecular targets.

	Compound	Cellular target	References
Eryptosis inducers	Amiodarone	Ion channel blocker (used for treatment of cardiac arrhythmias)	Nicolay et al., 2007
	Amphotericin B	Forms cation channels in membranes (used as an anti-fungal and anti-parasite)	Mahmud et al., 2009
	Anandamide	Cannabinoid receptor agonist; induces apoptosis in diverse cell types	Bentzen and Lang, 2007
	Aurothiomalate	Rheumatoid arthritis gold-containing drug	Sopjani et al., 2008
	Azathioprine	Induces apoptosis of lymphocytes (used as an immunosuppressive drug)	Geiger et al., 2008
	Chlorpromazine	Dopamine antagonist, anti-serotonergic and antihistaminic (used as an antipsychotic drug)	Akel et al., 2006
	Cyclosporine	Inhibits gene transcription in nucleated cells (used as an immunosuppressive drug)	Niemoeller et al., 2006
	Dimethylfumarate	Decreases intracellular GSH hence induces oxidative stress (used as an anti-inflammatory drug)	Ghashghaeinia et al., 2016
	Lead	Decreases erythrocytes ATP concentration, and activates erythrocyte K^+ channels	Kempe et al., 2005
	L-NAME	Inhibits synthase of nitric oxide (NO)	Koka et al., 2008b; Nicolay et al., 2008
	Paclitaxel	Blocks mitosis and cytoskeleton organization (used as anti-cancer drugs)	Lang et al., 2006b
Eryptosis inhibitors	Amitriptyline	Inhibits sphingomyelinase (hence ceramide production)	Brand et al., 2008; Lang et al., 2015b
	Flufenamic acid	Inhibits Cl^- sensitive and PGE_2-triggered Ca^{2+} entry	Kasinathan et al., 2007

*Compounds described as eryptosis inducers or inhibitors (see references therein), their cellular/molecular target and current use. These compounds have been further utilized in the context of malaria infections (see **Tables 3**, **4**).*

G6PD deficiency (Lang et al., 2002). The clinical relevance of red blood cell death in health and disease, has stimulated numerous studies over the last 20 years attempting to define the cellular and molecular mechanisms of eryptosis. Although much remains to be described, the section below summarizes our current knowledge of the regulatory mechanisms of eryptosis.

ERYPTOSIS—WHAT DO WE KNOW ABOUT ITS REGULATORY MECHANISMS?

Eryptosis can be triggered by various signals, including osmotic shock (Huber et al., 2001; Lang et al., 2004), energy depletion (Klarl et al., 2006), oxidative stress (Lang K. et al., 2005; Lang et al., 2014), and xenobiotics (Lang and Lang, 2015; Pretorius et al., 2016). Regardless of the trigger, induction of an eryptotic state generally involves entry of extracellular calcium ions into the cell (Lang K. S. et al., 2003), which induces changes in membrane asymmetry/exposure of PS, cell shrinkage and membrane blebbing, detailed below and summarized in **Figure 2**.

Changes in Cell Membrane Asymmetry With Phosphatidylserine Exposure

In normal conditions, the RBC lipid bilayer is asymmetric, with specific lipids predominantly present on the inner or the outer leaflet. This is the case of the phospholipid phosphatidylserine, which is mainly present within the cytosolic monolayer (Leventis and Grinstein, 2010). The asymmetry is maintained by active membrane proteins termed flippases, that translocate phosphatidylserine and other phospholipids from the outer to the inner membrane leaflet (Sharom, 2011; Segawa and Nagata, 2015). In eryptotic cells, however, high intracellular calcium concentrations lead to the inactivation of flippases (Suzuki et al., 2010, 2013), leading to the rupture of membrane asymmetry and exposure of PS on the outer leaflet of the RBC membrane (Bratosin et al., 2001; Segawa and Nagata, 2015). High intracellular calcium levels also lead to the activation of another family of membrane proteins termed scramblases that translocate phospholipids non-specifically and bidirectionally in an ATP-independent manner (Segawa and Nagata, 2015). In addition, caspase 3 can also cleave and thus irreversibly activate scramblases and inactivate flippases (Berg et al., 2001; Schoenwaelder et al., 2009; Suzuki et al., 2010), committing the cell to PS exposure. The increased and abnormal exposure of PS on the outer RBC membrane is recognized by macrophages (McEvoy et al., 1986), which remove eryptotic cells from the circulation (Boas et al., 1998). "Flippase" and "scramblase" are generic terms used to describe lipid-transport enzymatic activities. The exact proteins responsible for PS exposure during eryptosis remain to be identified.

Cell Shrinkage and Gardos Channels Activation

Increased concentration of cytosolic calcium activates calcium-sensitive potassium channels, or Gardos channels (Bookchin et al., 1987; Brugnara et al., 1993), which allow the exit of K^+ (Lang P. A. et al., 2003). The loss of intracellular K^+ hyperpolarises the cell membrane, forcing the exit of Cl^- (Lang P. A. et al., 2003). Consequently, the loss of water through osmosis leads to cell shrinkage (Lang P. A. et al., 2003). Cell shrinkage activates phospholipase A, which produces platelet-activating factor (PAF) (Lang P. A. et al., 2005). PAF in turn stimulates

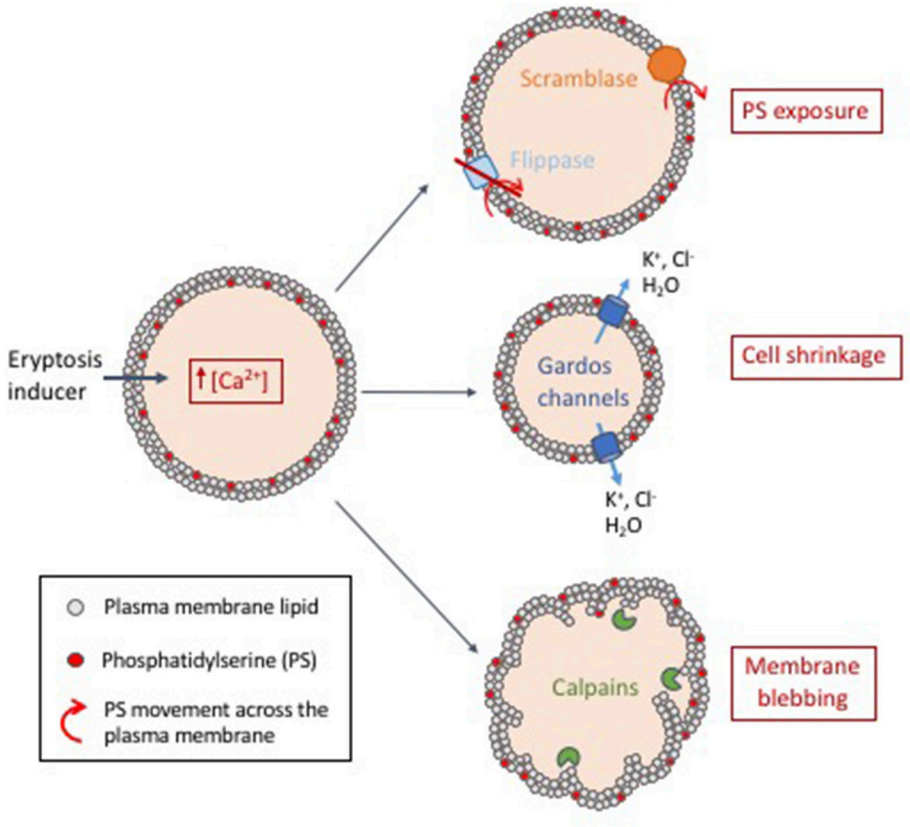

FIGURE 2 | Proposed model of eryptosis mechanisms. Induction of eryptosis (energy depletion, oxidative stress or exposure to xenobiotics) leads to an increase of intracellular calcium concentration. (i) Intracellular calcium activates scramblases (membrane proteins that transport lipids non-specifically and bidirectionally) and inactivates flippases (membrane proteins that actively maintain phosphatidylserine (PS) in the membrane inner leaflet). This leads to exposure of PS at the surface of the cell, a signal that is recognized by macrophages, which then mediate clearance of eryptotic cells. (ii) Intracellular calcium activates calcium-sensitive potassium channels known as Gardos channels. This is followed by exit of potassium and chlorine, leading to loss of water by osmosis and subsequent cell shrinkage. (iii) Increased concentration of free intracellular calcium activates calpains (calcium-activated proteases). Calpains degrade cytoskeleton proteins which leads to membrane ruffling and blebbing.

sphingomyelinase, an enzyme that breaks down sphingomyelin (Lang P. A. et al., 2005), the most prevalent sphingolipid in the cell membrane (Barenholz and Thompson, 1980). This leads to the formation of ceramide, a well-known inducer of eryptosis (Lang et al., 2004) and apoptosis (Dbaibo et al., 1997; Birbes et al., 2002). The role of ceramide in eryptosis has been review by Lang et al. (2015b).

Membrane Blebbing and Calpain Activation

Increased intracellular calcium concentration leads to the activation of calpains (Berg et al., 2001), a family of cytosolic calcium-dependent thiol proteases. Calpains I (or μ-calpains) are activated by micromolar amounts of calcium, whereas activation of calpains II (or M-calpains) requires millimolar amounts of calcium (Perrin and Huttenlocher, 2002). Activated calpains target RBC cytoskeleton proteins, such as spectrin, actin, and band 3/AE1 (Murachi et al., 1981; Schwarz-Ben Meir et al., 1991), whose degradation ultimately leads to ruffling and blebbing of the RBC membrane (Larsen et al., 2008).

Depending on the eryptotic trigger, different pathways can be activated. For instance, eryptosis due to oxidative stress seems to activate caspases (Matarrese et al., 2005), although there is some controversy about the activity of caspases in RBCs (Berg et al., 2001). Interestingly, it has been observed that not all erythrocytes have the same sensitivity to oxidative stress-induced eryptosis, differences being attributed to age and oxidative stress "history" of the cell (Ghashghaeinia et al., 2012). Eryptosis triggered by energy depletion has been shown to involve a number of kinases—further discussed below—as well as an impairment in antioxidant glutathione (GSH) replenishment, which requires energy (Tang et al., 2015).

Although some of the mechanisms leading to eryptosis have been described, the molecular players and signaling pathways underpinning eryptosis remain yet to be fully characterized. So far, a few key regulators of classical apoptotic pathways, protein kinases and "death" receptors have been suggested as putative molecular regulators of eryptosis and are summarized in the next section.

MOLECULAR REGULATORS OF ERYPTOSIS

Death or apoptotic proteins, protein kinases and cell surface receptors are proposed to have a role in the execution or the inhibition of eryptotic pathways. The section below (and **Table 2**) summarizes available information on such molecular regulators of eryptosis, and highlights the many gaps in knowledge that remain to be filled.

Apoptotic Proteins Involved in Erythrocyte Survival

Many cell death proteins are present in mature RBCs, including members of the BCL-2 family such as the pro-apoptotic proteins BAD, BID, BCL10, BAK, BAX, and the anti-apoptotic protein BCL-X_L (Walsh et al., 2002; Roux-Dalvai et al., 2008; Lange et al., 2014). These proteins play crucial roles in mitochondria-dependent apoptosis, and are key gatekeepers of viability in nucleated cells.

In healthy nucleated cells, pro-survival BCL-X_L and BCL-2 sequester BAX and BAK, while pro-apoptotic BAD is sequestered in a phosphorylation-dependent manner by protein 14-3-3 to repress apoptosis. When apoptotic signals overcome survival signals, the phosphorylation status of BAD changes, causing its release from 14-3-3 and binding to pro-survival BCL-X_L and BCL-2, unleashing the apoptotic pore forming BAK and BAX. Perforation of the mitochondrial outer membrane commits the cell to apoptosis: cytochrome c is released, an apoptosome is formed, and effector caspases are activated, ultimately leading to DNA fragmentation, PS exposure and membrane blebbing.

BCL-X_L is known to be crucial during haematopoiesis and is particularly strongly expressed during the late stages of erythroblasts maturation (Gregoli and Bondurant, 1997), while expression of BAX and BAK decreases during development of erythroid lineage cells (Gregoli and Bondurant, 1997). In reticulocytes (immature erythrocytes containing a mitochondrion), inhibition of BCL-X_L leads to caspase-dependent apoptosis (Delbridge et al., 2017). Similarly, the interaction between BCL-X_L and BAK in the plasma membrane is required for the survival of mature RBCs (which lack mitochondria) (Walsh et al., 2002). Indeed, rupture of this interaction using a BAK-mimetic small molecule (resulting in the release of BAK) increases intracellular calcium concentrations and induces PS exposure (Walsh et al., 2002). Interestingly, eryptosis induction through this pathway is inhibited by the addition of serum, suggestive of a key role for serum survival factors in erythrocyte viability. Nevertheless, the role of death proteins within mature erythrocytes, if any, remains to be investigated.

Protein Kinases Involved in Eryptosis

Phosphorylation is a key regulatory mechanism of all intracellular processes, including apoptosis in nucleated cells. Noteworthy, phosphorylation and other post-translational modifications are possibly even more important in mature erythrocytes, as these cells cannot synthesize *de novo* proteins. Accordingly, numerous protein kinases have been shown to regulate eryptosis. Some, including CK1α, p38 MAP kinase, PKC, and JAK3, stimulate eryptosis; others, such as AMPK, cGKI, PAK2, Raf kinase, and MSK1/2, inhibit this process. The section below summarizes the currently knowledge regarding the mechanisms by which these kinases stimulate or inhibit eryptosis in mature RBCs (also see **Table 2**).

Eryptosis Stimulator: Casein Kinase 1

Casein kinase 1 (CK1) is a serine/threonine protein kinase with seven isoforms in humans, and plays a role in very diverse cellular processes, including cell cycle, gene expression, cytoskeleton modifications, cell adhesion, and modulation of receptor-mediated signaling (Schittek and Sinnberg, 2014). In the context of apoptosis in nucleated cells, CK1α phosphorylates BCL10, BID and Fas-associated death domain (FADD, further described below) (Schittek and Sinnberg, 2014). In RBCs, stimulation of CK1α enhances eryptosis following energy depletion, oxidative stress and osmotic shock (Kucherenko et al., 2012; Zelenak et al., 2012). Conversely, CK1α inhibition blunts eryptosis in these same conditions.

Eryptosis Stimulator: p38 MAP Kinase

p38 mitogen-activated protein kinase (p38 MAPK) is activated by diverse stimuli, such as UV light, heat, osmotic shock and cytokines (Zarubin and Han, 2005). In the context of apoptosis, p38 MAP kinase can have pro- and anti-apoptotic roles depending on the cell type and on the stimulus. In RBCs, p38 MAP kinase is phosphorylated upon osmotic shock, and participates in calcium uptake, PS exposure and cell shrinkage (as p38 MAP kinase inhibition blunts these effects) (Gatidis et al., 2011).

Eryptosis Stimulator: Protein Kinase C

Protein Kinase C (PKC) molecules constitute a family of eight serine/threonine protein kinase isoforms that are activated upon increase of Ca^{2+} and diacylglycerol (Mochly-Rosen et al., 2012). Upon activation, PKC is recruited to the membrane where it phosphorylates its substrates. PKC can regulate an important number of processes, including gene expression, protein secretion, cell division and inflammation (Mochly-Rosen et al., 2012). In RBCs, activation of PKC leads to increased calcium intake, cell shrinkage and PS exposure, whereas PKC inhibition prevents calcium entry and PS exposure (Andrews et al., 2002; de Jong et al., 2002). Furthermore, glucose depletion induces PKCα translocation to the membrane, significantly increasing PKC activity and phosphorylation of membrane proteins (Klarl et al., 2006). Interestingly, PS exposure following energy depletion was blunted with PKC-specific inhibitors (Klarl et al., 2006), consistent with a direct role of PKC on PS exposure.

Eryptosis Stimulator: Janus Kinase 3

Janus kinase 3 (JAK3) is a cytosolic tyrosine kinase, part of the larger JAK family, which includes JAK1, JAK2, and TYK2. All Janus kinases play a role in signaling triggered by extracellular cytokines and growth factors. Typically, upon binding of a cytokine to its receptors, the receptors multimerize, specific JAK kinases are recruited to the receptor cytosolic domain, and trans-phosphorylate (Rawlings et al., 2004). Janus kinases

TABLE 2 | Molecular regulators of eryptosis.

	Protein	Proposed role in eryptosis	References
Apoptotic proteins	BCL-X_L/BAK	**Anti-eryptotic** effect observed when BCL-X_L/BAK complex detected at the plasma membrane and in the absence of serum	Walsh et al., 2002
Kinases	Casein Kinase 1	**Pro-eryptotic**	Kucherenko et al., 2012; Zelenak et al., 2012
	p38 MAP Kinase	**Pro-eryptotic** Phosphorylated upon osmotic shock	Gatidis et al., 2011
	Protein Kinase C	**Pro-eryptotic** Translocates to the membrane upon absence of glucose Direct role on PS exposure	Andrews et al., 2002; de Jong et al., 2002; Klarl et al., 2006
	Janus Kinase 3	**Pro-eryptotic** Phosphorylated/Activated in the absence of glucose	Nosaka et al., 1995; Bhavsar et al., 2011
	AMP-activated Kinase	**Anti-eryptotic** In the absence of glucose	Föller et al., 2009b ; Wang et al., 2010
	cGMP-dependent Kinase I	**Anti-eryptotic**	Föller et al., 2008
	p21-Activated Kinase 2	**Anti-eryptotic** In the absence of glucose	Zelenak et al., 2011
	Raf Kinase	**Anti-eryptotic**	Lupescu et al., 2012
	Mitogen and Stress activated Kinase 1 and 2	**Anti-eryptotic** During hyperosmotic shock and in the absence of glucose	Lang et al., 2015a
Receptor-mediated eryptosis	Glycophorin-C receptor	**Pro-eryptotic** Stimulation leads to PS exposure and hemolysis	Head et al., 2005a
	CD47 receptor	**Pro-eryptotic** Upon conformational change due to oxidative stress or aging Stimulation leads to PS exposure and hemolysis	Head et al., 2005b; Burger et al., 2012
	CD94/Fas receptor	**Pro-eryptotic** Upon oxidative stress (or aging), Fas receptors, Fas ligands, FADD and caspase 8 accumulate within lipid rafts	Mandal et al., 2005

Molecular modulators of eryptosis published to date. For each factor, their suggested role in eryptosis is indicated. Further investigation is required to confirm involvement in eryptosis and elucidate the exact mechanisms of action.

substrates include STATs (signal transduction and activators of transcription) which then enter the nucleus and regulate transcription. Of relevance, JAK/STAT signaling is crucial for haematopoiesis and JAK3 is predominantly expressed in haematopoietic cells (Nosaka et al., 1995, p. 3). In RBCs, following glucose depletion, JAK3 is phosphorylated on the activating Tyrosine 980 (Nosaka et al., 1995, p. 3). Further, inhibition of JAK3 (or absence of JAK3 in the case of *jak3*$^{-/-}$ mice) blunts the exposure of PS upon glucose depletion, but has no effect on cell size (Bhavsar et al., 2011). Overall, JAK3 is thought to be implicated in membrane scrambling upon energy depletion.

Eryptosis Inhibitor: AMP-Activated Kinase

AMP-activated kinase (AMPK) is a serine/threonine kinase that is activated by adenosine monophosphate (AMP) and plays a crucial role in energy homeostasis. Increased concentration of AMP (and a decrease in ATP concentration) is an indication of energy depletion. Upon activation, AMPK switches on catabolic processes that produce ATP, such as glycolysis, and switches off anabolic pathways that consume ATP, such as lipogenesis. Interestingly, mice lacking the AMPK subunit α exhibit erythrocytes with a shorter lifespan compared to their wild-type counterpart (Wang et al., 2010). Additionally, inhibition of AMPK exacerbates eryptosis phenotypes induced by glucose depletion: in an energy depletion context, inhibition of AMPK further increases PS exposure and intracellular calcium, suggesting a role of AMPK in protecting against eryptosis (Föller et al., 2009b).

Eryptosis Inhibitor: cGMP-Dependent Kinase I

cGMP-dependent protein kinase I (cGKI) is a serine/threonine kinase activated by cyclic guanosine monophosphate (cGMP), and is implicated in calcium regulation, platelet activation and many other processes (Butt et al., 1994). Noteworthy, mice lacking cGKI display increased levels of eryptosis, as detected by elevated PS exposure, faster RBC clearance and a higher rate of RBC turnover (Föller et al., 2008).

Eryptosis Inhibitor: p21-Activated Kinase 2

The p21-activated kinase (PAK) family of serine/threonine kinases comprises 6 members in humans. PAK1, 2 and 3 are effector kinases of the Rho-GTPase CDC42 and Rac, two key cytoskeletal regulatory proteins. PAK2 can also be activated by proteolytic cleavage by caspase 3 during apoptosis (Rane and Minden, 2014). In erythrocytes, PAK2 inhibition leads to PS exposure in the absence of glucose, an effect not exacerbated

by the absence of AMPK (*ampk* knock-out mice), suggesting that both these enzymes are acting within the same pathway (Zelenak et al., 2011). Overall AMPK and PAK2 appear to have a pro-survival role during energy depletion.

Eryptosis Inhibitor: Raf Kinase

The Rapid accelerated fibrosarcoma (Raf) kinase family of serine/threonine kinases comprises 3 members that act upstream of mitogen-activated protein kinase (MAPK) pathways: A-Raf, B-Raf, and C-Raf. Typically, growth factor receptors activate the Ras GTPase, which activates Raf, which in turn phosphorylates MEK, leading to activation of ERK (Matallanas et al., 2011). Raf is implicated in apoptosis, and a specific inhibitor, Sorafenib, has been developed for cancer treatment (Wilhelm et al., 2004). In erythrocytes, inhibition of Raf with Sorafenib leads to eryptosis, suggesting a protective role of Raf against eryptosis (Lupescu et al., 2012).

Eryptosis Inhibitor: Mitogen and Stress Activated Kinase 1 and 2

MSK1 and MSK2 are serine kinases involved in the MAPK cascade. Once activated by ERK1 and 2, they phospho-activate transcription factors, which then promote cellular proliferation (Wiggin et al., 2002, p. 1). Mice lacking MSK1/2 present a higher turnover of erythrocytes (Lang et al., 2015a). Although in normal conditions, the levels of PS exposure were similar compared to their wild-type counterpart, when MSK1/2-deficient erythrocytes were stressed with hyperosmotic shock or energy depletion, eryptosis (as indicated by PS exposure and cell shrinkage) was significantly enhanced.

Although numerous protein kinases have been shown to be involved in eryptosis, the mechanisms leading to their activation, as well as the specific downstream effectors, are yet to be identified. This represents an important gap in knowledge in the field that requires further investigation.

Receptor-Mediated Eryptosis

The third category of molecular regulators of eryptosis encompasses cellular receptors that have the ability to transform extracellular signals into an intracellular cell death cascade. Indeed, similar to apoptosis of nucleated cells, eryptosis can be triggered upon the binding of specific extracellular ligands to various red blood cell surface receptors. RBC receptors that have been shown to trigger eryptosis include glycophorin-C, CD47, and CD95/Fas. We are yet to fully understand the links between activation of these surface receptors and the trigger of eryptosis; and this section summarizes the current knowledge of receptor-mediated eryptosis activation (also see **Table 2**).

Glycophorin-C Receptor

Glycophorin-C (GPC) is an important membrane glycoprotein that interacts with the membrane skeleton and plays a role in the maintenance of the shape of the erythrocyte (Tanner, 1993). Interestingly, it has been reported that binding of anti-GPC antibodies leads to PS exposure and hemolysis (Head et al., 2005a).

CD47 Receptor

Cluster of Differentiation 47 (CD47) is a transmembrane protein that has long been described as a "don't eat-me" signal directed toward the macrophage receptor SIRPα (Oldenborg et al., 2000, p. 47). However, recent studies indicate that CD47 can switch to an "eat-me" signal in aging and oxidative-stressed erythrocytes (Burger et al., 2012, p. 47). Indeed, oxidative stress induces a conformational change of CD47 which, despite retaining binding to the same macrophage SIRPα receptor, will under these conditions induce phagocytosis (Burger et al., 2012). Interestingly, induction of CD47 signaling through binding of its TSP-1 ligand, as well as anti-CD47 antibodies and a specific CD47-binding peptide, trigger PS exposure and hemolysis of RBCs (Head et al., 2005b).

CD94/Fas Receptor

Fas receptor (or CD94 or APO-1) is a well-studied death receptor in the context of apoptosis and other programmed cell death pathways (Schulze-Osthoff et al., 2001). Upon binding of the Fas ligand FasL (either as transmembrane proteins on cytotoxic T lymphocytes, or as soluble proteins) to the Fas receptors on the target cell, the latter form death-inducing signaling complexes (DISC). Aggregation of Fas receptors allows the recruitment of proteins that carry Fas-associated death domain (FADD), leading to the recruitment and activation of caspase 8. Caspase 8 in turn can cleave, and hence activate, BID (with subsequent mitochondria-dependent apoptosis activation) and/or directly activate effector caspase 3. Mandal et al. (2005) showed that Fas receptors, Fas ligands, FADD and caspase 8 accumulate within lipid rafts in old erythrocyte membranes, as well as in oxidative-stressed erythrocytes. Caspase 8 is activated in both old and oxidative-stressed erythrocytes, followed by activation of caspase 3 and reduced activity of flippases (and hence increased PS exposure).

STUDYING ERYPTOSIS: THE TOOLS OF THE TRADE

As emphasized above, the molecular events leading to eryptosis remain largely unknown. A number of challenges, inherent to the specific cell type we are considering, explain this gap in knowledge. A key step toward further dissecting the molecular mechanisms of eryptosis relies on robust technical approaches. However, cell death detection techniques relying on nuclear DNA fragmentation or mitochondrial activity cannot be used in this context, for obvious reasons. Nevertheless, a key phenotypic hallmark of eryptosis (and apoptosis) is the cell surface exposure of phosphatidyl serine, which allows flow cytometry to be a key technique commonly used to detect and quantify eryptosis. The binding of fluorescent Annexin V to externalized PS and the cell volume (measured via forward scatter values) are the most common parameters used to assess eryptosis. Additionally, intracellular calcium concentrations can be measured with cell-permeable fluorescent indicators, such as Fluo-3 AM dye.

Intracellular ceramide levels can be detected with ceramide-specific antibodies, and the redox state of the cells can be assessed through measurement of GSH/GSSG ratio (reviewed in Pretorius et al., 2016; Jemaà et al., 2017).

Another key hurdle is the study of the RBC proteome given the overwhelming relative amounts of the two most abundant proteins: hemoglobin represents 97% of RBCs' total proteins, and carbonic anhydrase I 1% (Barasa and Slijper, 2014). This implies that all other proteins are present in a much lower relative abundance, and therefore difficult to identify and quantify.

At the genetic level, as RBCs are enucleated, experiments requiring genetic manipulations aimed at investigating the role of specific genes in eryptosis cannot be conducted. However, recent advances in *in vitro* stem cell culture and haematopoietic lineage differentiation, as well as advances in genome editing, offer exciting perspectives to address a number of these issues in the near future (Hockemeyer and Jaenisch, 2016; Caulier et al., 2017). For example, with major advances in *in vitro* stem cell differentiation methods being made, *in vitro* production of large amounts of human mature erythrocytes for transfusion could become a reality (Lapillonne et al., 2010; Caulier et al., 2017). Further, genetic manipulation of stem cells, followed by maturation into erythrocytes, would allow the investigation of molecular events and signaling pathways essential for mature erythrocyte survival. This has indeed been recently explored in the context of indirect areas of RBC research, notably with respect to infection of RBCs with malaria parasites (Egan, 2017; Kanjee et al., 2017).

Finally, other challenges to the study of eryptosis (and erythrocytes in general) include RBC origin, availability, purification, storage conditions and the lack of well-characterized cell lines.

PLASMODIUM-INFECTED ERYTHROCYTES: A FIGHT BETWEEN LIFE AND DEATH

It is well documented that many pathogens manipulate (i.e., inhibit) the apoptotic pathway of their host cell in order to achieve intracellular survival (viruses: Hay and Kannourakis, 2002; parasites: James and Green, 2004; bacteria: Ashida et al., 2011). In the case of malaria parasites, this has been demonstrated during the infection of liver cells (van de Sand et al., 2005). However, little is known about host-parasite interactions of the erythrocytic stages of infection. Unraveling the molecular regulation of eryptosis is key to our understanding of the interrelationship between *Plasmodium* parasites and their host red cell. *Plasmodium* imposes oxidative stress and induces phosphatidylserine exposure on the host red blood cells, but the clinical outcome arising from PS-exposing *Plasmodium*-infected RBCs is debated. In the context of the tools currently available to study eryptosis, this section reviews published evidence and proposed models that attempt to characterize the interplay between *Plasmodium* and host RBC death mechanisms (also see **Figure 3**).

Plasmodium Imposes Oxidative Stress on Its Host Cell

During the 48h of its erythrocytic asexual cycle, *Plasmodium falciparum* increases its body mass by up to 32-fold. This requires a considerable supply of nutrients, which the parasite obtains from the digestion of hemoglobin (Zarchin et al., 1986). The ensuing generation of H_2O_2 and OH radicals imposes oxidative stress on the host cell (Atamna and Ginsburg, 1993; Ginsburg and Atamna, 1994), which, as discussed above, can lead to erythrocyte's death, which would represent a non-favorable outcome for the parasite (**Figure 3**).

Extensive Digestion of Hemoglobin Prevents Bursting of the Host Cell

In addition to the nutrients provided by hemoglobin degradation, parasite survival further relies on the import of nutrients and metabolites from the extracellular milieu, and on a mechanism of waste disposal to the extracellular environment (Kirk, 2001). For this purpose, *Plasmodium* exports parasite encoded transporters to the red cell membrane known as the New Permeability Pathways (NPP) transporters (Kirk, 2001; Huber et al., 2005). Consequently, during trophozoite development, extensive changes take place on the red cell membrane, leading to a dramatic decrease in K^+, and increase in Na^+ concentrations in the host cell cytosol to levels resembling those of the extracellular space (Kirk, 2001). The increased cytosolic Na^+ concentration poses a risk of cell swelling and hemolysis. To prevent this and ensure osmotic stability, the parasite decreases the intracellular colloid osmotic pressure by digesting more hemoglobin than metabolically needed, and exports the excess of amino acids through the NPP transporters, consequently reducing cell swelling and decreasing risks of hemolysis (Lew et al., 2003) (**Figure 3**).

Plasmodium Might Sequester Intracellular Calcium to Delay Host Cell Death

In normal conditions, erythrocytes maintain low intracellular Ca^{2+} levels, corresponding to a concentration that is $\sim$ 40,000-fold lower than that of free-Ca^{2+} in the blood plasma (Bogdanova et al., 2013). However, upon *P. falciparum* infection, the erythrocyte's calcium content increases by 10- to 20-fold (Kirk, 2001). Intracellular calcium is crucial for parasite invasion and development (Wasserman et al., 1982) and is thought to be key for many parasite signaling pathways (Enomoto et al., 2012). Interestingly, an increase of free Ca^{2+} in the RBC cytosol is not observed during infection; it is thought that *Plasmodium* accumulates Ca^{2+} in its own cytosol to maintain a low level of free Ca^{2+} in the host cell (Adovelande et al., 1993; Tiffert et al., 2000) (**Figure 3**). Ca^{2+} sequestration inside the parasite is thought to delay eryptosis, however direct measurements of *in vivo* calcium concentrations in the parasite are required to formally determine whether this is the case. Interestingly, during the liver stage of infection *Plasmodium* sequesters intracellular calcium from hepatocytes, therefore preventing/delaying PS exposure (Sturm et al., 2006). Noteworthy, calcium sequestration mechanisms

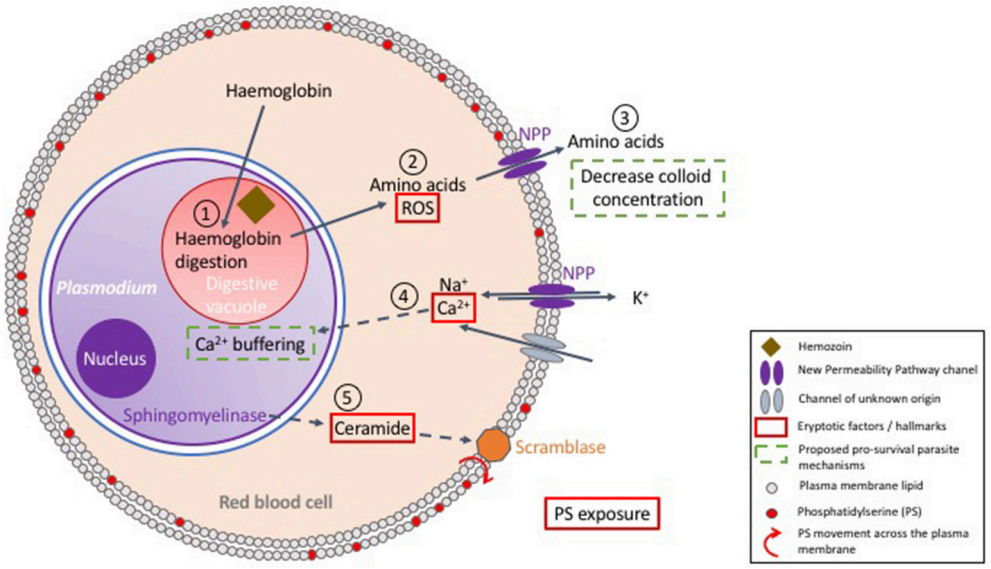

FIGURE 3 | Proposed model of the interactions between *Plasmodium* and its host red blood cell. Upon erythrocyte invasion, *Plasmodium* digests host cell hemoglobin in its digestive vacuole (1). In this process, heme is detoxified by polymerisation into hemozoin and amino acids are utilized for parasite development. The surplus of amino acids is exported to the RBC cytosol (2), and further secreted to the extracellular milieu to decrease colloid concentration (3), which is proposed to enhance survival of the host cell. Digestion of hemoglobin also produces reactive oxygen species (ROS) (2), which enhances eryptosis. New Permeability Pathways (NPPs) and/or other transporters allow Ca^{2+} entry into the red cell cytosol, a key player in triggering eryptosis (4). However, it has been suggested that *Plasmodium* uptakes most of the intracellular calcium in its own cytosol, thus achieving delay of host cell death (4). Nevertheless, active parasite sphingomyelinase has been proposed to break down sphingomyelin, producing ceramide (5), which enhances exposure of phosphatidylserine (PS), and hence recognition and clearance by macrophages.

of erythrocytic stages, if demonstrated, would likely be considered one of the basic foundations for parasite-manipulated eryptosis.

Increased Phosphatidylserine Exposure During Infection

Despite the fact that *Plasmodium* is proposed to control the levels of free Ca^{2+} in the RBC cytosol, an increase in PS exposure is observed in *Plasmodium*-infected RBCs (iRBCs) when compared to uninfected erythrocytes (uRBCs) (Schwartz et al., 1987). This has been observed not only *in vitro* with *P. falciparum* infection of human RBCs (Schwartz et al., 1987), but also *in vivo* in animal models of malaria infection, such as *P. yoelii* infection of mice (Totino et al., 2010) and *P. knowlesi* infection of monkeys (Joshi et al., 1987). Overall, PS-exposure tends to increase in the mature stages of parasite development (Joshi et al., 1987; Schwartz et al., 1987). A possible explanation for this phenomenon involves the formation of ceramides, a component of sphingomyelin, one of the major structural lipids of cell membranes. Hydrolysis of sphingomyelin, catalyzed by sphingomyelinase, generates ceramide, which, in erythrocytes, leads to PS exposure (see above) even at low cytosolic Ca^{2+} concentrations (Lang et al., 2004) (see **Figure 3**). Interestingly, erythrocytic forms of *P. falciparum* express a sphingomyelinase that is active during blood stages (Hanada et al., 2000). In line with this observation, a marked decrease of the sphingomyelin content is observed in RBC membranes upon infection by *P. falciparum* (Maguire and Sherman, 1990). Besides the role of ceramide in PS-exposure during infection, it is also interesting that GPC (an erythrocyte receptor able to mediate eryptosis) is used by *P. falciparum* to invade RBCs (Maier et al., 2003), and it has been suggested that this could be the trigger for PS exposure during early stages of parasite development (Head et al., 2005a).

Overall, *Plasmodium* induces eryptosis in the infected cell, by imposing oxidative stress, possibly by producing ceramide, activating GPC-pathways and modulating the erythrocyte intracellular ionic composition. At the same time, *Plasmodium* might also prevent / delay eryptosis and hemolysis by sequestering calcium, and exporting amino acids to the extracellular milieu, as summarized in **Figure 3**. A balance between induction and prevention (or delay) of eryptosis of the host cell by *Plasmodium* is likely to translate into a successful vs. unsuccessful infection. Although this appears key to our understanding of the clinical outcomes of malaria infections, much is yet to be uncovered in this area.

PLASMODIUM INDUCES ERYPTOSIS OF BYSTANDER ERYTHROCYTES

Further to the eryptosis that *Plasmodium* induces on its own infected cell, it has been observed that malaria infection induces eryptosis of bystander uninfected erythrocytes. In a study using a rodent malaria model, increased numbers of eryptotic uRBCs have been observed in mice 6–7 days post-infection with *P.*

yoelii (Totino et al., 2013). Similarly, incubation of human RBCs with serum from patients infected with *P. falciparum* leads to increased PS exposure and decreased cell size of uRBCs (Totino et al., 2014), suggesting that *P. falciparum* is able to induce cell death of non-infected erythrocytes. Interestingly, this has not been observed in the case of *P. vivax* infections, so one cannot exclude that the proinflammatory response common in *P. falciparum* infections, but not in *P. vivax* infections, could be at least partially responsible for this observation (Totino et al., 2014). Further, another *in vitro* study where the role of proinflammatory responses cannot be taken into account, suggests the increase of PS exposure on bystander uRBCs is partially attributed to the presence of methaemoglobin in the extracellular medium. Methaemoglobin is a form of hemoglobin, in which the iron in the heme group is in the Fe^{3+} (ferric) state, not the Fe^{2+} (ferrous) of normal hemoglobin. Upon RBC lysis, hemoglobin is released and oxidized by oxygen to methaemoglobin, which in turn leads to PS exposure of bystander RBCs through oxidative stress (Balaji and Trivedi, 2013). Overall, increased eryptosis of uRBC is thought to be a major contributor of anemia observed during severe malaria infections (Jakeman et al., 1999; Totino et al., 2016), alongside the loss of iRBCs and decreased erythropoiesis (Pathak and Ghosh, 2016). Consequently, a full understanding of the molecular events leading to eryptosis of bystander uRBCs during a malaria infection is crucial to comprehensively address the clinical symptoms of severe anemia in malaria patients.

A CONTROVERSIAL ROLE OF ERYPTOSIS DURING MALARIA INFECTION—IS IT GOOD OR BAD?

While it has been established that *Plasmodium* infection contributes to eryptosis of the host cell, the clinical benefit of the phenomenon is debated. On one hand it is argued that PS-mediated clearance of infected cells is favorable to the host. On the other hand it is argued that PS exposure contributes to parasite immune evasion and malaria pathogenesis. This section summarizes the studies that have led to such observations.

Phosphatidylserine Exposure of *Plasmodium*-Infected Erythrocytes Implicated in Severe Disease

It has been argued that PS exposure of iRBCs may play a role in the cytoadherence of *P. falciparum* and enhance tissue sequestration of *P. vivax* (Eda and Sherman, 2002; Totino and Lopes, 2017). Adherence of PS-exposing RBCs to endothelial cells has been demonstrated to occur in various medical conditions and in *in vitro* experiments (Wali et al., 1988; Closse et al., 1999; Bonomini et al., 2002; Setty et al., 2002; Wautier et al., 2011). Therefore, it is plausible that exposure of PS in *Plasmodium*-infected RBCs contributes to adherence and sequestration, as well as to cell aggregation and rosetting (Ho et al., 1991). Consequently, increased PS exposure of iRBCs has two major detrimental effects for malaria patients: sequestered and adherent *Plasmodium*-iRBCs avoid immune clearance; and adherence to the endothelium and other cells induces thrombo-occlusion, which leads to severe disease. Both these events are well characterized in the case of *P. falciparum* infections, and have been to date mainly attributed to the cell surface exposure of PfEMP1, a parasite-derived molecule. Interestingly, in the case of *P.* vivax (which do not express PfEMP1), PS exposure might lead to a more severe course of infection, and there is some evidence that *P. vivax*-iRBCs are able to adhere to endothelial walls and to rosette, due at least in part to phosphatidylserine exposure (Costa et al., 2011; Totino and Lopes, 2017).

Does Phosphatidylserine Exposure of *Plasmodium*-Infected Erythrocytes Benefit Disease Outcome?

Despite the data discussed above suggesting that PS exposure in iRBCs is beneficial to parasite survival, two studies propose that eryptosis of *Plasmodium*-infected RBCs is beneficial for the outcome of malaria infection. One study has shown that *P. falciparum* preferentially invades non-eryptotic RBCs (Totino et al., 2010), therefore eryptosis of uninfected RBCs has been interpreted as "a host mechanism to fight malaria" (Totino et al., 2010). The decreased susceptibility of infection of eryptotic cells may in part be attributed to cytoskeleton changes in the host cell (Totino et al., 2010), since actin, spectrin and band 3 proteins, which are crucial for invasion by the parasite (Koch and Baum, 2016), are degraded during eryptosis (Murachi et al., 1981; Schwarz-Ben Meir et al., 1991). In this case, enhanced eryptosis is suggested to correlate with lower parasite burden. Another study proposed that PS-based clearance of ring stage-iRBCs prevents the formation of late-stage parasites, and hence sequestration and associated clinical complications (Föller et al., 2009a). The authors suggest that this may be part of the mechanisms leading to the relative protection against severe malaria in sickle-cell trait, homozygous hemoglobin-C and G6PD-deficiency (Cappadoro et al., 1998; Ayi et al., 2004).

INDUCING ERYPTOSIS TO TREAT MALARIA?

Following from the idea that increased PS exposure of *Plasmodium*-infected RBCs benefits clearance and therefore disease outcome, numerous studies have assessed the effect of eryptosis modulators in the context of malaria. In the section below (and in **Tables 2**, **3**), we summarize the studies that have attempted to date to induce or inhibit eryptosis with the aim of modulating malaria infection, and we further discuss the limitations of such approaches.

The Effect of Eryptosis Modulators on the Course of a Malaria Infection

Given the interrelationship between malaria and eryptosis, numerous studies have assessed the effect of eryptosis modulators

TABLE 3 | Effect of eryptosis inducers and inhibitors on *P. falciparum in vitro* development.

	Compound	Eryptosis		Parasitemia decrease	References
		uRBC	iRBC		
Eryptosis inducers	Amiodarone* 10 μM	ns	↗	60%	Bobbala et al., 2010b
	Amphotericin B* 5 μM	ns	↗	90%	Siraskar et al., 2010
	Aurothiomalate* 50 μM	ns	↗	29%	Alesutan et al., 2010
	Azathioprine* 1 μM	ns	↗	11%	Bobbala et al., 2009
	Anandamide* 50 μM	ns	ns	70%	Bobbala et al., 2010a
	Chlorpromazine 10 μM	↗	↗	75%	Koka et al., 2008a
	Cyclosporine	↗ 0.01 μM	↗ 0.001 μM	33% 0.01 μM	Bobbala et al., 2008
	Paclitaxel	↗ 0.1 μM	↗ 0.001 μM	10% 0.01 μM	Koka et al., 2009
	Lead	↗ 5 μM	↗ 1 μM	ns up to 100 μM	Koka et al., 2007
	L-NAME 10 μM	↗	↗	ns up to 100 μM	Koka et al., 2008b
Eryptosis inhibitors	Amitriptyline* 50 μM	ns	↘	90%	Brand et al., 2008
	Flufenamic acid* 25 μM	ns	↘ Early stages	19%	Kasinathan et al., 2007

*Eryptosis features of infected red blood cells (iRBC) and bystander uninfected red blood cells (uRBC), as well as parasitemia were measured after 24 or 48 h of treatment with each compound. For clarity purposes, the eryptosis phenotype observed is based only on reported PS exposure measurements. Although not represented in the table, PS exposure of iRBCs was significantly superior to that of uRBCs in all studies. "Parasitemia decrease" indicates the decreased percentage in parasitemia of treated cultures when compared to the untreated control at a given compound concentration (value calculated based on data provided in the original publication). Compounds previously described as inducers or inhibitors or eryptosis (see **Table 1**) but which do not induce a significant increase or decrease in eryptosis of uRBC in the indicated studies are represented by *. Flufenamic acid induced a decrease of PS exposure of RBC infected with early stage parasites only. ns, not significant; ↗, significant increase of PS exposure compared to untreated control; ↘, significant decrease of PS exposure compared to untreated control.*

in the context of malaria (**Tables 2**, **3** and references therein). Interestingly, various compounds described to induce or inhibit eryptosis in naïve RBCs (**Table 1**) fail to modulate eryptosis in bystander uRBCs of a *Plasmodium* culture (**Table 3**, compounds indicated by *). This discrepancy can be attributed to differences between naïve RBCs and *Plasmodium in vitro* culture conditions. Indeed, eryptosis of naïve RBCs is assessed in Ringer solution at 0.4% haematocrit (see references of **Table 1**), whereas eryptosis of *Plasmodium* cultures is assessed in complete RPMI medium at 4% haematocrit (see references of **Table 3**). Noteworthy, all but one of the eryptosis inducers tested on malaria parasites (regardless of their ability to induce eryptosis on bystander uRBCs), induce eryptosis of *Plasmodium*-infected RBCs, often at a lower concentration than the one required to induce eryptosis of uRBCs. Further, most of the compounds presented in **Table 3** somehow affect parasite viability albeit at variable (and in some cases high) concentrations. Together, these observations provide the main argument in favor of the use of eryptosis inducers as anti-malarial treatments, particularly for those compounds where uRBCs remain unaffected at the concentrations required to affect infected cells. Similar observations were made when using *in vivo* mouse malaria models of infection (**Table 4**). Five eryptosis inducers have been reported to not modulate eryptosis in bystander uRBCs, while inducing eryptosis of iRBCs. Overall, these *in vivo* studies indicate that inducing eryptosis has a beneficial effect for the host. Indeed, a decrease of parasitemia and increase in mice survival are observed (**Table 4**). Importantly, few studies measured anemia levels of treated mice, although this is a crucial side effect to consider when testing the use of eryptosis manipulators *in vivo* (**Table 4**). With respect to the above studies, the possibility has not been excluded that some of the compounds may have off-targets in the parasite. Finally, it is interesting to note that some antimalarial drugs such as

TABLE 4 | Effect of eryptosis inducers on *P. berghei in vivo* development.

Compound	Eryptosis		Parasitemia decrease	Mice survival	Anemia effect	References
		uRBC	iRBC			
Amiodarone*	ns	↗	64%	70%	N/A	Bobbala et al., 2010b
Anandamide*	ns	↗	67%	70%	N/A	Bobbala et al., 2010a
Aurothiomalate*	ns	↗	44%	55%	↗	Alesutan et al., 2010
Dimethylfumarate*	ns	↗	83%	60%	ns	Ghashghaeinia et al., 2010
Amphotericin B*	ns	↗	ns	50%	N/A	Siraskar et al., 2010

*Eryptosis compounds were administered to P. berghei-infected mice 8 days post-parasite infection. Eryptosis features of infected red blood cells (iRBC) and bystander uninfected red blood cells (uRBC), as well as parasitemia levels, mice survival outcome, and anemia levels effects were measured every day. For clarity purposes, the eryptosis phenotype observed is based only on reported PS exposure measurements. "Parasitemia decrease" indicates the decreased percentage in parasitemia of treated mice when compared to the untreated control (value calculated based on data provided in the original publication) when the difference reached significance. "Mice survival" indicates the percentage of viable treated mice when untreated controls reached 100% lethality rate. Compounds previously described as eryptotic inducers (see **Table 1**) that did not induce a significant increase in eryptosis of uRBC in these studies are indicated by *. ns, not significant; ↗, significant increase of PS exposure compared to untreated control; N/A, parameter not discussed in the publication.*

artesunate, mefloquine and quinine, have been shown to induce eryptosis (Alzoubi et al., 2014; Bissinger et al., 2015; Mischitelli et al., 2016), raising the question of a possible interference with the eryptotic process to their antimalarial effect.

Inducing Eryptosis to Treat Malaria—Is It Realistic?

The majority of studies discussed in this review (and summarized in **Tables 3**, **4**) support the notion that enhancing eryptosis of parasitised RBCs represents an attractive anti-malaria strategy. This is based on the hypothesis that exposing RBCs to eryptotic inducers could lead to early clearance of ring stages, preventing trophozoite development and sequestration, and therefore leading to a less severe course of infection. However, it is worth emphasizing that eryptosis inducers that do not specifically target iRBCs, will also increase PS exposure of non-infected RBCs and are therefore likely to lead to anemia. Perhaps the only exception to this, consists in the argument that iRBCs are stressed by the presence of the parasite, therefore the threshold to induce eryptosis may be lower for iRBCs than for uRBCs. Hence the idea of inducing eryptosis selectively (or predominantly) in *Plasmodium*-iRBC may be considered achievable by some authors. It is our view, however, that further work is required to assess the overall potential clinical benefits of eryptosis inducers in the context of a malaria infection. On the other hand, assuming that *Plasmodium* actively inhibits eryptosis of its host cell, an anti-malarial strategy aiming to prevent this inhibition appears more attractive and is discussed in the following section.

PREVENTING *PLASMODIUM* FROM INHIBITING ERYPTOSIS—A NOVEL APPROACH TO TREAT MALARIA?

Plasmodium interferes with apoptosis of its host cells in the liver of the vertebrate host (Heussler et al., 2006; Kakani et al., 2016) and in the mosquito midgut (Ramphul et al., 2015; Kakani et al., 2016). The parasite thus has a proven track record of manipulating host cell death pathways, and, as alluded to above, also appears to do so during infection of RBCs. Upon RBC invasion, buffering of host cell intracellular calcium and secretion of unused amino acids (**Figure 3**) have been proposed as the first signs of eryptosis manipulation by the parasite (Adovelande et al., 1993; Tiffert et al., 2000; Kirk, 2001). Consistent with this idea, inhibition of a *P. falciparum* cation-transporting ATPase was shown to induce eryptosis of the iRBC and its rapid clearance *in vivo* (Jiménez-Díaz et al., 2014), as if this inhibition reversed eryptosis silencing. Further, *P. falciparum* activates and relies on human kinases such as mitogen-activated protein kinase kinase (MEK) and p21 activated kinase (PAK), for its development inside RBCs (Sicard et al., 2011). Interestingly, PAK kinases have the ability to inhibit eryptosis in energy depletion conditions, as discussed above (Zelenak et al., 2011) and are often subverted by pathogens for different cellular functions, including manipulation of apoptosis (John von Freyend et al., 2017). Overall, even though there is currently no direct evidence that PAK activation in iRBCs is linked to eryptosis manipulation, it is an exciting hypothesis that opens great perspectives for anti-malaria intervention strategies. Indeed, inhibition of host kinases required by the parasite for survival would ensure disease treatment with smaller risks of emergence of parasite resistance. In addition, host-directed approaches offer the possibility of repurposing human kinase inhibitors already available in the drug-market (Doerig, 2004).

CONCLUSIONS AND FUTURE DIRECTIONS

Although the complexity of eryptosis regulation in healthy individuals remains to be fully understood, numerous molecular mechanisms have been described to date. Understanding eryptosis regulation is particularly relevant to further our knowledge of *Plasmodium*-erythrocyte interactions. Indeed, manipulation of host cell pathways is a widely used strategy

by a multitude of pathogens and offers novel and attractive host-direct therapy opportunities. Manipulation of eryptosis by *Plasmodium* parasites is an emergent area of research that has attracted attention in recent years, and where much is yet to be done. Importantly, host-directed antimalarial therapy offers the considerable advantage of limiting the major pathways toward drug resistance, namely the selection of mutated parasite-encoded targets. However, before this is realized, major gaps in knowledge prevail and need to be addressed. Below, we outline some of the key questions that need to be addressed.

Potential Manipulation of Eryptosis by *Plasmodium*

Although infection of erythrocytes by *Plasmodium* induces cell death hallmarks, it has been proposed that the parasite inhibits host cell death by buffering intracellular calcium levels (Adovelande et al., 1993), exporting amino acids (Lew et al., 2003), and manipulating host cell kinases (reviewed in Carvalho et al., 2016). Specific molecular mechanisms of calcium sequestration and host ceramide production for example are yet to be elucidated. However, host molecular mechanisms that are shown to be manipulated by the parasite represent exciting opportunities for host-directed therapy. In this context, modulators of eryptosis appear to have a protective effect toward the host in murine models, although possible off-target effects on parasite-encoded factors cannot be excluded, and the influence of these treatments on anemia levels are yet to be determined in most cases.

Role of PS Exposure During *Plasmodium* Infection

The clinical outcome arising from PS-exposing *Plasmodium*-infected RBCs is controversial. On the one hand, PS-exposure of erythrocytes infected by young parasites is thought to lead to early parasite clearance, hence being favorable to the host (Föller et al., 2009a). On the other hand it is argued that PS exposure enhances the cytoadherence of infected red blood cells, and therefore contributes to parasite immune evasion and malaria pathogenesis (Totino and Lopes, 2017). Although it is clear that *Plasmodium* infection enhances PS exposure of the host erythrocyte, the physiological role of this phenomenon remains to be elucidated and further *in vivo* studies are required to address this question.

Eryptosis of Bystander Erythrocytes

Another notable finding in malaria-related eryptosis is the increased eryptosis of uninfected bystander erythrocytes during a malaria infection (Totino et al., 2010, 2013). This is believed to be a key mechanism leading to malaria-induced anemia and the severe outcome of disease (Jakeman et al., 1999). However, the molecular mechanisms underpinning this phenomenon, including a possible role of the immune response, are not understood. There is little doubt that unraveling the mechanism underlying eryptosis of bystander erythrocytes can lead to critical clinical applications in malaria patients suffering from severe anemia.

AUTHOR CONTRIBUTIONS

CB and TC drafted the manuscript. CD edited and commented on the manuscript.

FUNDING

The current work was conducted with funding from La Trobe University and Monash University.

REFERENCES

Adovelande, J., Bastide, B., Délèze, J., and Schrével, J. (1993). Cytosolic free calcium in *Plasmodium falciparum*-infected erythrocytes and the effect of verapamil: a cytofluorimetric study. *Exp. Parasitol.* 76, 247–258.

Akel, A., Hermle, T., Niemoeller, O. M., Kempe, D. S., Lang, P. A., Attanasio, P., et al. (2006). Stimulation of erythrocyte phosphatidylserine exposure by chlorpromazine. *Eur. J. Pharmacol.* 532, 11–17. doi: 10.1016/j.ejphar.2005.12.037

Alesutan, I., Bobbala, D., Qadri, S. M., Estremera, A., Föller, M., and Lang, F. (2010). Beneficial effect of aurothiomalate on murine malaria. *Malar. J.* 9, 118. doi: 10.1186/1475-2875-9-118

Alzoubi, K., Calabrò, S., Bissinger, R., Abed, M., Faggio, C., and Lang, F. (2014). Stimulation of suicidal erythrocyte death by artesunate. *Cell. Physiol. Biochem. Int. J. Exp. Cell. Physiol. Biochem. Pharmacol.* 34, 2232–2244. doi: 10.1159/000369666

Andrews, D. A., Yang, L., and Low, P. S. (2002). Phorbol ester stimulates a protein kinase C-mediated agatoxin-TK-sensitive calcium permeability pathway in human red blood cells. *Blood* 100, 3392–3399. doi: 10.1182/blood.V100.9.3392

Antony, H. A., and Parija, S. C. (2016). Antimalarial drug resistance: an overview. *Trop Parasitol* 6, 30–41. doi: 10.4103/2229-5070.175081

Arese, P., Turrini, F., and Schwarzer, E. (2005). Band 3/complement-mediated recognition and removal of normally senescent and pathological human erythrocytes. *Cell. Physiol. Biochem.* 16, 133–146. doi: 10.1159/000089839

Ashida, H., Mimuro, H., Ogawa, M., Kobayashi, T., Sanada, T., Kim, M., et al. (2011). Cell death and infection: a double-edged sword for host and pathogen survival. *J. Cell Biol.* 195, 931–942. doi: 10.1083/jcb.201108081

Atamna, H., and Ginsburg, H. (1993). Origin of reactive oxygen species in erythrocytes infected with *Plasmodium falciparum*. *Mol. Biochem. Parasitol.* 61, 231–241.

Autino, B., Corbett, Y., Castelli, F., and Taramelli, D. (2012). Pathogenesis of malaria in tissues and blood. *Mediterr. J. Hematol. Infect. Dis.* 4:e2012061. doi: 10.4084/MJHID.2012.061

Ayi, K., Turrini, F., Piga, A., and Arese, P. (2004). Enhanced phagocytosis of ring-parasitized mutant erythrocytes: a common mechanism that may explain protection against falciparum malaria in sickle trait and beta-thalassemia trait. *Blood* 104, 3364–3371. doi: 10.1182/blood-2003-11-3820

Balaji, S. N., and Trivedi, V. (2013). Extracellular methemoglobin primes red blood cell aggregation in malaria: an *in vitro* mechanistic study. *FEBS Lett.* 587, 350–357. doi: 10.1016/j.febslet.2012.12.015

Barasa, B., and Slijper, M. (2014). Challenges for red blood cell biomarker discovery through proteomics. *Biochim. Biophys. Acta* 1844, 1003–1010. doi: 10.1016/j.bbapap.2013.10.002

Barenholz, Y., and Thompson, T. E. (1980). Sphingomyelins in bilayers and biological membranes. *Biochim. Biophys. Acta Biomembr.* 604, 129–158. doi: 10.1016/0005-2736(80)90572-6

Baynes, J. W. (2005). "Oxygen and life," in *Medical Biochemistry*, eds J. W. Baynes, and M. H. Dominiczak (Philadelphia, PA: Elsevier Health Sciences), 497–506.

Bentzen, P. J., and Lang, F. (2007). Effect of anandamide on erythrocyte survival. *Cell. Physiol. Biochem.* 20, 1033–1042. doi: 10.1159/000110714

Berg, C. P., Engels, I. H., Rothbart, A., Lauber, K., Renz, A., Schlosser, S. F., et al. (2001). Human mature red blood cells express caspase-3 and caspase-8, but are devoid of mitochondrial regulators of apoptosis. *Cell Death Differ.* 8, 1197–1206. doi: 10.1038/sj.cdd.4400905

Bhavsar, S. K., Gu, S., Bobbala, D., and Lang, F. (2011). Janus kinase 3 is expressed in erythrocytes, phosphorylated upon energy depletion and involved in the regulation of suicidal erythrocyte death. *Cell. Physiol. Biochem.* 27, 547–556. doi: 10.1159/000329956

Birbes, H., Bawab, S. E., Obeid, L. M., and Hannun, Y. A. (2002). Mitochondria and ceramide: intertwined roles in regulation of apoptosis. *Adv. Enzy. Regul.* 42, 113–129. doi: 10.1016/S0065-2571(01)00026-7

Bissinger, R., Barking, S., Alzoubi, K., Liu, G., Liu, G., and Lang, F. (2015). Stimulation of suicidal erythrocyte death by the antimalarial drug mefloquine. *Cell. Physiol. Biochem.* 36, 1395–1405. doi: 10.1159/000430305

Boas, F. E., Forman, L., and Beutler, E. (1998). Phosphatidylserine exposure and red cell viability in red cell aging and in hemolytic anemia. *Proc. Natl. Acad. Sci. U.S.A.* 95, 3077–3081.

Bobbala, D., Alesutan, I., Föller, M., Huber, S. M., and Lang, F. (2010a). Effect of anandamide in *Plasmodium berghei*-infected mice. *Cell. Physiol. Biochem.* 26, 355–362. doi: 10.1159/000320559

Bobbala, D., Alesutan, I., Föller, M., Tschan, S., Huber, S. M., and Lang, F. (2010b). Protective effect of amiodarone in malaria. *Acta Trop.* 116, 39–44. doi: 10.1016/j.actatropica.2010.05.005

Bobbala, D., Koka, S., Geiger, C., Föller, M., Huber, S. M., and Lang, F. (2009). Azathioprine favourably influences the course of malaria. *Malar. J.* 8:102. doi: 10.1186/1475-2875-8-102

Bobbala, D., Koka, S., Lang, C., Boini, K. M., Huber, S. M., and Lang, F. (2008). Effect of cyclosporine on parasitemia and survival of *Plasmodium berghei* infected mice. *Biochem. Biophys. Res. Commun.* 376, 494–498. doi: 10.1016/j.bbrc.2008.09.005

Bogdanova, A., Makhro, A., Wang, J., Lipp, P., and Kaestner, L. (2013). Calcium in red blood cells-a perilous balance. *Int. J. Mol. Sci.* 14, 9848–9872. doi: 10.3390/ijms14059848

Bonomini, M., Sirolli, V., Gizzi, F., Di Stante, S., Grilli, A., and Felaco, M. (2002). Enhanced adherence of human uremic erythrocytes to vascular endothelium: role of phosphatidylserine exposure. *Kidney Int.* 62, 1358–1363. doi: 10.1111/j.1523-1755.2002.kid560.x

Bookchin, R. M., Ortiz, O. E., and Lew, V. L. (1987). Activation of calcium-dependent potassium channels in deoxygenated sickled red cells. *Prog. Clin. Biol. Res.* 240, 193–200.

Brand, V., Koka, S., Lang, C., Jendrossek, V., Huber, S. M., Gulbins, E., et al. (2008). Influence of amitriptyline on eryptosis, parasitemia and survival of *Plasmodium berghei*-infected mice. *Cell. Physiol. Biochem.* 22, 405–412. doi: 10.1159/000185482

Bratosin, D., Estaquier, J., Petit, F., Arnoult, D., Quatannens, B., Tissier, J.-P., et al. (2001). Programmed cell death in mature erythrocytes: a model for investigating death effector pathways operating in the absence of mitochondria. *Cell Death Differ.* 8, 1143–1156. doi: 10.1038/sj.cdd.4400946

Brugnara, C., de Franceschi, L., and Alper, S. L. (1993). Inhibition of Ca(2+)-dependent K+ transport and cell dehydration in sickle erythrocytes by clotrimazole and other imidazole derivatives. *J. Clin. Invest.* 92, 520–526. doi: 10.1172/JCI116597

Buehler, P. W., Baek, J. H., Lisk, C., Connor, I., Sullivan, T., Kominsky, D., et al. (2012). Free hemoglobin induction of pulmonary vascular disease: evidence for an inflammatory mechanism. *Am. J. Physiol. Lung. Cell. Mol. Physiol.* 303, L312–L326. doi: 10.1152/ajplung.00074.2012

Burger, P., Hilarius-Stokman, P., de Korte, D., van den Berg, T. K., and van Bruggen, R. (2012). CD47 functions as a molecular switch for erythrocyte phagocytosis. *Blood* 119, 5512–5521. doi: 10.1182/blood-2011-10-386805

Butt, E., Abel, K., Krieger, M., Palm, D., Hoppe, V., Hoppe, J., et al. (1994). cAMP- and cGMP-dependent protein kinase phosphorylation sites of the focal adhesion vasodilator-stimulated phosphoprotein (VASP) *in vitro* and in intact human platelets. *J. Biol. Chem.* 269, 14509–14517.

Cappadoro, M., Giribaldi, G., O'Brien, E., Turrini, F., Mannu, F., Ulliers, D., et al. (1998). Early phagocytosis of glucose-6-phosphate dehydrogenase (G6PD)-deficient erythrocytes parasitized by *Plasmodium falciparum* may explain malaria protection in G6PD deficiency. *Blood* 92, 2527–2534.

Carvalho, T. G., Morahan, B., John von Freyend, S., Boeuf, P., Grau, G., Garcia-Bustos, J., et al. (2016). The ins and outs of phosphosignalling in Plasmodium: parasite regulation and host cell manipulation. *Mol. Biochem. Parasitol.* 208, 2–15. doi: 10.1016/j.molbiopara.2016.05.006

Caulier, A., Guyonneau Harmand, L., and Garçon, L. (2017). Immortalisation érythrocytaire pour production de globules rouges *in vitro*. *Transfus. Clin. Biol.* 24, 263–267. doi: 10.1016/j.tracli.2017.06.030

Cimen, M. Y. B. (2008). Free radical metabolism in human erythrocytes. *Clin. Chim. Acta* 390, 1–11. doi: 10.1016/j.cca.2007.12.025

Closse, C., Dachary-Prigent, J., and Boisseau, M. R. (1999). Phosphatidylserine-related adhesion of human erythrocytes to vascular endothelium. *Br. J. Haematol.* 107, 300–302.

Costa, F. T. M., Lopes, S. C. P., Ferrer, M., Leite, J. A., Martin-Jaular, L., Bernabeu, M., et al. (2011). On cytoadhesion of *Plasmodium vivax*: raison d'être? *Mem. Inst. Oswaldo Cruz* 106(Suppl. 1), 79–84. doi: 10.1590/S0074-02762011000900010 ·

D'Alessandro, U., and Buttiëns, H. (2001). History and importance of antimalarial drug resistance. *Trop. Med. Int. Health* 6, 845–848. doi: 10.1046/j.1365-3156.2001.00819.x

Dbaibo, G. S., Perry, D. K., Gamard, C. J., Platt, R., Poirier, G. G., Obeid, L. M., et al. (1997). Cytokine Response Modifier A (CrmA) inhibits ceramide formation in response to Tumor Necrosis Factor (TNF)-α: CrmA and Bcl-2 target distinct components in the apoptotic pathway. *J. Exp. Med.* 185, 481–490.

de Jong, K., Rettig, M. P., Low, P. S., and Kuypers, F. A. (2002). Protein kinase C activation induces phosphatidylserine exposure on red blood cells. *Biochemistry* 41, 12562–12567. doi: 10.1021/bi025882o

Delbridge, A. R., Aubrey, B. J., Hyland, C., Bernardini, J. P., Rago, L. D., Garnier, J.-M., et al. (2017). The BH3-only proteins BIM and PUMA are not critical for the reticulocyte apoptosis caused by loss of the pro-survival protein BCL-XL. *Cell Death Dis.* 8:e2914. doi: 10.1038/cddis.2017.304

Doerig, C. (2004). Protein kinases as targets for anti-parasitic chemotherapy. *Biochim. Biophys. Acta ProteinsProteomics* 1697, 155–168. doi: 10.1016/j.bbapap.2003.11.021.

Eda, S., and Sherman, I. W. (2002). Cytoadherence of malaria-infected red blood cells involves exposure of phosphatidylserine. *Cell. Physiol. Biochem.* 12, 373–384. doi: 10.1159/000067908

Egan, E. S. (2017). Beyond hemoglobin: screening for malaria host factors. *Trends Genet.* 34, 133–141. doi: 10.1016/j.tig.2017.11.004

Enomoto, M., Kawazu, S., Kawai, S., Furuyama, W., Ikegami, T., Watanabe, J., et al. (2012). Blockage of spontaneous Ca^{2+} oscillation causes cell death in intraerythrocitic *Plasmodium falciparum*. *PLoS ONE* 7:e39499. doi: 10.1371/journal.pone.0039499

Föller, M., Bobbala, D., Koka, S., Huber, S. M., Gulbins, E., and Lang, F. (2009a). Suicide for survival–death of infected erythrocytes as a host mechanism to survive malaria. *Cell. Physiol. Biochem.* 24, 133–140. doi: 10.1159/000233238

Föller, M., Feil, S., Ghoreschi, K., Koka, S., Gerling, A., Thunemann, M., et al. (2008). Anemia and splenomegaly in cGKI-deficient mice. *Proc. Natl. Acad. Sci. U.S.A.* 105, 6771–6776. doi: 10.1073/pnas.0708940105

Föller, M., Sopjani, M., Koka, S., Gu, S., Mahmud, H., Wang, K., et al. (2009b). Regulation of erythrocyte survival by AMP-activated protein kinase. *FASEB J.* 23, 1072–1080. doi: 10.1096/fj.08-121772

Franco, R. S. (2012). Measurement of red cell lifespan and aging. *Transfus Med. Hemother.* 39, 302–307. doi: 10.1159/000342232

Gatidis, S., Zelenak, C., Fajol, A., Lang, E., Jilani, K., Michael, D., et al. (2011). p38 MAPK activation and function following osmotic shock of erythrocytes. *Cell. Physiol. Biochem.* 28, 1279–1286. doi: 10.1159/000335859.

Geiger, C., Föller, M., Herrlinger, K. R., and Lang, F. (2008). Azathioprine-induced suicidal erythrocyte death. *Inflamm. Bowel Dis.* 14, 1027–1032. doi: 10.1002/ibd.20433

Ghashghaeinia, M., Bobbala, D., Wieder, T., Koka, S., Brück, J., Fehrenbacher, B., et al. (2010). Targeting glutathione by dimethylfumarate protects against experimental malaria by enhancing erythrocyte cell membrane scrambling. *Am. J. Physiol. Cell Physiol.* 299, C791–C804. doi: 10.1152/ajpcell.00014.2010

Ghashghaeinia, M., Cluitmans, J. C. A., Akel, A., Dreischer, P., Toulany, M., Köberle, M., et al. (2012). The impact of erythrocyte age on eryptosis. *Br. J. Haematol.* 157, 606–614. doi: 10.1111/j.1365-2141.2012.09100.x

Ghashghaeinia, M., Giustarini, D., Koralkova, P., Köberle, M., Alzoubi, K., Bissinger, R., et al. (2016). Pharmacological targeting of glucose-6-phosphate dehydrogenase in human erythrocytes by Bay 11-7082, parthenolide and dimethyl fumarate. *Sci. Rep.* 6:28754. doi: 10.1038/srep28754

Ginsburg, H., and Atamna, H. (1994). The redox status of malaria-infected erythrocytes: an overview with an emphasis on unresolved problems. *Parasite* 1, 5–13. doi: 10.1051/parasite/1994011005

Gregoli, P. A., and Bondurant, M. C. (1997). The roles of Bcl-XL and apopain in the control of erythropoiesis by erythropoietin. *Blood* 90, 630–640.

Hanada, K., Mitamura, T., Fukasawa, M., Magistrado, P. A., Horii, T., and Nishijima, M. (2000). Neutral sphingomyelinase activity dependent on Mg^{2+} and anionic phospholipids in the intraerythrocytic malaria parasite *Plasmodium falciparum*. *Biochem. J.* 346(Pt 3), 671–677. doi: 10.1042/bj3460671

Hattangadi, S. M., and Lodish, H. F. (2007). Regulation of erythrocyte lifespan: do reactive oxygen species set the clock? *J. Clin. Invest.* 117, 2075–2077. doi: 10.1172/JCI32559

Hay, S., and Kannourakis, G. (2002). A time to kill: viral manipulation of the cell death program. *J. Gen. Virol.* 83, 1547–1564. doi: 10.1099/0022-1317-83-7-1547

Head, D. J., Lee, Z. E., Poole, J., and Avent, N. D. (2005a). Expression of phosphatidylserine (PS) on wild-type and Gerbich variant erythrocytes following glycophorin-C (GPC) ligation. *Br. J. Haematol.* 129, 130–137. doi: 10.1111/j.1365-2141.2005.05407.x

Head, D. J., Lee, Z. E., Swallah, M. M., and Avent, N. D. (2005b). Ligation of CD47 mediates phosphatidylserine expression on erythrocytes and a concomitant loss of viability *in vitro*. *Br. J. Haematol.* 130, 788–790. doi: 10.1111/j.1365-2141.2005.05668.x

Heussler, V., Sturm, A., and Langsley, G. (2006). Regulation of host cell survival by intracellular Plasmodium and Theileria parasites. *Parasitology* 132, S49–S60. doi: 10.1017/S0031182006000850

Ho, M., Davis, T. M., Silamut, K., Bunnag, D., and White, N. J. (1991). Rosette formation of *Plasmodium falciparum*-infected erythrocytes from patients with acute malaria. *Infect. Immun.* 59, 2135–2139.

Hockemeyer, D., and Jaenisch, R. (2016). Induced pluripotent stem cells meet genome editing. *Cell Stem Cell* 18, 573–586. doi: 10.1016/j.stem.2016.04.013

Huber, S. M., Duranton, C., and Lang, F. (2005). Patch-clamp analysis of the "new permeability pathways" in malaria-infected erythrocytes. *Int. Rev. Cytol.* 246, 59–134. doi: 10.1016/S0074-7696(05)46003-9

Huber, S. M., Gamper, N., and Lang, F. (2001). Chloride conductance and volume-regulatory nonselective cation conductance in human red blood cell ghosts. *Pflügers. Arch. Eur. J. Physiol.* 441, 551–558. doi: 10.1007/s004240000456

Jakeman, G. N., Saul, A., Hogarth, W. L., and Collins, W. E. (1999). Anaemia of acute malaria infections in non-immune patients primarily results from destruction of uninfected erythrocytes. *Parasitology* 119 (Pt 2), 127–133.

James, E. R., and Green, D. R. (2004). Manipulation of apoptosis in the host–parasite interaction. *Trends Parasitol.* 20, 280–287. doi: 10.1016/j.pt.2004.04.004

Jemaà, M., Fezai, M., Bissinger, R., and Lang, F. (2017). Methods employed in cytofluorometric assessment of eryptosis, the suicidal erythrocyte death. *Cell. Physiol. Biochem.* 43, 431–444. doi: 10.1159/000480469

Jiménez-Díaz, M. B., Ebert, D., Salinas, Y., Pradhan, A., Lehane, A. M., Myrand-Lapierre, M.-E., et al. (2014). (+)-SJ733, a clinical candidate for malaria that acts through ATP4 to induce rapid host-mediated clearance of Plasmodium. *Proc. Natl. Acad. Sci. U.S.A.* 111, E5455–E5462. doi: 10.1073/pnas.1414221111

John von Freyend, S., Kwok-Schuelein, T., Netter, H. J., Haqshenas, G., Semblat, J.-P., and Doerig, C. (2017). Subverting host cell P21-activated kinase: a case of convergent evolution across pathogens. *Pathogens* 6:E17. doi: 10.3390/pathogens6020017

Joshi, P., Dutta, G. P., and Gupta, C. M. (1987). An intracellular simian malarial parasite (*Plasmodium knowlesi*) induces stage-dependent alterations in membrane phospholipid organization of its host erythrocyte. *Biochem. J.* 246, 103–108.

Kakani, P., Suman, S., Gupta, L., and Kumar, S. (2016). Ambivalent outcomes of cell apoptosis: a barrier or blessing in malaria progression. *Front. Microbiol.* 7:302. doi: 10.3389/fmicb.2016.00302

Kanjee, U., Grüring, C., Chaand, M., Lin, K.-M., Egan, E., Manzo, J., et al. (2017). CRISPR/Cas9 knockouts reveal genetic interaction between strain-transcendent erythrocyte determinants of *Plasmodium falciparum* invasion. *Proc. Natl. Acad. Sci. U.S.A.* 114, E9356–E9365. doi: 10.1073/pnas.1711310114.

Kasinathan, R. S., Föller, M., Koka, S., Huber, S. M., and Lang, F. (2007). Inhibition of eryptosis and intraerythrocytic growth of *Plasmodium falciparum* by flufenamic acid. *Naunyn. Schmiedebergs Arch. Pharmacol.* 374, 255–264. doi: 10.1007/s00210-006-0122-x

Kaushansky, A., Metzger, P. G., Douglass, A. N., Mikolajczak, S. A., Lakshmanan, V., Kain, H. S., et al. (2013). Malaria parasite liver stages render host hepatocytes susceptible to mitochondria-initiated apoptosis. *Cell Death Dis.* 4:e762. doi: 10.1038/cddis.2013.286

Kempe, D. S., Lang, P. A., Eisele, K., Klarl, B. A., Wieder, T., Huber, S. M., et al. (2005). Stimulation of erythrocyte phosphatidylserine exposure by lead ions. *Am. J. Physiol. Cell Physiol.* 288, C396–C402. doi: 10.1152/ajpcell.00115.2004

Kirk, K. (2001). Membrane transport in the malaria-infected erythrocyte. *Physiol. Rev.* 81, 495–537. doi: 10.1152/physrev.2001.81.2.495

Klarl, B. A., Lang, P. A., Kempe, D. S., Niemoeller, O. M., Akel, A., Sobiesiak, M., et al. (2006). Protein kinase C mediates erythrocyte "programmed cell death" following glucose depletion. *Am. J. Phys. Cell Physiol.* 290, C244–C253. doi: 10.1152/ajpcell.00283.2005

Koch, M., and Baum, J. (2016). The mechanics of malaria parasite invasion of the human erythrocyte – towards a reassessment of the host cell contribution. *Cell Microbiol.* 18, 319–329. doi: 10.1111/cmi.12557

Koka, S., Bobbala, D., Lang, C., Boini, K. M., Huber, S. M., and Lang, F. (2009). Influence of paclitaxel on parasitemia and survival of *Plasmodium berghei* infected mice. *Cell. Physiol. Biochem.* 23, 191–198. doi: 10.1159/000204107

Koka, S., Huber, S. M., Boini, K. M., Lang, C., Föller, M., and Lang, F. (2007). Lead decreases parasitemia and enhances survival of *Plasmodium berghei*-infected mice. *Biochem. Biophys. Res. Commun.* 363, 484–489. doi: 10.1016/j.bbrc.2007.08.173

Koka, S., Lang, C., Boini, K. M., Bobbala, D., Huber, S. M., and Lang, F. (2008a). Influence of chlorpromazine on eryptosis, parasitemia and survival of Plasmodium berghe infected mice. *Cell. Physiol. Biochem.* 22, 261–268. doi: 10.1159/000149804

Koka, S., Lang, C., Niemoeller, O. M., Boini, K. M., Nicolay, J. P., Huber, S. M., et al. (2008b). Influence of NO synthase inhibitor L-NAME on parasitemia and survival of *Plasmodium berghei* infected mice. *Cell. Physiol. Biochem.* 21, 481–488. doi: 10.1159/000129641

Kucherenko, Y., Zelenak, C., Eberhard, M., Qadri, S. M., and Lang, F. (2012). Effect of casein kinase 1α activator pyrvinium pamoate on erythrocyte ion channels. *Cell. Physiol. Biochem.* 30, 407–417. doi: 10.1159/000339034

Lang, E., Bissinger, R., Fajol, A., Salker, M. S., Singh, Y., Zelenak, C., et al. (2015a). Accelerated apoptotic death and *in vivo* turnover of erythrocytes in mice lacking functional mitogen- and stress-activated kinase MSK1/2. *Sci. Rep.* 5:17316. doi: 10.1038/srep17316

Lang, E., Bissinger, R., Gulbins, E., and Lang, F. (2015b). Ceramide in the regulation of eryptosis, the suicidal erythrocyte death. *Apoptosis* 20, 758–767. doi: 10.1007/s10495-015-1094-4

Lang, E., and Lang, F. (2015). Triggers, inhibitors, mechanisms, and significance of eryptosis: the suicidal erythrocyte death. *Bio Med. Res. Int.* 2015:e513518. doi: 10.1155/2015/513518

Lang, F., Abed, M., Lang, E., and Föller, M. (2014). Oxidative stress and suicidal erythrocyte death. *Antioxid. Redox Signal.* 21, 138–153. doi: 10.1089/ars.2013.5747

Lang, F., and Föller, M. (2012). *Erythrocytes: Physiology and Pathophysiology*. Basel: World Scientific Publishing Company.

Lang, K., Lang, P., Bauer, C., Duranton, C., Wieder, T., Huber, S., et al. (2005). Mechanisms of suicidal erythrocyte death. *CPB* 15, 195–202. doi: 10.1159/000086406

Lang, K. S., Duranton, C., Poehlmann, H., Myssina, S., Bauer, C., Lang, F., et al. (2003). Cation channels trigger apoptotic death of erythrocytes. *Cell Death Differ.* 10, 249–256. doi: 10.1038/sj.cdd.4401144

Lang, K. S., Myssina, S., Brand, V., Sandu, C., Lang, P. A., Berchtold, S., et al. (2004). Involvement of ceramide in hyperosmotic shock-induced death of erythrocytes. *Cell Death Differ.* 11, 231–243. doi: 10.1038/sj.cdd.4401311

Lang, K. S., Roll, B., Myssina, S., Schittenhelm, M., Scheel-Walter, H.-G., Kanz, L., et al. (2002). Enhanced erythrocyte apoptosis in sickle cell anemia, thalassemia and glucose-6-phosphate dehydrogenase deficiency. *Cell. Physiol. Biochem.* 12, 365–372. doi: 10.1159/000067907

Lang, P. A., Beringer, O., Nicolay, J. P., Amon, O., Kempe, D. S., Hermle, T., et al. (2006a). Suicidal death of erythrocytes in recurrent hemolytic

uremic syndrome. *J. Mol. Med.* 84, 378–388. doi: 10.1007/s00109-006-0058-0

Lang, P. A., Huober, J., Bachmann, C., Kempe, D. S., Sobiesiak, M., Akel, A., et al. (2006b). Stimulation of erythrocyte phosphatidylserine exposure by paclitaxel. *Cell. Physiol. Biochem.* 18, 151–164. doi: 10.1159/000095190

Lang, P. A., Kaiser, S., Myssina, S., Wieder, T., Lang, F., and Huber, S. M. (2003). Role of Ca^{2+}-activated K^+ channels in human erythrocyte apoptosis. *Am. J. Physiol., Cell Physiol.* 285, C1553–C1560. doi: 10.1152/ajpcell.00186.2003

Lang, P. A., Kempe, D. S., Tanneur, V., Eisele, K., Klarl, B. A., Myssina, S., et al. (2005). Stimulation of erythrocyte ceramide formation by platelet-activating factor. *J. Cell Sci.* 118, 1233–1243. doi: 10.1242/jcs.01730

Lange, P. F., Huesgen, P. F., Nguyen, K., and Overall, C. M. (2014). Annotating N termini for the human proteome project: N termini and Nα-acetylation status differentiate stable cleaved protein species from degradation remnants in the human erythrocyte proteome. *J. Proteome Res.* 13, 2028–2044. doi: 10.1021/pr401191w

Lapillonne, H., Kobari, L., Mazurier, C., Tropel, P., Giarratana, M.-C., Zanella-Cleon, I., et al. (2010). Red blood cell generation from human induced pluripotent stem cells: perspectives for transfusion medicine. *Haematologica* 95, 1651–1659. doi: 10.3324/haematol.2010.023556

Larsen, A. K., Lametsch, R., Elce, J. S., Larsen, J. K., Thomsen, B., Larsen, M. R., et al. (2008). Genetic disruption of calpain correlates with loss of membrane blebbing and differential expression of RhoGDI-1, cofilin and tropomyosin. *Biochem. J.* 411, 657–666. doi: 10.1042/BJ20070522

Leventis, P. A., and Grinstein, S. (2010). The distribution and function of phosphatidylserine in cellular membranes. *Annu. Rev. Biophys.* 39, 407–427. doi: 10.1146/annurev.biophys.093008.131234.

Lew, V. L., Tiffert, T., and Ginsburg, H. (2003). Excess hemoglobin digestion and the osmotic stability of *Plasmodium falciparum*-infected red blood cells. *Blood* 101, 4189–4194. doi: 10.1182/blood-2002-08-2654

Lu, S. C. (2009). Regulation of glutathione synthesis. *Mol. Aspects Med.* 30, 42–59. doi: 10.1016/j.mam.2008.05.005

Lupescu, A., Shaik, N., Jilani, K., Zelenak, C., Lang, E., Pasham, V., et al. (2012). Enhanced erythrocyte membrane exposure of phosphatidylserine following sorafenib treatment: an *in vivo* and *in vitro* study. *CPB* 30, 876–888. doi: 10.1159/000341465

Lutz, H. U. (2004). Innate immune and non-immune mediators of erythrocyte clearance. *Cell. Mol. Biol.* 50, 107–116.

Lutz, H. U., and Bogdanova, A. (2013). Mechanisms tagging senescent red blood cells for clearance in healthy humans. *Front. Physiol.* 4:387. doi: 10.3389/fphys.2013.00387

Maguire, P. A., and Sherman, I. W. (1990). Phospholipid composition, cholesterol content and cholesterol exchange in *Plasmodium falciparum*-infected red cells. *Mol. Biochem. Parasitol.* 38, 105–112.

Mahmud, H., Mauro, D., Qadri, S. M., Föller, M., and Lang, F. (2009). Triggering of suicidal erythrocyte death by amphotericin B. *Cell. Physiol. Biochem.* 24, 263–270. doi: 10.1159/000233251.

Maier, A. G., Duraisingh, M. T., Reeder, J. C., Patel, S. S., Kazura, J. W., Zimmerman, P. A., et al. (2003). *Plasmodium falciparum* erythrocyte invasion through glycophorin C and selection for Gerbich negativity in human populations. *Nat. Med.* 9, 87–92. doi: 10.1038/nm807

Mandal, D., Mazumder, A., Das, P., Kundu, M., and Basu, J. (2005). Fas-, caspase 8-, and caspase 3-dependent signaling regulates the activity of the aminophospholipid translocase and phosphatidylserine externalization in human erythrocytes. *J. Biol. Chem.* 280, 39460–39467. doi: 10.1074/jbc.M506928200

Matallanas, D., Birtwistle, M., Romano, D., Zebisch, A., Rauch, J., von Kriegsheim, A., et al. (2011). Raf family kinases. *Genes Cancer* 2, 232–260. doi: 10.1177/1947601911407323

Matarrese, P., Straface, E., Pietraforte, D., Gambardella, L., Vona, R., Maccaglia, A., et al. (2005). Peroxynitrite induces senescence and apoptosis of red blood cells through the activation of aspartyl and cysteinyl proteases. *FASEB J.* 19, 416–418. doi: 10.1096/fj.04-2450fje

McClure, N. S., and Day, T. (2014). A theoretical examination of the relative importance of evolution management and drug development for managing resistance. *Proc. R. Soc. Lond. B Biol. Sci.* 281:20141861. doi: 10.1098/rspb.2014.1861

McEvoy, L., Williamson, P., and Schlegel, R. A. (1986). Membrane phospholipid asymmetry as a determinant of erythrocyte recognition by macrophages. *Proc. Natl. Acad. Sci. U.S.A.* 83, 3311–3315.

Menard, D., and Dondorp, A. (2017). Antimalarial drug resistance: a threat to malaria elimination. *Cold. Spring Harb. Perspect Med.* 7:a025619. doi: 10.1101/cshperspect.a025619

Mischitelli, M., Jema,à, M., Almasry, M., Faggio, C., and Lang, F. (2016). Stimulation of erythrocyte cell membrane scrambling by Quinine. *Cell. Physiol. Biochem.* 40, 657–667. doi: 10.1159/000452578

Mochly-Rosen, D., Das, K., and Grimes, K. V. (2012). Protein kinase C, an elusive therapeutic target? *Nat. Rev. Drug Dis.* 11, 937–957. doi: 10.1038/nrd3871

Murachi, T., Tanaka, K., Hatanaka, M., and Murakami, T. (1981). Intracellular Ca^{2+}-dependent protease (CALPAIN) and its high-molecular-weight endogenous inhibitor (CALPASTATIN). *Adv. Enzy. Regul.* 19, 407–424. doi: 10.1016/0065-2571(81)90026-1

Nicolay, J. P., Bentzen, P. J., Ghashghaeinia, M., Wieder, T., and Lang, F. (2007). Stimulation of erythrocyte cell membrane scrambling by amiodarone. *Cell. Physiol. Biochem.* 20, 1043–1050. doi: 10.1159/000110713

Nicolay, J. P., Liebig, G., Niemoeller, O. M., Koka, S., Ghashghaeinia, M., Wieder, T., et al. (2008). Inhibition of suicidal erythrocyte death by nitric oxide. *Pflüg. Arch. Eur. J. Physiol.* 456, 293–305. doi: 10.1007/s00424-007-0393-1

Niemoeller, O. M., Akel, A., Lang, P. A., Attanasio, P., Kempe, D. S., Hermle, T., et al. (2006). Induction of eryptosis by cyclosporine. *Naunyn. Schmiedebergs Arch. Pharmacol.* 374, 41–49. doi: 10.1007/s00210-006-0099-5

Nosaka, T., van Deursen, J. M., Tripp, R. A., Thierfelder, W. E., Witthuhn, B. A., McMickle, A. P., et al. (1995). Defective lymphoid development in mice lacking Jak3. *Science* 270, 800–802.

Oldenborg, P.-A., Zheleznyak, A., Fang, Y.-F., Lagenaur, C. F., Gresham, H. D., and Lindberg, F. P. (2000). Role of CD47 as a marker of self on red blood cells. *Science* 288, 2051–2054. doi: 10.1126/science.288.5473.2051

Pathak, V. A., and Ghosh, K. (2016). Erythropoiesis in malaria infections and factors modifying the erythropoietic response. *Anemia* 2016:e9310905. doi: 10.1155/2016/9310905

Perrin, B. J., and Huttenlocher, A. (2002). Calpain. *Int. J. Biochem. Cell Biol.* 34, 722–725. doi: 10.1016/S1357-2725(02)00009-2.

Pretorius, E., Plooy, J. N., du, and Bester, J. (2016). A comprehensive review on eryptosis. *CPB* 39, 1977–2000. doi: 10.1159/000447895

Ramphul, U. N., Garver, L. S., Molina-Cruz, A., Canepa, G. E., and Barillas-Mury, C. (2015). *Plasmodium falciparum* evades mosquito immunity by disrupting JNK-mediated apoptosis of invaded midgut cells. *Proc. Natl. Acad. Sci. U.S.A.* 112, 1273–1280. doi: 10.1073/pnas.1423586112

Rane, C. K., and Minden, A. (2014). P21 activated kinases. *Small GTPases* 5:e28003. doi: 10.4161/sgtp.28003

Rawlings, J. S., Rosler, K. M., and Harrison, D. A. (2004). The JAK/STAT signaling pathway. *J. Cell Sci.* 117, 1281–1283. doi: 10.1242/jcs.00963

Roux-Dalvai, F., Gonzalez de Peredo, A., Sim,ó, C., Guerrier, L., Bouyssié, D., Zanella, A., et al. (2008). Extensive analysis of the cytoplasmic proteome of human erythrocytes using the peptide ligand library technology and advanced mass spectrometry. *Mol. Cell Proteomics* 7, 2254–2269. doi: 10.1074/mcp.M800037-MCP200

Schaer, D. J., Buehler, P. W., Alayash, A. I., Belcher, J. D., and Vercellotti, G. M. (2013). Hemolysis and free hemoglobin revisited: exploring hemoglobin and hemin scavengers as a novel class of therapeutic proteins. *Blood* 121, 1276–1284. doi: 10.1182/blood-2012-11-451229

Schieber, M., and Chandel, N. S. (2014). ROS function in redox signaling and oxidative stress. *Curr. Biol.* 24, R453–R462. doi: 10.1016/j.cub.2014.03.034

Schittek, B., and Sinnberg, T. (2014). Biological functions of casein kinase 1 isoforms and putative roles in tumorigenesis. *Mol Cancer* 13:231. doi: 10.1186/1476-4598-13-231

Schoenwaelder, S. M., Yuan, Y., Josefsson, E. C., White, M. J., Yao, Y., Mason, K. D., et al. (2009). Two distinct pathways regulate platelet phosphatidylserine exposure and procoagulant function. *Blood* 114, 663–666. doi: 10.1182/blood-2009-01-200345

Schulze-Osthoff, K., Ferrari, D., Los, M., Wesselborg, S., and Peter, M. E. (2001). Apoptosis signaling by death receptors. *Eur. J. Biochem.* 254, 439–459. doi: 10.1046/j.1432-1327.1998.2540439.x

Schwartz, R. S., Olson, J. A., Raventos-Suarez, C., Yee, M., Heath, R. H., Lubin, B., et al. (1987). Altered plasma membrane phospholipid organization

in *Plasmodium falciparum*-infected human erythrocytes. *Blood* 69, 401–407.

Schwarz-Ben Meir, N., Glaser, T., and Kosower, N. S. (1991). Band 3 protein degradation by calpain is enhanced in erythrocytes of old people. *Biochem. J.* 275 (Pt 1), 47–52.

Segawa, K., and Nagata, S. (2015). An apoptotic 'Eat Me' signal: phosphatidylserine exposure. *Trends Cell Biol.* 25, 639–650. doi: 10.1016/j.tcb.2015.08.003.

Setty, B. N. Y., Kulkarni, S., and Stuart, M. J. (2002). Role of erythrocyte phosphatidylserine in sickle red cell-endothelial adhesion. *Blood* 99, 1564–1571. doi: 10.1182/blood.V99.5.1564

Sharom, F. J. (2011). Flipping and flopping–lipids on the move. *IUBMB Life* 63, 736–746. doi: 10.1002/iub.515

Sicard, A., Semblat, J.-P., Doerig, C., Hamelin, R., Moniatte, M., Dorin-Semblat, D., et al. (2011). Activation of a PAK-MEK signalling pathway in malaria parasite-infected erythrocytes. *Cell Microbiol.* 13, 836–845. doi: 10.1111/j.1462-5822.2011.01582.x

Siraskar, B., Ballal, A., Bobbala, D., Föller, M., and Lang, F. (2010). Effect of amphotericin B on parasitemia and survival of *plasmodium berghei*-infected mice. *Cell. Physiol. Biochem.* 26, 347–354. doi: 10.1159/000320558

Sopjani, M., Föller, M., and Lang, F. (2008). Gold stimulates Ca^{2+} entry into and subsequent suicidal death of erythrocytes. *Toxicology* 244, 271–279. doi: 10.1016/j.tox.2007.12.001

Sturm, A., Amino, R., van de Sand, C., Regen, T., Retzlaff, S., Rennenberg, A., et al. (2006). Manipulation of host hepatocytes by the malaria parasite for delivery into liver sinusoids. *Science* 313, 1287–1290. doi: 10.1126/science.1129720

Suzuki, J., Fujii, T., Imao, T., Ishihara, K., Kuba, H., and Nagata, S. (2013). Calcium-dependent phospholipid scramblase activity of TMEM16 protein family members. *J. Biol. Chem.* 288, 13305–13316. doi: 10.1074/jbc.M113.457937

Suzuki, J., Umeda, M., Sims, P. J., and Nagata, S. (2010). Calcium-dependent phospholipid scrambling by TMEM16F. *Nature* 468, 834–838. doi: 10.1038/nature09583

Tang, H., Ho, H., Wu, P., Chen, S., Kuypers, F. A., Cheng, M., et al. (2015). Inability to maintain GSH pool in G6PD-deficient red cells causes futile AMPK activation and irreversible metabolic disturbance. *Antioxid. Redox. Signal.* 22, 744–759. doi: 10.1089/ars.2014.6142

Tanner, M. J. (1993). The major integral proteins of the human red cell. *Baillieres Clin. Haematol.* 6, 333–356.

Tiffert, T., Staines, H. M., Ellory, J. C., and Lew, V. L. (2000). Functional state of the plasma membrane Ca^{2+} pump in *Plasmodium falciparum*-infected human red blood cells. *J. Physiol.* 525, 125–134. doi: 10.1111/j.1469-7793.2000.00125.x

Tilley, L., Straimer, J., Gnädig, N. F., Ralph, S. A., and Fidock, D. A. (2016). Artemisinin action and resistance in *Plasmodium falciparum*. *Trends Parasitol.* 32, 682–696. doi: 10.1016/j.pt.2016.05.010

Tolosano, E., Hirsch, E., Patrucco, E., Camaschella, C., Navone, R., Silengo, L., et al. (1999). Defective recovery and severe renal damage after acute hemolysis in hemopexin-deficient mice. *Blood* 94, 3906–3914.

Totino, P. R., and Lopes, S. C. (2017). Insights into the cytoadherence phenomenon of *Plasmodium vivax*: the putative role of phosphatidylserine. *Front. Immunol.* 8:1148. doi: 10.3389/fimmu.2017.01148

Totino, P. R., Magalhaes, A. D., Silva, L. A., Banic, D. M., Daniel-Ribeiro, C. T., and Ferreira-da-Cruz Mde F. (2010). Apoptosis of non-parasitized red blood cells in malaria: a putative mechanism involved in the pathogenesis of anaemia. *Malar. J.* 9:350. doi: 10.1186/1475-2875-9-350

Totino, P. R. R., Daniel-Ribeiro, C. T., and Ferreira-da-Cruz, M., de F. (2016). Evidencing the role of erythrocytic apoptosis in malarial anemia. *Front. Cell Infect. Microbiol.* 6:176. doi: 10.3389/fcimb.2016.00176

Totino, P. R. R., Magalhães, A. D., Alves, E. B., Costa, M. R. F., de Lacerda, M. V. G., Daniel-Ribeiro, C. T., et al. (2014). *Plasmodium falciparum*, but not *P. vivax,* can induce erythrocytic apoptosis. *Parasit. Vectors* 7:484. doi: 10.1186/s13071-014-0484-8

Totino, P. R. R., Pinna, R. A., De-Oliveira, A. C. A. X., Banic, D. M., Daniel-Ribeiro, C. T., and Ferreira-da-Cruz Mde, F. (2013). Apoptosis of non-parasitised red blood cells in *Plasmodium yoelii* malaria. *Mem. Inst. Oswaldo Cruz* 108, 686–690. doi: 10.1590/0074-0276108062013003

van de Sand, C., Horstmann, S., Schmidt, A., Sturm, A., Bolte, S., Krueger, A., et al. (2005). The liver stage of *Plasmodium berghei* inhibits host cell apoptosis. *Mol. Microbiol.* 58, 731–742. doi: 10.1111/j.1365-2958.2005.04888.x

Wali, R. K., Jaffe, S., Kumar, D., and Kalra, V. K. (1988). Alterations in organization of phospholipids in erythrocytes as factor in adherence to endothelial cells in diabetes mellitus. *Diabetes* 37, 104–111.

Walsh, M., Lutz, R. J., Cotter, T. G., and O'Connor, R. (2002). Erythrocyte survival is promoted by plasma and suppressed by a Bak-derived BH3 peptide that interacts with membrane-associated Bcl-XL. *Blood* 99, 3439–3448. doi: 10.1182/blood.V99.9.3439.

Wang, S., Dale, G. L., Song, P., Viollet, B., and Zou, M. (2010). AMPKα1 deletion shortens erythrocyte life span in mice. *J. Biol. Chem.* 285, 19976–19985. doi: 10.1074/jbc.M110.102467

Wasserman, M., Alarcón, C., and Mendoza, P. M. (1982). Effects of Ca++ depletion on the asexual cell cycle of *Plasmodium falciparum*. *Am. J. Trop. Med. Hyg.* 31, 711–717.

Wautier, M.-P., Héron, E., Picot, J., Colin, Y., Hermine, O., and Wautier, J.-L. (2011). Red blood cell phosphatidylserine exposure is responsible for increased erythrocyte adhesion to endothelium in central retinal vein occlusion. *J. Thromb. Haemost.* 9, 1049–1055. doi: 10.1111/j.1538-7836.2011.04251.x

WHO|Global Technical Strategy for Malaria (2016–2030). WHO. Available online at: http://www.who.int/malaria/areas/global_technical_strategy/en/ (Accessed May 1, 2018).

WHO|World Malaria Report (2017). WHO. Available online at: http://www.who.int/malaria/publications/world-malaria-report-2017/report/en/ (Accessed February 12, 2018).

Wiggin, G. R., Soloaga, A., Foster, J. M., Murray-Tait, V., Cohen, P., and Arthur, J. S. C. (2002). MSK1 and MSK2 are required for the mitogen- and stress-induced phosphorylation of CREB and ATF1 in fibroblasts. *Mol. Cell. Biol.* 22, 2871–2881. doi: 10.1128/MCB.22.8.2871-2881.2002

Wilhelm, S. M., Carter, C., Tang, L., Wilkie, D., McNabola, A., Rong, H., et al. (2004). BAY 43-9006 exhibits broad spectrum oral antitumor activity and targets the RAF/MEK/ERK pathway and receptor tyrosine kinases involved in tumor progression and angiogenesis. *Cancer Res.* 64, 7099–7109. doi: 10.1158/0008-5472.CAN-04-1443

Wu, G., Fang, Y.-Z., Yang, S., Lupton, J. R., and Turner, N. D. (2004). Glutathione metabolism and its implications for health. *J. Nutr.* 134, 489–492. doi: 10.1093/jn/134.3.489

Zappulla, D. (2008). Environmental stress, erythrocyte dysfunctions, inflammation, and the metabolic syndrome: adaptations to CO_2 increases? *J. Cardiometab Syndr.* 3, 30–34. doi: 10.1111/j.1559-4572.2008.07263.x

Zarchin, S., Krugliak, M., and Ginsburg, H. (1986). Digestion of the host erythrocyte by malaria parasites is the primary target for quinoline-containing antimalarials. *Biochem. Pharmacol.* 35, 2435–2442.

Zarubin, T., and Han, J. (2005). Activation and signaling of the p38 MAP kinase pathway. *Cell Res.* 15, 11–18. doi: 10.1038/sj.cr.7290257

Zelenak, C., Eberhard, M., Jilani, K., Qadri, S. M., Macek, B., and Lang, F. (2012). Protein kinase CK1α regulates erythrocyte survival. *Cell. Physiol. Biochem.* 29, 171–180. doi: 10.1159/000337598

Zelenak, C., Föller, M., Velic, A., Krug, K., Qadri, S. M., Viollet, B., et al. (2011). Proteome analysis of erythrocytes lacking AMP-activated protein kinase reveals a role of PAK2 kinase in eryptosis. *J. Proteome Res.* 10, 1690–1697. doi: 10.1021/pr101004j

Conflict of Interest Statement: The authors declare that the research was conducted in the absence of any commercial or financial relationships that could be construed as a potential conflict of interest.

Copyright © 2018 Boulet, Doerig and Carvalho. This is an open-access article distributed under the terms of the Creative Commons Attribution License (CC BY). The use, distribution or reproduction in other forums is permitted, provided the original author(s) and the copyright owner(s) are credited and that the original publication in this journal is cited, in accordance with accepted academic practice. No use, distribution or reproduction is permitted which does not comply with these terms.

Chapter 3

Materials & Methods

Table 3.1: List of solutions used in this project. This table lists the names and composition of all solutions referred to in the method sections, and indicates the final and stock concentrations, solvents/diluents, providers and other specifications, such as the pH, sterilization method and storage conditions.

Solution name	Component	Final concentration	Other specifications	Provider
***P. falciparum* cell culture**				
10% GIEMSA	Giemsa's azur Eosin Methylene-blue	10% (v/v)	in water	Merck
Made fresh at least every 2 days				
iRPMI (incomplete RPMI)	RPMI 1640 Medium HEPES	16.2g/L	-	Life Technologies
	Hypoxanthine	50mg/L	Dissolved in 1M NaOH (0.1g/mL)	Sigma
	Gentamicin	10mg/L	50mg/ml stock solution	Life Technologies
in MilliQ water, pH 6.74, filter-sterilised. Stored at 4°C until use.				
cRPMI (complete RPMI)	Sodium bicarbonate	2.25g/L	7.5% (w/v) stock solution in MilliQ water, filter-sterilised	Merck
	AlbuMAX II Lipid-rich BSA	5g/L	20% (w/v) stock solution in iRPMI, filter-sterilised and frozen until use	Gibco
Add sodium bicarbonate and Albumax to iRPMI before use.				
5% sorbitol	Sorbitol	5% (w/v)	in MilliQ water, filter-sterilised, stored at 4°C	Unilab

List of the solutions used in this project

Solution name	Component	Final concentration	Other specifications	Provider
SYBR Gold reaction solution	Tris buffer	20mM	1M stock, pH 7.5, in MilliQ water	Invitrogen
	EDTA (EthyleneDiamine Tetra Acetic Acid Disodium Salt)	5mM	0.5M stock, pH 8.0, in MilliQ water	Ajax Finechem
	Saponin	0.008% (w/v)	1% (w/v) saponin stock, in MilliQ water	Sigma
	Triton X100	0.08% (v/v)	1% (v/v) stock in MilliQ water	Sigma
	SYBR Gold nucleic acid stain	1X	10'000X stock	ThermoFisher
Protect from light.				

Flow cytometry				
Ringer solution	Sodium chloride	125mM	5M stock	ChemSupply
	Potassium chloride	5mM	1M stock	Univar
	Magnesium sulfate	1mM	1M stock	Unilab
	HEPES	32mM	1M pH 7.4 stock	Sigma
	Glucose	5mM	1M stock	Univar
	Calcium chloride	1mM	100mM stock	ChemSupply
In MilliQ water, pH 7.4, filter sterilised and aliquoted. Stored at room temperature.				
Flow cytometry staining solution	Sodium chloride	125mM	5M stock, stored at room temperature	ChemSupply
	Potassium chloride	5mM	1M stock	Univar
	Magnesium sulfate	1mM	1M stock	Unilab
	HEPES	32mM	1M pH 7.4 stock	Sigma
	Glucose	5mM	1M stock	Univar
	Calcium chloride	5mM	100mM stock	ChemSupply
In MilliQ water, pH 7.4, filter sterilised and aliquoted. Stored at room temperature.				

Extracellular Vesicles				
70% ethanol	Ethanol	70% (v/v)	in MilliQ water, filter sterilised	ChemSupply
20% ethanol	Ethanol	20% (v/v)	in MilliQ water, filter sterilised	ChemSupply
VivaCell soaking solution	Ethanol	60% (v/v)	-	ChemSupply
	1M Hydrochloric acid (HCl)	40% (v/v)	in MilliQ water	ChemSupply
Filter-sterilised.				

List of the solutions used in this project

Solution name	Component	Final concentration	Other specifications	Provider
DPBS	DPBS	100% (v/v)	-	Life Technologies

Protein work				
MPER PPI (MPER with Protease and Phosphatase Inhibitors)	MPER	100%	-	ThermoFisher
	Protease Inhibitors Cocktail (PIC), EDTA-free, Roche	1X	10X or 25X stock in PBS, stored at -20°C	Sigma
	Sodium fluoride	20mM	200 or 500mM stock, stored at -20°C	Sigma
	Sodium orthovanadate	100µM	100mM stock, stored at -20°C	Sigma
	PMSF (phenyl-methanesulfonyl fluoride)	1mM	200mM stock	Rowe Scientific
	β-glycerophosphate	10mM	500mM stock, stored at -20°C	Sigma
Make fresh and keep on ice.				
PBS PPI (PBS with Protease and Phosphatase Inhibitors)	PBS (Phosphate buffered saline)	1X	in MilliQ water	ThermoFisher
	Protease Inhibitors Cocktail (PIC), EDTA-free, Roche	1X	10X or 25X stock in PBS, stored at -20°C	Sigma
	Sodium fluoride	20mM	200 or 500mM stock, stored at -20°C	Sigma
	Sodium orthovanadate	100µM	100mM stock, stored at -20°C	Sigma
	PMSF (phenyl-methanesulfonyl fluoride)	1mM	200mM stock	Rowe Scientific
	β-glycerophosphate	10mM	500mM stock, stored at -20°C	Sigma
Make fresh and keep on ice.				
Saponin PPI (0.1% saponin with Protease and Phosphatase Inhibitors)	Saponin	0.1-0.15% (w/v)	5% (w/v) in PBS	Sigma
	Protease Inhibitors Cocktail (PIC), EDTA-free, Roche	1X	10X or 25X stock in PBS, stored at -20°C	Sigma
	Sodium fluoride	20mM	200 or 500mM stock, stored at -20°C	Sigma
	Sodium orthovanadate	100µM	100mM stock, stored at -20°C	Sigma

List of the solutions used in this project

Solution name	Component	Final concentration	Other specifications	Provider
	PMSF (phenyl-methanesulfonyl fluoride)	1mM	200mM stock	Rowe Scientific
	β-glycerophosphate	10mM	500mM stock, stored at -20°C	Sigma
Make fresh and keep on ice.				
Laemmli buffer	2X Laemmli sample buffer	1X	in protein sample	Sigma
Laemmli buffer	4X Laemmli sample buffer	1X	in protein sample	BioRad
	2-β-mercoptoethanol	10% (v/v)	in 4X Laemmli buffer	Sigma
1X running buffer	5X Tris/Glycin/SDS running buffer	1X	in MilliQ water	BioRad
1X transfer buffer	5X Tans-Blot Turbo transfer buffer	1X	in MilliQ water	BioRad
	Methanol	20% (v/v)	in MilliQ water	Merck
TBST (Tris-buffered saline Tween-20)	Tris	20mM	-	Invitrogen
	NaCl	150mM	-	ChemSupply
	Tween-20	0.1% (v/v)	-	BioRad
In MilliQ water; store at 4°C.				
5% BSA-TBST	Bovine Serum Albumin (BSA)	5% (w/v)	in TBST	Moregate Biotech
Stored at 4°C.				
ECL solution	Clarity™ Western ECL substrate Peroxide Reagent	50% (v/v)	-	BioRad
	Clarity™ Western ECL substrate Luminol /Enhancer Reagent	50% (v/v)	-	BioRad
Prepare ECL solution and immediately soak membrane abundantly with it.				
TBST PPI (TBST with Protease and Phosphatase Inhibitors)	TBST	-	-	-
	Protease Inhibitors Cocktail (PIC), EDTA-free, Roche	1X	10X or 25X stock in PBS, stored at -20°C	Sigma
	Sodium fluoride	20mM	200 or 500mM stock, stored at -20°C	Sigma
	Sodium orthovanadate	100µM	100mM stock, stored at -20°C	Sigma

List of the solutions used in this project

Solution name	Component	Final concentration	Other specifications	Provider
	PMSF (phenyl-methanesulfonyl fluoride)	1mM	200mM stock	Rowe Scientific
	β-glycerophosphate	10mM	500mM stock, stored at -20°C	Sigma
Make fresh and keep on ice.				

Mass spectrometry analysis				
DDA (data-dependent acquisition) peptide library solutions (day 1)	Sodium-deoxycholate (SDC)	4% (v/v)	in 100mM HEPES pH 8.1. Chilled.	Sigma Aldrich
	tris(2-carboxy ethyl)phosphine (TCEP)	10mM	in protein samples with 4% SDC	Sigma Aldrich
	Iodoacetamide	40mM	in protein samples with 4% SDC	Sigma Aldrich
	Trypsin	20µg per mg of sample	in provider's resuspension buffer	Promega
	Ethylacetate	100% (v/v)	-	Sigma Aldrich
	Ethylacetate	50% (v/v)	in 0.5% (v/v) formic acid (Fisher Scientific) in MilliQ water	Sigma Aldrich
	Formic acid	0.1% (v/v)	in MilliQ water	Fisher Scientific
	Ammonium acetate	1M	in MilliQ water	Sigma Aldrich
Elution buffer 1	Ammonium acetate	75mM	in MilliQ water	Sigma Aldrich
	Acetonitrile (ACN)	20% (v/v)		Merck
	Formic acid (FA)	0.5% (v/v)		Fisher Scientific
Elution buffer 2	Ammonium acetate	100mM	in MilliQ water	Sigma Aldrich
	Acetonitrile (ACN)	20% (v/v)		Merck
	Formic acid (FA)	0.5% (v/v)		Fisher Scientific
Elution buffer 3	Ammonium acetate	125mM	in MilliQ water	Sigma Aldrich
	Acetonitrile (ACN)	20% (v/v)		Merck
	Formic acid (FA)	0.5% (v/v)		Fisher Scientific
Elution buffer 4	Ammonium acetate	150mM	in MilliQ water	Sigma Aldrich
	Acetonitrile (ACN)	20% (v/v)		Merck
	Formic acid (FA)	0.5% (v/v)		Fisher Scientific
Elution buffer 5	Ammonium acetate	175mM	in MilliQ water	Sigma Aldrich
	Acetonitrile (ACN)	20% (v/v)		Merck
	Formic acid (FA)	0.5% (v/v)		Fisher Scientific
Elution buffer 6	Ammonium acetate	225mM	in MilliQ water	Sigma Aldrich

List of the solutions used in this project

Solution name	Component	Final concentration	Other specifications	Provider
	Acetonitrile (ACN)	20% (v/v)		Merck
	Formic acid (FA)	0.5% (v/v)		Fisher Scientific
Elution buffer 7	Ammonium acetate	250mM	in MilliQ water	Sigma Aldrich
	Acetonitrile (ACN)	20% (v/v)		Merck
	Formic acid (FA)	0.5% (v/v)		Fisher Scientific
Elution buffer 8	Ammonium acetate	275mM	in MilliQ water	Sigma Aldrich
	Acetonitrile (ACN)	20% (v/v)		Merck
	Formic acid (FA)	0.5% (v/v)		Fisher Scientific
Elution buffer 9	Ammonium acetate	300mM	in MilliQ water	Sigma Aldrich
	Acetonitrile (ACN)	20% (v/v)		Merck
	Formic acid (FA)	0.5% (v/v)		Fisher Scientific
Elution buffer 10	Ammonium acetate	325mM	in MilliQ water	Sigma Aldrich
	Acetonitrile (ACN)	20% (v/v)		Merck
	Formic acid (FA)	0.5% (v/v)		Fisher Scientific
Elution buffer 11	Ammonium acetate	350mM	in MilliQ water	Sigma Aldrich
	Acetonitrile (ACN)	20% (v/v)		Merck
	Formic acid (FA)	0.5% (v/v)		Fisher Scientific
Elution buffer 12	Acetonitrile (ACN)	80% (v/v)	in MilliQ water	Merck
	Ammonium hydroxide	5% (v/v)		Sigma Aldrich
DDA peptide library solutions (day 2)	Formic acid	5% (v/v)	in MilliQ water	Fisher Scientific
	Ethylacetate	50% (v/v)	in MilliQ water	Sigma Aldrich
	Formic acid	0.5% (v/v)		Fisher Scientific
Easy phospho (EP) loading buffer	Trifluoroacetic acid (TFA)	6% (v/v)	in MilliQ water	Sigma Aldrich
	Acetonitrile (ACN)	80% (v/v)		Merck
EP enrichment buffer	Trifluoroacetic acid (TFA)	48% (v/v)	in MilliQ water	Sigma Aldrich
	Potassium phosphate, monobasic	8mM		Sigma Aldrich
EP wash buffer	Trifluoroacetic acid (TFA)	5% (v/v)	in MilliQ water	Sigma Aldrich
	Isopropanol	60% (v/v)		Merck
EP transfer buffer	Trifluoroacetic acid (TFA)	0.1% (v/v)	in MilliQ water	Sigma Aldrich
	Isopropanol	60% (v/v)		Merck
EP elution buffer	Ammonia	17.8% (v/v)	Prepare fresh. In MilliQ water	Sigma Aldrich
	Acetonitrile (ACN)	32% (v/v)		Merck

List of the solutions used in this project

Solution name	**Component**	**Final concentration**	**Other specifications**	**Provider**
SDB-RPS loading buffer / wash buffer 1	Trifluoroacetic acid (TFA)	1% (v/v)	in isopropanol (Merck)	Sigma Aldrich
SDB-RPS wash buffer 2	Trifluoroacetic acid (TFA) Acetonitrile (ACN)	0.2% (v/v) 5% (v/v)	in MilliQ water	Sigma Aldrich Merck
SDB-RPS elution buffer	Ammonia Acetonitrile (ACN)	0.44% (v/v) 60% (v/v)	in MilliQ water	Sigma Aldrich Merck
C18 elution buffer	Acetonitrile (ACN) Formic acid (FA)	70% (v/v) 0.1% (v/v)	in MilliQ water	Merck Fisher Scientific
MS loading buffer	Acetonitrile (ACN) Formic acid (FA) iRT (indexed retention time) peptides	2% (v/v) 0.1% (v/v) 1:300 dilution	in MilliQ water	Merck Fisher Scientific Biognosys

3.1 *P. falciparum* culture methods

3.1.1 *P. falciparum* culture

Plasmodium falciparum 3D7 parasites were cultured *in vitro* in human erythrocytes provided by the Australian Red Cross (La Trobe University Research Ethics HEC17-013 and Australian Red Cross Blood Service Agreement 19-05VIC-01). Cultures were performed as previously described by Trager and Jensen (1976) [140], using complete RPMI (see details in Table 3.2), at 4% hematocrit and incubated at 37°C in 1% O2, 5% CO2 and 94% N2. Parasitemia was assessed by thin blood smear, fixed in 100% methanol and stained in 10% (v/v) GIEMSA (Azur Eosin Methylene-blue), observed under light microscopy at a 1000x oil immersion magnification, on an Olympus CX41 microscope (and Olympus DP22 digital camera).

3.1.2 *P. falciparum* culture synchronisation by sorbitol treatment

Overview. Sorbitol is a sugar that induces lysis of mature parasites-infected erythrocytes, but not of ring-iRBCs or uRBCs [141].

Sorbitol treatment. High ring cultures were centrifuged (5min at 700xg), the cell pellet was resuspended in 4-12ml warm 5% (w/v) sorbitol, and incubated 10min at 37°C. Cells were then washed in incomplete RPMI (iRPMI) and the culture was transferred into a new dish.

3.1.3 Parasite growth inhibition assay

Overview. IC_{50} is the concentration at which 50% of parasite growth is inhibited.

Culture preparation. IC_{50} assays were conducted in a 96-well plate using an asynchronous parasite culture at 0.25% parasitemia in 2% hematocrit, exposed to compounds (see Table 3.3) at concentrations from 0.2nM to 20 or 50µM. 20 or 50µM artemisinin and chloroquine were used as the growth inhibition positive control, while the negative control consisted of the vehicle (typically DMSO), at a volume equivalent to the highest drug concentration. 50µl triplicates of each conditions were prepared and incubated in a humidified chamber at 37°C in a gas mixture of 1% O2, 5% CO2, 94% N2 for 72 hours.

DNA staining. After 72 hours, plates were sealed and placed at -80°C overnight. Once thawed, 140µl of SYBR Gold reaction solution (Table 3.2) was added to each sample to stain double- or single-stranded DNA or RNA and incubated for 1 hour at room temperature protected from light.

Fluorescence reading and analysis. Fluorescence was measured using a CLARIOstar® microplate reader (BMG Labtech) with the following settings: Excitation: 495nm; Emission: 537nm; Gain: 1000; Number of flashes: 20. Data was exported from MARS Data Analysis Software (BMG Labtech) and transformed in Excel. Percentage inhibition was

calculated according to the following formula:

$$1 - \frac{average(sample) - average(Art\&CQ)}{average(DMSO) - average(Art\&CQ)} * 100$$

Percent inhibition was graphed against logarithm of concentration using GraphPad Prism® 7.03 software to produce a non-linear regression (curve fit) indicating the log concentration (µM) at which 50% of parasite growth was inhibited (IC_{50}) (log (inhibitor) vs. response – variable slope – 4 parameters).

Table 3.3: Compounds used in this thesis.

Compound	Provider	Product number
A-1155463	Sapphire Bioscience	S7800
A-1331852	Sapphire Bioscience	S7801
ABT-199	Sapphire Bioscience	A12500
ABT-263	Sapphire Bioscience	A10022
ABT-737	Sapphire Bioscience	A10255
Amiodarone HCl	Selleck Chem	S1979
Apigenin	Selleck Chem	S2262
Artemisinin	Sapphire Bioscience	11816
BAY 43-9006	AdipoGen Life Sciences	AG-CR1-0025
Benzethonium chloride	Selleck Chem	S4162
Chloroquine	Sigma	C6628
Cordycepin	Cayman Chemicals	14426
Ionomycin	ThermoFisher	I24222
Oridonin	Selleck Chem	S2335
WEHI-539	Sapphire Bioscience	S7100

3.1.4 Trophozoite-infected cells enrichment

Overview. As parasites digest haemoglobin, free heme, a toxic component once detached from the protein, is released. To detoxify heme, *Plasmodium* converts it into a pigment called hemozoin. Importantly, hemozoin possesses paramagnetic properties that allow magnetic purification of hemozoin-containing cells (*i.e.* RBCs infected with a mature parasite) [142].

iRBC purification. A high trophozoite culture was loaded on column containing a ferromagnetic matrix (MS Column, Miltenyi Biotec) previously equilibrated with iRPMI, inserted on a VarioMACS™ Separator (Miltenyi Biotec). Flow rate was adjusted to 1 drop per second. Once the culture has completely passed through (but never allowing the matrix to dry), the column was washed with iRPMI until the flow-through appeared clear. After detaching the column from the magnet, infected-RBCs were eluted with 20mL cRPMI, and efficiency of enrichment was assessed by thin blood smear.

3.1.5 Cell counting with a haemocytometer

10µl of homogenously diluted cells were loaded on a counting chamber of a haemocytometer (Neubauer) covered with a glass coverslip. Number of erythrocytes were counted in nine non-adjacent central 'mini-squares' (0.2mm side) using a 400x magnification on an Olympus CX41 microscope (and Olympus DP22 digital camera). The following formula was then applied to estimate the density of cells in the original culture:

$$average\ number\ of\ RBC\ per\ minisquare * 25 * dilution\ factor * 10^4 = results\ in\ cells/ml$$

3.1.6 Immunofluorescence assay (IFA)

500µl of high parasitemia (>5%) mix stages culture was washed in PBS and resuspended in 1ml PBS. All the centrifugation steps were carried out for 1min at 1,600rpm, and all the incubations were performed on a rocker. The cells were fixed for 30min in 1ml 4% (v/v) paraformaldehyde (PFA) and 0.0075% (v/v) glutaraldehyde at room temperature. Samples were then washed in PBS and permeabilised for 10min in 1ml of 0.1% (v/v) Triton X-100 at room temperature. Following another PBS wash, cells were blocked in 3% (v/v) BSA-PBS (cf. Table 3.2) overnight at 4°C. The cells were incubated with the primary antibody (cf. Table 3.5) in 3% (v/v) BSA-PBS overnight at 4°C. Following three PBS washes of 10min each, cells were resuspended in the secondary antibody (cf. Table 3.5) in 3% (v/v/) BSA-PBS for 1h at room temperature in the dark. After three 10min washes in PBS, 2µl of packed cells were added onto a coverslip and mixed with 1µl of 2µg/ml DAPI in VectaShield. A thin coverslip was applied and cells gently spread. The coverslip was finally sealed with nail polish. Cells were imaged on a Zeiss Axioscope microscope in combination with an Orca Digitalcamera (1,000 magnification).

3.2 Eryptosis measurement: Assay designs, Flow Cytometry and Hemolysis

3.2.1 Eryptosis assays and Flow Cytometry Analysis

Overview. Infected and uninfected red blood cells (uRBCs and iRBCs) were analysed by flow cytometry. The presence and developmental stage of the parasite were quantified using a DNA stain (Hoechst) and an RNA stain (Thiazole Orange), as previously described by Grimberg (2011) [143]. Eryptosis hallmarks were also measured: phosphatidylserine (PS) exposure (using Annexin V PE binding), intracellular calcium content (using x-Rhod1 AM or Fluo-4 AM fluorescent dies), cell size (based on forward scatter measurements).

Assay cultures. Assays were conducted in triplicates, with 50µl culture volumes, incubated as described in *P. falciparum in vitro* cultures. Where specified, cells were incubated in incomplete RPMI (iRPMI) instead of complete RPMI (cRPMI). Where specified, cells were incubated in the presence of a a given inhibitor (DMSO was used as a vehicle). As a negative control, cells were incubated in DMSO alone. The volume of DMSO added to

the negative control corresponds to that used in the highest drug concentration condition within the same assay.

Staining procedure. Subsequent centrifugation steps of the 96-well plate were carried out for 5min at 200xg. Cells were washed once in 100µl PBS, then resuspended in the same volume of Thiazole Orange (BD Retic-Count™, BD Bioscience) containing 4µM Hoechst 33342 (Invitrogen), and incubated for 40min at room temperature in the dark. Cells were washed once in staining buffer (Table 3.2), and resuspended in staining buffer containing 0.3µM x-Rhod1 AM (Invitrogren) or 5µM Fluo-4 AM (Abcam), and incubated 30min in the dark. Following another wash, cells were incubated with Annexin V PE (BD Bioscience) (1:20 in staining buffer) for 20min in the dark. Cells were finally centrifuged and resuspended in 200µl staining buffer, and analysed within the hour.

Flow cytometry. Cells were analysed on a CytoFLEX S flow cytometer (Beckman Coulter), where 100,000 total events were recorded for each condition at a flow rate of 10µl/min. Details for channels used, excitation and emission wavelength are shown in table 3.4.

Data analysis. Data was analysed using FlowJo V10. Erythrocytes were gated based on forward scatter height (FSC-H) and side scatter height (SSC-H); uRBCs, ring-, trophozoite- and schizont-iRBCs were gated based on their DNA and RNA content (Hoechst and Thiazole Orange fluorescence); PS exposing cells were gated based on the naïve uRBCs with no drug condition. Mean forward scatter height (FSC-H), percentage of Annexin V positive cells, mean x-Rhod-1 AM fluorescence area (PE-A) or mean Fluo-4 AM fluorescence area (FITC-A) were acquired. For each of these measures, the average over the technical triplicates were kept. The number of independent experiments is specified under each graphic. Graphic representation and statistical analysis were performed using GraphPad Prism 8. Unless stated otherwise, values of individual experiments are shown along with the mean +/- standard deviation (SD). Unless stated ptherwise, When comparing multiple conditions, a one-way ANOVA with multiple Tukey's comparison tests was performed to calculate the p value. When comparing two conditions, a t-test was used.
ns : p>0.05; * : $p \leq 0.05$; ** : $p \leq 0.01$; *** : $p \leq 0.001$; **** : $p \leq 0.0001$.

Table 3.4: Specifications for the flow cytometry settings on CytoFLEX S (Beckman Coulter).

Stain	Provider	Molecular target	Final concentration & incubation time	Excitation max (nm)	Emission max (nm)	CytoFLEX channel name	Laser; Filters
Hoechst 33342	Thermo-Fisher	DNA	4µM; 40min	350	461	PB450	405nm; 450/45 BP
Thiazole Orange (Retic-Count)	BD Bioscience	RNA	100%; 40min	475	530	FITC	488nm; 525/40 BP
PE Annexin V	BD Bioscience	PS exposure on the cell surface	1:20; 20min	496	578	PE	488nm; 585/42 BP
x-Rhod-1 AM	Thermo-Fisher	Intracellular calcium content	300nM; 30min	580	602	PE	488nm; 585/42 BP
Fluo-4 AM	Abcam	Intracellular calcium content	5µM; 30min	475	530	FITC	488nm; 525/40 BP

3.2.2 Hemolysis

Following an incubation in conditioned specified under each graphic, cultures were span down 5min at 200xg and 50µl cell free media was aliquoted for each replicate. Absorbance was read at 405nm using the plate reader CLARIOstar®. The mean of absorbance of the media alone (in triplicate) was subtracted to the mean of the triplicate for each condition. The number of independent experiments is specified under each graphic. Graphic representation and statistical analysis was performed using GraphPad Prism 8. Unless stated otherwise, values of individual experiments are shown along with the mean +/- standard deviation (SD). One-way ANOVA with multiple Tukey's comparison tests or t-test were performed to calculate the p value.
ns : $p>0.05$; * : $p\leq 0.05$; ** : $p \leq 0.01$; *** : $p \leq 0.001$; **** : $p \leq 0.0001$.

3.2.3 Time-course analysis of eryptosis

A *P. falciparum* culture was synchronized with two sorbitol treatments 6h apart. Early morning at the start of the time-course, the culture was sorbitol-treated again, diluted to 1% parasitemia and split into 5ml cultures, in the presence of 10µM BAY 43-9006, 1µM WEHI-539 or the equivalent volume of DMSO, in triplicate for each condition. Every 12h for the following 84h, a thin blood smear of each condition was made, and flow cytometry analysis (described above, with x-Rhod-1 AM as the calcium dye) of each replicate of each condition was conducted. In addition to the measures mentioned in the flow cytometry analysis section, mean Hoechst fluorescence area (PB450-A), mean Thiazole Orange fluorescence

area (FITC-A) and percentage of Hoechst positive cells (parasitemia – percentage of iRBCs) were collected.

3.2.4 Conditioned media 1 (asynchronous, filter 0.45µm or 0.22µm; 48h)

Objective. To test the impact of parasite secreted factors on eryptosis, we incubated fresh RBCs with conditioned media from parasite cultures or from uRBC cultures.

Conditioned media 1. An asynchronous *P. falciparum* culture and a culture of naïve uRBCs were incubated in cRPMI for 48h. This conditioned media was collected following two centrifugation steps (5min at 700xg) and was filtered using a 0.22µm or a 0.45µm filter, to exclude bigger EVs or simply exclude merozoites and cell debris respectively. Fresh uRBCs were added (for a final hematocrit of 4%), and distributed in triplicates, along with a cRPMI control condition. These cultures were incubated 48h, after which flow cytometry analysis was performed.

3.2.5 Conditioned media 2 (synchronous, glucose supplementation)

Objective. To test the impact of parasite secreted factors on eryptosis of uRBCs, excluding those secreted upon schizont egress, and to test the contribution of glucose depletion, we incubated fresh RBCs with conditioned media from synchronised parasite cultures or from uRBC cultures, supplemented or not with glucose.

Conditioned media 2. A synchronized culture of high parasitemia rings (>6%) and a culture of uRBCs were incubated 24h in cRPMI. This conditioned medium was then collected following two centrifugation steps (5min at 700xg); pH was measured; conditioned medium was filtered through a 0.22µm filter. 11mM glucose was added or not in each conditioned medium. Fresh uRBCs (washed once in iRPMI) were then added to create a 5ml culture at 4% hematocrit. A control culture was also prepared with cRPMI. Cultures were incubated in usual *Plasmodium* conditions for 2, 4 and 7 days. At each time point, a thin blood smear was prepared, and each condition was aliquoted in triplicate in a 96-well plate to conduct flow cytometry analysis. Hemolysis assays were also conducted, using the original conditioned media (cRPMI, uRBC or iRBC conditioned media) as a blank.

3.3 Extracellular Vesicles (EVs)

3.3.1 EVs enrichment

Cultures. Nine 30ml cultures of synchronized, high parasitemia (>6% rings) were sorbitol-treated at the beginning of the EVs enrichment process. Nine 30ml cultures of uRBCs were prepared. Media was harvested after 30h incubation in this media (*i.e.* collect EVs produced by both ring and trophozoite stages).

Media harvest. Medium was collected following a number of centrifugation steps to eliminate cells and debris: twice 5min at 700xg; 10min at 3,000rpm at 4°C; 1h at 10,500rpm

at 4°C (using a Sorvall RC 5 Plus high speed centrifuge, rotor SLA-1500). At all time, the medium was maintained on ice / at 4°C. Supernatant was then filtered through a 0.45µm filter unit.

EVs concentration. Vivacell® 100 100,000 MWCO PES (Sartorius) were used to concentrate EVs and eliminate smaller molecules. The centrifugation steps were carried out at 4°C at 700xg, for 5min, unless stated otherwise, in a swing out rotor. Vivacell® units were washed with 70% (v/v) ethanol, and twice with sterile MilliQ water. The filtered medium was then added, concentrated (*i.e.* centrifuged) and the concentrated fraction gently transferred to an ultracentrifuge tube. This was repeated for the remain of the medium. Typically, 30min centrifugation for 50ml medium was required. Vivacell® units were reused: washed twice with MilliQ water, soaked 30min at 37°C with a slow shake (60RPM) in 60% ethanol 40% 1M HCl, washed twice with MilliQ water, and kept at 4°C in 20% ethanol.

Ultracentrifugation. DPBS (Gibco) was used to balance the tubes. Filtered, concentrated media was ultracentrifuged overnight (no more than 16h) at 37,000 RPM at 4°C, in a Hitachi Ultracentrifuge CP100NX (fixed angle rotor P70AT-1285). The pellet was then gently washed with 1ml cold DPBS, and carefully resuspended in 100-200µl iRPMI and kept at 4°C until use (the time required to analyse them with ZetaView® and prepare the Transmission Electron Microscopy samples).

3.3.2 Nanoparticle Tracking Analysis of EVs

Overview. Nanoparticle tracking analysis (NTA), such as the ZetaView® analyser, uses the Brownian movements of particles (captured on videos) to calculate some of their physical parameters (size, concentration, surface charge) (as described in the manufacturer's website https://www.particle-metrix.de/en/products/zetaview-nanoparticle-tracking).

Nanoparticle Tracking Analysis. NTA was performed using ZetaView® Basic PMX-120. Briefly, the standard NTA cell cassette was cleaned with water and PBS. Autofocus and alignment were performed using 102nm polystyrene beads (ThermoFisher) diluted 1:250,000 in DPBS. Samples were diluted at different concentrations in DPBS to reach an acceptable number of particles per frame (50-200 particles/frame); 1ml of sample was injected and the cell was cleaned between each sample/dilution. For each measurement, 60 frames captured per second for 11 positions. The CMOS camera sensitivity was 80. The cell temperature was 25°C. Laser settings were 68mW at 405nm. After capture, analysis was performed by ZetaView Software 8.05.12 SP1.

3.3.3 Transmission Electron Microscopy (TEM) imaging of EVs

TEM imaging was performed with the kind help of Dr Julian Ratcliffe from the La Trobe BioImaging Platform. Glow discharge of carbon-coated grids 300 mesh (ProSciTech) was performed for 1min at 20mA sputtering, at a pressure of $2x10^{-1}$mbar (Emitech K950X with K350 power supply). 5µl of EVs (diluted 1:50-1:20 in iRPMI) were added to the grid and

allowed to settle for 1min. Excess liquid was blotted off, 5µl of 2% (w/v) uranyl acetate (Bio-Rad) was added for 10sec, excess liquid blotted off again, and staining repeated once more. TEM images were taken using a Jeol JEM-2100 instrument, at 200kV. A minimum of 20 images of each EV samples were taken. Images were analysed with a GMS 3 software. The size of 92 uRBC-derived EVs and 62-iRBC-derived EVs were measured manually on the GMS 3 software, and plotted using GraphPad Prism 8, as a violin plot which shows the median, the 25^{th} and 75^{th} quartiles. A Kolmogorov-Smirnov test was used to test the difference in size between uRBC- and iRBC-derived EVs.

3.3.4 EVs incubation with fresh uRBCs

Using the particle concentration measured on the ZetaView, a controlled number of EVs (from 10^5 to 10^8 EVs per µl of culture) were added to uRBC cultures which contained fresh uRBCs (washed in iRPMI) at 4% hematocrit, in iRPMI. Triplicates of 50µl were prepared and incubated 48h before flow cytrometry analysis. A culture of the same uRBCs in iRPMI (no EVs added) was prepared as negative control.

3.4 Protein work

3.4.1 Protein extraction: MPER - Whole cell

Overview. M-PER™ (Thermo Scientific) is a commercially available Mammalian Protein Extraction Reagent, which lyses mammalian membranes.

Protein preparation. uRBCs and magnet-purified trophozoite-iRBCs cell numbers were determined using a hemocytometer. For Western Blots, 10^8 cells were dispensed in microcentrifuge tubes, resuspended in 80µl of MPER PPI (see Table 3.2 for details) and incubated 10min on ice. For immunoprecipitation (IP), 10^9 cells were lysed with 800µl MPER PPI for 15min.

Post-treatment. Haemoglobin was removed for Western Blots but not for immunoprecipitations (see 'Haemoglobin removal' or 'Immunoprecipitation' sections).

3.4.2 Protein extraction: Saponin supernatant - RBC's cytosol

Overview. Saponin is a molecule extracted from *Quillaja* bark, and typically used to isolate the parasites from its host erythrocyte. Saponin solubilises the erythrocytic and parasitophorous vacuole membranes, but leaves the parasite's membrane intact [144]. Here, we use saponin to separate the erythrocyte cytosolic proteins (soluble fraction) from the parasite's and the membranes' proteins (insoluble fraction).

Protein preparation. uRBCs were counted, trophozoite-iRBCs were magnet-purified and counted: for Western blot application, 10^8 cells were typically dispensed in microcentrifuge tubes, and dry cells resuspended in 160µl of 0.1% saponin PPI (see Table 3.2 for details) and incubated 10min on ice. For mass spectrometry analysis, 10^9 cells were resuspended

in 600µl 0.1% saponin PPI. After lysis, samples were centrifuged 5min at 16,200xg at 4°C. The supernatant was carefully collected.

Post-treatment. For both Western Blots and proteomics analysis, haemoglobin was subsequently removed (see 'Haemoglobin removal' section for more information).

3.4.3 Protein extraction: Saponin pellet - RBC's membrane (and parasite)

After saponin lysis, centrifugation, and removal of the supernatant, the pellet was lysed a second time with 300µl 0.15% saponin PPI (see Table 3.2). The sample was incubated 10min on ice, centrifuged 5min at max speed at 4°C. The pellet was washed three times with 500µl PBS PPI to ensure removal of haemoglobin and other RBCs cytosolic proteins (centrifugation steps carried out for 5min at 16,200xg at 4°C). Finally, samples were denatured with Laemmli Buffer, boiled at 98°C for 5min and stored at -20°C.

3.4.4 Haemoglobin removal

Overview. Haemoglobin represents 97% of all RBCs' proteins[124]. This sur-representation of haemoglobin makes it difficult to identify and detect other proteins. For certain applications (here, Western Blots and generation of a mass spectrometry peptide library), it was therefore necessary to deplete protein samples from haemoglobin. This was done using TALON® Metal Affinity Resin (Takara). These beads are coupled to cobalt ions and were developed for purification of His-tagged proteins. The interaction between positively charged cobalt and negatively charged haemoglobin allows depleting samples from haemoglobin [145].

Haemoglobin removal. TALON resin was thoroughly resuspended and washed in an equal volume of PBS PPI (see table 3.2), with centrifugation steps carried out for 2min at 600xg. Protein samples (MPER or saponin supernatant) were added on the resin. 100µl of resin slurry was typically used for MPER samples (10^8 cells with 80µl MPER PPI), 300µl resin for the saponin supernatant samples (10^8 cells with 160µl 0.1% saponin PPI), and 600µl of resin for the proteomic analysis (10^9 cells in 600µl 0.1% saponin PPI). Protein samples were then incubated with this resin 10min at 4°C on a rotating wheel, to allow a thorough mixing. After that, samples were centrifuged (2min at 2,400rpm). If the supernatant was still red (*i.e.* if it still contained haemoglobin), it was added on freshly washed beads, and incubated again at 4°C. Otherwise, the supernatant was transferred into a clean microcentrifuge tube, centrifuged 2min at 2,400xg, and transferred into a final clean tube (this step was repeated until all beads were removed).

Post-treatment. For Western blot applications, samples were denatured with Laemmli Buffer, boiled at 98°C for 5min and stored at -20°C.

3.4.5 Western Blots

Gel run. The equivalent of 10^7 cells were added per lane in a Mini-PROTEAN® TGX™ pre-cast 4-15% gel, along with 5-8µl of Precision Plus Protein™ Standards (10 to 250kDa), and 3-8µl of MDA-MB 231 (breast cancer cell line) protein sample, kindly provided by Dr Delphine Merino (Olivia Newton-John Institute). The gel was assembled on a Mini-PROTEAN® Tetra Vertical Electrophoresis cell and run with 1X running buffer (see table 3.2) at 160V for 40min. Stain free gels were activated, and a total protein image taken using a ChemiDoc MP (auto-activation and rapid auto-exposure) to ensure correct run of proteins.

Membrane transfer. Proteins were transferred onto mini PVDF membranes (0.2µm) using a Trans-Blot® Turbo™. Briefly, the membrane was soaked in 100% methanol until translucent, then soaked in 1X transfer buffer (see table 3.2), along with two transfer stacks. The appropriate Turbo transfer program was used. Finally, efficiency of transfer was assessed by imaging stain-free total protein on the ChemiDoc MP.

Membrane probing. The membrane was washed twice with TBST and blocked overnight at 4°C with a slow shake in 5% BSA-TBST. After a couple of washes with TBST, the membrane was probed with primary antibody in 5% BSA-TBST (with 0.02% sodium azide to prevent growth of microbes). Typically, a 1:1,000 or 1:5,000 dilution was used (see details in table 3.5); the membrane was probed overnight at 4°C, with a slow rotation. After 3 washes of 10min each in TBST, the membrane was probed with the secondary antibody (1:5,000 dilution of anti-rabbit- or anti-mouse-HRP (Cell Signaling) in 5% BSA-TBST) for 1h at room temperature with a slow shake. The membrane was then washed 3x 10min in TBST and incubated with ECL solution for 5min. The membrane was imaged using the ChemiDoc MP: with auto-exposure, manual signal accumulation mode (*e.g.* 10 images from 10sec to 15min) and colorimetric imaging. Image analysis was carried out using Image Lab™ 6.0.1 (BioRad).

Membrane stripping and storage. The membrane was rinsed in TBST, stripped with Restore™ Western Blot Stripping Buffer (Thermo Scientific) for 15min at room temperature with a slow shake, washed 3x 10min in TBST, and blocked again. After last use, the membrane was air dried and stored in a plastic zip-log bag.

Table 3.5: Antibodies used in this thesis. WB: Western blot. IP: Immunoprecipitation. IFA: Immunofluorescent Assay

Antibody against:	**Provider**	**Product number**	**Origin**	**Purpose**	**Dilution**
BAD	Cell Signaling	9239	Rabbit	IFA	1:150
BCL-x_L	Cell Signaling	2764	Rabbit	WB	1:1,000
				IP	1:100
	Santa Cruz	sc-8392	Mouse	IFA	1:150
µ-Calpain (Calpain 1)	Cell Signaling	2556	Rabbit	WB	1:1,000
Carbonic Anhydrase I	Abcam	ab108367	1:4,000	WB (Fig6.6)	1:4,000
	ThermoFisher	PA5-49698	Rabbit	WB (Fig6.9)	1:4,000
PfHSP70.1	Kindly provided by Prof Gilson and Prof Crabb (Burnet institute)	N/A	Rabbit	WB	1:5,000
PfHSP101	Kindly provided by Prof Gilson and Prof Crabb (Burnet institute)	N/A	Rabbit	WB	1:5,000
Protein 4.1	Kindly provided by Dr Proellocks and Prof Cooke (Monash university)	N/A	Rabbit	WB	1:500
Spectrin	Sigma Aldrich	S1515	Rabbit	WB	1:10,000
Rabbit-HRP	Cell Signaling	7074	N/A	WB (secondary antibody)	1:5,000
Rabbit-Alexa Fluor 594	Cell Signaling	8889	N/A	IFA (secondary antibody)	1:1,000
Mouse-HRP	Cell Signaling	7076	N/A	WB (secondary antibody)	1:5,000
Mouse-Alexa Fluor 488	Cell Signaling	4408	N/A	IFA (secondary antibody)	1:1,000

3.4.6 Proteomics and Phosphoproteomics: peptide library

Samples. A total of 10^{10} uRBCs and 10^{10} iRBCs were prepared by saponin lysis, keeping only the supernatant (*i.e.* cytosolic fraction of the RBCs) and depleting haemoglobin as described above (Sections 3.1.4, 3.1.5, 3.4.2 and 3.4.4). The cells were collected 10^9 uRBCs and 10^9 iRBCs at a time, using different batches of donors. Following removal of haemoglobin, proteins were precipitated from the sample using 1:20 (v/v) trichloroacetic acid (TCA), incubated for 10min on ice, pelleted (5min at 16,200xg, 4°C), then washed with 1ml of acetone (5min at 16,200xg, 4°C). Acetone was removed and pellets were dried out for 30sec at 95°C, and finally stored at -80°C until further preparation. All the subsequent steps were performed with (peptide preparation) or by (data acquisition and analysis) Dr Ghizal Siddiqui (Creek Laboratory, Monash Institute of Pharmaceutical Sciences).

Peptide preparation. Cold 4% sodium deoxycholate (SDC) in 100mM HEPES was added to each pellet (1ml per 100µl pellet size), heated at 90°C for 5min, and sonicated 3 times for 30sec (Model Q55, Qsonica). Once the samples had reached room temperature, TCEP and iodoacetamide were added (final concentrations of 10mM and 40mM respectively (Table 3.2), and samples were heated again for 5min at 95°C. Samples were centrifuged for 5min at 21,000xg at 4°C to remove any insoluble material. A Bicinchonic Acid (BCA) assay (ThermoFisher Scientific) was conducted to measure the protein concentration as per manufacturer's protocol. Quickly, BSA standards were prepared (concentrations from 125µg/ml to 2,000µg/ml), samples and BSA solutions were dispensed in triplicate, the BCA reagent was added and incubated for 30min at 37°C, and colorimetry measured using a plate-reader (Perkin Elmer Ensight Plate Reader). Once the samples' concentrations have been measured, 20µg of trypsin (Promega) was added per mg of sample and incubated overnight at 37°C while shaking (2000rpm) (Multi-Therm, Benchmark). The following day, samples were pooled together and acidified using 5% (v/v) formic acid. SDC was removed by adding an equal volume of 100% (v/v) ethyl acetate, samples were vortexed and then centrifuged at 2,000xg for 5min to remove to upper layer (hydrophobic peptides and the detergent SDC). MilliQ water was then added to the pooled sample to dilute concentration of 100mM HEPES to 20mM prior to fractionation.

Fractionation. Fractionation of peptides was conducted using a strong cation exchange (SCX) column (Agilent), as previously described [146]. The SCX cartridge was fitted into a vacuum manifold apparatus (Waters), and set for a flow of 1 drop per second. The column was activated with 1ml of 100% (v/v) methanol, washed with 1ml of 0.1% (v/v) formic acid. Samples were loaded onto the SCX column, which was then washed three times with 1ml of 50% (v/v) ethyl acetate and 0.5% (v/v) formic acid, then washed three times with 1ml of 0.1% (v/v) formic acid. The peptides were eluted in fractions using 500µl of SCX elution solutions 1-12 (Table 3.2). Fractions were dried using a Speedvac (Labconco). Fractions were then resuspended in 100mM Tris-HCl (up to 300µl).

Phosphopeptide enrichment. The enrichment of phosphopeptides was done using the EasyPhos (EP) method [147]. 400µl of 100% (v/v) isopropanol was added to the samples,

and mixed using a thermal shaker (Multi-Therm, Benchmark) at 1,500rpm for 30sec. 100µl of EP enrichment solution (Table 3.2) was then added and the samples mixed again. To eliminate any precipitates, the samples were centrifuged at 2,000xg for 15min. For 300µg of peptides, 5mg of TiO_2 beads (Kinesis) were weighted and resuspended in EP loading buffer (Table 3.2) at a concentration of 1mg/µl. Beads were thoroughly resuspended and added to the samples: phosphopeptides were allowed to bind to the TiO_2 beads for 5min at 40°C at 1,500rpm. Beads were pelleted at 2,000xg for 1min: the supernatant (containing non-phosphorylated peptides) was collected in clean tubes and desalted (see "Desalting proteomics samples"). The beads were washed four times in 1ml of EP wash buffer (Table 3.2) (vortexed, shaken at 1,500rpm for 30sec, centrifuged at 1,000xg for 1min). The beads were resuspended in a total of 150µl of EP transfer buffer (Table 3.2), in two steps, and loaded onto C8 stage tips. C8 stage tips consisted of a 200µl pipette tip containing one layer of C8 material (Thermofisher Scientific), mounted onto a microcentrifuge tube. These were centrifuged until complete dryness at 1,500xg (for at least 7min). The stage tips were mounted onto new microcentrifuge tubes and phosphopeptides were eluted twice using 30µl of EP elution buffer (Table 3.2) and centrifugation at 1,500xg until dryness. Samples were then partially dried using Speedvac, until their volume was less than 15µl, and desalted (see "Desalting phosphoproteomics samples").

Desalting proteomics samples. The unbound peptides were dried down to 50µl. 100µl of 0.1% (v/v) formic acid was added, and the pH was adjusted to 2-3 using 2M NaOH. C18 stage tips were made to desalt these proteomics samples: two layers of C18 material (Thermofisher Scientific) were added into a 200µl pipette tip, as previously described [148] and mounted on microcentrifuge tubes. The C18 stage tips were activated with 40µl methanol. All centrifuge steps were performed at 1,200xg at room temperature until all liquid had passed through the tips. Stage tips were then washed twice with 40µl of 0.1% (v/v) formic acid. The samples were loaded, span down, the stage tips were washed three times using 50µl of 0.1% formic acid. The samples were eluted into clean tubes with 100µl of C18 elution buffer (Table 3.2) in two steps, with a centrifugation at 800xg for 5min. Samples were then dried using Speedvac until complete dryness. Finally, proteomics samples were resuspended in 12µl of MS loading solution (Table 3.2), sonicated in a waterbath (Soniclean) for 15min and then agitated on a centrifuge/vortex multispin instrument (MSC-600, BioSan) for 10 cycles (vortexed at maximum speed for 15sec and centrifuged at 6,000xg for 10sec). Samples were stored at -80°C until required for LC-MS/MS analysis (see "Data Independent Acquisition").

Desalting phosphoproteomics samples. SDB-RPS stage tips were made to desalt phosphoproteomic samples: two layers of styrenedivinylbenzene-reverse phase sulfonate (SDB-RPS) material (Thermofisher Scientific) were added into 200µl pipette tips, mounted on microcentrifuge tubes. 100µl of SDB-RPS loading buffer (Table 3.2) was added to samples, loaded in the stage tips, and centrifuges at 1,500xg for 8min (or until dryness). The stage tips were washed once with 100µl of SDB-RPS wash buffer 1, then with 100µl of SDB-RPS wash buffer 2 (Table 3.2), and finally eluted with 60µl of SDB-RPS elution buffer (Table 3.2)

into clean tubes. Samples were then dried using Speedvac until complete dryness. Finally, phosphoproteomics samples were resuspended in 7µl of MS loading solution (Table 3.2), sonicated in a waterbath (Soniclean) for 15min and then agitated on a centrifuge/vortex multispin instrument (MSC-600, BioSan) for 10 cycles. Samples were stored at -80°C until required for LC-MS/MS analysis (see "Data Independent Acquisition").

Data Dependent Acquisition. LC-MS/MS analysis was performed as described previously [149, 146]. Briefly, a nanoLC (Thermofisher Scientific) paired with a Q-Exactive Orbitrap Mass Spectrometer (Thermofisher Scientific) was used for LC-MS/MS analysis. Samples (2µl for proteomics; 6µl for phosphoproteomics) were loaded onto a reversed-phase trap column (Acclaim PepMap media, 100µm x 2cm; Dionex) at a flow rate of 15µl/min at 40°C. Peptides were then separated over a reversed-phase capillary column (LC Packing, 75µm x 50cm; Dionex) at a flow rate of 0.250µL/min over a 158min gradient. Mobile phase (A) was 0.1% (v/v) formic acid and mobile phase (B) was 100% (v/v) acetonitrile. The gradient reached 30% mobile phase (B) at 123min, increased to 34% (B) at 126min, increased to 79.2% (B) at 131min, decreased to 2% (B) at 138min and held at 2% (B) until 158min. The MS operated in DDA mode at a mass resolution of 70,000 from m/z 375-1575 Da in positive ionisation mode. The 20 most abundant precursor peptides with charge states 2-6 were selected for fragmentation with a normalised collision energy of 27.0, an activation time of 15 milliseconds and dynamic exclusion enabled.

DDA analysis. The Maxquant (version 1.6.0.1) analysis software was used to analysed DDA data, as previously described [150]. The DDA files were searched against *P. falciparum* (UP000001450, release version 2016_04) and *Homo sapiens* (UP000005640, release version 2017_05) UniProt fasta database and the Biognosys iRT peptides database. Carbamidomethylation of cysteines was set as a fixed modification. Oxidation of methionine, and protein N-terminal acetylation were set as variable modifications. Parent mass error tolerance and fragment mass tolerance were set at 20ppm, and the false discovery rate at 1%. For phosphoproteomics, the same default setting as above was used with the exception that Phospho(STY) was also included as variable modification. MaxQuant search results were imported as spectral libraries into Spectronaut with default settings.

The peptide libraries (both proteomics and phosphoproteomics) are available with this thesis.

3.4.7 BCL-x_L ImmunoPrecipitation (IP)

Objective. To investigate the role of erythrocyte BCL-x_L during infection, I investigated the changes in BCL-x_L binding partners. To do so, I immunoprecipitated BCL-x_L from uRBCs and from iRBCs, exposed or not to the BCL-x_L inhibitor WEHI-539.

Beads preparation. In microcentrifuge tubes, 50µl of Protein A magnetic beads (GenScript) slurry was washed 3x with 500µl TBST and resuspended in 200µl TBST (control without antibody) or in 200µl TBST with 1:100 anti-BCL-x_L antibody (Cell Signaling

#2764). Beads were incubated overnight at 4°C on a rotating wheel. The following day, unbound antibodies were removed: beads supernatant was discarded and the beads were washed gently 3x in 500µl TBST-PPI (Table 3.2).

uRBCs and iRBCS preparation. Parasites from 10x 30ml cultures of synchronised trophozoites (>8% parasitemia) were magnet-purified and placed back in culture: half of the sample was incubated in 30ml cRPMI containing 10µM WEHI-539, the other half in 30ml cRPMI with an equivalent volume of DMSO and then incubated at 37°C in low oxygen conditions for 4h. Similarly, 10µM WEHI-539 or DMSO was added to a 10ml fresh RBCs culture and incubated 4h in identical conditions.

Protein preparation and incubation. 10^9 cells (uRBCs or magnet-purified iRBCs, exposed or not to WEHI-539) were lysed with MPER-PPI as described in section 3.4.1, and added to the washed beads. For the controls where beads alone (*i.e.* no antibody) were used, the samples consisted of $5x10^8$ WEHI-539-treated cells and $5x10^8$ DMSO-treated cells. The samples were incubated overnight at 4°C on a rotating wheel.

BCL-X_L pull-down. The following day, unbound proteins were removed: supernatant was discarded, the beads were gently washed 3-5x in 1ml TBST-PPI (Table 3.2). Finally, beads were resuspended in 100µl 4X Laemmli buffer, boiled 5min on a 95°C heat-bloc and kept at -20°C before mass spectrometry analysis. A $1/10^{th}$ of the samples was analysed by Western Blot to confirm presence of BCL-x_L in the immunoprecipitate.

3.4.8 Mass spectrometry analysis of BCL-x_L IP

The mass spectrometry sample preparation and acquisition were performed by Dr Ghizal Siddiqui (Creek Laboratory, Monash Institute of Pharmaceutical Sciences). I analysed the results with her guidance and input.

Mass spectrometry samples preparation. The samples were pelleted by centrifugation for 3min at 21,100xg at 4 °C, and the supernatants (100µl) of each sample were resolved on a pre-cast 1D PAGE gel (Mini-PROTEAN® TGXTM, Bio-Rad Laboratories) using 1x mix of a 10x pre-mixed electrophoresis buffer (25mM Tris, 192mM glycine, 0.1% SDS, pH 8.3, BioRad) at 200V / 0.04A / 8W for 5min. The gel was incubated in Instant Blue stain (Expedion Ltd) for 30min on a shaker to fix and visualize the protein bands. MilliQ water was then used to de-stain the gel for 1h (fresh MilliQ water every 20min) prior to further processing. Briefly, the entire region where the proteins had resolved were excised and subjected to an in-gel trypsin digestion procedure, as described previously [151]. Peptides were extracted, dried in a Speed-Vac, and stored at -20°C until analysis. On the day of analysis, samples were reconsituted in 20µl of 2% acetonitrile (ACN), 0.1% formic acid and LC-MS/MS analysis was carried out as previously described with minor modifications [149]. Reconstituted samples were loaded as per above data independent acquisition. For label-free proteomics analysis, the HPLC gradient was set to 98min using a gradient that reached 30% ACN after 63min, 34% after 66min, 79.2% after 71min for 6min, following which there was an equilibration phase of 20min at 2% ACN. Peptide sequences (and protein identity) were

determined using the MaxQuant software (version 1.6.0.1) by matching protein database *P. falciparum* (UP000001450, release version 2016_04) and *Homo sapiens* (UP000005640, release version 2017_05) uniport fasta database and label free quantification of identified proteins was then carried out as previously described [151].

Data analysis. Potential contaminants, reversely identified peptides and proteins only identified by site were removed. The Q-value threshold was set at 10^{-2}. The number of LFQ intensities were used in the analysis as an indication of the protein being identified; subsequently the average of LFQ intensities over replicates were sometimes also used. BCL-x_L was successfully identified in all IPs (3 to 6 peptides in each replicate; n=4 for uRBC DMSO, uRBC WEHI-539 and iRBC WEHI-539; n=5 for iRBC DMSO). A single peptide was identified in a beads-alone control of iRBC, otherwise BCL-x_L was not identified in beads-alone controls (n=3 for iRBC; n=2 for uRBC). Identified BCL-xL peptides were aligned with the full length BCL-x_L sequence using the https://blast.ncbi.nlm.nih.gov/ website. BH domains, transmembrane domain, phosphorylation sites and caspase 1 cleavage site on BCL-x_L were extracted from UniProt. Proteins identified (even once) in the beads alone controls were deleted. For proteins identified in uRBC DMSO but not uRBC WEHI-539, we selected all proteins with LFQ intensity counts of 2 or more from uRBC DMSO, and we accepted proteins with LFQ intensity counts of 0 or 1 from uRBC WEHI-539. Proteins are then shown with decreasing average LFQ intensities for uRBC DMSO. Highlighted are the ones with the most interesting characteristics (largest difference of counts and/or intensities between DMSO and WEHI-539 conditions). Similar analysis was done for proteins identified in iRBC DMSO but not iRBC WEHI-539; and for proteins identified in iRBC DMSO, but neither iRBC WEHI-539 nor uRBC DMSO.

Chapter 4

Effect of eryptosis inducers on *Plasmodium falciparum* infection & Recent additions to the study of the Raf inhibitor BAY 43-9006

This chapter consists of two parts:

- an article under revision at Frontiers in Cellular and Infection Microbiology (2020) entitled "Previously described eryptosis inducers impair *Plasmodium falciparum* growth via an eryptosis-independent mechanism", authored by C. Boulet, TL. Gaynor and TG. Carvalho. In this article, we investigated the best methodology to measure eryptosis hallmarks within a *P. falciparum in vitro* culture. We tested a subset of eryptosis inducers and discovered that, while some impaired parasite development, they were doing so without inducing eryptosis.
- a report on additional work on one of these eryptosis inducers displaying an antimalarial activity discussed in the paper above: the Raf kinase inhibitor, BAY 43-9006.

(A) Previously described eryptosis inducers impair *Plasmodium falciparum* growth via an eryptosis-independent mechanism

C. Boulet, TL. Gaynor and TC. Carvalho, under revision at *Front Cell Inf Microbiol* (2020)

4.1 Abstract

Erythrocytes possess an unusual programmed cell death mechanism termed eryptosis. Several compounds have been shown to induce eryptosis *in vitro*. Malaria parasites (genus *Plasmodium*) reside in erythrocytes during the pathogenic part of their life cycle, and the potential of several eryptosis inducers to act as antimalarials has been tested in recent years. However, the eryptosis-inducing capacity of these compounds varies significantly between erythrocyte biology findings and malaria investigations. In this study, we investigated the reasons for these discrepancies. We show that eryptosis induction *in vitro* is dependent on culture conditions and that some compounds do not induce eryptosis when culture parameters that closely mimic physiological conditions are used. We demonstrate that six "eryptosis-inducing" compounds (selected on the basis of their current or prospected clinical use, known molecular target and/or antimalarial activities) do not affect the viability of naïve or *P. falciparum*-infected erythrocytes *in vitro*. Further, three of these compounds do impair parasite development *in vitro*, but this occurs through a mechanism that is not related to eryptosis. Careful consideration of the experimental set up is key for the accurate assessment of eryptosis-inducing potential of compounds and their evaluation as potential antimalarials. The identification of three "eryptosis inducers" with antiparasitic effects independent of eryptosis opens exciting new research avenues for malarial drug discovery.

4.2 Introduction

Malaria is a devastating infectious disease that considerably affects the lives of millions worldwide. Despite a recent global decrease in malaria incidence, malaria cases continue to increase in high burden countries [1]. Challenges, such as the lack of a long-lasting efficient vaccine and the spread of antimalarial drug resistance, represent a serious threat to malaria elimination [152, 153]. Therefore, novel alternative treatment options are urgently needed. Infection of erythrocytes by *Plasmodium spp.* parasites leads to the development of all symptoms associated with malaria, hence most antimalarials developed to date target the parasite in its blood stages. However, parasites quickly develop resistance against these antimalarials. For this reason, host-directed therapies have emerged in recent years as an attractive and novel strategy to tackle malaria [114], combining a reduced likelihood for drug resistance to emerge and drug repurposing opportunities. Many intracellular pathogens, including the *Plasmodium* liver stages [107], have been shown to inhibit or delay host cell death pathways to promote their own survival. As such, host cell death factors appear as ideal targets for antipathogen therapeutics [154]. Further, compounds that inhibit human cell death factors are available, many of which were developed for cancer therapies, and could be utilised in the development of new host-directed therapeutics for malaria.

Erythrocytes display a form of programmed cell death distinct from senescence termed eryptosis [112]. Eryptosis hallmarks closely resemble those of apoptosis and include (i) an increase in intracellular calcium levels, (ii) phosphatidylserine (PS) exposure to the cell surface (leading to erythrocyte clearance by macrophages), (iii) cell shrinkage and (iv) membrane blebbing [112, 155]. The potential of eryptosis-inducer compounds in antimalarial drug discovery has drawn attention in recent years [156, 157]. Most of the eryptosis-inducers tested affect parasite viability *in vitro* and in murine models [71]. However, although all eryptosis-inducers did induce PS exposure of infected erythrocytes, less than half of those tested *in vitro* induced PS exposure of uninfected erythrocytes [71]. This unexpected observation might stem from significant differences in the experimental approaches used. Indeed, eryptosis-focused studies maintain erythrocytes in Ringer solution (a basic saline buffer), at 0.4% hematocrit – conditions that would not support *Plasmodium* growth [158]. On the other hand, *Plasmodium in vitro* cultures are conducted in RPMI 1640 media complemented with Albumax (a serum replacement) at 4% hematocrit [140].

To address major discrepancies in the literature and to interrogate the potential of eryptosis inducers as antimalarial candidates, we compared cell culture methodologies used for uninfected erythrocytes and for erythrocytes infected with *P. falciparum*, the most virulent human malaria parasite. Our study demonstrates that little PS exposure and hemolysis of uninfected cells are observed when used in *Plasmodium* culture conditions, compared to erythrocytes-only culture conditions. We identify this discrepancy as being predominantly attributed to Albumax supplementation. Further, none of the eryptosis-inducers tested induced eryptosis of naïve or *P. falciparum*-infected erythrocytes in our culture

conditions, although three compounds impaired *P. falciparum* growth *in vitro*. Overall, the present study unveils reasons behind discrepancies observed between eryptosis-focused studies and those conducted in the context of malaria infections. Moreover, we have shown that "eryptosis-inducers" exert their antiparasitic effects independently of eryptosis. We explore and discuss the potential of the compounds tested in this study as antimalarials, considering their current and potential use in the clinic.

4.3 Methods

4.3.1 *In vitro* cell culture

Use of human erythrocytes was approved by the La Trobe University Research Ethics Committee (ethics number HEC17-013) and an Australian Red Cross Blood Service Agreement (Deed 19-05VIC-01). Naïve (non-infected) erythrocytes and *Plasmodium falciparum* 3D7-infected erythrocytes were cultured at 37°C, in low oxygen conditions (1% O_2, 5% CO_2, 94% N_2), at 4% or 0.4% hematocrit, in incomplete RPMI media (RPMI 1640 HEPES, 50mg/L hypoxanthine, 10mg/L gentamicin, pH 6.74), complete RPMI media (incomplete RPMI supplemented with 2.25g/L sodium bicarbonate and 5g/L AlbuMAX II) or Ringer solution (1mM $CaCl_2$, 5mM glucose, 32mM HEPES pH 7.4, 5mM KCl, 1mM $MgSO_4$, 125mM NaCl). *P. falciparum* standard *in vitro* culture conditions were conducted as previously described [140].

4.3.2 Eryptosis assay and flow cytometry analysis

Previously described eryptosis inducers were selected based on their use (or potential use) in the clinic, their known targets and/or their previously described antimalarial activity (Table 4.1): amiodarone HCl (Selleck Chem, #S1979), apigenin (Selleck Chem, #S2262), BAY 43-9006 (AdipoGen Life Sciences, #AG-CR1-0025), benzethonium chloride (Selleck Chem, #S4162), cordycepin (Cayman Chemicals, #14426), ionomycin (ThermoFisher, #I24222) and oridonin (Selleck Chem, #S2335). Drug assays measuring eryptosis were carried out in 100µl or 500µl culture when using 4% or 0.4% hematocrit conditions, respectively. DMSO, the vehicle, was used for the no-drug conditions. Cells were incubated at 37°C, in low oxygen conditions for 1h - 48h depending on the assay. Each experiment was performed in triplicate unless otherwise indicated and cells were analysed by flow cytometry. Cells were washed in PBS, resuspended in Thiazole Orange (BD Retic-Count™, BD Bioscience) containing 4µM Hoechst 33342 (Invitrogen) for parasite RNA and DNA detection, respectively [143], and incubated in the dark for 40min at 37°C. Cells were washed in staining buffer (5mM $CaCl_2$, 5mM glucose, 32mM HEPES pH7.4, 5mM KCl, 1mM $MgSO_4$, 125mM NaCl), resuspended in 0.3µM of intracellular calcium dye x-Rhod-1 AM (Invitrogen) and incubated in the dark at 37°C for 30min. Subsequently, cells were washed in staining buffer and incubated with Annexin V-PE (1:20 dilution; BD Bioscience) at 37°C for 20min in the dark for the staining of surface-exposed phosphatidylserine. Cells were resuspended in 200µl staining buffer and analyzed within the hour using a CytoFLEX S flow cytometer (Beckman Coulter). 100,000

total events were recorded for each condition at a flow rate of 10µl/min. Data were analysed using FlowJo V10. For PS exposure measure, gating was set using data obtained with naïve erythrocytes DMSO control. Infected cells were gated using Hoechst fluorescence. The percentage of Annexin V-PE positive cells, the mean forward scatter height (FSC-H) and mean x-Rhod-1 fluorescence area (PE-A) were acquired for naïve and infected-erythrocytes.

4.3.3 Hemolysis assay

Following drug incubation, cells were spun down at 200g for 5min, the supernatant was collected, and absorbance was read at 405nm on a CLARIOstar® microplate reader. Absorbance of culture media alone was considered as baseline.

4.3.4 Parasite growth inhibition assay

Asynchronous parasite cultures (0.25% parasitemia, 2% hematocrit) were incubated with increasing drug concentrations (up to 50µM) over 72h in standard culture conditions, subject to a freeze/thaw cycle and incubated with the DNA intercalant SYBR Gold following manufacturer instructions (SYBR™ Gold Nucleic Acid Stain, Invitrogen). Fluorescence was measured at 495nm using a CLARIOstar® microplate reader and analysed as a proxy of parasite replication. Percentage of growth inhibition was plotted against the logarithm of drug concentration using GraphPad Prism v8. The resulting non-linear regression curve determines the compound concentration (µM) that inhibits growth of 50% of the parasite population (IC_{50}). 50µM of artemisinin and chloroquine were used as a positive growth inhibition control, and DMSO as a negative control. For each compound five independent biological replicates were performed in triplicate.

4.3.5 Statistical analysis

Data is expressed as the mean +/- standard deviation (SD). One-way ANOVA with Tukey's multiple comparisons test was performed to calculate the p value (ns : $p>0.05$; * : $p\leq0.05$; ** : $p\leq0.01$; *** : $p\leq0.001$; **** : $p\leq0.0001$.) using GraphPad Prism v8.

4.4 Results

4.4.1 Establishing a baseline of eryptosis for *Plasmodium in vitro* conditions

We first explored the impact of cell culture media (Ringer solution vs. RPMI), hematocrit (0.4% vs. 4%) and supplementation (or not) of Albumax to the baseline eryptosis of non-infected erythrocytes, in the absence of drugs. We then tested the strong eryptosis inducer, ionomycin, in these different culture conditions, in order to validate it as a positive control.

Culture in Ringer solution and at low hematocrit increases baseline levels of PS exposure and hemolysis in erythrocytes

Previous eryptosis studies have focused exclusively on naïve (non-infected) erythrocytes, consistently incubating cells in Ringer solution at 0.4% hematocrit [158], while human malaria parasites are cultured in complete RPMI (cRPMI) media at 4% hematocrit [140]. To test the influence of specific culture conditions on eryptosis, naïve erythrocytes were incubated in either Ringer solution (at 0.4 or 4% hematocrit) or in cRPMI at 4% hematocrit (Figure 4.1A and B). These parameters have been named "erythrocyte" and "*Plasmodium*" culture conditions, respectively. Following 48h incubation, PS exposure and hemolysis were measured. A significantly higher level of PS exposure was observed under the erythrocyte culture conditions at 0.4% hematocrit when compared to the *Plasmodium* culture conditions (p=0.0127). When increasing hematocrit to 4%, although PS exposure was 10-fold higher in Ringer solution than in cRPMI, the difference was not significant. Similarly, hemolysis (normalised to hematocrit) was significantly higher under erythrocyte culture conditions at 0.4% hematocrit compared to *Plasmodium* culture conditions (p=0.0219). After adjusting for hematocrit, no difference in hemolysis was observed compared to the *Plasmodium* culture conditions. To compare the impact of the media type alone, erythrocytes were incubated in Ringer solution or incomplete RPMI (iRPMI; the contribution of Albumax supplementation is assessed below) at 4% hematocrit. PS exposure and hemolysis were measured after 48h (Figure 4.1C and D). In Ringer solution, ∼4-fold more cells exposed PS (p=0.0103) and there was ∼2-fold more hemolysis (p=0.0134) than in iRPMI. This reveals that Ringer solution primes erythrocytes for eryptosis and/or that iRPMI protects erythrocytes from eryptosis.

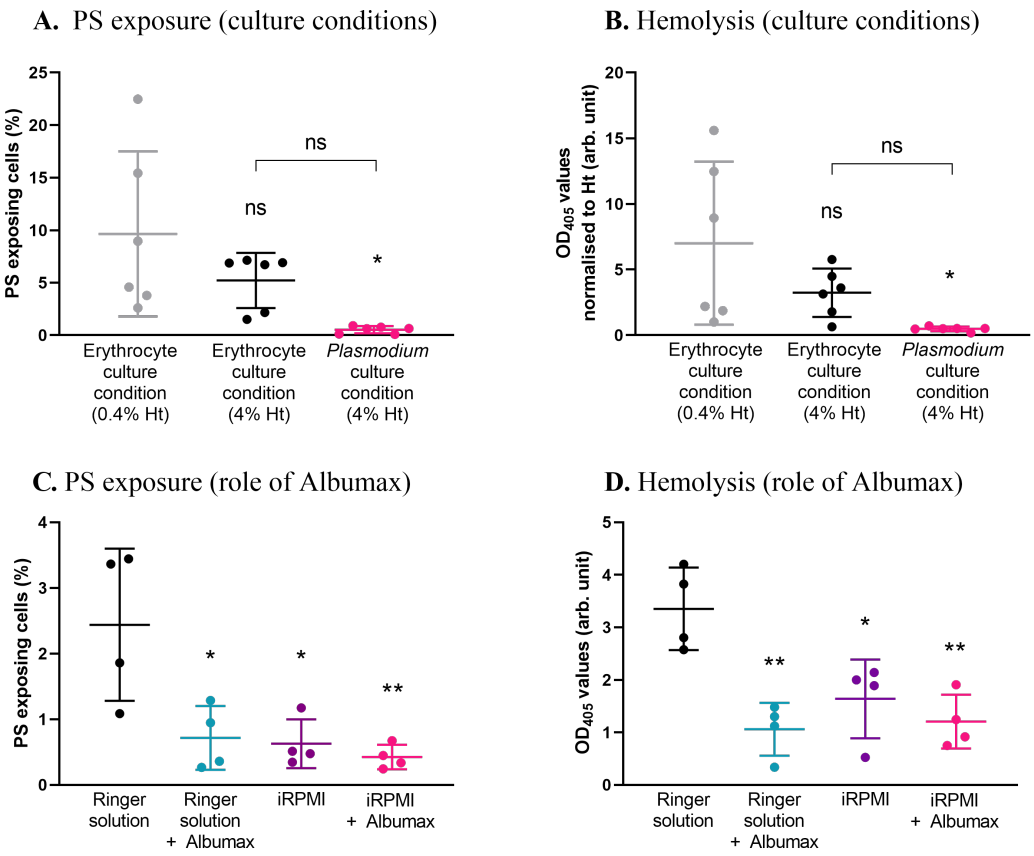

Figure 4.1: PS exposure and hemolysis levels of naïve erythrocytes strongly depend on cell culture parameters. Percentage of PS-exposing cells **(A)** and hemolysis (normalised by hematocrit) **(B)** of erythrocytes cultured for 48h in either erythrocyte culture condition (*i.e.* Ringer solution) at 0.4% or 4% hematocrit, or in *Plasmodium* culture conditions (*i.e.* complete RPMI, 4% hematocrit). N=6 independent experiments performed in triplicate. Percentage of PS-exposing cells **(C)** and hemolysis levels **(D)** of erythrocytes cultured for 48h in either Ringer solution or incomplete RPMI (iRPMI) supplemented or not with Albumax (all conditions at 4% hematocrit). N=4 independent experiments performed in triplicate. Individual data points represent the means of the 3 technical replicates for each experiment. The bars represent the mean and SD of the 4-6 independent experiments (biological replicates). Unless indicated otherwise, compare to the first condition. ns : $p>0.05$; * : $p\leq0.05$; ** : $p\leq0.01$; *** : $p\leq0.001$; **** : $p\leq0.0001$.

Albumax strongly protects erythrocytes from increased PS exposure and hemolysis

Albumax (a serum replacement) is a component used for successful *Plasmodium in vitro* culture but is not used in erythrocyte culture conditions. To determine whether Albumax was a contributing factor for the difference in PS exposure and hemolysis observed between culture conditions, we incubated erythrocytes in Ringer solution +/- Albumax or in incomplete RPMI (iRPMI) +/- Albumax for 48h at 4% hematocrit (Figure 4.1C and D). Compared to Ringer solution alone, addition of Albumax to Ringer solution significantly reduced both PS exposure (p= 0.0143) and hemolysis levels (p= 0.0016) by ~3-fold. Similarly, compared to iRPMI alone, addition of Albumax to iRPMI decreased PS exposure and hemolysis levels, though not significantly. We conclude that the addition of Albumax protects erythrocytes from increased PS exposure and hemolysis.

Ionomycin induces PS exposure in all conditions tested

We then tested the well-known calcium ionophore and previously described eryptosis inducer ionomycin as a potential positive control for subsequent experiments [112, 159]. Erythrocytes were cultured in either Ringer solution (+/- Albumax) or iRPMI (+/- Albumax), in the presence of 1µM ionomycin, at 4% hematocrit for 48h (Figure 4.2A and B). Ionomycin significantly increased PS exposure in all conditions (when compared to the DMSO control): Ringer (2.4% to 24%, p=0.0004), Ringer+Albumax (0.72% to 22%, p=0.0005), iRPMI (0.63% to 23%, p=0.0003) and iRPMI+Albumax (0.43% to 15%, p=0.0329). Similarly, hemolysis increased significantly in the presence of ionomycin, both in Ringer and iRPMI (p<0.0001). However, addition of Albumax to either media was sufficient to abolish ionomycin-induced hemolysis. Ionomycin-induced hemolysis in iRPMI was less pronounced than in Ringer (OD_{405}=5.5 vs. 20.5, respectively, p<0.0001). Taken together, these results suggest that Ringer solution sensitises erythrocytes to hemolysis, and that Albumax protects erythrocytes from ionomycin-induced lysis. Moreover, given that ionomycin induces PS exposure in all conditions, it appears as an effective positive control to test eryptosis levels *in vitro*.

Induction of PS exposure in erythrocytes is a fast process

To investigate the dynamics of PS exposure stimulated by ionomycin, erythrocytes were incubated with 1µM ionomycin and PS exposure was measured between 1 and 48 hours (Figure 4.2C and D). In the absence of drug, PS exposure of erythrocytes slowly increased over time, both in Ringer solution (24-fold increase after 48h, p=0.0011) and in iRPMI (6.4-fold increase after 48h, p=0.0068). The dynamic of PS exposure was much faster in response to ionomycin. Indeed, 1h after the addition of ionomycin, a strong increase in PS exposure was observed both in Ringer solution (62-fold increase compared to the no-drug condition, p<0.0001) and in iRPMI (45-fold increase, p=0.0032).

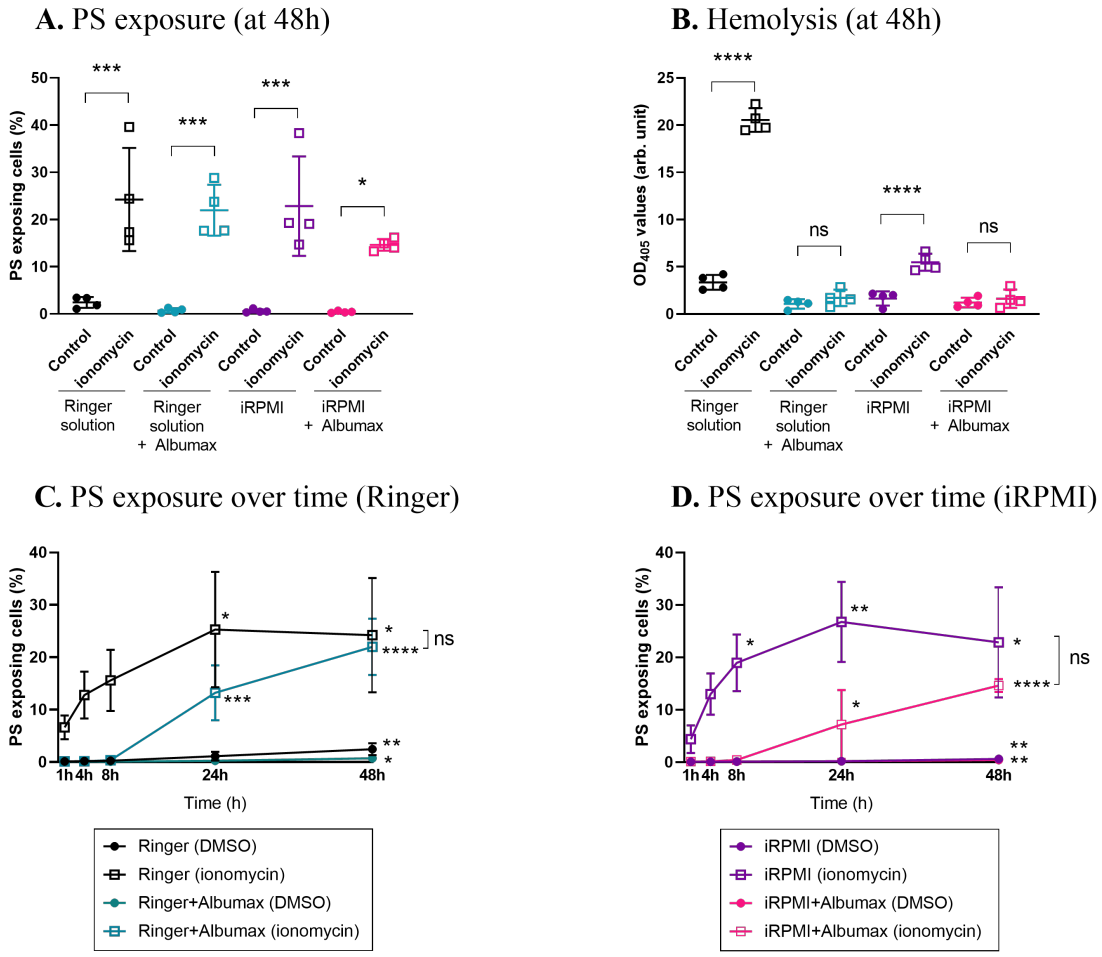

Figure 4.2: Ionomycin induces PS exposure in all conditions but Albumax delays eryptosis. Erythrocytes were cultured in Ringer (+/- Albumax) or incomplete RPMI (+/- Albumax) in the presence of the calcium ionophore ionomycin (1µM) or carrier control (DMSO). PS exposure **(A)** and hemolysis **(B)** levels were measured after 48h. Further, PS levels were determined after 1, 4, 8, 24 and 48h of incubation in Ringer **(C)** or iRPMI **(D)**. N=4 independent experiments performed in triplicate. Individual data points represent the means of the 3 technical replicates for each experiment. The bars represent the mean and SD of the 4 independent experiments (biological replicates). ns : $p>0.05$; * : $p\leq0.05$; ** : $p\leq0.01$; *** : $p\leq0.001$; **** : $p\leq0.0001$. For (C) and (D): unless indicated otherwise, compare each timepoint to T_{1h} within each condition; only significant differences are indicated.

Albumax supplementation delays ionomycin-induced PS exposure for up to 24h

Compared to erythrocytes cultured in Ringer solution alone (T_{1h}=0.1% and T_{48h}=2.4%; p=0.0011), the increase in baseline PS exposure was significantly dampened by the addition of Albumax (T_{1h}=0.1% and T48h=0.7%; p=0.0212) (Figure 4.2C). When ionomycin was added to erythrocytes, the increase in PS exposure was more pronounced in the no-Albumax condition. The increase was significant after only 1h incubation in Ringer alone (T_{1h}=0.1% in Ringer DMSO vs. 6.6% in Ringer ionomycin; p<0.0001), but after 24h in Ringer+Albumax (T_{24h}=0.3% DMSO vs. 13.2% ionomycin; p=0.0476).

When cells were incubated in iRPMI, similar observations were made (Figure 4.2D). Baseline PS exposure increased modestly but significantly over time in both iRPMI alone (T_{1h}=0.1% and T_{48h}=0.6%; p=0.0068) and iRPMI+Albumax (T_{1h}=0.1% and T_{48h}=0.4%;

p=0.0084). The addition of ionomycin to iRPMI alone induced a rapid and significant increase of PS exposure after only 1h incubation (T_{1h}=0.1% in DMSO vs. 4.4% in ionomycin; p=0.0032). In iRPMI+Albumax however, ionomycin only induced a significant increase in PS exposure after 48h (T_{48h}=0.4% DMSO vs. 14.6% ionomycin; p=0.0120). Overall, Albumax appears to delay ionomycin-induced eryptosis by up to 24h.

BAY 43-9006 induces eryptosis exclusively in erythrocyte culture conditions

Following the measure of baseline and ionomycin-stimulated PS exposure and hemolysis, we sought to investigate the impact of culture conditions on eryptosis induction using a previously published eryptosis inducer BAY 43-9006 [160], a Raf kinase inhibitor and approved anti-cancer drug. Erythrocytes were exposed to 0, 1 and 10µM of BAY 43-9006 for 48h under either erythrocyte (0.4 and 4% hematocrit) or *Plasmodium* culture conditions (Figure 4.3). As anticipated, BAY 43-9006 significantly increased the percentage of PS-exposing cells at 10µM (from 10% to 41%; p=0.0003) in erythrocyte culture conditions when compared to the no-drug control. The increase in PS-exposing cells was still observed, albeit to a lesser extent, when adjusting the hematocrit to 4% (from 5% to 10% of PS-exposing cells, p=0.0083). However, no significant increase in PS exposure was observed under *Plasmodium* culture conditions in the presence of 10µM of BAY 43-9006. Similarly, 10µM of BAY 43-9006 significantly induced hemolysis exclusively under erythrocyte culture conditions at 0.4% hematocrit (p=0.0012), but not at 4% hematocrit or in *Plasmodium* culture conditions. These results demonstrate that BAY 43-9006 increases PS exposure and hemolysis levels under erythrocyte culture conditions but not under *Plasmodium* culture conditions.

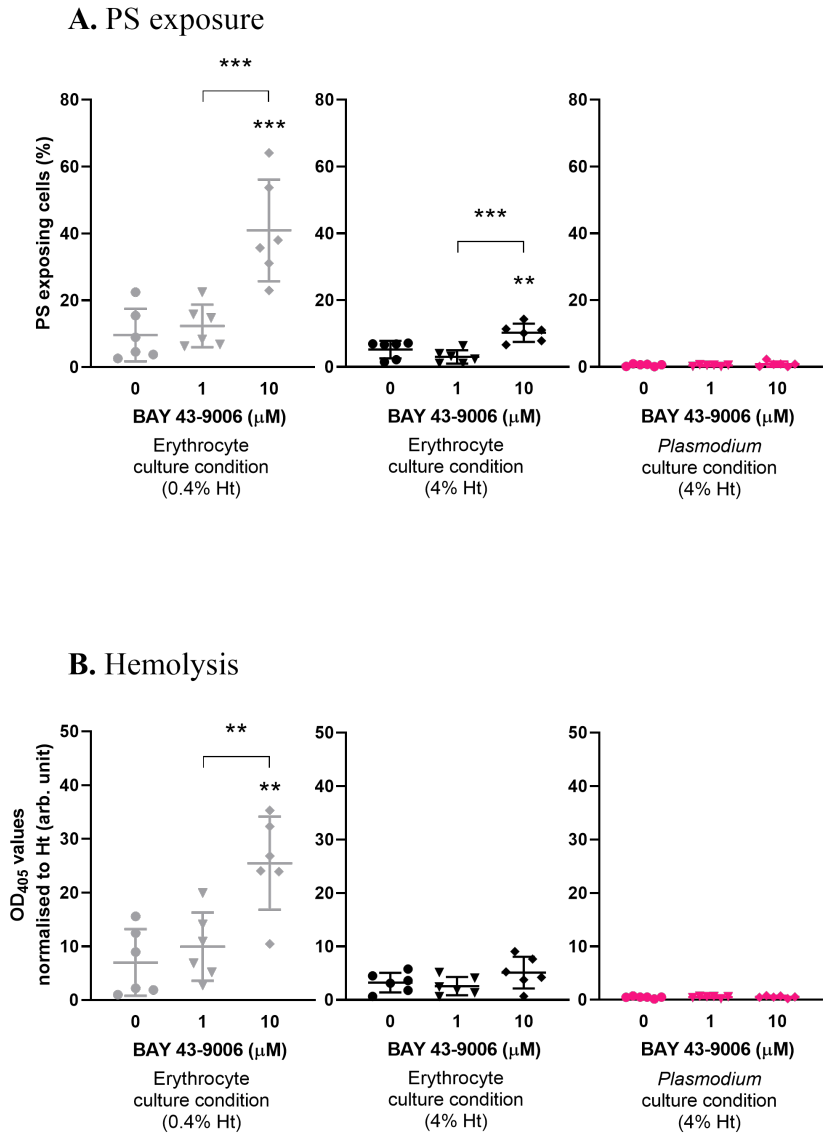

Figure 4.3: The previously described eryptosis inducer BAY 43-9006 does not induce an increase of PS exposure or hemolysis of naïve erythrocytes in malaria culture conditions. Percentage of PS-exposing cells **(A)** and hemolysis (normalised by hematocrit) **(B)** of naïve erythrocytes cultured for 48h in the presence of 0, 1 or 10µM BAY 43-9006 in erythrocyte culture conditions (*i.e.* Ringer solution) at 0.4% or 4% hematocrit, or in malaria culture conditions (*i.e.* complete RPMI, 4% hematocrit). N=6 independent experiments performed in triplicate. Individual data points represent the means of the 3 technical replicates for each experiment. The bars represent the mean and SD of the 6 independent experiments (biological replicates). Unless indicated otherwise, compare to the first condition. ns : $p>0.05$; * : $p\leq 0.05$; ** : $p \leq 0.01$; *** : $p \leq 0.001$; **** : $p \leq 0.0001$.

4.4.2 Testing the effect of "eryptosis inducers" on *P. falciparum* cultures

After establishing the baseline conditions of eryptosis for malaria parasite cultures and using ionomycin as a positive control, we tested the effect of selected eryptosis inducers on the viability of naïve and *P. falciparum*-infected erythrocytes within *in vitro* cultures.

Six selected "eryptosis inducers" do not induce eryptosis of naïve and P. falciparum-infected erythrocytes

We tested the effect of six eryptosis inducers on naïve and *P. falciparum*-infected erythrocytes. Based on our previous data, we measured eryptosis following a 4h drug incubation in iRPMI (without Albumax) at 4% hematocrit: these conditions allowed both the detection of any changes in eryptosis while supporting the growth of *P. falciparum*. PS exposure, cell size, intracellular calcium levels and hemolysis were measured for each compound as proxies for eryptosis. Figure 4.4 presents the eryptosis data on naïve and *P. falciparum*-infected erythrocytes for one of the six tested compounds, oridonin (one of the most clinically promising candidate), along with the positive control ionomycin. While ionomycin expectedly induced a significant increase of PS exposure and a decrease in cell size, both in naïve ($p<0.0001$) and in *P. falciparum*-infected erythrocytes ($p<0.0008$), oridonin did not induce statistically significant changes in eryptosis markers in naïve or *P. falciparum*-infected erythrocytes. Table 2 4.2 summarises the eryptosis observations for all "eryptosis-inducers" tested (benzethonium, oridonin, amiodarone, BAY 43-9006, cordycepin and apigenin): none induced eryptosis hallmarks of naïve or infected-erythrocytes (Supplementary Figures 4.6-4.10).

Three "eryptosis inducers" impact parasite viability

We assessed the *Plasmodium* growth inhibitory effect of "eryptosis inducers" (Figure 4.5 and Table 4.2). Cordycepin and apigenin did not impact parasite growth (IC_{50} of 12 and 66µM, respectively), while four other compounds revealed an IC_{50} below 10µM. In particular, benzethonium presents a sub-micromolar IC_{50} value of 490nM, and the IC_{50} of oridonin and amiodarone were ∼2µM. These results suggest that some "eryptosis inducers" have antiparasitic effects that are independent of eryptosis induction.

Table 4.1: Eryptosis inducers tested in this study.

Compound	Molecular target	Clinical use or potential use	Published eryptosis induction concentration	Effect of *P. falciparum* / *P. berghei*
		Clinically approved		
Amiodarone	Calcium, potassium and sodium channels inhibitor	Anti-arrhythmic agent [161, 162]	5µM [163]	Reduced parasitemia (Pf, Pb) and increased mice survival (Pb) [156]
BAY 43-9006 (Sorafenib, Nexavar)	Raf kinase inhibitor	Anti-cancer (hepatocellular carcinoma) [164]	1µM [160]	-
		Clinical trials		
Cordycepin	AMPK activator	Isolated from the fungus *Cordyceps militaris*, Clinical trials I/II: Anti-cancer capacities [165]	31µM [166]	-
		Herbal medicine compoumds		
Apigenin	Kinases inhibitor	Extracted from chamomile, Anti-inflammatory, anti-cancer capacities [167]	15µM [168]	Decreased parasitemia (Pb) [169]
Oridonin	Not well understood	Extracted from *Isodon rubescens*, Anti-inflammatory, anti-cancer capacities [170, 171]	25µM [172]	-
		Other		
Benzethonium	Disrupts lipid bilayer (cationic detergent)	FDA-approved as a skin disinfectant and preservative in vaccines [173, 174]. Anti-cancer capacities [175]	5µM [158]	-

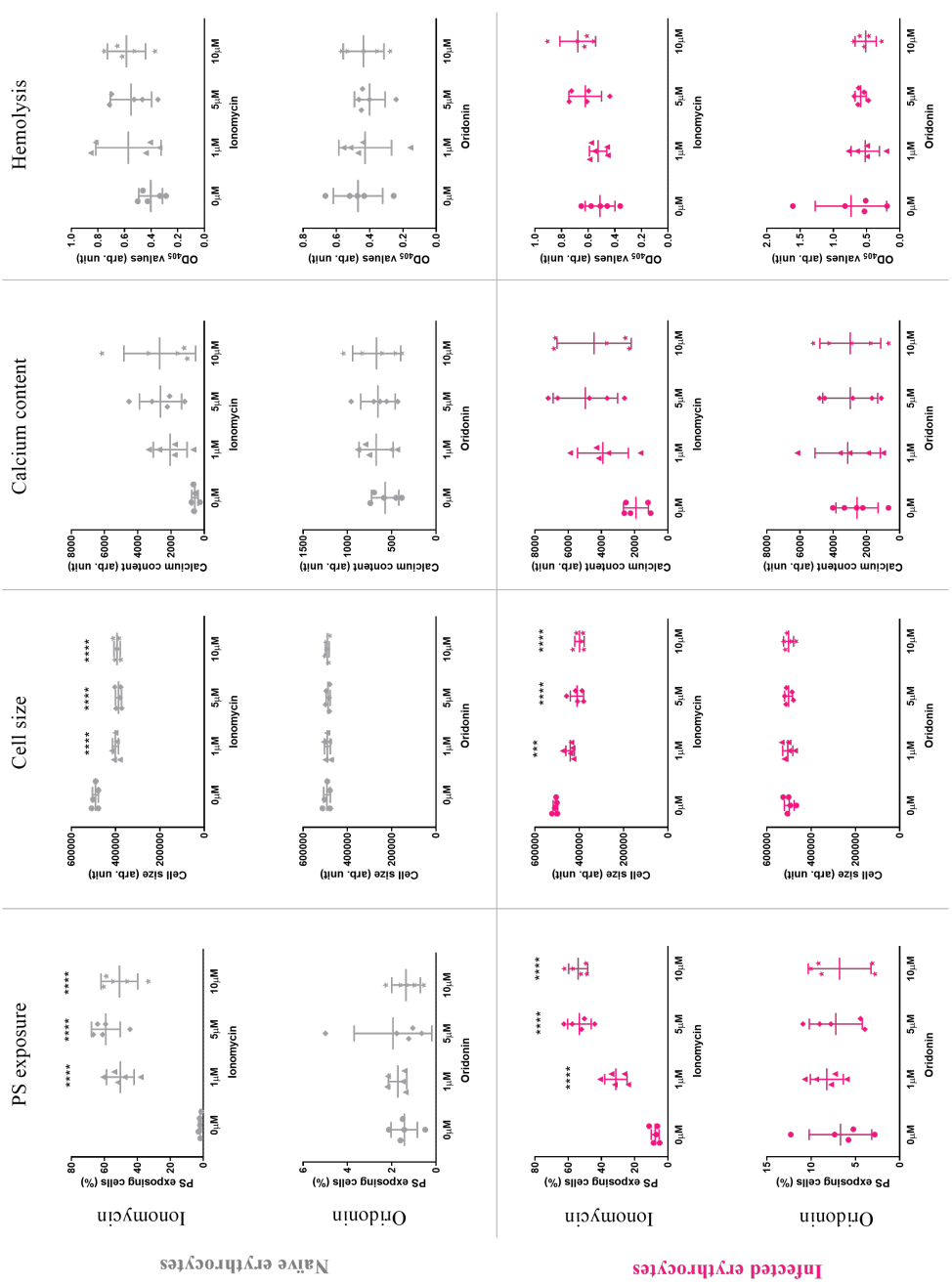

Figure 4.4: Effect of ionomycin and oridonin on eryptosis hallmarks of naïve and *P. falciparum*-infected erythrocytes. Significant increase of PS exposure and significant decrease of cell size were observed in naïve and infected erythrocytes exposed to 1µM of ionomycin (4h in incomplete RPMI). However, no significant increase in these eryptosis hallmarks was observed in naïve and *P. falciparum*-infected erythrocytes exposed up to 10µM of oridonin. N=5 independent experiments performed in triplicate. Individual data points represent the means of the 3 technical replicates for each experiment. The bars represent the mean and SD of the 5 independent experiments (biological replicates).

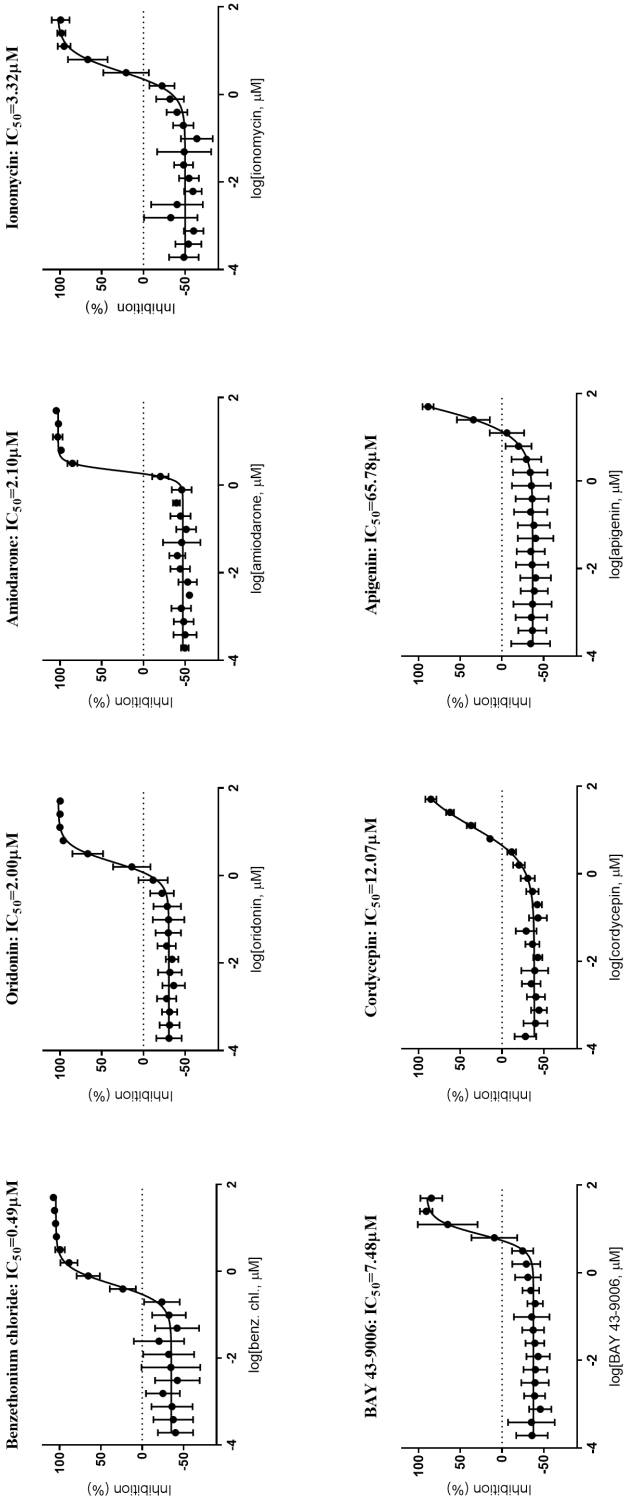

Figure 4.5: Growth-inhibition curves of *P. falciparum* exposed to seven eryptosis inducers. *In vitro* asynchronous cultures of *P. falciparum* were cultured with a range of concentrations of compounds (up to 50µM) for 72h. DNA content was measured as a proxy for parasite growth. IC_{50} concentrations are indicated for each compound in µM. N=5 independent experiments performed in triplicate. Data are represented as the mean and SD of the 5 independent experiments.

Table 4.2: Eryptosis hallmarks of naïve and *P. falciparum*-infected erythrocytes exposed to seven eryptosis inducers and growth inhibition (IC_{50}) on *P. falciparum*. Eryptosis hallmarks include PS exposure, cell size, intracellular calcium levels and hemolysis data (see Figure 4.4 4 and Supplementary Figures 4.6 - 4.10 for detailed data on each compound). Ionomycin is used as a positive control. Significant changes (↑ = increase or ↓ = decrease) are indicated with the concentration at which the effect is observed. *: infected erythrocytes incubated with 5µM benzethonium have an increase in hemolysis which is not observed at 10µM.

Compound	Eryptosis hallmarks		*P. falciparum* IC_{50} (µM)
	Naïve erythrocytes	*P. falciparum*-infected erythrocytes	
Ionomycin	**↑ PS exposure** **↓ Cell Size (1µM)**	**↑ PS exposure** **↓ Cell Size** (1µM)	3.32
Benzethonium	Ns	Ns *	0.49
Oridonin	Ns	Ns	2.00
Amiodarone	↑ Calcium (5µM)	Ns	2.10
BAY 43-9006	Ns	Ns	7.48
Cordycepin	Ns	Ns	12.07
Apigenin	Ns	Ns	65.78

4.5 Discussion

4.5.1 Ringer solution sensitises erythrocytes to eryptosis

Culture media differs substantially between erythrocyte and *Plasmodium* culture conditions. We hypothesised that this underpins the discrepancies observed in the literature, where compounds described as eryptosis inducers, have not been observed to induce PS exposure of non-infected erythrocytes when tested in malaria culture conditions [71]. By measuring PS exposure levels and hemolysis of naïve erythrocytes as a proxy for eryptosis, we were able to confirm that these compounds induce eryptosis when using erythrocyte culture conditions. However, eryptosis levels were significantly reduced in *Plasmodium* culture conditions. Specifically, we showed that Ringer solution primes erythrocytes to eryptosis when compared to incomplete RPMI (iRPMI) media. *Plasmodium* culture media is optimised to mimic physiological blood conditions, while Ringer solution is a nutrient-poor solution. For example, glucose levels are higher in *Plasmodium* culture media (11mM) than in Ringer solution (5mM). These differences in culture media composition could modulate eryptosis induction and the nutrient-poor Ringer solution might weaken erythrocytes and pre-dispose them to eryptosis.

4.5.2 A lower hematocrit exacerbates eryptosis phenotypes

In addition to the difference in media, we investigated the impact of cell density on eryptosis induction. We demonstrated that a lower hematocrit exacerbated PS exposure and hemolysis in the absence of eryptosis inducers and in response to the eryptosis compound BAY 43-9006. This increased susceptibility to BAY 43-9006-induced eryptosis occurring at a lower hematocrit may be, at least partly, attributed to the higher proportion of drug per

cell. Additionally, erythrocytes, similar to other cell types, appear to show better viability outcomes with a higher cell density, better reflecting physiological conditions [176, 177].

4.5.3 Albumax protects erythrocytes from eryptosis

Albumax supplementation (a serum replacement) is required for the growth of *P. falciparum in vitro*. In contrast, eryptosis inducers have been tested *in vitro* in the absence of human serum or a synthetic replacement. Here, we show that addition of Albumax (to Ringer solution or iRPMI media) is sufficient to protect erythrocytes from PS exposure and hemolysis. This is particularly striking when eryptosis is induced following addition of the calcium-ionophore ionomycin where PS exposure remains unchanged for 8h and hemolysis is not observed.

Walsh and colleagues suggested that human plasma contains pro-survival factors as it has the capacity to inhibit erythrocytic PS exposure induced by the apoptosis inducer BH3-mimetics [125]. Although our study did not use human serum, our results suggest that Albumax might also contain pro-survival factors that prevent eryptosis induction. Further, it is reasonable to hypothesise that direct sequestration of the drug by components of Albumax might prevent eryptosis induction [178]. Noteworthy, ionomycin had an impact on *P. falciparum* growth and was, therefore, unaffected by Albumax components. Another possible explanation for the protective role of Albumax might relate to its high lipid content. Indeed, some lipids can protect against cell death and stress, as demonstrated with lipid droplets in nucleated cells [179, 180]. Similar to nucleated cells, the presence of lipids in the culture media could improve erythrocyte viability and reduce their susceptibility to cell death induction [181]. It will be interesting in the future to fractionate Albumax in order to identify the factor(s) responsible for this protective effect against eryptosis [182].

4.5.4 The dynamics of PS exposure over time

Although induction of PS exposure in nucleated cells occurs in a matter of minutes [183], eryptosis has predominantly been studied 48h post-stimulation. Here we demonstrated that induction of PS exposure in erythrocytes has a rapid onset (of less than 1h), consistent with observations in other cell types. Moreover, we demonstrated that PS exposure levels increased over time regardless of culture conditions, which corroborates findings suggesting aging erythrocytes are recognised and cleared from circulation through increased PS exposure during senescence [158, 160, 168].

4.5.5 Eryptosis inducers do not induce eryptosis of naïve or *Plasmodium*-infected erythrocytes, and three do not impair *Plasmodium* growth

We tested the effects of six eryptosis inducers based on their use (or prospective use) in the clinic, their known molecular targets and/or their previously demonstrated antimalarial effects. We found that none of these compounds induced eryptosis hallmarks in our culture

conditions. In the case of oridonin, cordycepin and apigenin, this could be due to drug concentration, as previously published eryptosis inducing concentrations (25µM, 31µM and 15µM, respectively [172, 166, 168]) were higher than our maximum concentration of 10µM. In the case of BAY 43-9006, benzethonium and amiodarone [158, 160, 163], the differences between previously published studies and our findings are due to experimental conditions, as discussed above. A recent study reported a decrease in *Plasmodium berghei* parasitemia in mice administered with apigenin [169]. This finding contrasts with the absence of *P. falciparum* growth inhibition we observed in response to apigenin *in vitro*. This discrepancy might be due to the different *Plasmodium* species, different hosts/cultures or differences in read-outs.

4.5.6 Benzethonium, amiodarone and oridonin impair *Plasmodium* growth via an eryptosis-independent mechanism

We identified three "eryptosis inducers" displaying a low *P. falciparum* IC_{50} (benzethonium, oridonin and amiodarone). Benzethonium displayed the lowest IC_{50} (0.49µM) and could therefore be considered a promising antimalarial. However, its toxicity effects [174, 184] will need to be abrogated before being investigated further as a potential antimalarial. Benzethonium is used as an antimicrobial, acting by disrupting lipid bilayers, and has been identified as an anti-cancer compound by inducing apoptosis [175]. However, no consistent significant increase in hemolysis was observed both in naïve and *P. falciparum*-infected erythrocytes, suggesting that membrane disruption is not the mode of action. It is therefore possible that benzethonium targets a parasite-specific pathway.

Amiodarone, a clinically used antiarrhythmic drug, inhibited *P. falciparum* growth with an IC_{50} of 2.10µM. This antiparasitic effect is in agreement with a study describing reduced parasitemia of *P. falciparum in vitro* and *P. berghei in vivo* [156]. Interestingly, a typical 400mg dose of amiodarone in adults leads to a peak plasma concentration in the same order of magnitude as the IC_{50} value we measured here [185]. However, amiodarone can cause serious side effects, and is only recommended in case of life-threatening arrythmia [185]; more work is therefore required before it can be proposed as a novel antimalarial candidate. As an antiarrhythmic agent, amiodarone acts by inhibiting calcium, potassium and sodium channels. Inhibition of ion channels on either the erythrocyte surface or the parasite interface could be part of the mechanism of action.

Oridonin displayed a low IC_{50} (2µM). One oridonin derivative (HAO472) is currently in phase I clinical trials in China for the treatment of leukemia [170]. As such, this compound might be the most promising antimalarial candidate tested in this study. In cancer cells lines, oridonin and oridonin-like compounds were shown to regulate many pathways, including NF-ϰB, ROS, p53/p21, to inhibit proliferation and induce apoptosis [170]. At this stage, it is therefore difficult to infer the mechanism of action behind oridonin antimalarial activity.

4.5.7 PS exposure during a malaria infection: Turning the tables on *Plasmodium*

PS exposure at the surface of infected and non-infected erythrocytes during a malaria infection could be detrimental to the host. PS exposure by infected cells has been linked with an increase in their cytoadhesion and sequestration, both in *P. falciparum* [186] and in *P. vivax* malaria [187]. Further, PS exposure of uninfected erythrocytes and increased levels of anti-PS auto-antibodies have been proposed as key mechanisms leading to the loss of non-infected erythrocytes, therefore contributing to malarial anaemia [70, 48, 188]. However, compared to their non-infected counterparts, a larger proportion of infected erythrocytes expose PS [74]. This propensity of infected erythrocytes to expose PS could be used to target antimalarials specifically to infected cells using peptides that accumulate predominantly in PS-exposing cells [189] or with liposomes conjugated to PS binding peptides [190]. These techniques offer promising alternatives for antimalarial development that could be explored in the future.

4.5.8 Conclusions and future directions

We have shown that experimental culture conditions typically used to study eryptosis weaken erythrocytes and predispose them to eryptosis. Media supplementation with Albumax strongly protects against eryptosis, even in the presence of strong eryptosis inducers. Compounds initially identified as eryptosis inducers failed to induce eryptosis of naïve and *P. falciparum*-infected erythrocytes. However, some compounds showed promising antiparasitic activity, including amiodarone and oridonin, the most promising antimalarial leads in this study. Given the potential detrimental effect of increased PS exposure by erythrocytes in malaria-infected individuals, the identification of compounds with parasitic activity independent of eryptosis offers promising avenues in designing novel host-directed antimalarial strategies.

Acknowledgements

Professor Freya Fowkes (Burnet Institute) for assisting with statistical analysis. Dr Philippe Boeuf (Burnet Institute) and Professor Christian Doerig (RMIT) for helpful discussions and feedback on the manuscript. Professor Patrick Humbert (La Trobe University) for providing access to flow cytometry equipment. The Australian Red Cross Blood Bank for the supply of human erythrocytes.

Authorship contributions

CB, TG and TGC planned the experimental work and analysed the data. CB and TG performed the experimental work. CB and TGC wrote the manuscript.

Disclosure of conflicts of interest

The authors declare no conflict of interest.

4.6 Supplementary information

Supplementary Figure 1.

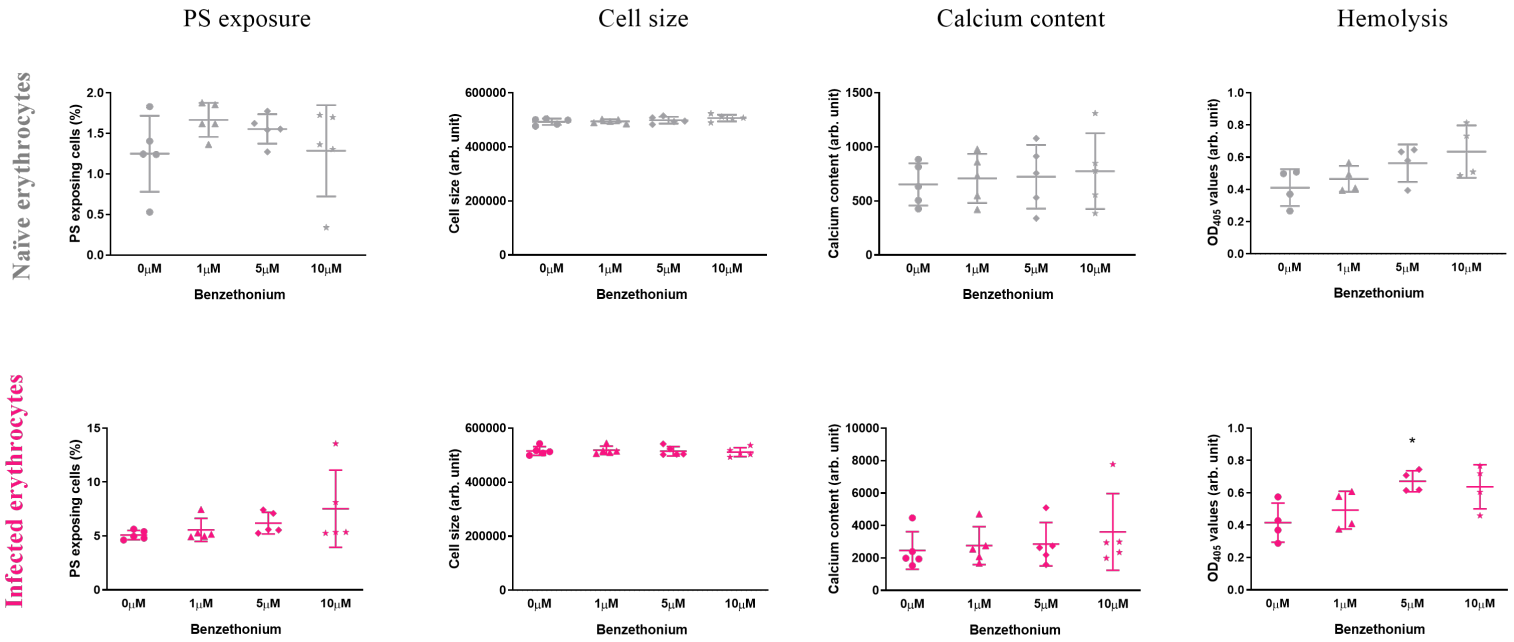

Figure 4.6: Effect of benzethonium on eryptosis levels of naïve and *P. falciparum*-infected erythrocytes. Naïve erythrocytes or *P. falciparum* cultures were incubated in incomplete RPMI for 4h in presence of 0, 1, 5 or 10µM benzethonium. PS exposure, cell size, calcium levels were measured by flow cytometry, and hemolysis was measured by absorbance assay. N=5, except for hemolysis where n=4. Mean and SD.

Supplementary Figure 2.

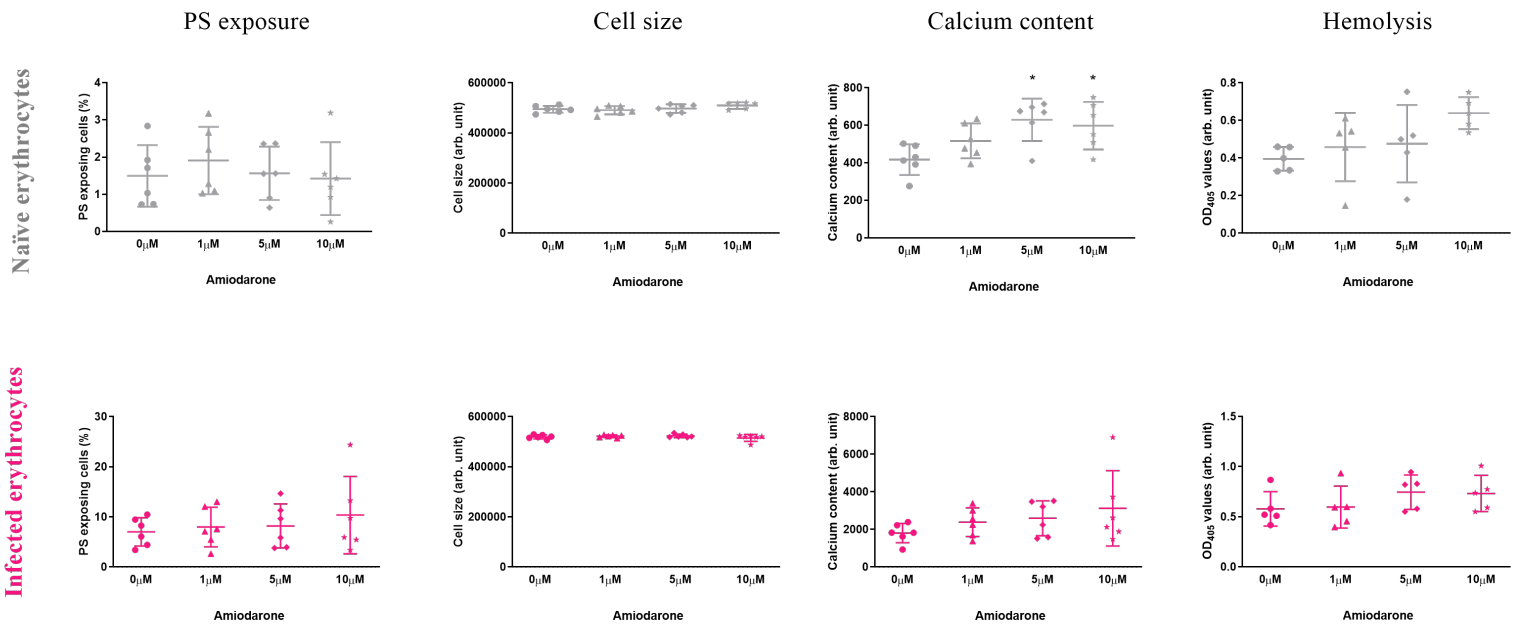

Figure 4.7: Effect of amiodarone on eryptosis levels of naïve and P. *falciparum*-infected erythrocytes. Naïve erythrocytes or *P. falciparum* cultures were incubated in incomplete RPMI for 4h in presence of 0, 1, 5 or 10µM amiodarone. PS exposure, cell size, calcium levels were measured by flow cytometry, and hemolysis was measured by absorbance assay. N=6 naïve, except for hemolysis where n=5. Mean and SD.

Supplementary Figure 3.

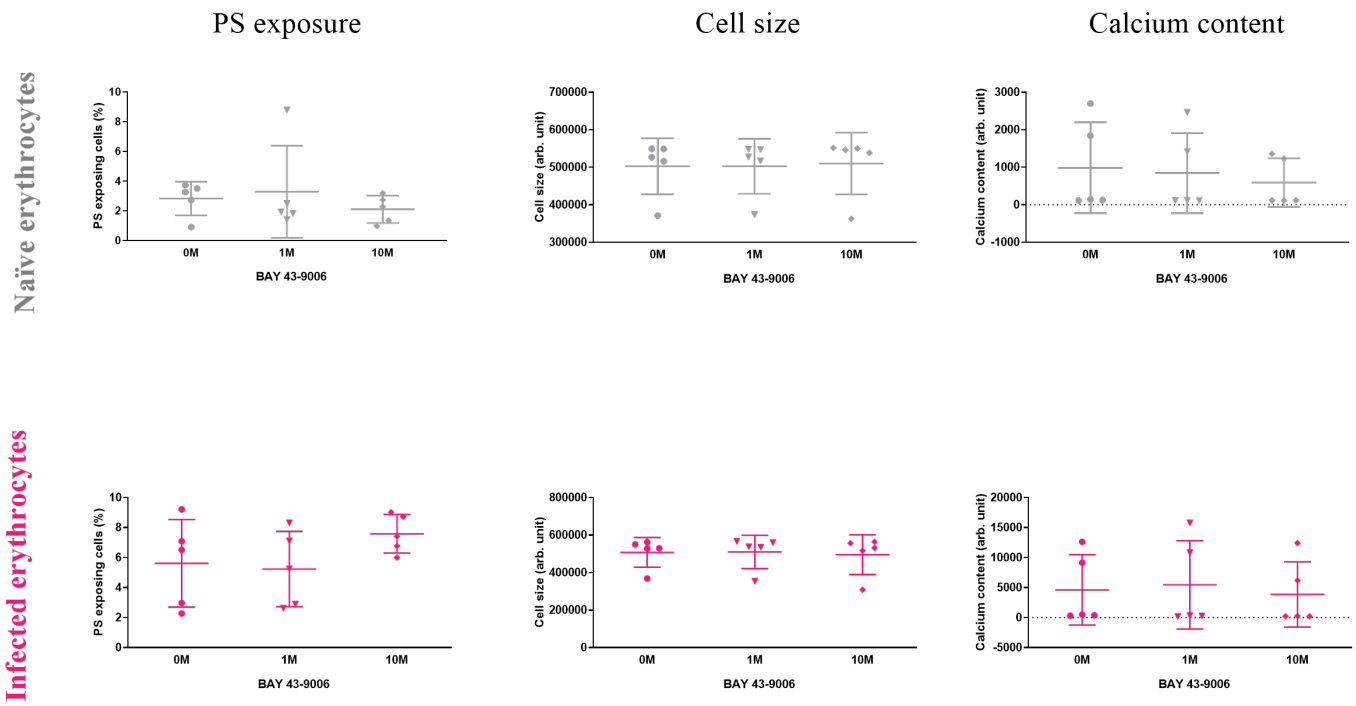

Figure 4.8: Effect of BAY 43-9006 on eryptosis levels of naïve and *P. falciparum*-infected erythrocytes. Naïve erythrocytes or *P. falciparum* cultures were incubated in incomplete RPMI for 4h in presence of 0, 1 or 10µM BAY 43-9006. PS exposure, cell size and calcium levels were measured by flow cytometry. N=5. Mean and SD.

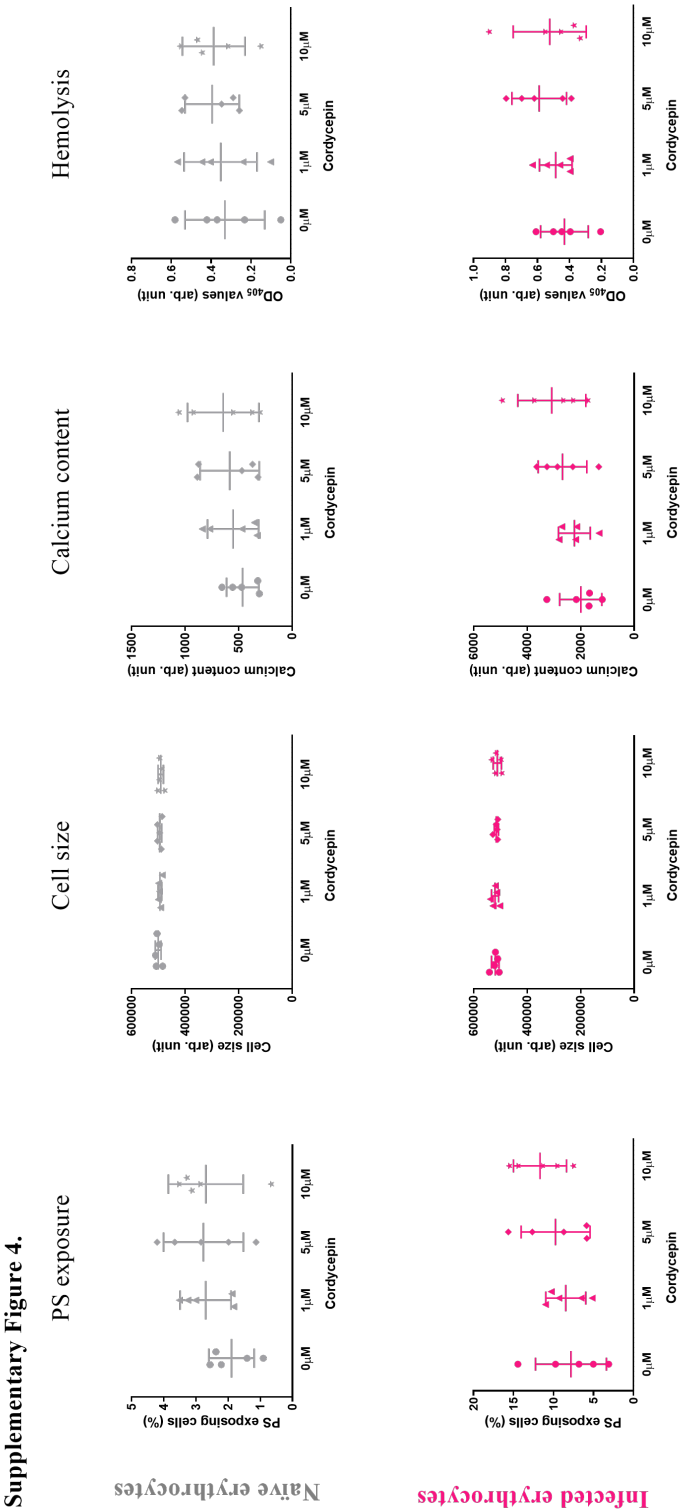

Figure 4.9: Effect of cordycepin on eryptosis levels of naïve and *P. falciparum*-infected erythrocytes. Naïve erythrocytes or *P. falciparum* cultures were incubated in incomplete RPMI for 4h in presence of 0, 1, 5 or 10µM cordycepin. PS exposure, cell size, calcium levels were measured by flow cytometry, and hemolysis was measured by absorbance assay. N=5. Mean and SD.

Supplementary Figure 5.

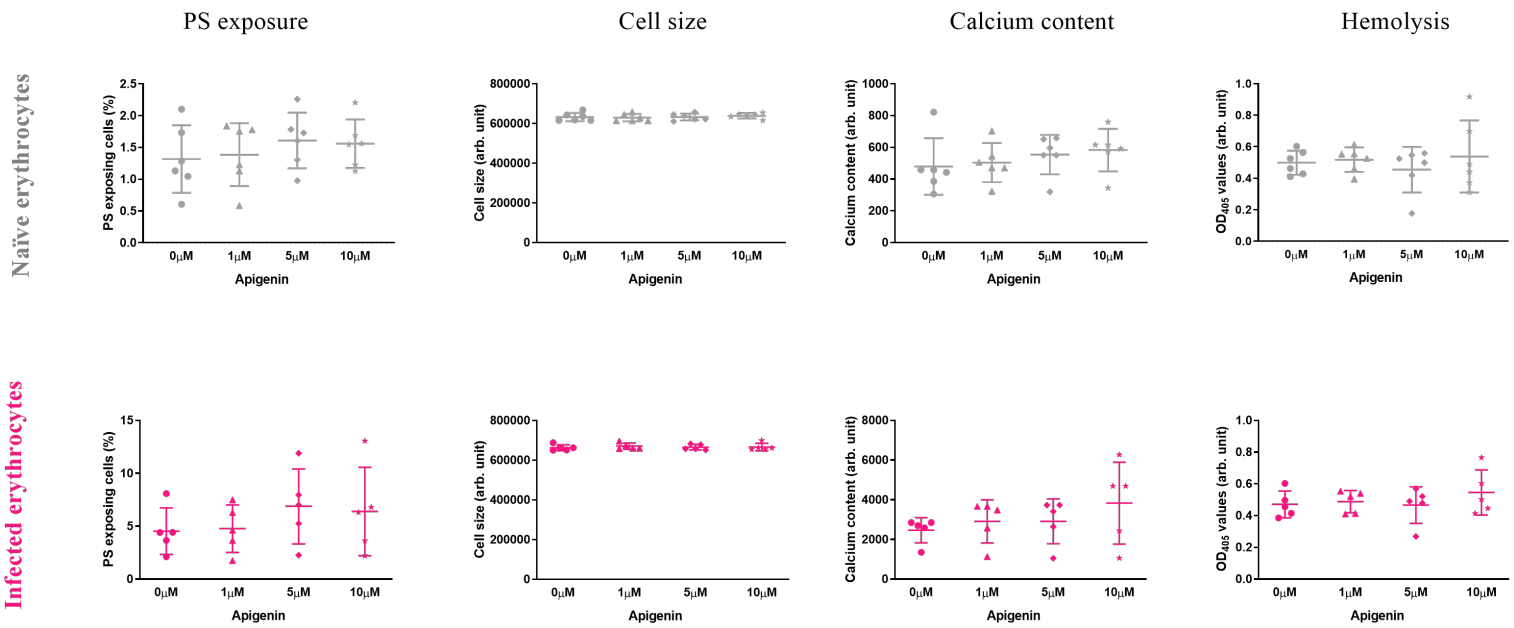

Figure 4.10: Effect of apigenin on eryptosis levels of naïve and *P. falciparum*-infected erythrocytes. Naïve erythrocytes or *P. falciparum* cultures were incubated in incomplete RPMI for 4h in presence of 0, 1, 5 or 10µM apigenin. PS exposure, cell size, calcium levels were measured by flow cytometry, and hemolysis was measured by absorbance assay. N=6 for naïve and N=5 for infected erythrocytes. Mean and SD.

(B) Effect of the Raf kinase inhibitor, BAY 43-9006, on eryptosis and parasite development

4.7 Introduction

We have demonstrated that BAY 43-9006 (Sorafenib), a human Raf kinase inhibitor used in the clinic to treat hepatocellular carcinoma, impairs *P. falciparum* growth *in vitro* (IC_{50}=7.48µM) (Chapter 4A). This result was recently confirmed by Adderley *et al.* (2020) [191], who demonstrated that two different Raf inhibitors, BAY 43-9006 and SB-590885, impaired *P. falciparum* development.

The human Raf (Rapidly Accelerated Fibrosarcoma) family is comprised of three paralogs: A-Raf, B-Raf and C-Raf (also known as Raf-1). The Raf kinases are part of a Mitogen-Activated Protein Kinase (MAPK) cascade: the Ras-Raf-MEK-ERK pathway [192]. Raf acts as a MEK kinase (MEKK) downstream of Ras (itself activated by receptor tyrosine kinases), and upstream of MEK-ERK (see Figure 4.11). Raf phosphorylates MEK1/2, which phosphorylate ERK1/2, which can then activate over 150 nuclear and cytosolic substrates [192]. Raf is regulated by many phosphorylation sites, resulting in changes in binding partners as well as changes in its cellular localisation. Although MEK1 and MEK2 are the only widely accepted substrates of Raf kinase, Raf can also inhibit apoptosis independently of its own kinase activity [192].

Importantly in the context of malaria, no Raf orthologs have been identified in *Plasmodium spp.* yet [193]. Moreover, Adderley *et al* (2020) [191] demonstrated that both B-Raf and C-Raf (Raf-1) kinases are differentially phosphorylated in infected red blood cells (iRBCs) compared to uninfected red blood cells (uRBCs), suggesting that infection by *P. falciparum* modifies their activity. Therefore, the antiparasitic activity of BAY 43-9006 might be due to the inhibition of the host RBC Raf kinase. This is particularly relevant in nucleus-deprived erythrocytes, which must heavily rely on post-translational signalling, of which phosphorylation is a major mechanism. Although BAY 43-9006 had previously been described as an eryptotic inducer [160], we've shown that it did not induce eryptosis hallmarks in naïve or infected erythrocytes in our conditions (Chapter 4A). However, we have investigated the impact of BAY 43-9006 on all iRBCs, but the specific impact of BAY 43-9006 on different stages of the parasite is yet to be determined.

In this chapter, we investigate the impact of BAY 43-9006 on *P. falciparum* erythrocytic stages. We first measured impacts of BAY 43-9006 in a static manner (*i.e.* measuring eryptosis of an asynchronous culture at a single timepoint), then in a dynamic fashion

(measuring eryptosis of a synchronised culture over two *Plasmodium* erythrocytic cycles).

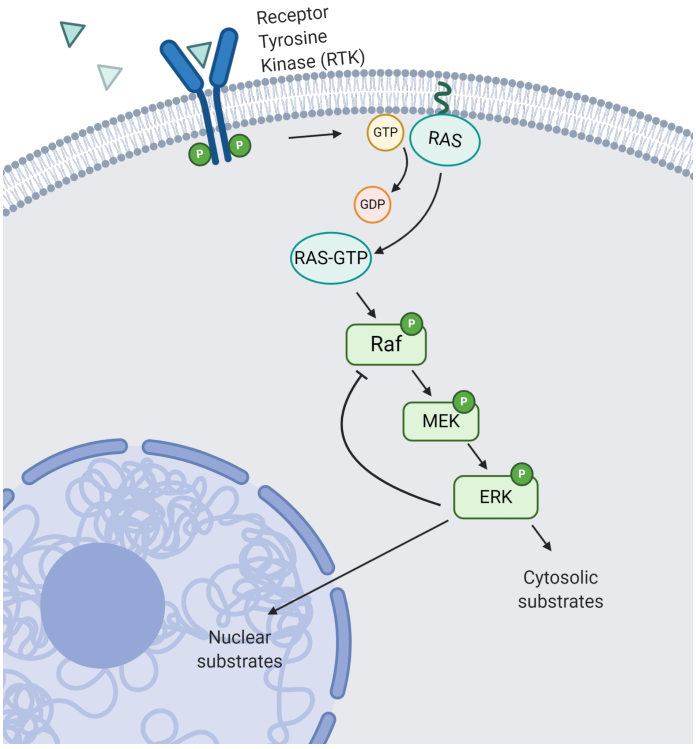

Figure 4.11: The Ras-Raf-MEK-ERK pathway. The Ras/Raf/KEK/ERK pathway is one of four mitogen-activated protein kinase (MAPK) cascade. Upon stimulation of a receptor tyrosine kinase (RTK), the inactive GDP-bound Ras becomes activated (GTP-bound Ras). GTP-bound Ras activates Raf kinase, which phosphorylates / activates MEK, which in turn phosphorylates / activates ERK, which finally phosphorylates many downstream effectors, including a negative feedback loop to deactivate Raf.

4.8 Results

4.8.1 Impact of BAY 43-9006 on the parasite viability

To study the impact of BAY 43-9006 on the viability and physiology of different stages of *P. falciparum*, asynchronous cultures were incubated with 10µM of BAY 43-9006 in incomplete RPMI (iRPMI) for 4h, as described earlier (Chapter 4A). Parasite stages were identified by flow cytometry based on their RNA and DNA content (with Thiazole Orange and Hoechst fluorescence respectively, as described previously [143]): the gating strategy is shown in Figure 4.12. Ring stages contain low amount of DNA and RNA, trophozoite stages contain more RNA and schizont stages contain more DNA and even more RNA. Interestingly, in the presence of BAY 43-9006, all the iRBC populations appeared to shift towards the left (*i.e.* less RNA detection), making the differentiation between ring and trophozoite stages difficult. Another gating strategy was therefore adopted, whereby young parasites (*i.e.* rings and trophozoites) were gated together. Figure 4.12 also shows representative images of each stage, with and without BAY 43-9006. We observed that after only 4h incubation with 10µM BAY 43-9006, ring stages, and even more so, trophozoite and schizont stages,

present a condensed, darker and rounded appearance detected by light microscopy, the characteristic phenotype of dead parasites.

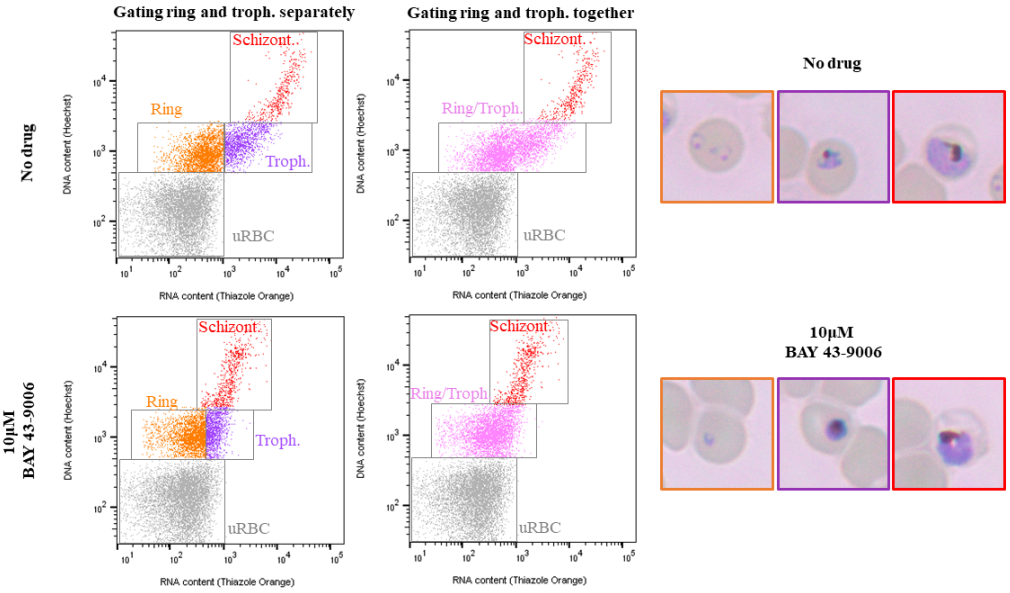

Figure 4.12: Gating of an asynchronous *P. falciparum* culture with or without 10µM BAY 43-9006. Two different gating strategies of a mix *P. falciparum* culture in absence (top panels) or presence (bottom panels) of 10µM BAY 43-9006 (4h in iRPMI). Rings (orange), trophozoites (purple), schizonts (red) and uninfected RBCs (grey) were gated separately (left panels), or rings and trophozoites were gated together (pink, right panels). Representative microscopy images of rings, trophozoites and schizonts with or without BAY 43-9006 are also shown.

Using the latter gating strategy (rings and trophozoites together; schizonts separately), Figure 4.13 shows the mean RNA and DNA contents of iRBCs. Although the DNA content per iRBC was not affected by BAY 43-9006, the RNA content was significantly decreased in both young (p=0.0303) and mature parasites (p=0.004) by the presence of BAY 43-9006 when compared to the no drug control.

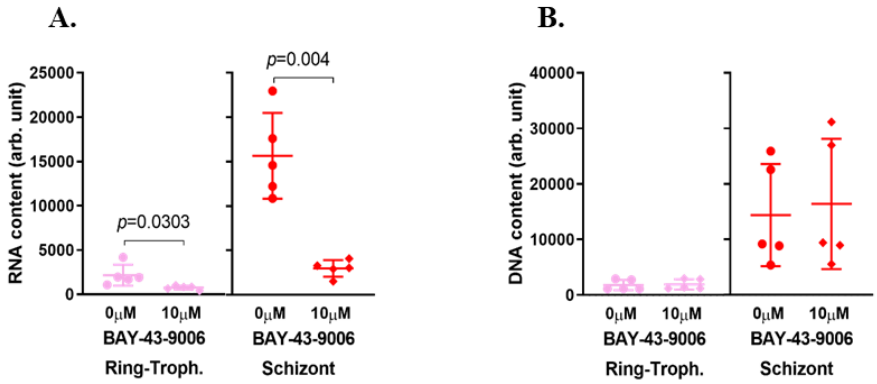

Figure 4.13: RNA and DNA content of young vs. mature parasites with or without 10µM BAY 43-9006. (A) Average RNA content and **(B)** DNA content of young parasites (rings and trophozoites, in pink) and mature parasites (schizonts, in red), with or without 10µM BAY 43-9006. Asynchronous *P. falciparum* cultures were incubated in iRPMI for 4h with BAY 43-9006 or the carrier control (DMSO) and analysed by flow cytometry. N=5 independent experiments in triplicate. t-test.

4.8.2 Impact of BAY 43-9006 on eryptosis of different parasite stages

As BAY 43-9006 is an inhibitor of the human Raf kinase, we wondered if BAY 43-9006 had an impact on the viability of the RBC itself (by measuring various eryptosis hallmarks) at different parasite stages. Figure 4.14 shows the PS exposure, cell size and intracellular calcium content of bystander uRBCs, young stages (rings and trophozoites) and mature stages (schizonts). The only effect of BAY 43-9006 (indicated in red) was to increase PS exposure of schizonts (compared to the no drug control) (p=0.0193).

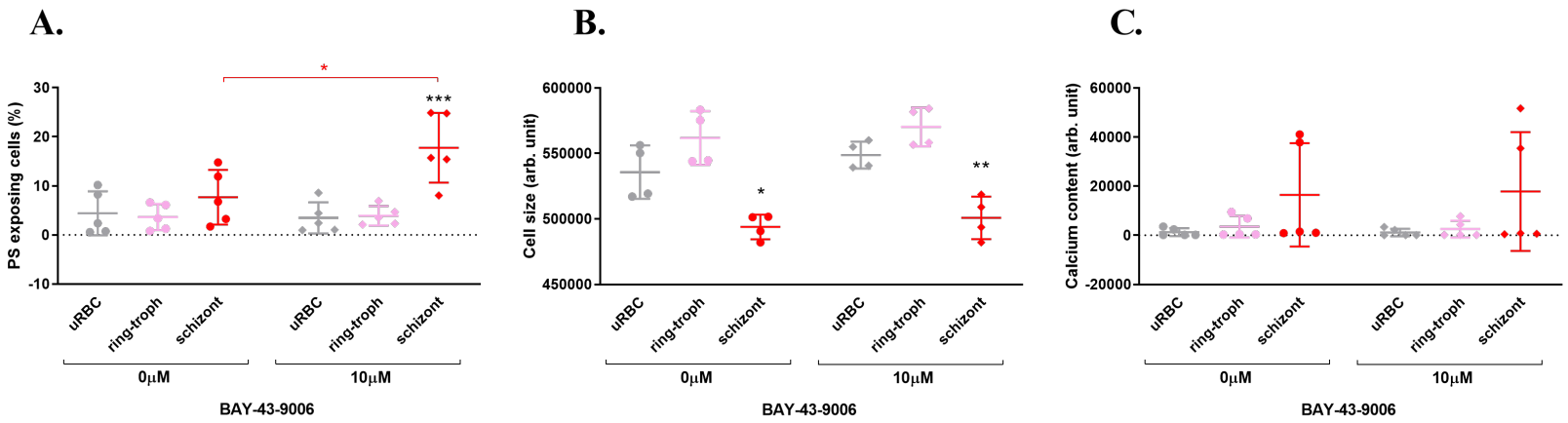

Figure 4.14: Impact of BAY 43-9006 on eryptosis hallmarks of different *P. falciparum* stages. Asynchronous *P. falciparum* cultures were incubated with 0 or 10µM BAY 43-9006 for 4h in iRPMI, then analysed by flow cytometry. Populations were gated as shown in 4.12: uRBCs (grey), rings/trophozoites (pink) and schizonts (red). **(A)** PS exposure , **(B)** cell size and **(C)** intracellular calcium content were measured. Individual values and mean (SD) for n=5 independent experiments in triplicate are shown. Unless indicated otherwise, compare to the uRBC within the same condition using a one-way ANOVA with multiple Tukey tests.

4.8.3 Impact of BAY 43-9006 on *P. falciparum* over two cycles

To precisely investigate the antiparasitic activity of BAY 43-9006, we analysed a highly synchronised culture of *P. falciparum* over time, starting with 1% rings and following the parasite culture over two erythrocytic cycles. A time-course analysis of eryptosis has been conducted, and the results of this experiment are described in this current chapter (Chapter 4B) and Chapter 5. In this chapter, we will focus on the impact of BAY 43-9006. In Chapter 5, we will focus on evolution of eryptosis in the absence of drug. Figure 4.15 shows the distribution of iRBCs (and uRBCs) according to their RNA and DNA content over time, with or without 10µM of BAY 43-9006. In addition, representative microscopy images of iRBCs are shown for each time point. Using these microscopy images, it is striking to note that in the presence of BAY 43-9006, parasites are not able to progress through the erythrocytic cycle, being affected mainly at the trophozoite and schizont stages. From the age of 36h, the parasites appear dead as indicated by a very condensed and round phenotype, or extracellular forms (24h of cycle 2). Figure 4.16 shows the parasitemia, DNA content, RNA content, PS exposure, cell size and intracellular calcium content of iRBCs over time. The light grey lines show the evolution without BAY 43-9006, while the bright coloured lines indicate the evolution in the presence of BAY 43-9006.

In the presence of BAY 43-9006, the parasitemia either stalled over time (during cycle 1) or decreased, as at 24h, 36h and 48h of cycle 2 when compared to the first timepoint (p=0.0275, 0.0048 and 0.0013). Parasitemia diverged from the no-drug control at the start of the second cycle, when reinvasion occurred in the absence of drug (7.8% vs 1.2% parasitemia, p<0.0001).

Although parasite DNA increased over time in the presence of BAY 43-9006 (p=0.0489 at 48h of cycle 1 and p<0.0001 at 12h of cycle 2), it appears to be both delayed (maximum at t=12h of cycle 2 instead of the expected 48h of cycle 1) and well below the expected values. Indeed, DNA content only increased by 2.5-fold at its peak in the presence of BAY 43-9006, when compared to the first timepoint, while in the absence of drug, DNA content increased by 11-fold at its peak. The difference in DNA content between presence and absence of drug became significant at 36h of cycle 1 (p=0.0001).

In the presence of BAY 43-9006, the RNA content significantly increased, reaching a peak at t=48h of cycle 1 (p<0.0001), albeit to much lower levels than expected: a 2.7-fold increase between the first timepoint and t=48h in the presence of BAY 43-9006 vs. a 24-fold increase without drug. Importantly, BAY 43-9006 reduced RNA content of iRBCs almost throughout the whole time-course (p=0.0499 at 12h, p=0.0013 at 36h, p<0.0001 at 48h/0h compared to both the schizonts of cycle 1 and rings of cycle 2, p=0.0080 at 12h of cycle 2, p<0.0001 at 36h and 48h of cycle 2).

It was striking that following a 48h incubation (12h of cycle 2), all measured eryptosis hall-

marks (PS exposure, cell shrinkage and intracellular calcium) were significantly induced by BAY 43-9006, both when comparing to the first timepoint of the BAY 43-9006 condition and when comparing to the no drug condition. In the presence of BAY 43-9006, PS exposure increased significantly over time especially after 12h of cycle 2, increasing by nearly 7-fold by the end of the experiment (p=0.0003 at 12h, then p<0.0001). When compared to the control, addition of BAY 43-9906 significantly increased PS exposure during the second cycle, at 12h (p=0.0059), 24h (p=0.0002), 36h (p<0.0001), and 48h (p=0.0002).

In the presence of BAY 43-9006, iRBCs also decreased in size over the course of the experiment, reaching a significant difference at 12h of cycle 2 (p<0.0001, p=0.0004 at 48h of cycle 2). When compared to the no-drug control, the schizont stages appeared bigger in the presence of BAY 43-9006 both at cycle 1 (p=0.0012) and cycle 2 (p=0.0035). The ring and trophozoite stages of cycle 2, however, were smaller with BAY 43-9006 compared to the control (p=0.0011 at 12h, p=0.0033 at 24h, p=0.0004 at 36h).

Finally, the intracellular calcium levels were also affected by BAY 43-9006. In the presence of drug, the calcium content of iRBCs did not follow the same pattern as the control: calcium increased significantly at 12h of cycle 2 (p=0.0018) and then decreased back to baseline levels. When comparing to the no-drug control, differences were observed throughout the second cycle, albeit with different effects. During the beginning of the second cycle, calcium levels were higher in the presence of BAY 43-9006 (p=0.0026 at 0h, p=0.0123 at 12h, p<0.0001 at 24h). During the end of the second cycle however, calcium levels in the presence of BAY 43-9006 were lower (p=0.0395 at 36h and p=0.0001 at 48h).

Overall, it appears that BAY 43-9006 prevents the parasite from developing beyond the trophozoite stage (apparent from microscopy images and low levels of DNA and RNA). BAY 43-9006 also induces eryptosis hallmarks in iRBCs from 12h of the second cycle.

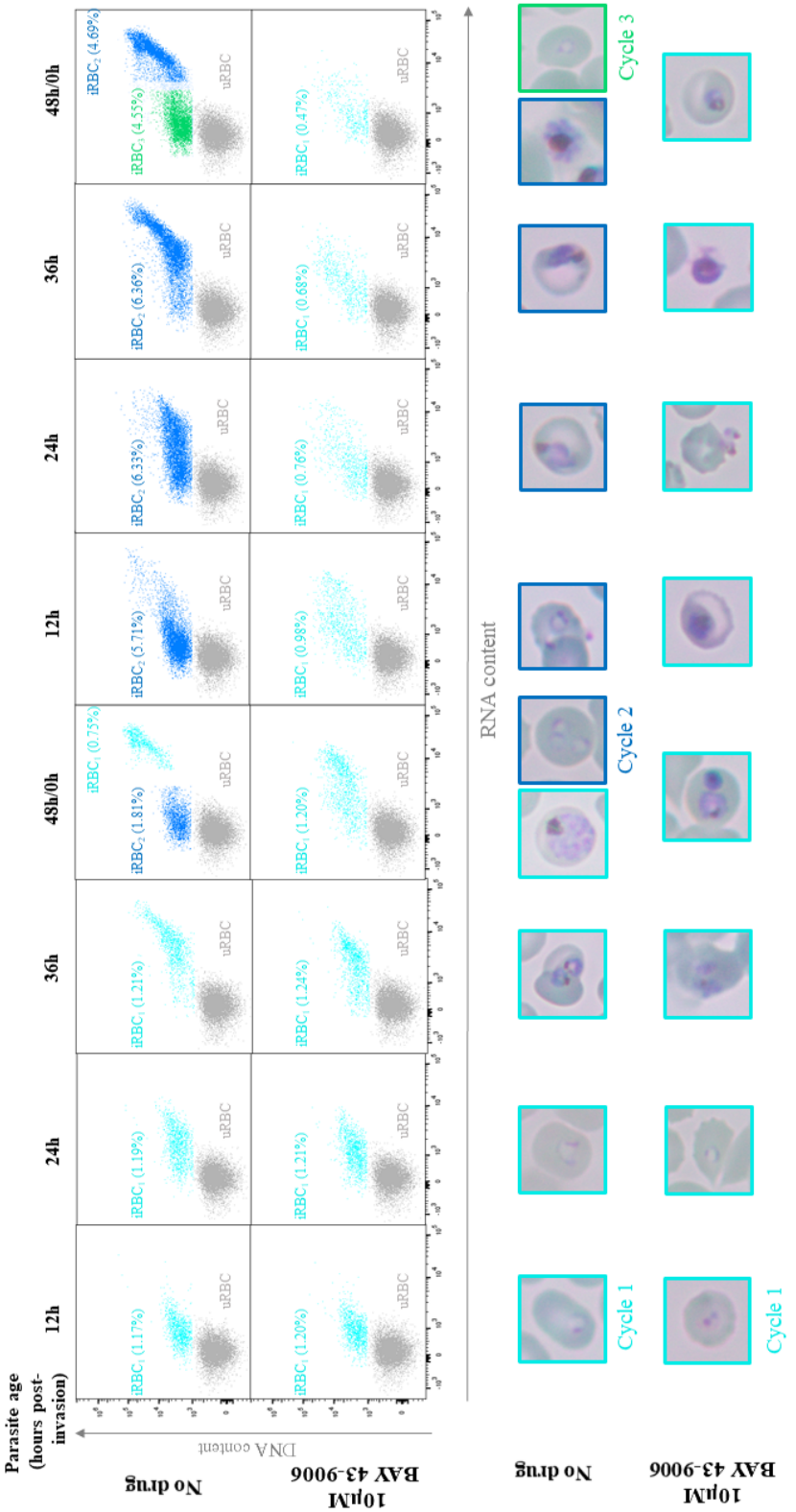

Figure 4.15: Evolution of the flow cytometry layout of iRBCs and uRBCs over time in the presence of 10µM BAY 43-9006. Distribution of uRBCs and iRBCs according to their levels of RNA and DNA content, every 12h over two *P. falciparum* cycles, with or without 10µM BAY 43-9006. The percentage of iRBCs (cycle 1 in light blue; cycle 2 in dark blue; cycle 3 in green) is indicated. Representative microscopy images of iRBCs for each time point are also shown.

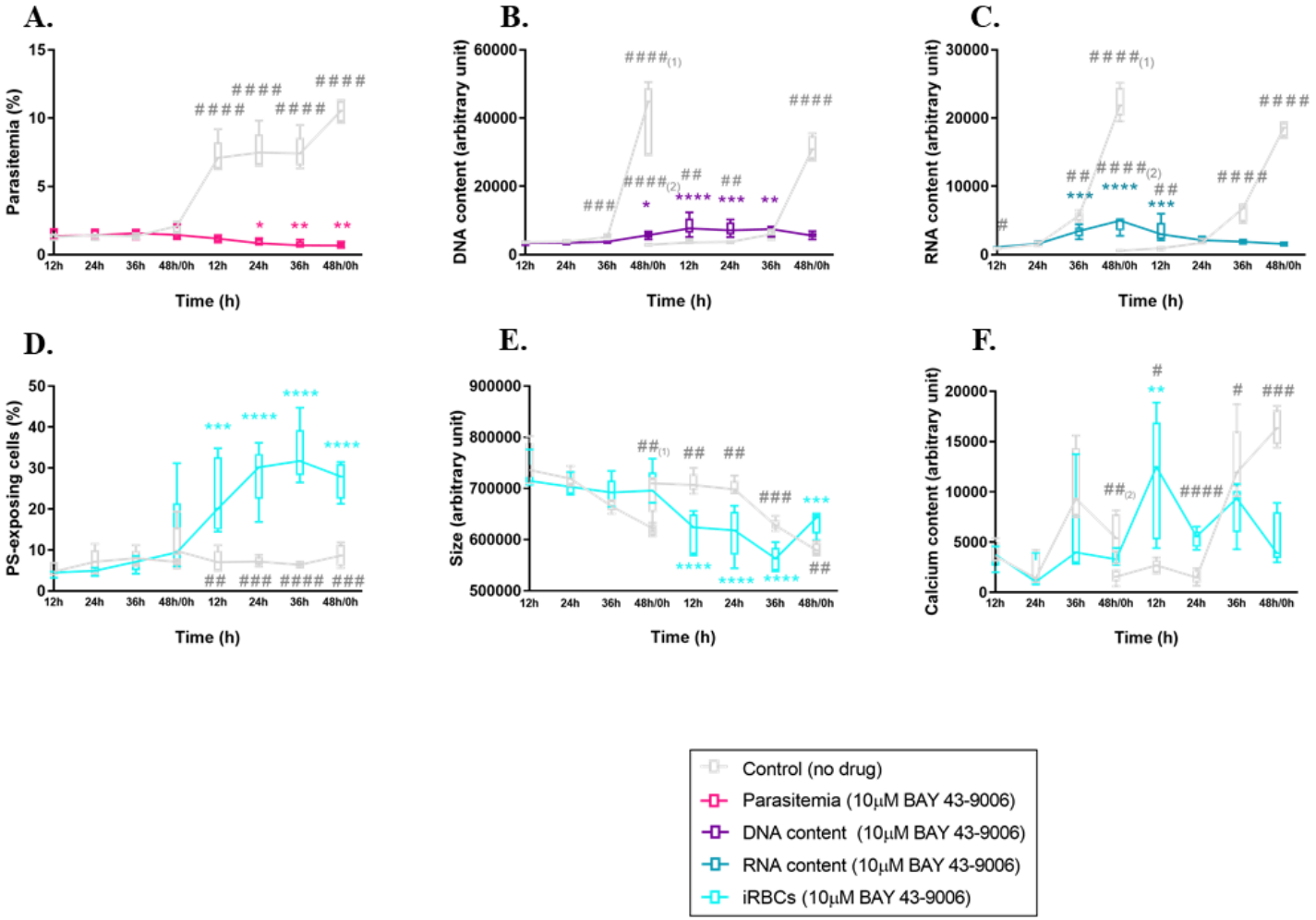

Figure 4.16: Eryptosis of iRBCs over time with or without 10µM BAY 43-9006. A synchronised culture of *P. falciparum* was analysed by flow cytometry every 12h with (coloured lines) or without (grey lines) 10µM of BAY 43-9006. **(A)** Parasitemia, **(B)** DNA content and **(C)** RNA content show the impact of BAY 43-9006 on the parasite development. **(D)** PS exposure, **(E)** cell size and **(F)** intracellular calcium levels show the impact of BAY 43-9006 on eryptosis hallmarks. Whisker boxes (median, 25^{th}, 75^{th}, max and min) for n=5 independent experiments in triplicates are shown. * indicates significant differences with the first point in presence of BAY 43-9006 (One way ANOVA with Dunnett's multiple comparisons test). # indicates significant differences between condition with and without BAY 43-9006 for each timepoint (t-tests). At 36h, $_{(1)}$ indicates that the difference is observed with the schizonts of cycle 1, $_{(2)}$ indicates that the difference is observed with the rings of cycle 2.

4.9 Discussion

4.9.1 BAY 43-9006 reduces parasite's RNA levels and impairs trophozoite development

After only 4h, BAY 43-9006 appeared to reduce the RNA content of iRBCs (Figure 4.13). To my knowledge, this is the first time BAY 43-9006 was found to hinder steady-state RNA levels (either decreasing transcription and/or increased degradation). Noteworthy, we measured RNA content with Thiazole Orange staining and fluorescence read-out by flow cytometry. A more accurate method to quantify RNA will be required to confirm this finding (for instance using phosphorous inductively coupled plasma–optical emission spectroscopy [194]). Further, BAY 43-9006 inhibited progression through schizogony. After only 4h of incubation, parasites appeared dead on microscopy images (Figure 4.12). Upon a longer incubation, BAY 43-9006 hindered both RNA and DNA levels, and resulted in a decreasing parasitemia (no newly formed rings) (Figure 4.16).

4.9.2 BAY 43-9006 induced eryptosis of mature stages of *P. falciparum*

BAY 43-9006 did not induce eryptosis of uRBCs, both after 4h incubation (as shown in Chapter 4A) and also during the time-course (data not shown), therefore Raf does not appear to play a role in constitutively repressing eryptosis. Raf may still play a more indirect role in eryptosis pathways, for instance its protective role may only become apparent upon chemical eryptosis induction.

Similarly, regarding iRBCs, we reported in Chapter 4A that 4h exposure to BAY 43-9006 did not significantly induce eryptosis of iRBCs in unsynchronised parasites. While investigating specific stages, however, we found that eryptosis levels of schizonts were actually impacted by BAY 43-9006 (Figure 4.14). On a longer timescale too, we found that BAY 43-9006 increased eryptosis of infected cells, especially after 48h of incubation with the drug. Since BAY 43-9006 did not induce eryptosis of uRBCs, both after 4h incubation and also during the time-course (data not shown), it is possible that BAY 43-9006 killed the parasite, which resulted in the parasite not being able to inhibit eryptosis of its host cell anymore, similar to what is believed to occur in hepatocytes [106] (also discussed in Chapter 5). It is also possible that schizont-iRBCs are more sensitive to cell death as they have been highly stressed by the presence of the parasite for ∼48h (further discussed in Chapter 5). Finally, BAY 43-9006 could also hypothetically inhibit a pathway only active in iRBCs, and more precisely, only active in mature stages, although such a pathway remains to be identified.

4.9.3 The role of erythrocyte Raf pathway during *P. falciparum* development

This work builds on previous studies showing that *P. falciparum* activates, and relies on, erythrocyte MAPK pathways. Indeed, erythrocyte MEK is phosphorylated in iRBCs (more

so than in uRBCs), a modification attributed to the erythrocyte PAK kinase [195]. Moreover, inhibition of either MEK or PAK resulted in an impairment in *P. falciparum* growth. Similar to MEK and Raf, no orthologs of PAK have been identified in *Plasmodium spp.* [195], supporting the idea that *P. falciparum* relies on these host kinases. In a recent paper, Adderley *et al.* (2020) used antibody microarrays to more comprehensively map differences in signalling pathway activation status in uRBCs vs iRBCs [191]. Interestingly, this study confirmed that the host erythrocyte MAPK pathway appears to be particularly activated by *P. falciparum*. Specifically, B-Raf and C-Raf were phosphorylated on several residues in iRBCs. C-Raf S296 was phosphorylated in all three stages (ring, trophozoite and schizont), supposedly by ERK, due to the negative feedback loop which is part of the MAPK pathway activation. Moreover, the authors observed an intriguing behaviour for B-Raf: phosphorylation on S446 and S447 was increased during the ring stages, and B-Raf appeared to be partially degraded during the trophozoite and schizont stages. Consistent with this, they showed that treatment with the B-Raf-selective inhibitor SB-590885 during the ring stage resulted in a decrease in parasitemia, whereas inhibition of B-Raf during later stages did not impact *P. falciparum* growth. This last observation contrasts with our own experiment, where a 4h incubation of an asynchronous culture with BAY 43-9006 resulted in the apparent death of trophozoites and schizonts (Figure 4.12). However, the inhibitors used were different (SB-590885 is highly selective towards B-Raf, while BAY 43-9006 primarily inhibits C-Raf), as well as the drug concentration and the type of assay, which probably accounts for the apparent discrepancy.

4.9.4 Molecular target of BAY 43-9006: erythrocyte Raf, erythrocyte kinases and/or parasite factors?

Although BAY 43-9006 is a Raf kinase inhibitor (mainly C-Raf and B-Raf), it can also inhibit other kinases within the receptor tyrosine kinases family (provider's specifications, https://www.caymanchem.com/product/10009644). Above 10µM, BAY 43-9006 was shown to inhibit ERK1 and MEK1 (provider's specifications, https://www.caymanchem.com). Overall, further work is required to identify the exact antiparasitic mode of action of BAY 43-9006, in particular whether it is through inhibition of erythrocyte Raf, of other erythrocyte kinases or of *P. falciparum* molecules (this is a possibility, even though no orthologs of Raf kinases have been identified in *Plasmodium spp.*). Follow-up experiments could include the phosphoproteomic analysis of uRBCs and iRBCs with or without BAY 43-9006 to map the phosphorylation changes. Ideally, development of *P. falciparum* in *raf* knock-out erythrocytes would be ideal, although this is a challenging experiment in human erythrocytes because it requires stem cell genetic manipulation, followed by differentiation into mature erythrocytes, which remains experimentally difficult and with a poor yield [196]. Another useful and more feasible approach would be to study the development of murine malaria parasites in *raf* knock-out mice. Such mice exist for the three different *raf* genes: while *a-raf* knock-out mice are born, they develop severe neurological and intestinal defects; *b-raf* and *c-raf* knock-out mice however, die in-embryo due to excessive apoptosis in various tissues

[197]. Conditional knock-out of *raf* genes in the hematopoietic lineage would be preferred to answer our question. Finally, another experiment that could provide us with precious information would be to attempt to develop resistant parasites: following continuous exposure to BAY 43-9006, resistant *P. falciparum* parasites may emerge. The whole-genome sequencing of their DNA could provide us with precious information regarding the mode of action of BAY 43-9006, in particular, whether it appears to target parasite proteins. If no resistant lines can be recovered, it would be an encouraging sign that BAY 43-9006 does indeed kill *P. falciparum* through inhibition of host molecules, hindering the parasite's ability to develop resistance.

4.10 Conclusion

Overall, it is unlikely that Raf is a direct and constitutive inhibitor of eryptosis pathways, since its inhibition does not lead to eryptosis in uRBCs. In iRBCs, only schizonts show an increase in PS exposure upon incubation with BAY 43-9006. Importantly however, BAY 43-9006 impairs *P. falciparum* growth (IC_{50}=7.48µM). In particular, BAY 43-9006 impaired trophozoite and schizont development, especially reducing the parasitic RNA content.

Although more work is required to confirm the mode of action of BAY 43-9006, erythrocyte Raf kinases are likely candidates. This opens exciting perspectives in both host-targeted therapies (targeting host molecules to eliminate a pathogen) and drug-repurposing (utilising an already approved drug for another indication than the one for which the drug was originally developed).

Chapter 5

Eryptosis of *Plasmodium falciparum*-infected erythrocytes

5.1 Introduction

Many intracellular apicomplexan parasites inhibit or delay their host cell apoptosis in order to survive and complete their own development [198]. Similarly, *Plasmodium* parasites have been described to inhibit apoptosis within their host hepatocytes [107]. Therefore, we hypothesise that *P. falciparum* also interferes with its host cell eryptosis in order to survive and avoid splenic clearance.

During the erythrocytic stages of development, *P. falciparum* induces major stress on the host red blood cell (RBC) [71]. This leads to *Plasmodium*-infected RBCs (iRBCs) globally exposing more phosphatidylserine (PS) on the RBC surface than uninfected RBCs (uRBCs) [75, 76]. PS is a key hallmark of programmed cell deaths, including eryptosis: while PS is maintained in the inner lipid bilayer of healthy cells, PS becomes exposed to the surface of eryptotic RBCs, leading to their recognition and phagocytosis by macrophages [73]. To date, eryptosis of *Plasmodium* erythrocytic stages has not been investigated in a stage-specific manner, and the eryptotic state of each intraerythrocytic parasite stage (ring, trophozoite and schizont) is yet to be described. This is relevant because intraerythrocytic stages are remarkably different to one another, therefore their interaction to the host cell eryptosis could also be variable.

We started by measuring eryptosis levels of iRBCs within an asynchronous *P. falciparum in vitro* culture. Then, we determined the dynamics over time of the eryptotic state of each *P. falciparum* erythrocytic stage within a tightly synchronised *in vitro* culture. This allowed us to demonstrate that ring and trophozoite stages display similar eryptosis levels as uRBCs, while schizont stages showed increased eryptosis. Moreover, we found that invasion by *P. falciparum* induces a peak in PS exposure on the host cell, which is then quickly reversed back to base levels. This indicates for the first time that *P. falciparum* may be actively repressing PS exposure during the ring and trophozoite stages.

5.2 Results

5.2.1 Measure of eryptosis of *P. falciparum*-infected RBCs within a parasite mixed population

Eryptosis hallmarks of asynchronous *P. falciparum in vitro* cultures were assessed using flow cytometry. Intraerythrocytic stages were identified based on their DNA and RNA content [143]: ring stages contain low levels of both DNA and RNA; trophozoite stages are transcriptionally active resulting in increased levels of RNA; and schizont stages undergo cell division resulting in increased levels of DNA. A representative example of such a mixed stages culture contained 3.4% of ring stages, 1.7% of trophozoite stages and 0.3% of schizont stages, with the rest of the cells being bystander uRBCs (Figure 5.1A).

For each cell subpopulation (*i.e.* uRBCs, rings, trophozoites and schizonts), the percentage of PS-exposing cells, the average cell size and the average intracellular calcium content were determined (Figure 5.1B-D). We found that schizonts, but not rings and trophozoites, present an increased percentage of PS-exposing cells, when compared to uRBCs ($p<0.0001$) (Figure 5.1B). Similarly, schizonts were also significantly smaller in size when compared to the other subpopulations ($p=0.0048$ compared to uRBCs, $p<0.0001$ compared to rings and trophozoites), while rings appeared significantly bigger ($p=0.0224$ compared to uRBCs, $p<0.0001$ compared to schizonts) (Figure 5.1C). Finally, the level of intracellular calcium content increased with the maturation of the parasite, with schizont reporting higher levels of calcium content than all the other stages (Figure 5.1D): trophozoites vs. uRBCs ($p=0.0008$), schizonts vs. uRBCs ($p=0.0001$). We concluded that overall, schizont stages, but not ring and trophozoite stages, display all tested hallmarks of eryptosis.

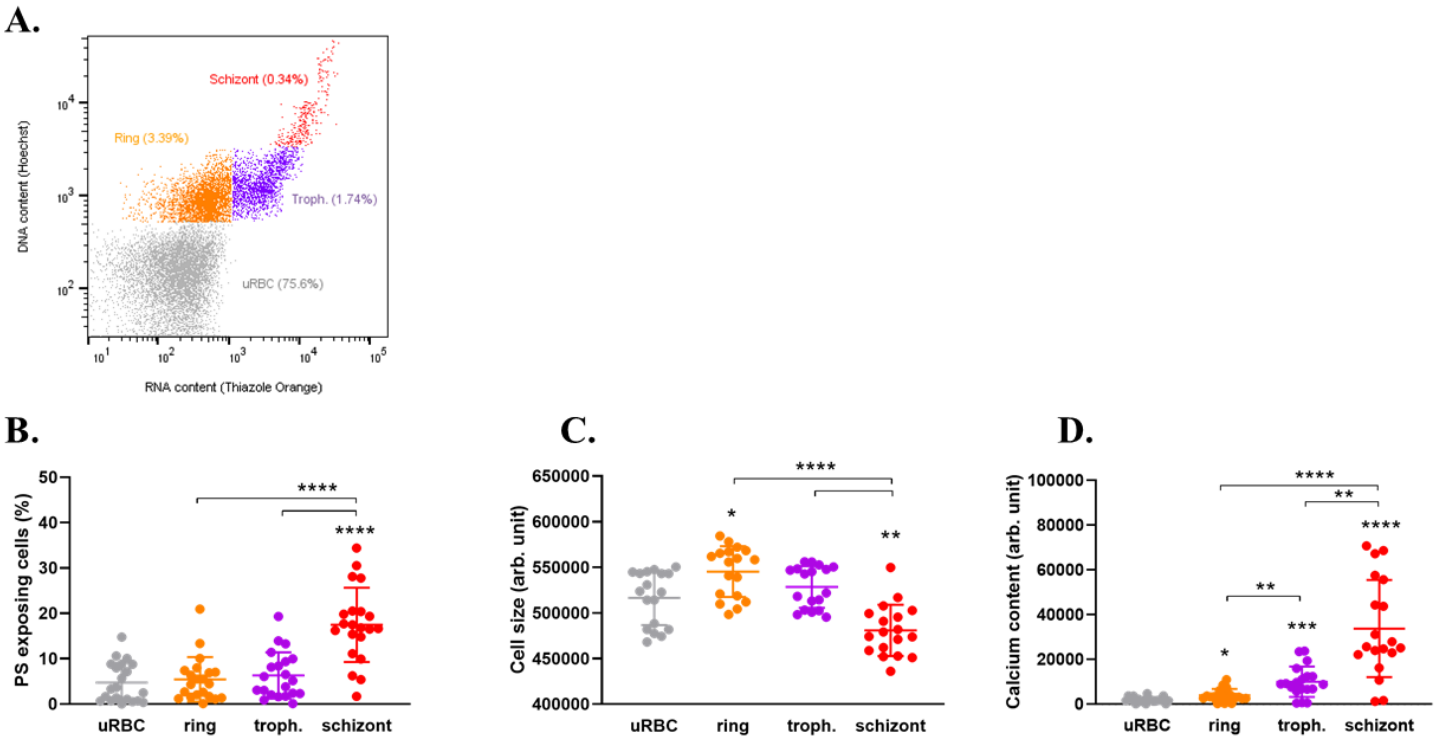

Figure 5.1: Eryptosis hallmarks measured in a mixed population of a *P. falciparum in vitro* culture. **(A)** Identification of uRBCs (grey), ring stages (orange), trophozoite stages (purple) and schizont stages (red) by flow cytometry. Cellular DNA and RNA contents were measured using Hoechst and Thiazole Orange stains respectively. **(B)** PS exposure, **(C)** cell size and **(D)** intracellular calcium content of uRBCs, ring-, trophozoite- and schizont-iRBCs within an asynchronous culture of *P. falciparum*. Individual values, mean and SD are shown for n=17 independent experiments each performed in triplicate. Statistical test: Brown-Forsythe and Welch ANOVA. Compare to bystander uRBCs, unless indicated otherwise.

5.2.2 Measure of eryptosis of *P. falciparum*-infected erythrocytes over time

To investigate the dynamics of eryptosis over the intraerythrocytic development of *P. falciparum* in finer details, we followed a tightly synchronised culture of *P. falciparum* over time. A synchronised *P. falciparum* 1% ring culture was prepared, and cells were analysed every 12h over a total of two complete erythrocytic cycles, *i.e.* 84h, as previously described in Chapter 4B (see Chapter 3 Section 3.2.3).

Parasite synchronicity and maturation progress were measured by flow cytometry and light microscopy (Figure 5.2). Ring stages were detected between 0h post-invasion and 24h, followed by trophozoites (24-36h) and then by schizonts (48h), both during cycle 1 and 2. Although parasite cultures were tightly synchronised, a mixture of late schizonts (44-48h) and young rings (0-2h) was observed towards the end of each cycle (Figure 5.2). However, overall specific parasite stages were exclusively detected at each time point.

To monitor parasite growth over time, we measured parasitemia, DNA and RNA cellular contents by flow cytometry (Figure 5.3). Parasitemia (1.3%) remained constant throughout the first cycle up until 48 hours (Figure 5.3A), after which it increased by a factor 5.6 (reaching 7.23%), corresponding to the re-invasion of RBCs. DNA content remained constant for the first 36h of parasite development, then increased dramatically at 48h (11-fold increase during the first cycle), as a result of parasite cell division (Figure 5.3B). Expectedly, the increase in RNA content was more progressive, as trophozoites, in addition to schizonts, are transcriptionally active: during the first cycle, we measured a 6-fold increase at 36h and a 24-fold increase by 48h (Figure 5.3C).

Next, we analysed several eryptosis hallmarks at each parasite stage, including PS exposure, cell size and intracellular calcium content of the infected erythrocytes. During the first cycle, PS exposure of iRBCs increased slightly during parasite's maturation, although not significantly (Figure 5.3D): this contrasts with the significant increase in PS exposure of schizont stages observed earlier (Figure 5.1). In the transition from the first to the second cycle, PS exposure of newly infected RBCs was significantly higher than that of schizonts: 12% of the new rings of cycle 2 exposed PS vs. 7% of the schizonts of cycle 1 (p=0.0408). This again, contrasts with the earlier observation whereby ring stages displayed similar PS exposure levels as uRBCs (Figure 5.1). Following this marked increase, PS exposure levels significantly dropped between 12h and 36h in cycle 2 (p<0.05 when compared to 0h of cycle 2), before increasing again at 48h. Increased PS exposure of newly formed rings was observed again in cycle 3, with 9% of schizonts from cycle 2 exposing PS, compared to 13% of newly formed rings of cycle 3 (p=0.0404). This is discussed in detail in the Discussion section.

The evolution of cell size over time (Figure 5.3E) was consistent with the observations made

earlier: rings were bigger and schizonts significantly smaller (12h ring vs. 48h schizont of cycle 1, $p<0.0001$). This reduction in cell size (as measured by the forward scatter) seemed to happen gradually over the parasite maturation. This size difference was also observed in newly formed rings when compared to the schizonts of the previous cycle (cycle 1-2: $p=0.0073$; cycle 2-3: $p<0.0001$).

Lastly, we measured the intracellular calcium content and observed an increase as the parasites matured (Figure 5.3F): in cycle 2, the intracellular calcium content increased by 8-fold at 36h ($p<0.0001$) and by 10-fold at 48h ($p<0.0001$) when compared to 0h, in accordance with our previous observations (Figure 5.1). Interestingly, the calcium content of the second cycle's schizonts was higher than that of the first cycle's schizonts ($p<0.0001$). Again, this difference in calcium content was observed between cycles (schizonts of previous cycle vs. new rings of a new cycle), both in between cycle 1 to 2 ($p=0.0027$) and cycle 2 to 3 ($p<0.0001$).

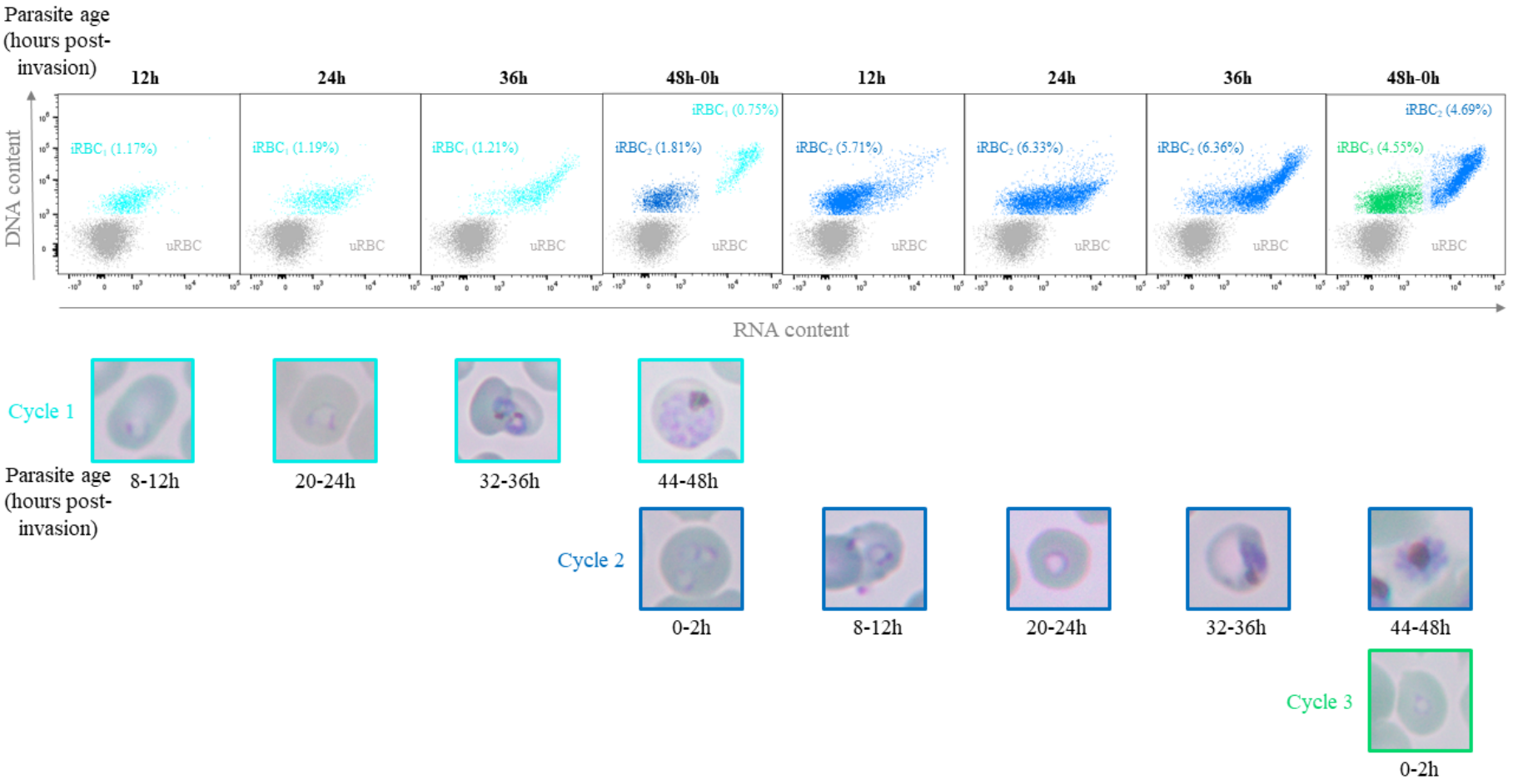

Figure 5.2: Progression of a tightly synchronised *P. falciparum* culture over two complete erythrocytic cycles. A synchronised *P. falciparum* culture was analysed by flow cytometry analysis every 12h for a total period of 84h (*i.e.* two complete parasite cycles). uRBCs and iRBCs were gated based on their DNA and RNA levels. The percentage of iRBCs at each time point is indicated. Representative microscopy images of iRBCs at each time point and the parasite age (in hours post-invasion) are also shown.

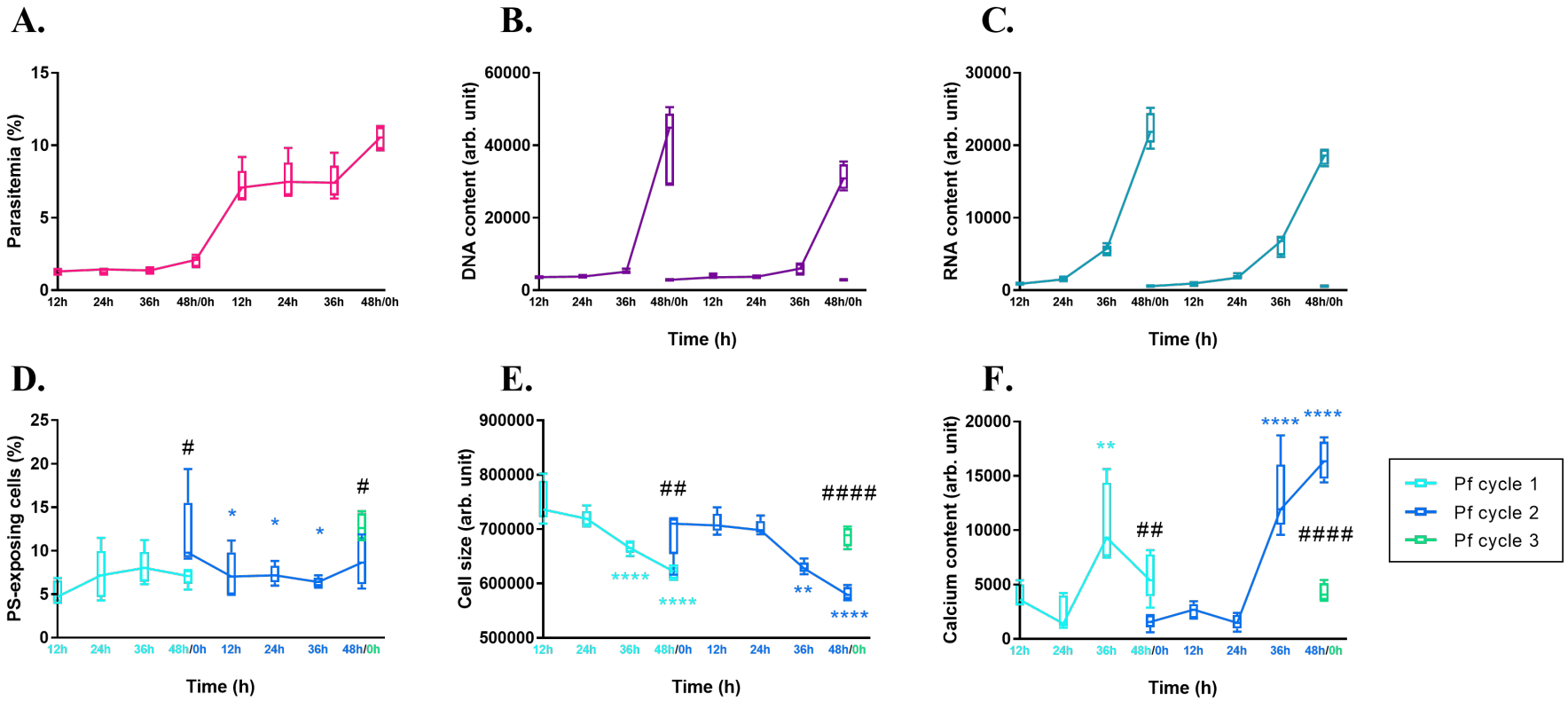

Figure 5.3: Detection of eryptosis hallmarks of iRBCs over time. **(A)** Parasitemia (percentage of DNA positive cells), **(B)** DNA content, **(C)** RNA content, **(D)** PS exposure, **(E)** cell size and **(F)** intracellular calcium content of a synchronised *P. falciparum* culture were measured every 12h over 84h. N=5 independent experiments performed in triplicates are shown with whisker boxes (median, 25th and 75th percentiles, max and min). * : indicates differences with the first point of the same cycle (One way ANOVA with Dunnett's multiple comparisons test). # indicates differences between cycle 1 and 2 and between cycle 2 and 3 (at 48h/0h) (t-test).

5.3 Discussion

5.3.1 *P. falciparum* appears to suppress PS exposure during early stages

- *P. falciparum* might actively suppress PS exposure shortly after invasion

We have demonstrated that in a *P. falciparum in vitro* mixed culture, ring and trophozoite stages expose similar levels of PS on their surface when compared to uRBCs (Figure 5.1). However, when analysing the dynamics of eryptosis hallmarks of iRBCs over time (Figure 5.3D), I discovered a more complex story: I have shown that, upon invasion, early ring stages display high percentage of PS exposure, which is followed by a dramatic decrease to base levels. Surprisingly, the peak in PS exposure observed in early rings is 1.5- to 1.7-fold higher than the levels of PS exposure observed in schizonts.

This observation suggests that the process of invasion leads to a disruption of membrane asymmetry. While this might not be surprising, as the invasion process by an external parasite represents a major trauma to the invaded cell, we discuss here a few explanations as to what could be driving the PS exposure peak.

A first explanation for this induction of PS exposure could be linked to the activation of the erythrocyte glycophorin C (GPC) protein during merozoite invasion [199]. Since the stimulation of GPC was shown to induce eryptosis [200], it is possible that the initial peak in PS exposure is due to the activation of this specific receptor. Moreover, previous studies have demonstrated that during the process of invasion, *Plasmodium* initiates an influx of calcium into the host cell [27]. Although in our assay we did not detect a peak in intracellular calcium upon invasion, which supposedly happens in a matter of seconds, it is also possible that this wave of calcium activates scramblases, leading to an increase in PS exposure [73].

Overall, it is very exciting to observe that following this initial PS exposure peak, the PS exposure levels significantly drop. This represents the first indication that *P. falciparum* could control eryptosis during its intracellular development.

- Schizont stages display increased exposure of PS

In a mixed *P. falciparum in vitro* culture, in contrast to ring and trophozoite stages, schizont stages display all eryptosis hallmarks tested, in particular, increased PS exposure (Figure 5.1). Our data builds on previous observations, whereby it was noted that iRBCs, on average, exposed more PS than uRBCs [75, 76]. Therefore, besides the supposedly short PS exposure peak upon invasion, only the very late stages of the parasite, the schizont stages, induce an increase in PS exposure on their host cell.

A possible explanation for this observation may be that the accumulation of stress over

∼40h-48h induced by *P. falciparum* has reached the host RBC maximum capacity. During schizogony, which only happens during the last ∼8h of the intraerythrocytic development, the parasite takes up a large volume of its host cell, ultimately growing nearly as big as an uninfected erythrocyte [201]. In addition, *Plasmodium* induces extreme changes in cell permeability; when similar changes were simulated in uRBCs, these cells were predicted to lyse after 48h [202]. It is therefore possible that the stress induced by *P. falciparum* ultimately results in eryptosis hallmarks on the host cell during the last few hours within the RBC.

A second hypothesis is that active induction of eryptosis by the parasite during the last few hours within its host RBC facilitates merozoite release. Indeed, induction of the host programmed cell death is a strategy used by some intracellular pathogens to exit their host cell. Flieger *et al.* (2018) described three strategies for a pathogen to exit a host cell [100]: exit without host cell destruction (*e.g. Plasmodium spp.* exit from hepatocytes), the active host cell destruction (*e.g. Plasmodium spp.* exit from erythrocytes) and initiation of the host programmed cell death (*e.g. Leishmania spp.* exit from macrophages). Importantly, exit strategies may be a combination of those. Schizont egress has been extensively studied and the molecular cascade is relatively well understood [203]. It involves various plasmodial kinases and proteases, combined with calcium signalling, first resulting in the lysis of the membrane of the parasitophorous vacuole and then the lysis of the RBC. Interestingly, *P. falciparum* has also been shown to hijack the host protein μ-calpain (or calpain-1) to exit the RBC [204]. Calpains are proteases also suggested to be involved in eryptotic membrane blebbing [205]. In line with this, we demonstrate in Chapter 6 that μ-calpain is recruited to the membrane fraction upon infection. In addition, it is known that *Plasmodium* egress is dependent on calcium signalling [206]. We found here that schizont stages display an increase in intracellular calcium, although our assay could not detect the localisation of this calcium (within the parasite or the host cell). Overall, it is possible that *P. falciparum* induces eryptosis, or stops inhibiting eryptosis, of its host cell to facilitate its exit.

- Inhibiting PS exposure of infected erythrocytes: *in vivo* considerations

Erythrocytes constantly circulate through the spleen, where damaged and senescent cells are detected and cleared. One of the 'defective cell' detection mechanisms by the immune system is the recognition of exposed PS [207]. To circumvent splenic clearance, *P. falciparum* sequesters to the blood vessels endothelium. However, sequestration only occurs at the trophozoite stage. Rings stages are found in the circulation and therefore pass through the spleen, risking clearance. Inhibition of PS exposure during the ring stages appears therefore beneficial to the parasite, by avoiding being recognised and eliminated by macrophages.

This does not explain why PS exposure seems to also be inhibited during the trophozoite stages. It is even more surprising considering the major stress induced by trophozoites: heavy modifications of the RBC, in particular the RBC membrane [30], digestion of consid-

erable amount of haemoglobin [208] and induction of oxidative stress [209]. There might be other advantages in inhibiting eryptosis in addition to avoiding macrophage surveillance, including inhibiting internal processes of eryptosis that would be detrimental to the parasite development. Better knowledge in the underlying molecular events is therefore crucial.

5.3.2 Size of the infected erythrocytes: adding to the controversy

We have shown that iRBCs appear to decrease in size as the parasite matures. Specifically, when compared to uRBCs, rings were bigger, trophozoites were of similar size and schizonts were smaller (Figure 5.1 and 5.3). This is counter-intuitive, as over the 48h of development, the parasite considerably increases its body mass, finishing with up to 32 newly formed merozoites.

However, volume variations of iRBCs during *Plasmodium* parasite growth is a subject of controversy. A mathematical model of homeostasis of parasitised cells predicts that the overall volume of iRBCs remains constant during the first 20h of parasite development, slightly drops at 26h, then increases over the last 20h to reach ∼1.5x the size of the original cell [201]. On the other hand, experimental observations do not support this model. Indeed, Esposito *et al.* (2010) used confocal microscopy to measure *P. falciparum*-infected RBCs size and concluded that only trophozoites (but not rings and schizonts) are significantly bigger than uRBCs [210].

These inconsistencies within the literature and our own data could stem from the use of different approaches (*i.e.* mathematical model, microscopy, flow cytometry). In our study, forward scatter was used to estimate the cell size. However, this readout is affected by the shape of the cell being measured. In the case of RBCs, we know that uRBCs have a discoid form whereas schizont-iRBCs tend to be rounder [210]. Considering the vast difference between uRBCs and iRBCs, comparing their forward scatter measurements to estimate their size difference might not be the best approach. Instead, confocal microscopy appears to be a more reliable method to estimate cell size across different parasite stages. The use of forward scatter to investigate cell size changes could still be considered when comparing the effect of treatment on similar stages (treated vs untreated ring-iRBCs for instance).

5.3.3 *P. falciparum* intracellular calcium levels increase during cycle progression

We have shown that the total amount of free calcium in iRBCs increases as the parasite matures. This is supported by other studies, including Kirk (2001) who estimated that the total calcium content within iRBCs increase by 10- to 20-fold during the course of parasite growth [31]. In addition to demonstrating an increase in intracellular calcium content within iRBCs, Adovelande, Bastide and Schrevel (1993) also found that this increase was focused primarily within the parasite and less so in the RBC cytosol [211]. This was later suggested to be a strategy utilised by the parasite to maintain a low content of free calcium

in the host cell, in order to prevent eryptosis induction.

Overall, we have demonstrated that *P. falciparum* appears to actively inhibit the host cell eryptosis hallmarks during the ring and trophozoite stages, primarily by maintaining low PS exposure levels. In the perspective of developing novel antimalarial drugs that would interfere with this eryptosis inhibition, we need to understand the underlying molecular events at play. However, little is known about the molecular pathways of eryptosis. Such is the focus of the following section.

5.3.4 What's next: phosphoproteome changes of erythrocytes upon *P. falciparum* infection

As the molecular events underlying eryptosis are yet to be identified, we cannot hypothesise what pathways and molecules *P. falciparum* could be interfering with to inhibit PS exposure during its intraerythrocytic development. However, as nucleus-deprived erythrocytes must rely on post-translational modifications of existing proteins for many processes, phosphoproteomics analysis of RBC components provides an unbiased and comprehensive approach to investigate parasite-host cell interactions.

Due to the sur-abundance of haemoglobin, proteomics analysis of erythrocytes has been challenging. The most comprehensive proteome of human (non-infected) erythrocytes to date identified 1,578 cytosolic proteins [124]. Importantly, the phosphoproteome of erythrocyte cytosol has never been established. Erythrocytic membrane proteins, on the other hand, have been more extensively studied: of particular interest, the phosphoproteome changes induced by *P. falciparum* at the erythrocyte membranes has been described [212]. We therefore aimed to establish the first proteome and phosphoproteome of RBC cytosolic proteins in uRBCs and in iRBCs.

To do so, the first step was to establish a peptide library for uRBCs and trophozoite-iRBCs, using Data-Dependent Acquisition (DDA) mass spectrometry. This was successfully conducted in collaboration with the Creek Laboratory (Monash Institute of Pharmaceutical Sciences). Briefly, a controlled number of uRBCs and magnet-purified trophozoite-iRBCs (in total 10^{10} uRBCs and 10^{10} iRBCs) were saponin-lysed, and only the soluble fraction (*i.e.* erythrocyte cytosolic content) was analysed by mass spectrometry. Proteins were trypsin digested, phospho-enrichment was performed using titanium dioxide (TiO_2) beads; finally, both phospho-enriched peptides and "unbound TiO_2" peptides were analysed by LC-MS/MS (Liquid chromatography–mass spectrometry) (see Chapter 3 section 3.4.6).

In our global proteomics library (the "unbound TiO_2" peptides), we identified a total of 1,205 proteins, of which 791 were human proteins and 414 were *P. falciparum* proteins. In the global phosphoproteomics, we identified a total 384 phosphorylated proteins: 223 human proteins and 161 *P. falciparu*m proteins. From the 384 proteins, there were 989

phospho-sites (779 serine, 202 threonine and 17 tyrosine) and of which 568 phospho-sites were greater than 70% in localisation confidence.

These peptide libraries (both proteomics and phosphoproteomics) are available alongside this thesis.

These findings compare to 1,578 cytosolic erythrocytic proteins identified by Roux-Dalvai *et al.* (2006) [124]. The lower number in human proteins in our study might be attributed to a number of experimental differences. First, we depleted haemoglobin using nickel beads, which can lead to the loss of proteins. Second, we performed a phospho-enrichment to establish a phosphoproteomics peptide library: this again, can affect the total number of proteins identified. Finally, we analysed both iRBCs and uRBCs together: some abundant plasmodial proteins could have "masked" low abundance human proteins.

Regarding *Plasmodium* proteins, the parasite secretome had been predicted to be comprised of ∼250 proteins [213], including a significant proportion known to be localised at the RBC membrane. Since we identified more *Plasmodium* proteins than expected, it is possible that a portion of proteins from the parasite contaminated our RBC cytosolic fraction. It will be important in follow-up studies to assess the quality of the separation between RBC cytosolic content and membrane / parasite fraction. Alternatively, it could indicate that the sensitivity of the method used here detected more "true" parasite proteins secreted in the RBC cytosol, which would be extremely exciting.

These are the first peptide and phosphopeptide libraries established for the cytosolic fraction of uRBCs and iRBCs. Now that this key database is available, the next step will be to establish the phosphoproteome of uRBCs and iRBCs separately in a Data Independent Acquisition (DIA) approach. Excitingly, this will allow for a global understanding of phosphorylation changes induced by the parasite. The impact of kinase inhibitors on these phosphoproteomes will also allow to decipher crucial signalling pathways taking place in the erythrocyte cytosol.

5.4 Conclusion

We demonstrated that among the *P. falciparum* erythrocytic stages, only schizont stages present several increased eryptosis hallmarks, namely increased PS exposure, calcium content and decreased cell size. Further, we have demonstrated for the first time that upon invasion, iRBCs display a peak in PS exposure which is reversed within less than 12 hours. Taken together, this suggests that *Plasmodium falciparum* invasion of RBCs triggers an increase in PS exposure, followed by a repression of PS exposure during the ring and trophozoite stages, and eventually by re-activation of eryptosis during late schizogony.

This offers great perspective for host-targeted therapies. Indeed, many compounds targeting "death proteins" and kinases already exist and are being used in the context of other diseases [115]. Importantly, targeting pathways being hijacked by the parasite (therefore potentially only active in iRBCs) could minimise off-target effects, whereby only iRBCs would be affected by the drug [106]. In order to develop such therapies, more work is required to decipher the molecular events of both eryptosis, and the manipulation of eryptosis by *P. falciparum*. In particular, global phosphoproteomic analysis of erythrocytes upon invasion by *P. falciparum* could significantly help filling this gap in knowledge.

Chapter 6

The Role of Erythrocytic BCL-x_L During *P. falciparum* Infection

6.1 Introduction

In the perspective of developing host-targeted therapies as a novel antimalarial strategy, host programmed cell death pathways are considered ideal targets. This is because apicomplexan parasites are known to manipulate their host cell death pathways in many different cell types [198]. Further, many compounds targeting cell death pathways are already available and clinically approved [115]. The manipulation of the host cell death often results in the pathogens being highly dependent on specific pathways, and can therefore become particularly susceptible to interference with such pathways. For instance, *P. falciparum* appears to be heavily reliant on mitochondria-driven apoptosis during the liver stage [106]. Indeed, inhibition of anti-apoptotic members of the BCL (B-cell lymphoma) family increased death of infected cells and reduced the parasites burden [106]. Of particular interest, the BH3-mimetic ABT-737 has been shown to eliminate liver stages of *Plasmodium spp.* both *in vitro* and in murine models [106]. Although mature erythrocytes lack a mitochondrion, BCL-x_L has been identified in this cell type by mass spectrometry [124]: its role in erythrocytes remains to be investigated. Interestingly, inhibition of BCL-x_L in mature erythrocytes was found to induce eryptosis [125]. We therefore hypothesise that, similar to liver stages, blood stages of *P. falciparum* interfere with its host cell eryptosis through BCL-x_L.

To elucidate if erythrocyte BCL-x_L plays a critical role during *P. falciparum* infection, we tested the impact of six BCL-x_L inhibitors (including one FDA-approved drug) on *P. falciparum* proliferation *in vitro*. To establish if BCL-x_L has a role in eryptosis, we measured eryptosis hallmarks of both uninfected red blood cells (uRBCs) and infected red blood cells (iRBCs) exposed to three BCL-x_L inhibitors. Finally, to define role of BCL-x_L in uRBCs and iRBCs, we determined its subcellular localisation and molecular binding partners.

6.2 Results

6.2.1 Impact of BCL-x_L inhibitors on *P. falciparum* growth *in vitro*

To determine whether erythrocytic BCL-x_L is required for *P. falciparum* development, we tested the antiparasitic ability of six BCL-x_L inhibitors (described in Table 6.1), including one FDA-approved compound (ABT-199) and one compound currently undergoing clinical trials (ABT-263). The results of growth inhibition assays for each of these compounds are shown in Figure 6.1. All six compounds significantly impacted *Plasmodium* proliferation, although at various degrees: IC_{50} values were between 0.74µM (for ABT-263) and 10.27µM (for A-1331852).

Table 6.1: BCL-x_L inhibitors tested on *P. falciparum* viability (IC_{50}) and their current clinical use. IC_{50}: half maximal inhibitory concentration. K_i: inhibitory constant (reflective of binding affinity).

Compound	Date of development	Current clinical trial	Indication	Molecular target	Peak plasma levels (in humans)	IC_{50} on *Pf in vitro*
ABT-737	2005 [128]	No	N/A (low solubility and bioavailability)	BCL-2 ∼BCL-x_L ∼BCL-w (K_i<1nM)	N/A	6.57µM
ABT-263 (Navitoclax)	2008 [129]	Phase I/II	Small Cell Lung Cancer; Lymphoid malignancies	BCL-2 ∼BCL-x_L ∼BCL-w (K_i<1nM)	∼5.75µM [130]	0.74µM
ABT-199 (Venclexta™, Venclyxto, Venetoclax)	2013 [133]	FDA-approved (2016)	Chronic lymphocytic leukemia	BCL-2 (K_i<0.01nM) BCL-x_L (K_i<48nM) BCL-w (K_i <245nM)	∼3.45µM [134]	4.60µM
WEHI-539	2013 [136]	Pre-clinical	N/A (poor physico-chemical properties)	BCL-x_L (IC_{50}=1.1nM)	N/A	0.93µM
A-1155463	2014 [137]	Pre-clinical	N/A	BCL-x_L (K_i<0.01nM)	N/A	4.70µM
A-1331852	2015 [138]	Pre-clinical	N/A	BCL-x_L (K_i<0.01nM) BCL-w (K_i=4nM) BCL-2 (K_i=6nM)	N/A	10.27µM

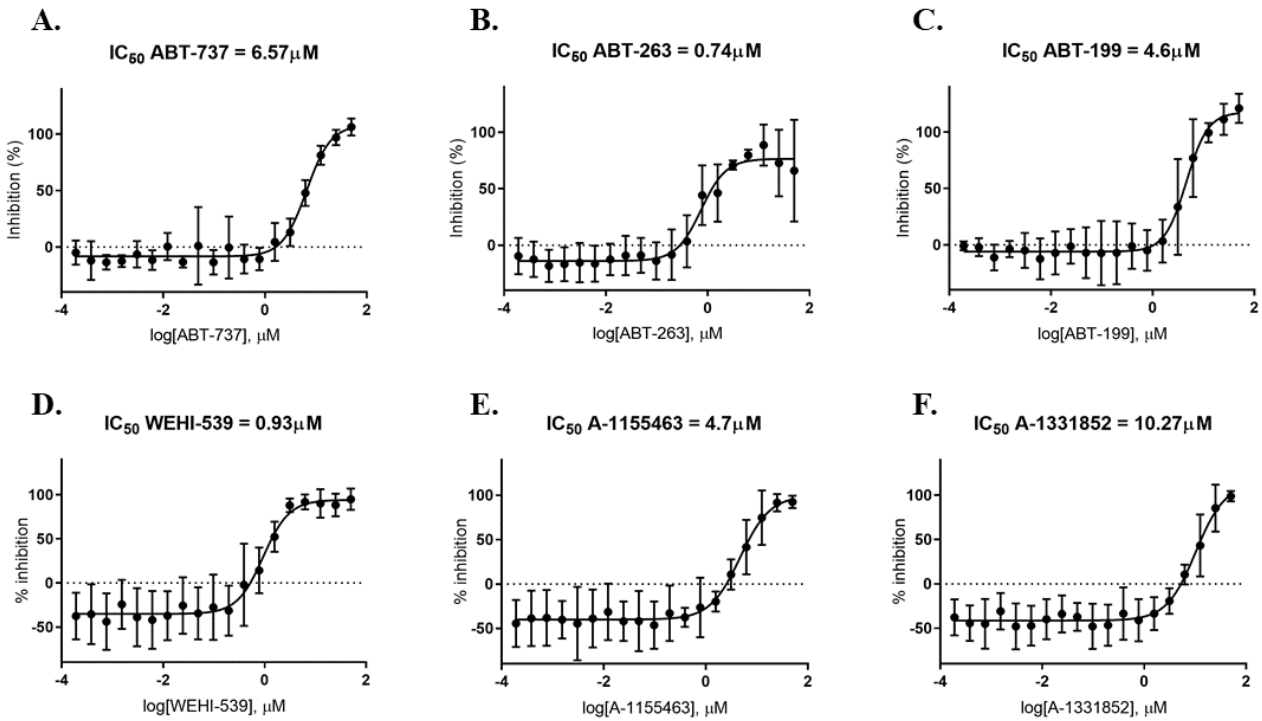

Figure 6.1: BCL-x_L inhibitors impair *P. falciparum* proliferation. *In vitro* asynchronous cultures of *P. falciparum* were cultured with a range of concentrations of BCL-x_L inhibitors (up to 50μM) for 72h. DNA content was measured as a proxy for parasite growth. IC_{50} concentrations are indicated for each compound in μM: ABT-737 (n=3), ABT-263 (n=3), ABT-199 (n=3), WEHI-539 (n=5), A-1155463 (n=6), A-1331852 (n=5). n: independent experiments, performed in triplicate. Data are represented as the mean and SD of independent experiments.

6.2.2 Impact of BCL-x_L inhibitors on eryptosis

In nucleated cells, BCL-x_L has an anti-apoptotic role; therefore BCL-x_L inhibitors induce apoptosis. We hypothesise that likewise, BCL-x_L has an anti-eryptotic role in mature RBCs. To challenge this hypothesis, we tested if BCL-x_L inhibitors induce erythrocyte death.

We tested three ABT compounds for eryptosis induction. These ABT compounds (ABT-737, ABT-263 and ABT-199) were designed to bind to the hydrophobic pocket of anti-apoptotic BCL-2 proteins, such as BCL-x_L, where BH3-only proteins (pro-apoptotic proteins, such as BAX) are usually sequestered [128, 129, 133].

Based on the ABT compounds respective IC_{50} values, we used 5µM for ABT-236 (∼6-fold the IC_{50}); since the IC_{50} for ABT-737 and ABT-199 were more elevated, we used 10µM (∼2-fold the IC_{50}). Cultures of asynchronous parasites and uRBCs were incubated with each compound for 4h in incomplete RPMI (iRPMI). Cells were then analysed by flow cytometry as described in Chapter 4. The presence and developmental stage of the parasite were detected based on RNA (Thiazole Orange) and DNA content (Hoechst), and eryptosis hallmarks were assessed (PS exposure, cell size, intracellular calcium content and hemolysis). Figure 6.2, 6.3 and 6.4 show eryptosis hallmarks of naïve RBCs, bystander RBCs, and RBCs infected with ring, trophozoite and schizont stages in the presence of ABT-737, ABT-263 and ABT-199. For each parasitic stage (ring, trophozoite and schizont) as well as for uninfected RBCs (naïve and bystander), we tested whether treatment induced eryptosis hallmarks compared to non-treated cells. We found that none of the compounds tested induced multiple hallmarks of eryptosis in any of these cell populations, although 10µM of ABT-199 induced hemolysis in *P. falciparum* cultures (p=0.059), but not in uRBCs cultures. ABT-263 appeared to slightly increase eryptosis hallmarks of schizonts, although not significantly.

Overall, BCL-x_L does not appear to have anti-eryptotic capacities in mature RBCs, given BCL-x_L inhibition did not induce eryptosis. This has led us to conclude that eryptosis is not the mechanism of action underpinning the antiparasitic activity of BCL-x_L inhibitors observed earlier.

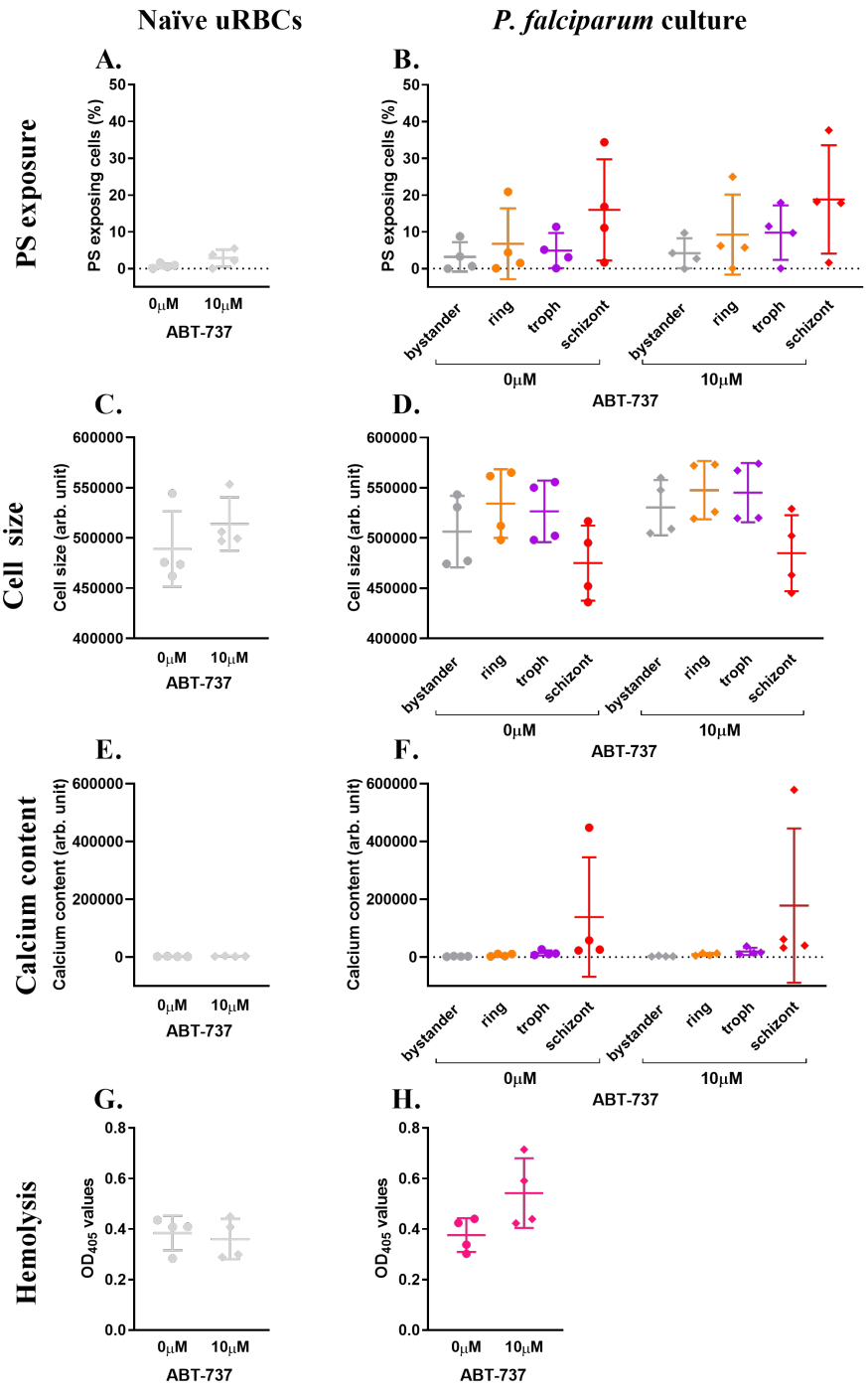

Figure 6.2: ABT-737 does not induce eryptosis of naïve erythrocytes or *Plasmodium* cultures. Naïve erythrocytes or asynchronous cultures of *P. falciparum* were incubated 4h in iRPMI with 0 or 10µM ABT-737 (n=4). PS exposure **(A, B)**, cell size **(C, D)** and calcium content **(E, F)** were assessed by flow cytometry for naïve uRBCs (light grey) **(A, C, E)**, bystander uRBCs (dark grey), rings (orange), trophozoites (purple), schizonts (red) **(B, D, F)**. Hemolysis was measured by absorbance of the cell-free media (OD_{405}) both for cultures of uRBCs (light grey) **(G)** and *P. falciparum* cultures (pink) **(H)**. Individual values of independent experiments in triplicates are shown with the mean and SD. A t-test (naïve uRBCs and hemolysis) or an Ordinary one-way Anova with multiple Tukey tests were performed. * : unless indicated otherwise, compare with bystander RBCs within the same condition. Treated vs. untreated cells (uRBCs, rings, trophozoites and schizonts) were also compared but not statistically different.

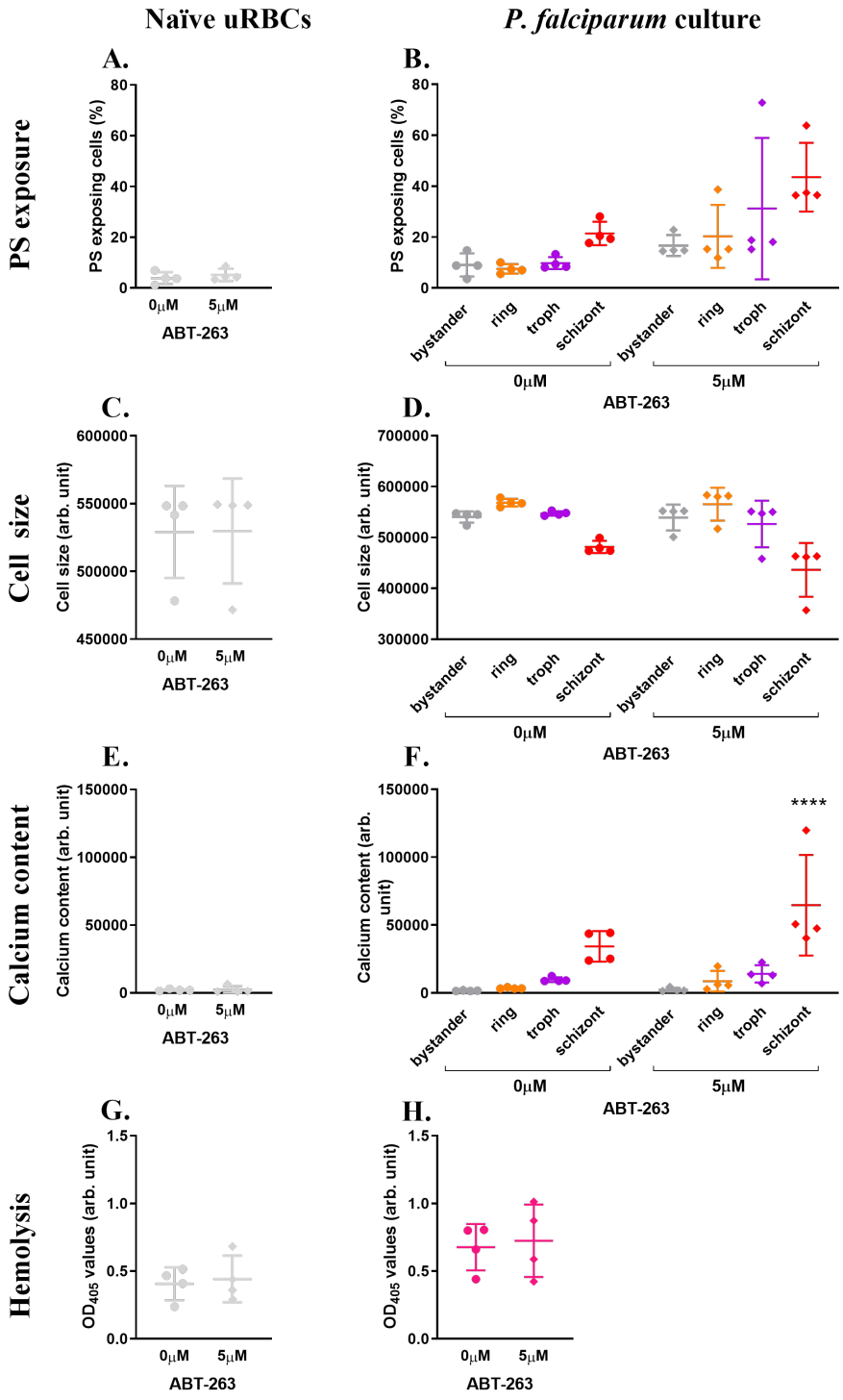

Figure 6.3: ABT-263 does not induce eryptosis of naïve erythrocytes or *Plasmodium* cultures. Naïve erythrocytes or asynchronous cultures of *P. falciparum* were incubated 4h in iRPMI with 0 or 5µM ABT-263 (n=4). PS exposure **(A, B)**, cell size **(C, D)** and calcium content **(E, F)** were assessed by flow cytometry for naïve uRBCs (light grey) **(A, C, E)**, bystander uRBCs (dark grey), rings (orange), trophozoites (purple), schizonts (red) **(B, D, F)**. Hemolysis was measured by absorbance of the cell-free media (OD_{405}) both for cultures of uRBCs (light grey) **(G)** and *P. falciparum* cultures (pink) **(H)**. Individual values of independent experiments in triplicates are shown with the mean and SD. A t-test (naïve uRBCs and hemolysis) or an Ordinary one-way Anova with multiple Tukey tests were performed. * : unless indicated otherwise, compare with bystander RBCs within the same condition. Treated vs. untreated cells (uRBCs, rings, trophozoites and schizonts) were also compared but not statistically different.

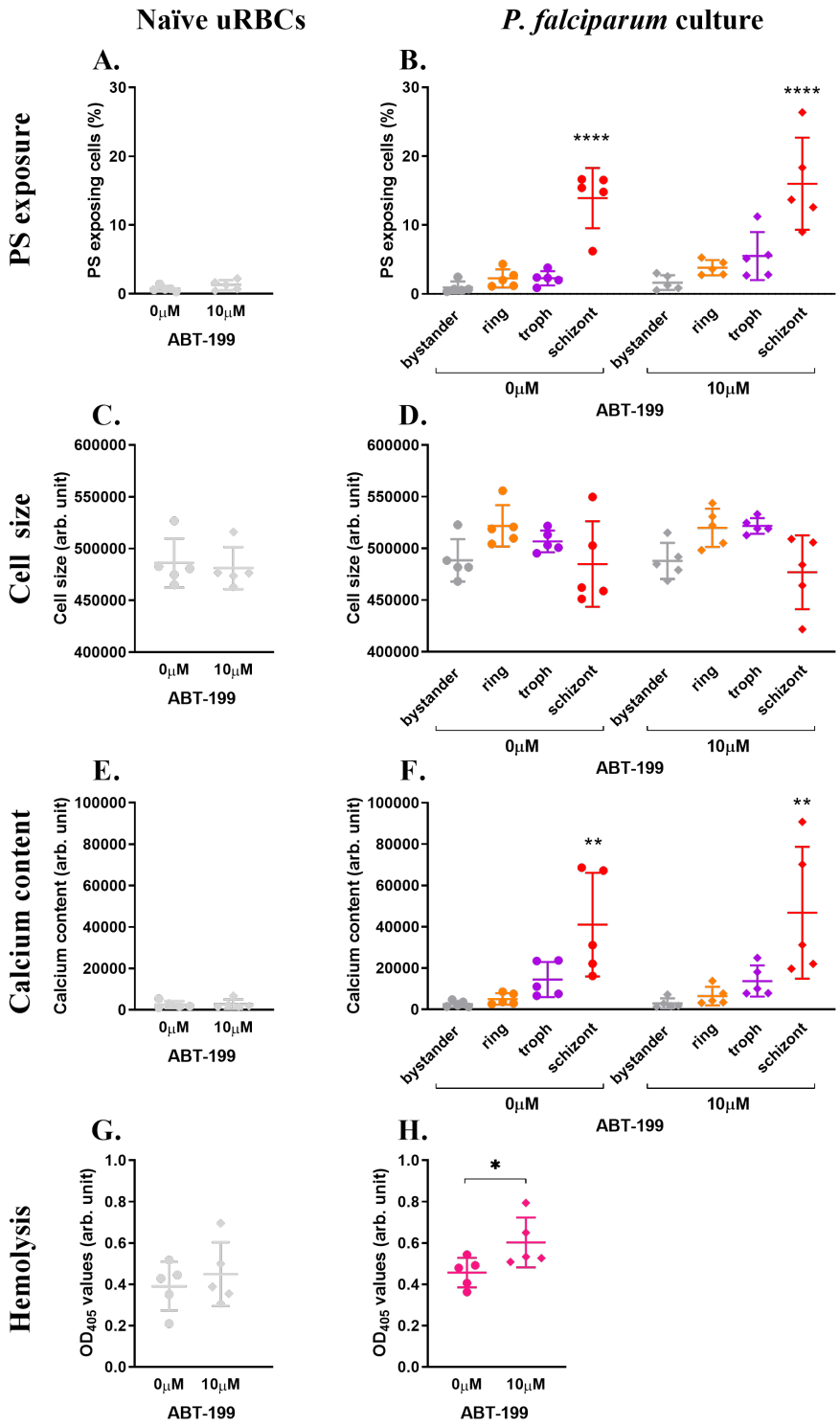

Figure 6.4: ABT-199 does not induce eryptosis of naïve erythrocytes or *Plasmodium* cultures. Naïve erythrocytes or asynchronous cultures of *P. falciparum* were incubated 4h in iRPMI with 0 or 10µM ABT-199 (n=5). PS exposure **(A, B)**, cell size **(C, D)** and calcium content **(E, F)** were assessed by flow cytometry for naïve uRBCs (light grey) **(A, C, E)**, bystander uRBCs (dark grey), rings (orange), trophozoites (purple), schizonts (red) **(B, D, F)**. Hemolysis was measured by absorbance of the cell-free media (OD_{405}) both for cultures of uRBCs (light grey) **(G)** and *P. falciparum* cultures (pink) **(H)**. Individual values of independent experiments in triplicates are shown with the mean and SD. A t-test (naïve uRBCs and hemolysis) or an Ordinary one-way Anova with multiple Tukey tests were performed. * : unless indicated otherwise, compare with bystander RBCs within the same condition. Treated vs. untreated cells (uRBCs, rings, trophozoites and schizonts) were also compared but not statistically different.

6.2.3 Effect of WEHI-539 on *P. falciparum* over time

Among the six BCL-x_L inhibitors tested, ABT-263 and WEHI-539 exhibited the lowest IC_{50} values (Figure 6.1, 0.74µM and 0.93µM, respectively). While ABT-263 targets two other molecules of the BCL-2 family (BCL-2 and BCL-w), WEHI-539 is a very specific inhibitor of BCL-x_L (see Table 6.1). We therefore decided to investigate the impact of WEHI-539 on parasite development and host cell eryptosis over two parasitic cycles.

As described in Chapter 4B (page 87) and Chapter 5, a synchronised culture of *P. falciparum* (set up at 1% ring stages), was analysed by flow cytometry every 12h, in the presence or absence of 1µM WEHI-539. Figure 6.5 shows the parasitemia, DNA and RNA content per iRBCs, eryptosis hallmarks (PS exposure, cell size and intracellular calcium content) of iRBCs, as well as representative images of iRBCs at each time point. We tested the impact of WEHI-539 (bright coloured lines) compared to the no-drug control (light grey lines).

We observed that WEHI-539 impacted parasitemia, seemingly at the schizont stage and/or at the reinvasion step (Figure 6.5A-C and G). Although between 12h and 36h of cycle 2 the difference in parasitemia between the presence and absence of WEHI-539 was not significant, there were replicates that were slightly affected by the presence of the drug, with only a small increase in parasitemia during the second cycle. The difference in parasitemia became significant at 48h of cycle 2 / 0h of cycle 3 (p=0.001): without drug, parasites multiplied to reach a parasitemia of 11%, while in the presence of the drug, parasitemia stalled at 4.2%. DNA replication seemed to be affected by the presence of WEHI-539, especially during the second cycle (the drug nearly halved the DNA content at 48h; p=0.0052). The RNA content was also slightly but significantly diminished by the presence of WEHI-539 at 36h of both cycle 1 and cycle 2 (p=0.0234 and 0.0399 respectively), and at 48h of cycle 2 (p=0.0166). Phenotypically, no striking differences were observed, although a subset of parasites appeared dead by microscopy from 36h of the second cycle in the presence of WEHI-539 (not shown).

Regarding the impact of WEHI-539 on eryptotic phenotypes of iRBCs, no significant changes of PS exposure and calcium contents were observed compared to the no-drug control. Regarding iRBC size, however, the schizonts appeared bigger in the presence of the drug, both in cycle 1 (p=0.047) and in cycle 2 (p=0.0069). On the other hand, the newly formed rings of cycle 3 appeared smaller than without the drug (p=0.0206).

Overall, it seemed that WEHI-539 impacted the parasite's ability to replicate (lowered parasitemia, DNA and RNA content), but did not appear to affect eryptosis induction, despite changes in cell size at the schizont stages.

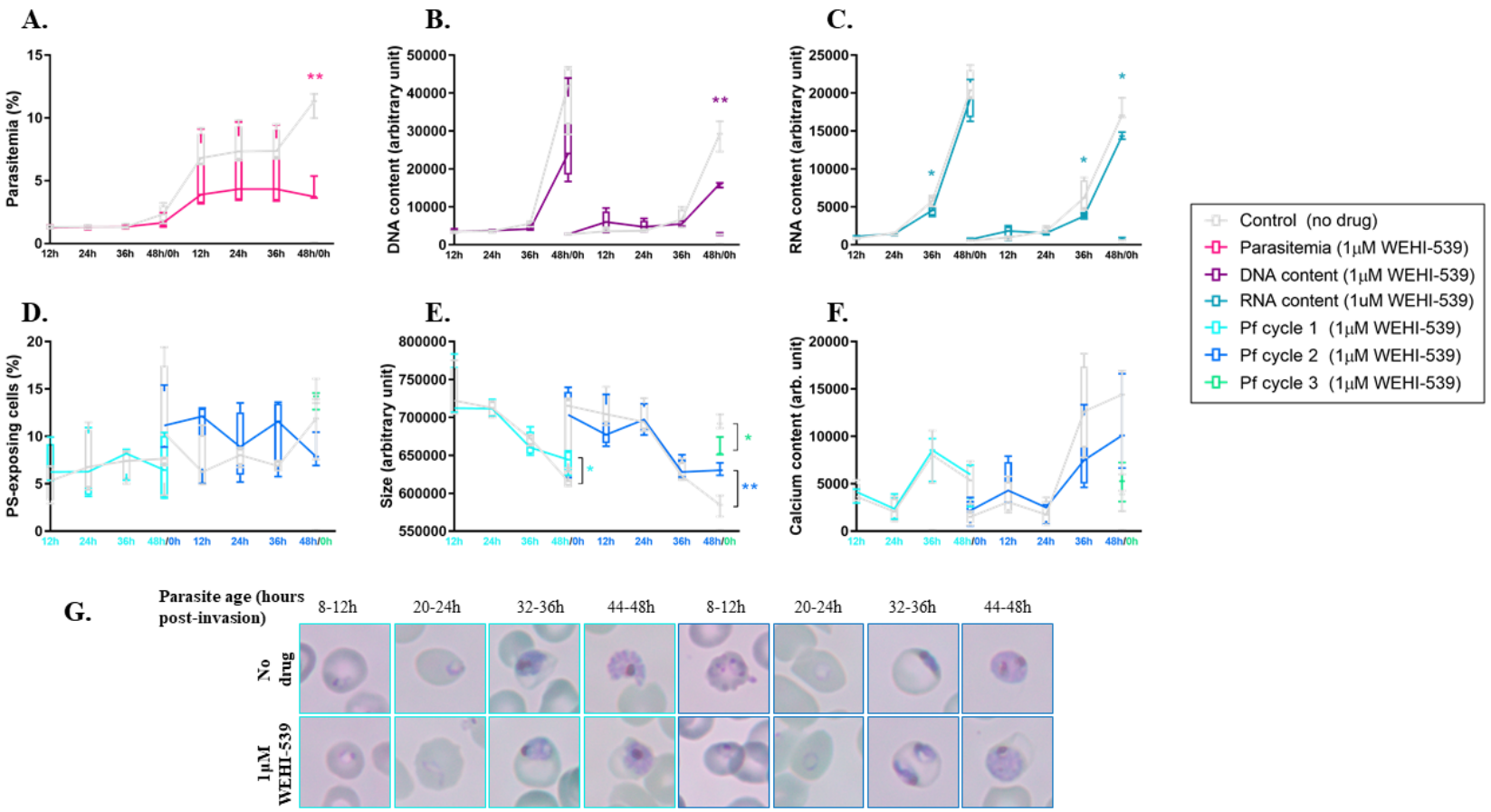

Figure 6.5: Time-course analysis of iRBC in the presence of 1µM WEHI-539 across two life-cycles. A synchronised culture of 1% ring with (bright colored lines) or without (light grey lines) 1µM WEHI-539 was analysed every 12h for 84h by flow cytometry: **(A)** parasitemia, **(B)** DNA content, **(C)** RNA content, **(D)** PS exposure, **(E)** cell size and **(F)** intracellular calcium content. **(G)** Phenotypic observation of parasites were conducted by thin blood smears. Whisker boxes (mean, 25^{th}, 75^{th} percentil, min and max) of N=4 independent experiments in triplicate are shown. T-tests were used to compare the condition with and without WEHI-539 at each timepoint.

6.2.4 Subcellular localisation of BCL-x_L in uRBCs and iRBCs

In nucleated cells, BCL-x_L role in apoptosis is highly dependent on its localisation. We therefore investigated the subcellular localisation of BCL-x_L in uRBCs and iRBCs.

Proteins from uRBCs and magnet-purified trophozoite-iRBCs were extracted, and samples normalised by cell number. The MPER detergent lysed all the membranes, providing the "total" protein content; saponin lysed the RBC membrane but not the parasite's membrane, therefore giving the RBC "cytoplasmic content" (*i.e.* the soluble fraction) and the "membranes fraction" (*i.e.* the insoluble fraction, which included the parasite in the case of iRBCs) (Figure 6.6A). The equivalent of 10^7 cells were loaded per lane, in addition to the breast cancer cell line (MDA-MB231) lysate as a positive control. The same Western Blot was probed with antibodies against BCL-x_L, Carbonic Anhydrase I (CA-I), protein 4.1 and PfHSP70.1 (Figure 6.6A). CA-I, Protein 4.1 and PfHSP70 were used as markers for the RBC cytosol, the RBC membrane and the parasite, respectively.

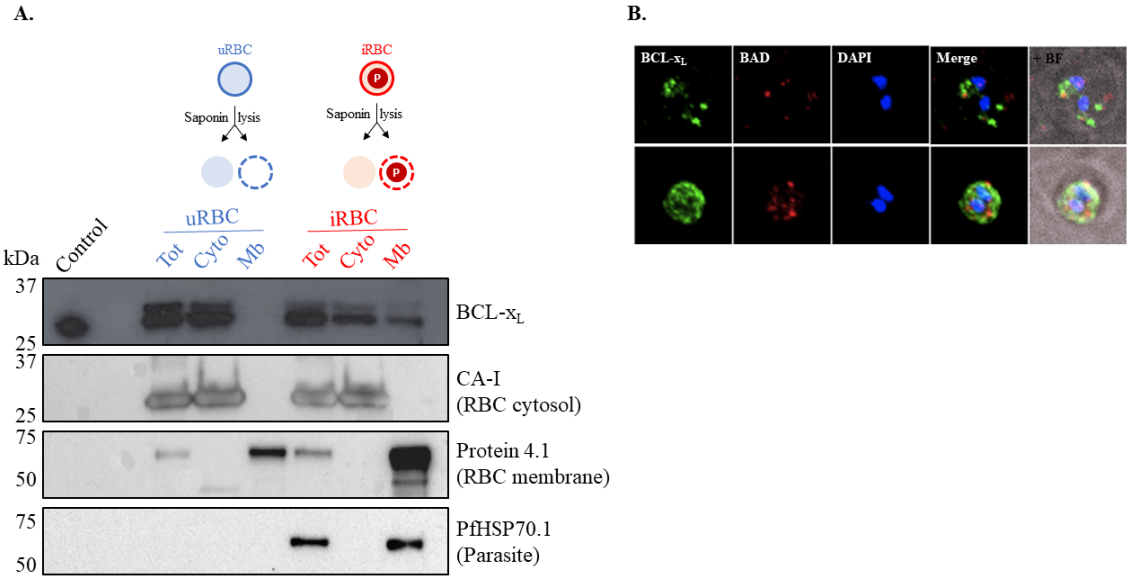

Figure 6.6: Erythrocytic BCL-x_L relocates upon infection. (A) Western Blot of 10^7 uRBCs or 10^7 iRBCs: total protein extraction (tot – solubilised with MPER), cytosolic content (cyto – soluble fraction of a saponin lysis) or membrane fraction (Mb – insoluble fraction of a saponin lysis; the whole parasite localises to the membrane fraction). BCL-x_L localises to the erythrocytic cytosolic fraction in uRBCs, and a proportion of BCL-x_L localises to the membrane fraction in iRBCs. Control is protein extraction from MDA-MB 231 (breast cancer cell line). **(B)** Immunofluorescence assay of *Plasmodium*-infected erythrocytes. Both BCL-x_L (in green) and BAD (in red) proteins are detected in the vicinity of the parasite. DAPI stains the parasite nucleus. The erythrocyte membrane is visible by Bright Field. (Credit: Dr Teresa Carvalho).

Carbonic Anhydrase-I (CA-I) is an abundant cytosolic enzyme in erythrocytes [145]: in Figure 6.6A, CA-I was only detected in total and cytosolic fractions of both uRBCs and iRBC. Protein 4.1 is a major cytoskeletal protein of erythrocytes [214] and was only detected in total and membrane fractions of both uRBCs and iRBCs (although the signal intensities were variable). PfHSP70.1 is a *P. falciparum* protein localised to the parasite

cytoplasm and nucleus [215]; it was only detected in the total and membrane fractions of the iRBCs. Overall, the controls indicate that the lysis was successful, and the membrane and cytosolic fractions were not cross-contaminated.

BCL-x_L was detected exclusively in the cytosol of uRBCs. However, in iRBCs, BCL-x_L is detected in both the cytosolic and the membrane fractions, suggesting that upon *P. falciparum* infection of RBCs, BCL-x_L becomes associated with RBC or parasite membranes, or is imported inside the parasite. Only one Western Blot is shown, but I was able to observe this localisation shift on Western Blots consistently.

The BCL-x_L signal on Western Blots appeared as a double band in RBCs, but not in the breast cancer cell control. Interestingly, the upper band (not found in the control) seemed to be mainly present in uRBCs, with a lower signal in iRBCs. This observation is discussed in details in the Discussion Section 6.3.

To further investigate the subcellular localisation of BCL-x_L in *P. falciparum* infected erythrocytes, we performed an immunofluorescence assay (IFA) (Figure 6.6B). BCL-x_L is shown in green, BAD (another apoptotic regulator not discussed here) in red, and the parasite nucleus in blue. BCL-x_L is detected surrounding the parasite and is not observed at the RBC membrane.

In summary, BCL-x_L was localised by Western Blot and IFA analysis in the cytosol of uRBCs and appears to be recruited near/to the parasite upon infection.

6.2.5 BCL-x_L changes in binding partners upon infection

The anti-apoptotic role of BCL-x_L in nucleated cells is strictly dependent on its binding partners. Typically, binding of BCL-x_L to BAX and BAK indicates anti-apoptotic activity, whereas binding of BCL-x_L to BAD indicates pro-apoptotic activity. Therefore, we aimed to identify the specific binding partners of BCL-x_L in uRBCs and iRBCs.

We performed a first immunoprecipitation of BCL-x_L from uRBCs and iRBCs: although BCL-x_L was successfully identified, we failed to identify any known binding partners of BCL-x_L previously described in nucleated cells. The reason behind this could be that BCL-x_L has specific binding partners in RBCs that are distinct from binding partners in nucleated cells. Therefore, we repeated the experiment, but this time, in the presence or absence of 5µM WEHI-539 for 4h. In nucleated cells, WEHI-539 inhibits BCL-x_L by displacing its binding partners from the BH3 domain-binding groove [136]. We therefore expected BCL-x_L binding partner candidates in RBCs to be displaced by WEHI-539.

- BCL-x_L was successfully pulled-down

uRBCs and trophozoite-iRBCs were incubated 4h in the presence of 5µM WEHI-539, or the vehicle DMSO. Cells were counted, proteins were extracted, and BCL-x_L was pulled-down using a specific antibody attached to magnetic beads (see details in Chapter 3 Section 3.4.7). As a negative control, similar protein samples were incubated with beads alone (without the BCL-x_L antibody). Overall, samples were: uRBC proteins incubated with beads alone, BCL-x_L immunoprecipitation (IP) from DMSO-treated uRBCs, BCL-x_L IP from WEHI-539-treated uRBCs, iRBC proteins incubated with beads alone, BCL-x_L IP from DMSO-treated iRBCs, BCL-x_L IP from WEHI-539-treated iRBCs.

Western Blot analysis of the BCL-x_L immunoprecipitation (IP) from three independent experiments was conducted to interrogate the successful pull-down on BCL-x_L (Figure 6.7): a band at the expected size (30kDa) confirmed the presence of BCL-x_L in the IP samples, but not in the negative controls (beads alone).

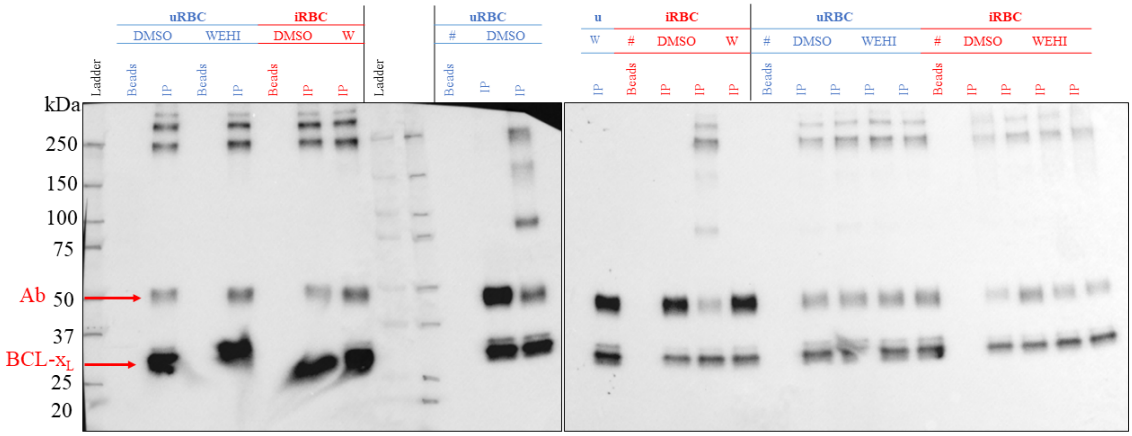

Figure 6.7: Western Blot analysis of BCL-x_L immunoprecipitation from uRBCs and iRBCs. Western Blot of BCL-x_L-IP from uRBCs, iRBCs exposed to 5µM of WEHI-539 for 4h. "Beads": protein lysate incubated with beads alone (without anti-BCL-x_L antibody). "IP": protein lysate incubated with beads and anti-BCL-x_L antibody. "DMSO": vehicle control; cells were incubated 4h in presence of DMSO. "WEHI" or "W": cells were incubated 4h in presence of the BCL-x_L inhibitor WEHI-539. "Ab": bands corresponding to the BCL-x_L antibody. "#": beads alone control consisting of half DMSO-treated cells and half of WEHI-539-treated cells.

The pull-down samples were further analysed by mass spectrometry, with the help of Dr Ghizal Siddiqui (Creek Laboratory, Monash Institute of Pharmaceutical Sciences). Numerous peptides were identified, including peptides belonging to the human protein BCL2-L1 (Table 6.2). Differential splicing of the *bcl2-l1* gene can produce either BCL-x_L or BCL-x_S proteins [216]. All peptides identified in this experiment shared 100% homology with BCL-x_L and most were identified several times across different samples. Importantly, peptides 3 and 5 are specific of BCL-x_L and do not align with BCL-x_S. Figure 6.8 maps these peptides on the BCL-x_L amino acid sequence: overall a significant coverage of the protein was achieved, including important domains of BCL-x_L such as BH1, BH3 and BH4.

Table 6.2: BCL-x_L peptides identified by mass spectrometry. All the BCL2-L1 peptides identified by mass spectrometry were aligned to the BCL-x_L amino acid sequence (using BLAST NCBI): an alignment schematic is presented in Figure 6.8. The total score (alignment score) is calculated by giving a value to each aligned amino acid and summing these over the length of the peptide sequence. E value, or Expected value, represents 'the number of hits one can "expect" to see by chance when searching a database of a particular size' (NCBI). In the last column, I summarised how many times we identified this specific peptide, and in how many different conditions. The first peptide was only identified in uRBCs.

Peptide number	**Peptide sequence**	**Peptide length**	**Total score**	**E value**	**Percentage identity)**	**Corresponding a.a. position in BCL-x_L**	**Peptide identified # times, in # different conditions**
Peptide 1	AFSDLTS QLHITPG TAYQSFE QVVNELFR	29	63.2	$6x10^{-19}$	100%	104-132	2 times 2 cond. (uRBCs)
Peptide 7	GYSWSQF SDVEENR	14	33.1	$5x10^{-8}$	100%	21-24	17 times 17 cond.
Peptide 6	ELVVDFLSYK	10	24.3	$7x10^{-5}$	100%	7-16	21 times 19 cond.
Peptide 4	EVIPMAAVK	9	21.9	$4x10^{-4}$	100%	79-87	26 times 14 cond.
Peptide 2	EAGDEFELR	9	21.6	$6x10^{-4}$	100%	92-100	17 times 17 cond.
Peptide 5	DGVNWGR	7	20.0	$2x10^{-3}$	100%	133-139	4 times 4 cond.
Peptide 3	EMQVLVSR	8	18.9	$5x10^{-3}$	100%	158-165	15 times 12 cond.

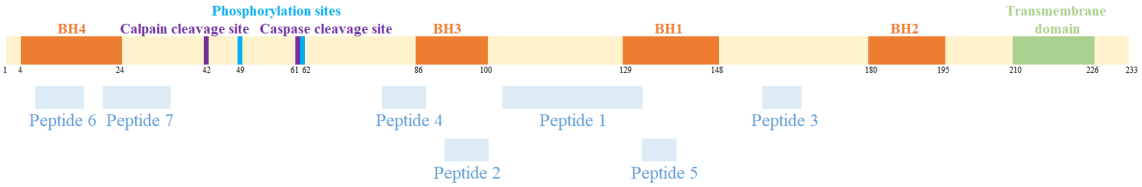

Figure 6.8: Mapping of BCL-x_L peptides identified in the IP experiment, on the BCL-x_L amino acid sequence. Peptides identified by mass spectrometry of the BCL-x_L IP (listed in Table 6.2) are shown in light blue. The BCL2-Homology domains (BH1-4) are shown in orange, the phosphorylation sites in blue, calpain and caspase cleavage sites in purple, and transmembrane domain in green.

The number of BCL-x_L peptides identified per sample and their average LFQ intensities (Label-Free Quantitation; an intensity normalised across all the samples) are summarised in Table 6.3. Overall, depending on the experiment, zero or one BCL-x_L peptide was identified in "beads alone" controls, with low intensities when a peptide was detected. In contrast, a minimum of three peptides per replicate was detected in the IP samples, with LFQ intensities in the 10^7-10^8 range. This demonstrates that we successfully pulled down BCL-x_L.

Table 6.3: Number and intensity of BCL-x_L peptides identified in each sample. For each condition (uRBC beads alone, uRBC DMSO, uRBC WEHI-539, iRBC beads alone, iRBC DMSO, iRBC WEHI-539), the number of replicates (n), the number of BCL-x_L peptides identified and their corresponding LFQ intensities are indicated. LFQ intensities are calculated through a normalisation procedure across all the samples [150].

uRBC Beads alone (n=2)		**uRBC DMSO** (n=4)		**uRBC WEHI** (n=4)		**iRBC Beads alone** (n=3)		**iRBC Beads DMSO** (n=5)		**iRBC Beads WEHI** (n=4)		
Number of BCL-x_L peptides identified	LFQ intensity	Number of BCL-x_L peptides identified	LFQ intensity	Number of BCL-x_L peptides identified	LFQ intensity	Number of BCL-x_L peptides identified	LFQ intensity	Number of BCL-x_L peptides identified	LFQ intensity	Number of BCL-x_L peptides identified	LFQ intensity	
0	-	6	$3.56x10^8$	5	$4.00x10^8$	1	-	6	$2.30x10^8$	6	$3.28x10^8$	Rep1
0	-	5	$3.80x10^8$	6	$3.43x10^8$	0	-	4	$1.20x10^8$	5	$1.31x10^8$	Rep2
		5	$3.84x10^8$	6	$1.28x10^8$	1	$1.95x10^6$	6	$1.60x10^8$	5	$5.40x10^7$	Rep3
		4	$1.28x10^8$	5	$1.45x10^8$			3	$2.92x10^7$	3	$3.45x10^7$	Rep4
								3	$7.40x10^7$			Rep5

- BCL-x_L binding partner candidates in uRBCs (disrupted by WEHI-539)

In order to identify potential BCL-x_L binding partners in uRBCs which are disrupted by the presence of the BCL-x_L inhibitor WEHI-539, we listed human proteins identified in DMSO-treated uRBCs, but not identified (or identified in low abundance) in WEHI-539-treated uRBCs (Table 6.4). The most promising candidate was calpain-1 (or µ-calpain), as it was identified in 3 of the 4 DMSO replicates and never identified in the WEHI-539 samples.

Table 6.4: BCL-x_L binding partner candidates: in uRBCs, disrupted by WEHI-539. Summary of the proteins identified in the uRBC DMSO samples, and not identified (or identified in low abundance) in presence of WEHI-539, *i.e.* specific BCL-x_L binding partners in uRBCs, displaced by the BCL-x_L inhibitor. I selected the proteins that have a count of 2 or more in uRBC DMSO, and a count of 0 or 1 in the uRBC WEHI samples. Sort from largest to smallest average LFQ intensity (uRBC DMSO). Based on the counts and average intensities, calpain-1 appears as the only likely BCL-x_L binding partner in this experiment.

uRBC DMSO (n=4)	Average Intensity	uRBC WEHI (n=4)	Average Intensity	Gene name	Protein
3	$1.33x10^7$	0	-	CAPN1	Calpain-1 catalytic subunit
2	$1.33x10^7$	1	$1.48x10^7$	PSMA1	Proteasome subunit alpha type-1
2	$8.35x10^6$	1	$9.23x10^6$	COPS6	COP9 signalosome complex subunit 6
2	$6.89x10^6$	1	$8.63x10^6$	PSMD6	26S proteasome non-ATPase regulatory subunit 6
4	$6.63x10^6$	1	$2.40x10^7$	ST13	Hsc70-interacting protein
2	$6.43x10^6$	0	-	PKP1	Plakophilin-1
2	$6.26x10^6$	0	-	ARIH2	E3 ubiquitin-protein ligase ARIH2
2	$5.18x10^6$	1	$3.31x10^6$	BLVRA	Biliverdin reductase A (Fragment)
2	$4.72x10^6$	0	-	GMPPA	Mannose-1-phosphate guanyltransferase alpha
2	$4.70x10^6$	1	$9.13x10^6$	ALDH16A1	Aldehyde dehydrogenase family 16 member A1
2	$4.61x10^6$	1	$7.71x10^6$	ALDH1A1	Retinal dehydrogenase 1
2	$2.82x10^6$	0	-	NSF	Vesicle-fusing ATPase

Building on the identification of µ-calpain as a binding partner candidate of BCL-x_L in uRBCs, and the relocalisation of BCL-x_L upon infection, I analysed the subcellular localisation of µ-calpain in uRBCs and iRBCs (Figure 6.9). An anti-spectrin antibody was used as a RBC membrane marker, and spectrin was successfully detected in the total and membrane fraction of iRBCs, but unfortunately not in uRBCs samples. PfHSP101, a parasite membrane marker, was detected only in iRBCs. PfHSP101 was identified in the total and membrane fractions, as expected, but a lower intensity signal was also observed in the cytosolic fraction, indicating possible contamination of the cytosolic fraction with material from the membrane fraction. Importantly, carbonic anhydrase-1 (CA-I), a RBC cytosolic marker, was only detected in the total and cytosolic fractions of both uRBCs and iRBCs,

indicating that no cytosolic content had "leaked" into the membrane fraction.

Overall, we observed that µ-calpain presented a similar pattern to BCL-x_L: it was localised in the cytosol of uRBCs and shifted to the membrane fraction in iRBCs.

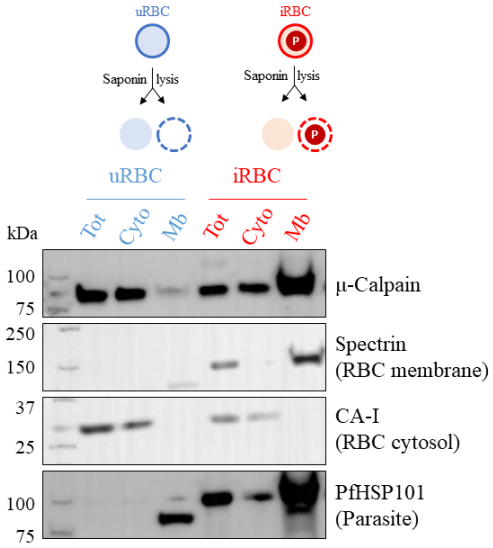

Figure 6.9: Erythrocytic µ-calpain relocates upon infection. Western Blot of 10^7 uRBCs or 10^7 iRBCs: total protein extraction (tot – solubilised with MPER), cytosolic content (cyto – soluble fraction of a saponin lysis) or membrane fraction (Mb – insoluble fraction of a saponin lysis; the whole parasite localises to the membrane fraction). µ-Calpain localises to the erythrocytic cytosolic fraction in uRBCs, and a proportion of µ-calpain localises to the membrane fraction in iRBCs.

- BCL-x_L binding partner candidates in iRBCs (disrupted by WEHI-539)

In order to identify potential BCL-x_L binding partners in iRBCs which are disrupted by the presence of the BCL-x_L inhibitor WEHI-539, we listed human and plasmodial proteins identified in DMSO-treated iRBCs, but not identified (or identified in low abundance) in WEHI-539-treated iRBCs (Table 6.5). The most promising candidate was the human protein SHOC-2, as well as, to a lesser extent, the malaria protein MAL13P1.36.

Table 6.5: BCL-x_L binding partner candidates: in iRBCs, disrupted by WEHI-539. These are the proteins found in the iRBC DMSO samples, and not identified (or identified in low abundance) in the presence of WEHI-539, *i.e.* specific BCL-x_L binding partners in iRBCs, displaced by the inhibitor. Proteins that had a count of 2 or more in iRBC DMSO, and a count of 0 or 1 in the iRBC WEHI samples were selected. Sorted from largest to smallest average LFQ intensity (iRBC DMSO).

Human proteins

iRBC DMSO (n=5)	Average Intensity	iRBC WEHI (n=4)	Average Intensity	Gene name	Protein
3	$6.28x10^7$	0	-	SHOC2	Leucine-rich repeat protein SHOC-2 (Fragment)
2	$8.43x10^6$	0	-	CCT6B	T-complex protein 1 subunit zeta-2
2	$5.00x10^6$	0	-	ANXA1	Annexin A1
2	$1.37x10^6$	0	-	ANP32A	Acidic leucine-rich nuclear phosphoprotein 32 family member A
3	$1.08x10^6$	1	$4.64x10^6$	PAICS	Multifunctional protein ADE2

Plasmodium proteins

iRBC DMSO (n=5)	Average Intensity	iRBC WEHI (n=4)	Average Intensity	Gene name	Protein
2	$9.94x10^6$	1	$5.72x10^6$	MAL13 P1.36	Uncharacterized protein
2	$5.47x10^6$	1	$3.74x10^6$	PF14_0111	Uncharacterized protein
2	$4.94x10^6$	0	-	MAL13 P1.284	Pyrroline carboxylate reductase
2	$3.27x10^6$	0	-	PFL0675c	Uncharacterized protein
2	$3.06x10^6$	1	$5.10x10^6$	PF11_0142	Uncharacterized protein

- BCL-x_L binding partner candidates specific of iRBCs (disrupted by WEHI-539, not found in uRBCs)

In order to identify BCL-x_L complexes formed upon *Plasmodium* infection specifically, and disrupted by the presence of WEHI-539, we listed human and plasmodial proteins identified in DMSO-treated iRBCs, but not identified (or identified in low abundance) in uRBCs and in WEHI-539-treated iRBCs (Table 6.6). The most promising candidate was again human SHOC-2 protein, detected in 3 out of 5 replicates of the DMSO-treated iRBC samples, with the highest intensity, and not identified at all in the other conditions.

Table 6.6: BCL-x_L binding partner candidates: specific to iRBCs, disrupted by WEHI-539. These are the proteins found in the iRBC DMSO but not uRBC DMSO or iRBC WEHI samples, *i.e.* binding partners of BCL-x_L specific of iRBCs and disrupted in the presence of the inhibitor. Proteins that had a count of 2 or more in iRBC DMSO, and 0 or 1 in uRBC DMSO and iRBC WEHI were selected.

Human proteins

iRBC DMSO (n=5)	Average Intensity	iRBC WEHI (n=4)	uRBC DMSO (n=4)	uRBC WEHI (n=4)	Gene name	Protein
3	$6.28x10^7$	0	0	0	SHOC2	Leucine-rich repeat protein SHOC-2 (Fragment)
2	$8.43x10^6$	0	1	1	CCT6B	T-complex protein 1 subunit zeta-2
2	$5.00x10^6$	0	1	1	ANXA1	Annexin A1

Plasmodium proteins

iRBC DMSO (n=5)	Average Intensity	iRBC WEHI (n=4)	uRBC DMSO (n=4)	uRBC WEHI (n=4)	Gene name	Protein
2	$9.94x10^6$	1	0	0	MAL13 P1.36	Uncharacterized protein
2	$5.47x10^6$	1	0	0	PF14_0111	Uncharacterized protein
2	$4.94x10^6$	0	0	0	MAL13 P1.284	Pyrroline carboxylate reductase
2	$3.27x10^6$	0	0	0	PFL0675c	Uncharacterized protein
2	$3.06x10^6$	1	0	0	PF11_0142	Uncharacterized protein
2	$2.89x10^6$	1	0	0	MAL8 P1.93	Uncharacterized protein
2	$2.84x10^6$	1	0	0	PFB0125c	Conserved *Plasmodium* protein
2	$2.40x10^6$	0	0	0	PFI1115c	Pre-mRNA splicing factor, putative

6.3 Discussion

6.3.1 BCL-x_L inhibitors impair erythrocytic growth of *P. falciparum*

We have demonstrated that six BCL-x_L inhibitors impair *in vitro* growth of *P. falciparum*. In particular, the FDA-approved drug ABT-199 displayed an IC_{50} of 4.6µM, within the same range as peak plasma concentrations observed in patients [134]. In addition, ABT-263 (a drug currently in clinical trials for solid tumors [130, 131]) and WEHI-539 (a highly specific inhibitor of BCL-x_L) displayed the lowest IC_{50} values (0.74 and 0.93µM respectively). Importantly, the IC_{50} value of ABT-263 was ∼2- to 8-fold lower than the peak plasma concentrations measured in treated humans: in an escalation study, the peak plasma concentrations reported were between 1.3µM and 5.75µM [130]. This indicates that its bioavailability should not be an issue, making both ABT-199 and ABT-263 promising candidates as antimalarial treatments.

Considering that the concentrations used here encompassed inhibition of several BCL-2 family members, we cannot exclude that the antiparasitic activity observed was due to the inhibition of members other than BCL-x_L. Unfortunately, very little is known about BCL-2 proteins in RBCs. Besides BCL-x_L, only BID, BCL-10, BAD [124] and BAK [125] have been identified by mass spectrometry and Western Blot, respectively. Importantly, BCL-2 has never been identified in erythrocytes, suggesting that the ABT compounds tested acted through inhibition of BCL-x_L.

In addition, although *P. falciparum* has not been found to express BCL-x_L orthologs [193], we cannot exclude the possibility that the compounds targeted a parasite factor. To address the possibility that *P. falciparum* factors are targeted, we could try to generate parasite lines resistant to these BCL-x_L inhibitors (via continuous exposure to high concentration of these drugs), and sequence the whole genome of such resistant parasites. To address the hypothesis that the host BCL-x_L is required for *P. falciparum* blood development, future experiments could include to genetically engineer human hematopoietic stem cells, knock-out the *bcl-2l1* gene, differentiate them into mature RBCs and assess *P. falciparum* ability to develop. Alternatively, a more accessible experiment would be to assess murine *Plasmodium spp.* ability to grow in BCL-x_L inducible knock-out mice [121].

BCL-x_L inhibitors have been found to impair *Plasmodium* liver stages [106]. We have demonstrated that they present a similar effect on *Plasmodium* blood stages, which opens exciting antimalaria therapeutical avenues. Having an antimalarial drug able to target several stages of the parasite would be extremely beneficial. In this instance, we could even rely on an already-approved drug (ABT-199) or a drug currently in clinical trials (ABT-263).

6.3.2 BCL-x_L inhibitors do not induce eryptosis

BCL-x_L inhibitors induce apoptosis in nucleated cells and a previous study found a BH3-mimetic induced eryptosis of mature RBCs [125]. We therefore hypothesised the BCL-x_L inhibitors we tested would induce eryptosis, both in uRBCs and iRBCs, and anticipated the antiparasitic effect of these compounds to be linked to eryptosis. However, none of the three ABT compounds tested (ABT-737, ABT-263 and ABT-199) induced eryptosis of uRBCs or iRBCs. This suggests that BCL-x_L does not have anti-eryptotic capacities, although it should be noted that it is possible that anti-eryptotic properties would manifest only in the presence of a pro-eryptotic signals. Moreover, the eryptosis assays were conducted upon a 4h incubation with the ABT compounds, while the IC_{50} assays consist of a 72h incubation: we can therefore not exclude that the ABT compounds would induce eryptosis upon a longer stimulation. However, inhibition of BCL-x_L with WEHI-539 over 84h (discussed below) did not induce significant eryptosis of iRBCs.

Overall, our data indicates that BCL-x_L inhibitors likely kill *P. falciparum* through a mechanism independent of eryptosis.

6.3.3 WEHI-539 impaired schizogony

The highly specific BCL-x_L inhibitor WEHI-539 displayed a sub-micromolar IC_{50} on *P. falciparum*. To investigate the effect of BCL-x_L inhibition on *P. falciparum* development and eryptosis hallmarks of different parasite stages over time, we analysed the effect of WEHI-539 on the development of synchronised *P. falciparum* and eryptosis of iRBCs along two erythrocytic cycles.

The observed reduction in parasitemia, DNA and RNA content at schizont stages indicated that WEHI-539 impaired schizogony. We also found that in the presence of the drug, schizonts appear larger than without the drug: considering that under normal conditions, schizont-iRBCs diminish in size (as measured by flow cytometry, see Chapter 5), we think that this is further indicative of impaired parasite development. However, eryptosis of the infected cells was not observed. In particular, there was no increase of PS exposure over the entire experiment.

The results from this experiment, together with the previous observations (eryptosis assays with ABT compounds), reject the hypothesis whereby BCL-x_L has a protective role against eryptosis. However, assuming BCL-x_L-specific inhibitors do not display off-target effects on parasites, our data indicates that the host BCL-x_L is required for the intra-erythrocytic development of *P. falciparum*.

6.3.4 BCL-x_L is recruited to the parasite upon infection

Considering that, in nucleated cells, the role of BCL-x_L is highly dependent on its localisation, we investigated its subcellular localisation in naïve and infected erythrocytes. We established that BCL-x_L is strictly cytosolic in naïve erythrocytes, and partially localises around the parasite upon infection. The cytosolic presence of BCL-x_L in mature RBCs is not in accordance with a previous study [125], where BCL-x_L was found to be localised at the membrane of RBCs. However, Walsh *et al.* did not control for successful lysis of the RBCs (*i.e.* no probing of cytosolic protein) and did not analyse the cytosolic fraction alone (only membrane and whole lysate); which may explain the discrepancy with our observations.

Additional preliminary data (Western Blot not shown) suggests that WEHI-539 did not prevent the localisation shift of BCL-x_L, suggesting that BCL-x_L recruitment towards the parasite is not performed by classical BCL-x_L binding partners.

The recruitment of BCL-x_L to the parasite (either to the parasitophorous vacuole membrane, the parasite membrane, or the parasite itself) was a novel and exciting finding. Indeed, *P. falciparum* is known to export considerable number of proteins to its host cell, including a majority to the RBC membrane, but only a few examples of human proteins have been shown to be recruited by the parasite. Beside the erythrocytic haemoglobin imported within the parasite as a nutrient source, *P. falciparum* was demonstrated to import the following human proteins into its cytosol: redox-active protein peroxiredoxin 2 (hPrx-2, hTPx1) [217], catalase, superoxide dismutase 1, flavin reductase, paraoxonase, and lactoferrin [218]. The human protein LANCL1 is also recruited, not into the parasite itself, but to the Maurer's clefts, localised in the RBC cytosol [219]. BCL-x_L might therefore be one of the few human proteins recruited to the parasite during infection. Further work using methods such as cryo super-resolution light and electron microscopy would enable to investigate the exact localisation of BCL-x_L (at the parasitophorous vacuole membrane, within the vacuole, at the parasite membrane or within the parasite).

6.3.5 Differential phosphorylation of host BCL-x_L upon infection?

In nucleated cells, BCL-x_L has been shown to be phosphorylated on Ser-49 by Polo Kinase 3, PLK3 [220], as well as on Ser-62 by Cyclin Dependent Kinase 1 and 2, CDK1 and 2 [221, 222]. In such systems, Ser-49 phospho-BCL-x_L (pBCL-x_L) has a role in cell cycle regulation, in particular stabilising G2 arrest before mitosis occurs [220]. Phosphorylation on Ser-62 by CDK1 and CDK2 was found to be pro-apoptotic, by reducing binding of pBCL-x_L to BAX, as well as leading to mitotic arrest [223, 221, 222].

Our Western Blot analyses have shown that the BCL-x_L signal appears as a double band in both uRBCs and iRBCs, but not in the cancer cell line positive control (Figure 6.6 and

6.7). Protein phosphorylation is one of the most common protein modifications and leads to slightly higher molecular weights; when detected on Western Blots, phosphorylated proteins therefore appear as a slightly higher band than the unphosphorylated protein [224]. Therefore, the BCL-x_L higher molecular weight band we observed may correspond to a phosphorylated version of BCL-x_L (pBCL-x_L). Interestingly, this potential pBCL-x_L signal appears weaker in iRBCs compared to uRBCs. In which case the invasion by *P. falciparum* would induce BCL-x_L dephosphorylation, either via a human or parasitic phosphatase. Unfortunately, our work did not identify phosphorylated BCL-x_L - either in the phosphoproteomic library described in Chapter 5, nor in the BCL-x_L immunoprecipitation (we did not identify any peptides covering the phosphorylation sites). Regarding kinases known to phosphorylate BCL-x_L in nucleated cells, our proteomic library did detect CDK1, 2 and 3, but not PLK3. Although human CDKs are known to be important for erythropoiesis [225], their role during *P. falciparum* infections has not been investigated. Interestingly, CDK inhibitors were reported to impair erythrocytic development of *Plasmodium spp.* and *Babesia bovis*, although the authors suggest this effect was due to the inhibition of parasitic kinases [226, 227].

Overall, the role of BCL-x_L and pBCL-x_L in nucleus- and mitochondrion-deprived erythrocytes remains a mystery. It would be interesting to further investigate phosphorylation status of BCL-x_L in uRBCs and iRBCs, for instance using phospho-specific BCL-x_L antibodies on uRBCs and iRBCs protein samples on Western Blots. In this project, to entangle the unknown role of BCL-x_L in erythrocytes, we aimed to identify molecular complexes of BCL-x_L in naïve and infected erythrocytes; this was done by immunoprecipitation of BCL-x_L.

6.3.6 Lack of classical BCL-x_L binding partners in erythrocytes

Surprisingly, we did not identify any known binding partners of BCL-x_L (BAK, BAX or BAD) in our pull-down experiments and all the co-immunoprecipitated proteins have never been described to form complexes with BCL-x_L and do not contain BH3-like domains which could explain such an interaction. Therefore, it is important we exercise caution in our interpretation of these results. Nevertheless, the possibility that BCL-x_L may have an unusual role and unusual binding partners in mature RBCs is intriguing and warrants further investigations.

- µ-Calpain as a binding partner of BCL-x_L in uRBCs

In uRBCs, the most prominent binding partner candidate we identified was µ-calpain (or calpain-1). µ-calpain is a calcium-dependent cysteine protease involved in apoptosis and eryptosis [228, 205]. Importantly, µ-calpain can cleave BCL-x_L N-terminus, on position 42 [216] and the generated sequences are expected to weigh 4.9kDa and 21.2kDa respectively (using a protein molecular weight calculator with the BCL-x_L amino acid sequence available on UniProt). It is therefore unlikely that this cleaved version of BCL-x_L explains the

double band observed on Western Blots. This would imply that in uRBCs, µ-calpain binds to BCL-x_L without cleaving it.

Interestingly, the subcellular localisation of µ-calpain (as detected on Western Blot, Figure 6.9) has a similar pattern to BCL-x_L. This could indicate that µ-calpain is also recruited to the parasite / parasitophorous vacuole, similarly to BCL-x_L, or to the RBC membrane (or a combination of those). However, it is important to note that µ-calpain was not identified as a binding partner candidate of BCL-x_L in iRBCs, suggesting that the relocalisation of µ-calpain is independent of BCL-x_L's own relocalisation. We know that *P. falciparum* hijacks human calpain at the schizont stage to facilitate egress. Indeed, Chandramohanadas *et al.* (2009) demonstrated the same shift in localisation we observed here (from cytosolic to membrane fraction) during the last hours of *P. falciparum* development (46-48h) [204]. This shift in localisation correlated with protease activation. However, the specific subcellular location of µ-calpain (at the RBC membrane, the parasitophorous vacuole membrane and/or the parasite) remains to be identified. Of note, µ-calpain is a protease activated by calcium binding: we have shown in Chapter 5 that schizonts display increased levels of intracellular calcium, although we did not investigate whether the increase was also observed in the RBC cytosol. The increased calcium might therefore be responsible for the activation of µ-calpain and its role in parasite egress.

Overall, the role of BCL-x_L and calpains in uRBCs is to be further explored. In future experiments, an immunoprecipitation of µ-calpain coupled with mass spectrometry would allow to confirm its interaction with BCL-x_L, and a more precise localisation of µ-calpain in iRBCs would provide us with further insights about its role during egress.

- SHOC-2 as a binding partner of BCL-x_L specifically in iRBCs

We identified the human protein SHOC-2 as a potential binding partner of BCL-x_L specifically in iRBCs. This suggests that upon invasion, a BCL-x_L-SHOC-2 complex might perform an important function for the parasite development.

SHOC-2 is comprised of many leucine-rich repeats, conferring its ability for protein-protein interactions. In nucleated cells, SHOC-2 was found to be a positive regulator in the RAS/ERK/MEK kinase signalling cascade: it can bind to M-Ras and Raf-1, and is targeted to late endosomes [229]. SHOC-2 also functions as a subunit of protein phosphatase 1c (PP1c), which dephosphorylates an inhibitory serine, and therefore activates, Raf-1 [230].

However, the role of SHOC-2 in human erythrocytes in unknown. In mice, *shoc2* knock-out resulted in early embryonic lethality, while in zebrafish, its deletion resulted in important defects in erythropoiesis, suggesting a role of SHOC-2 in erythrocytes generation [231].

Interestingly, it has been previously shown that *P. falciparum* relies on host proteins within

the MAPK pathway for its development, namely MEK, PAK [195] as well as Raf (Chapter 4B, [191]). It raises the intriguing possibility that this pathway is particularly important in iRBCs, and that BCL-x_L somehow plays an unusual role within it.

A pull-down of SHOC-2 would be required to confirm this observation. It would also be insightful to investigate the exact localisation of SHOC-2 during infection. In particular, conducting a time-course analysis of the localisation of BCL-x_L, SHOC-2 and µ-calpain would provide us with further information regarding the dynamics of these relocalisation events. Testing combinations of inhibitors of these proteins could also help us to decipher their interplay. Unfortunately, no SHOC-2 inhibitors exist to date, and researchers usually rely on genetic manipulations for functional studies.

6.4 Conclusion

We have demonstrated that inhibition of the host erythrocyte BCL-x_L protein impairs *P. falciparum* growth *in vitro*, and that ABT-199 (an FDA-approved drug) and ABT-263 (a drug in clinical trials for solid tumours) display a low micromolar and a submicromolar activity, respectively. We had hypothesised that, similar to a role in apoptosis, erythrocytic BCL-x_L played a role in eryptosis. However, our data suggests that antiparasitic activity of BCL-x_L inhibitors is unlikely to be due to eryptosis activation. In particular, the specific BCL-x_L inhibitor WEHI-539 appears to impair schizogony, without inducing eryptosis of iRBCs. We have demonstrated that BCL-x_L is exclusively cytosolic in uRBCs, and that it is recruited to the parasite/parasitophorous vacuole upon infection. The phosphorylation pattern of BCL-x_L, although not specifically investigated in this thesis, might be affected by the presence of *P. falciparum* and is worth of further investigation. Finally, we discovered that BCL-x_L forms unusual molecular complexes in RBCs: µ-calpain binds to BCL-x_L in uRBCs, while SHOC-2 binds to BCL-x_L in iRBCs. Although more work is required to confirm these results, this opens exciting possibilities of novel host pathways required for parasite development. Intriguingly, we did not identify yet *Plasmodium* proteins which could play a role in such a pathway.

Taken together, we uncovered an important and unusual role of erythrocytic BCL-x_L in *P. falciparum* development. Although the mechanistic of an erythrocyte-specific BCL-x_L role remains unclear, we have shown that chemical inhibition of erythrocyte BCL-x_L would be an interesting novel antimalarial strategy which would allow (i) host-targeted therapy opportunities, (ii) drug repurposing, and (iii) targeting several stages at once (blood and liver stages).

Chapter 7

Mechanisms of *Plasmodium falciparum*-Induced Bystander Erythrocyte Death

7.1 Introduction

Malarial anaemia is the most common symptom leading to malaria-related deaths. Surprisingly, the loss of uninfected red blood cells (uRBCs) is the main driver of severe anaemia during malarial infections. Indeed, for each infected RBC (iRBC) that is destroyed, it is estimated that up to 30 uRBCs are also lost [50]. However, the mechanisms behind this enhanced clearance of bystander RBCs remain poorly understood. Contributing factors include stiffening of uRBCs and therefore their mechanical clearance by the spleen [59], reduced splenic clearance threshold due to spleen reorganisation [57, 54], increased levels of auto-antibodies priming destruction of RBCs [70], as well as increased levels of PS exposure on bystander RBCs, leading to their phagocytosis by macrophages [49, 80]. The latter is the focus of this chapter. The increase in PS exposure of bystander RBCs is observed *in vitro* [80], suggesting the host immune response is not the only contributor of this phenomenon. Therefore, we hypothesize that three other factors may contribute to PS exposure: direct cell-to-cell contact (as observed with iRBC-induced apoptosis of endothelial cells [232]), secreted factors (molecules or extracellular vesicles) and cellular stress due to "collateral damage" (such as nutrient shortage, waste accumulation or pH changes). Since malarial anaemia is observed even at low parasitemia [50], we decided to exclude direct cell-to-cell contact from our study. Instead, we focused on secreted factors and "collateral damage", in particular, the contribution of extracellular vesicles and glucose depletion.

All cells are believed to produce extracellular vesicles (EVs), membrane-bound packages containing a wide range of molecules (DNA, RNA, proteins and lipids) [85]. In particular, it was demonstrated that *Plasmodium falciparum* use EVs to communicate between individual parasites [89, 88], as well as to modify surrounding hosts cells, including uRBCs [92].

During malarial infections, EVs derived from iRBCs are thought to promote pathogenicity, especially that associated with cerebral malaria [86]. However, the role of iRBC-derived EVs in malarial anaemia has never been investigated.

We hypothesise that extracellular vesicles (EVs) and/or other factors secreted by *P. falciparum*-iRBCs are responsible for the increased levels of PS exposure of bystander RBCs. To test this hypothesis, we studied the PS exposure levels of bystander RBCs in a mixed *P. falciparum in vitro* culture, as well as the changes in PS exposure levels of bystander cells within a synchronised parasite culture over time. Further, we tested the contribution of iRBC-derived EVs to the death phenotype of bystander cells, by exposing fresh RBCs to purified iRBCs- or uRBCs-derived EVs. To test the contribution of other secreted factors, we exposed fresh RBCs to filtered conditioned media from iRBCs and uRBCs. Finally, to assess the contribution of glucose depletion, we exposed fresh RBCs to conditioned media, with or without glucose supplementation.

7.2 Results

7.2.1 PS exposure of bystander RBCs within a mixed *P. falciparum in vitro* culture

A culture of naïve RBCs and an asynchronous (mixed stages) *P. falciparum* culture were analysed by flow cytometry to determine PS exposure levels of uRBCs. Bystander RBCs within a parasite culture were identified as the Hoechst negative population (*i.e.* DNA negative, see Chapter 5.2.1). We found that bystander RBCs cultured in the presence of parasites exposed significantly more PS than RBCs incubated in the same conditions, but in the absence of parasites (p=0.0144; Figure 7.1). Our data indicates that *P. falciparum* induces PS exposure of bystander RBCs *in vitro*.

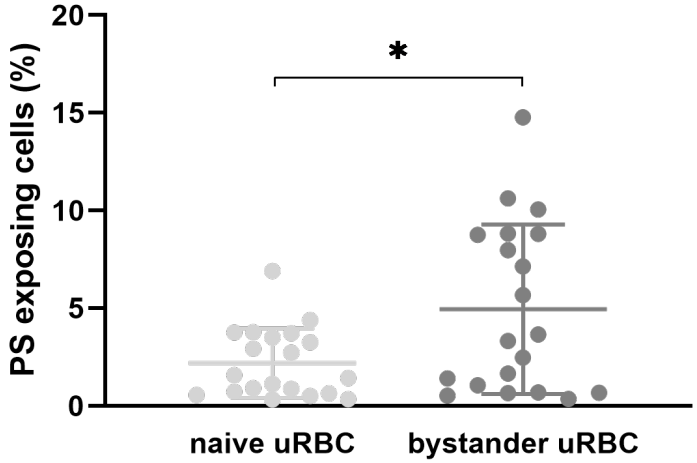

Figure 7.1: Bystander RBCs expose more PS than naïve RBCs. Naïve RBCs and asynchronous *P. falciparum* cultures were analysed by flow cytometry for PS exposure (Annexin V binding). uRBCs from the parasite culture (named bystander uRBCs) were gated based on their absence of Hoechst fluorescence (*i.e.* no DNA). Individual values, mean and SD for n=20 independent experiments in triplicate are shown. Welch's t test, p=0.0144.

7.2.2 PS exposure of bystander RBCs over time

P. falciparum has an intraerythrocytic cycle of 48h, during which it matures from the ring stage, to the trophozoite stage, to the schizont stage, after which newly formed merozoites leave the host RBC by lysing it, and finally invade new RBCs. To precisely pinpoint when the increase in PS exposure of bystander RBCs occurred, we determined the levels of PS exposure of uRBCs over time, *i.e.* during two erythrocytic cycles of *P. falciparum* as described in Chapter 5.2.2. A synchronised ∼1% rings *P. falciparum* culture was prepared, and PS exposure of bystander RBCs was measured every 12h by flow cytometry (Figure 7.2). The increase of parasitemia over time is also shown, along with representative microscopy images of iRBCs at each timepoint.

During the first cycle, from 12h to 36h, parasitemia remains constant (1.5%). This is expected as the parasites are maturing, and reinvasion has not occurred yet. At 48h, parasitemia doubles (3%), and further increases at 12h of cycle 2 (to 8%). This indicates that schizonts are rupturing and new merozoites are invading RBCs during these timepoints. Similar to the first cycle, during the second cycle, parasitemia plateaus again (8%) at 24h and 36h, before increasing to 14% at 48h.

PS exposure of bystander RBCs significantly increased at 24h (p=0.0118), and further at 36h (p=0.0004). This appears to indicate that bystander RBCs are affected by the maturation of the parasite. However, at 48h, no statistical difference was observed. Instead, a large distribution including some very high values were measured (from 1.6% up to 10.4% of PS-exposing cells). During the second parasite cycle, at 12h, 24h and even more so at 36h post invasion, PS exposure levels of bystander RBCs significantly increased again when compared to the very first timepoint of cycle 1 (p=0.0162, 0.235 and 0.0002 respectively).

Similar to the end of the first parasite cycle, at 48h of the second cycle, a very large spread of PS exposure values was observed (from 3% to 20.6% of PS-exposing cells, p=0.0106 compared to the first timepoint).

The release of intracellular factors upon egress can contribute to RBC death, in particular different forms of haemoglobin (methaemoglobin and malaria heme product hemin, [233, 234, 84]). Therefore, we hypothesised that the range of PS exposure values at 48h of both cycles was due to differences in egress levels. Replicates where PS exposure was extremely high might be replicates where schizont egress has occurred, while replicates where PS exposure was low might be replicates where schizonts egress has not been completed yet.

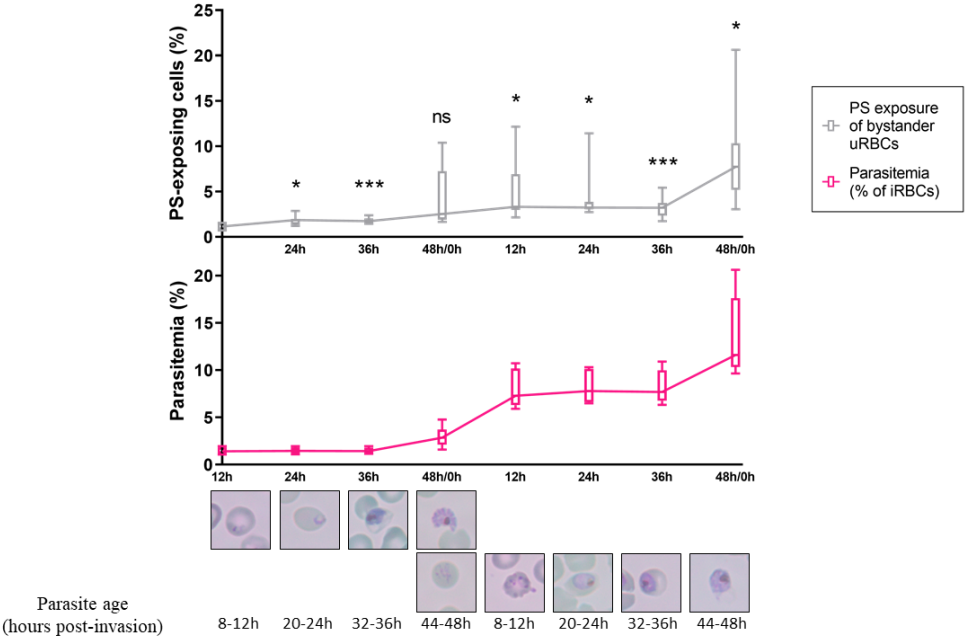

Figure 7.2: Changes in PS exposure on bystander RBCs within a synchronised culture of parasites over time. We analysed a synchronised culture of *P. falciparum* every 12h over two life cycles (*i.e.* 84h). Here, we show the PS exposure of bystander RBCs over time, and the corresponding parasitemia. Representative photos of iRBCs and their estimated age (hours post-invasion) are indicated for each time point. Box and whiskers representation (mean, 25th and 75th percentile, min and max) of n=11 independent experiments in triplicate are shown. Brown-Forsythe and Welch ANOVA tests; compare to the first timepoint (*i.e.* 12h of cycle 1).

7.2.3 Correlation between parasitemia and PS exposure of bystander RBCs

To test the hypothesis whereby increased schizont egress leads to increased PS exposure levels of bystander RBCs, we performed Pearson correlation tests between parasitemia (indicative of re-invasion at times 48h and 12h) and PS exposure of bystander RBCs (Figure 7.3 and Table 7.1). Strikingly, parasitemia did not correlate with PS exposure of bystander RBCs during ring and trophozoite developments within each timepoint (24h and 36h of both cycles). In contrast, PS exposure of bystander RBCs strongly correlated with parasitemia at 48h of cycle 1, 12h and 48h of cycle 2, suggesting that schizont egress induces PS exposure of bystander RBCs.

	Timepoint	r	*p* value	*P. falciparum* stages
Cycle 1	12h	0.5715	0.0662	Ring
	24h	0.5726	0.0656	Young trophozoite
	36h	0.4794	0.1356	Mature trophozoite
	48h	0.9224	<0.0001	Schizont (Ring)
Cycle 2	12h	0.6579	0.0278	Ring
	24h	0.3828	0.2452	Young trophozoite
	36h	0.03835	0.9109	Mature trophozoite
	48h	0.8775	0.0008	Schizont (Ring)

Table 7.1: Pearson correlation tests: Parasitemia vs PS exposure of bystander RBCs. For each timepoint, a Pearson correlation test was conducted for parasitemia against PS exposure of bystander RBCs (n=11 independent experiments in triplicate). The significant correlations are indicated in red. A positive correlation between PS exposure of uRBCs and parasitemia at 0h, 12h and 48h of cycle 2 was observed.

The absence of correlation at timepoints 12h (cycle 1), 24h and 36h (cycles 1 and 2) might stem from the corresponding low levels of parasitemia. This was especially true during the first cycle, where parasitemia was between 1% and 2%. To address this question, we combined together timepoints corresponding to similar parasite stages (12h for young rings; 24h for young trophozoites; 36h for mature trophozoites; and 48h/0h for schizonts/new rings). In this case, Pearson correlation results show that parasitemia correlated with PS exposure of bystander cells at all parasite stages (Figure 7.4).

In summary, we have demonstrated that *P. falciparum* induces an increase of PS exposure on bystander RBCs *in vitro*. Overall, the PS exposure levels increase over time: parasite trophozoite stages, and potentially schizont egress, induce more PS exposure when compared to ring stages. Finally, increase of parasitemia positively correlated with PS exposure of bystander RBCs, regardless of parasite stages.

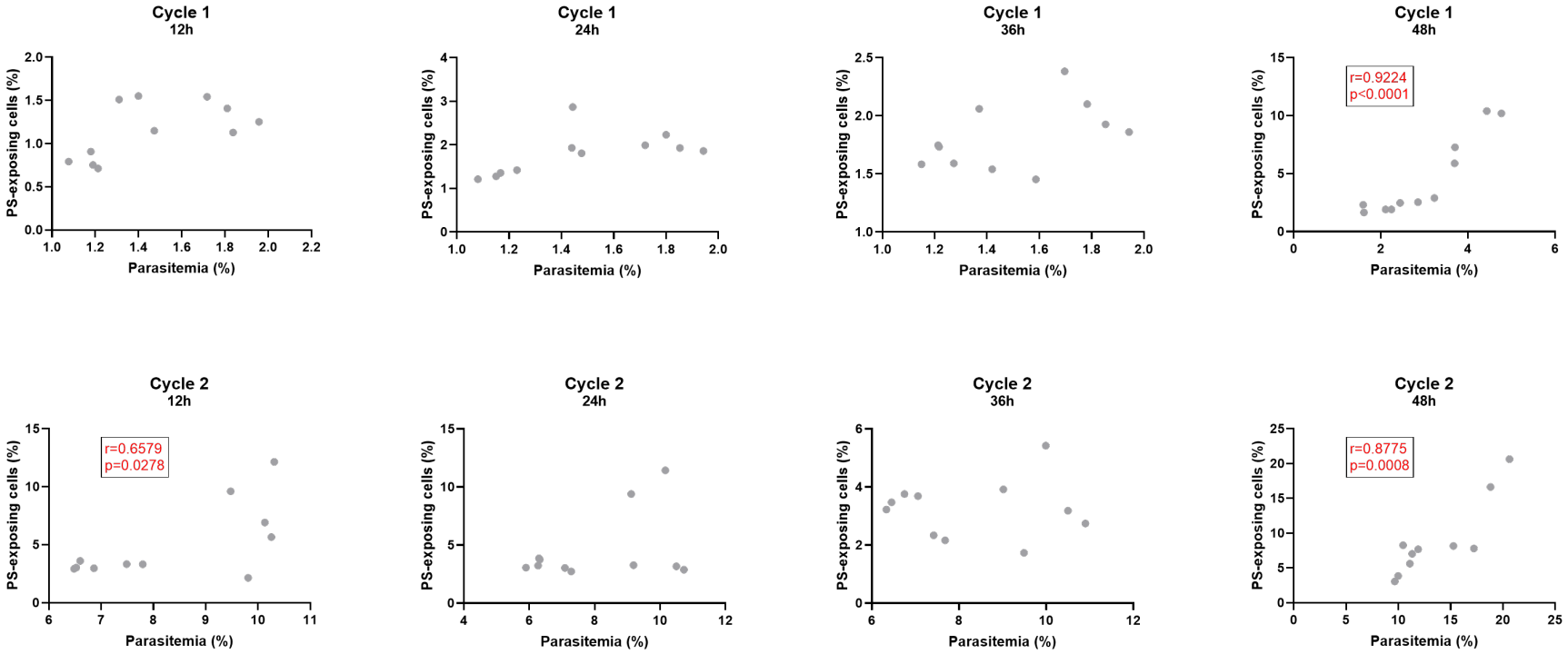

Figure 7.3: PS exposure of bystander RBCs correlates with parasitemia when reinvasion occurs. For each timepoint, a Pearson correlation test was conducted between parasitemia and PS exposure of bystander RBCs (n=11 independent biological replicates performed in triplicate). A positive correlation between PS exposure of uRBCs and parasitemia at t=48h of cycle 1, 12h and 48h of cycle 2 was demonstrated as indicated by r and p values in red (for further details on r and p values see Table 7.1).

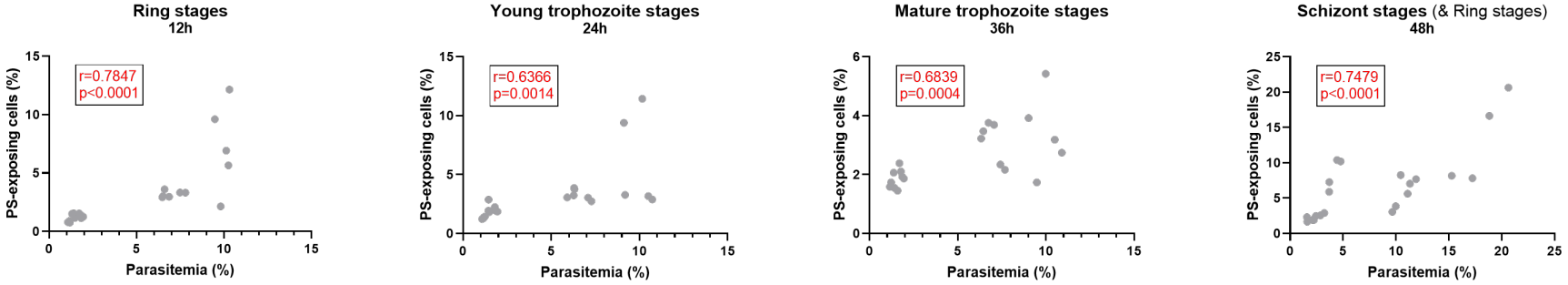

Figure 7.4: PS exposure of bystander RBCs correlates with parasitemia at all stages. Equivalent timepoints from cycle 1 and 2 were merged and a Pearson correlation test was conducted between parasitemia and PS exposure of bystander RBCs (n=11 independent biological replicates performed in triplicate). A positive correlation between PS exposure of uRBCs and parasitemia was identified for all parasite stages.

7.2.4 Role of iRBC-derived Extracellular Vesicles (EVs) on eryptosis of bystander RBCs

Purification of iRBC- and uRBC-derived EVs

We demonstrated that *P. falciparum* induces an increase in PS exposure of bystander RBCs, and that this effect was stronger during the trophozoite stages. Since extracellular vesicles (EVs) are key players in *P. falciparum* communication [89], and since their production by trophozoite stages is increased compared to ring stages [88], we decided to explore their role in the induction of PS exposure of bystander RBCs. To test the hypothesis that iRBC-derived EVs induce PS exposure of uRBCs, we isolated EVs from naïve RBCs and from *P. falciparum* cultures. Please note that when I refer to "iRBC-EVs" or "iRBC-derived EVs", I actually refer to EVs concentrated from a *P. falciparum* culture, which therefore include EVs derived from ring stages, trophozoite stages as well as bystander RBCs. Briefly, following a 24h incubation of synchronised *P. falciparum* culture or naïve RBCs, the culture medium was collected, cells and cell debris were eliminated through a series of centrifugation steps and EVs were concentrated using membrane filters of 100kDa cut-off (VivaCell® units). Following an overnight ultracentrifugation step, EVs were resuspended in incomplete RPMI medium (iRPMI) and EV's concentration and size distribution were determined using a ZetaView nanoparticle tracking analyser (Figure 7.5A). Further, to visualise their morphology and size, purified iRBC- and uRBC-derived EVs were imaged by Transmission Electron Microscopy (TEM) (Figure 7.5B and Figure 7.6).

Size distribution of uRBC- and iRBC-EVs was determined by ZetaView and TEM imaging (Figure 7.5). The ZetaView analysis indicates that EVs derived from uRBCs are bigger than those derived from iRBCs, with size peaks at 142.1nm and 130.3nm respectively. Further, the diameters of 92 uRBC-derived EVs and 62 iRBC-derived EVs measured by TEM confirmed that uRBC derived-EVs are significantly larger than those derived from iRBCs, with medians of 79.36nm and 63.95nm respectively (p=0.0205). Of note, the differences in size measured by ZetaView vs. TEM imaging are expected: indeed, during the TEM samples preparation, dehydration of EVs occur, leading to their shrinkage and an artificial cup-shaped morphology [235].

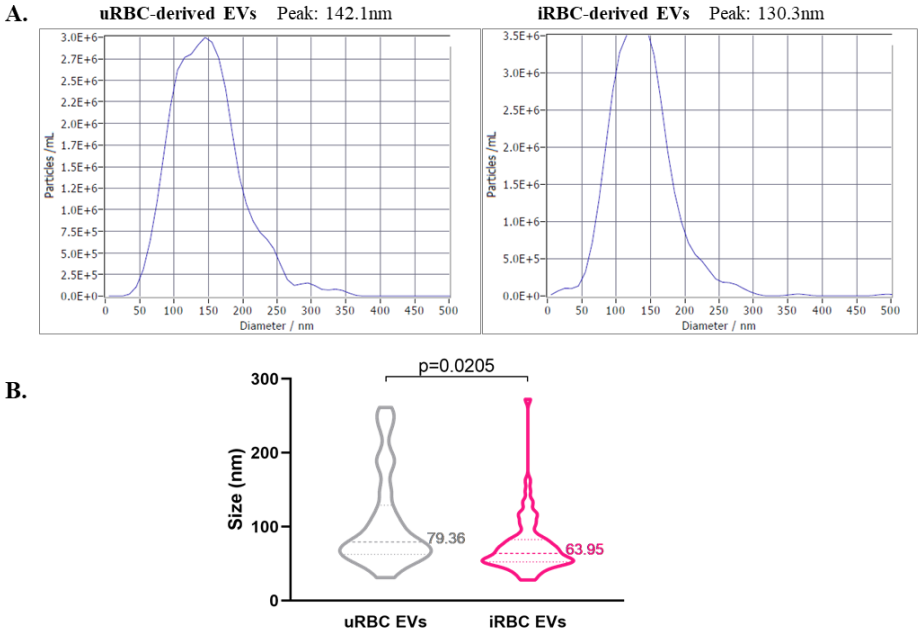

Figure 7.5: Size distribution of iRBC- and uRBC-derived EVs. (A) A representative example of the size distribution profile of uRBC- and iRBC-derived EVs determined by ZetaView. **(B)** Diameter of uRBC- and iRBC-derived EVs measured by negative staining TEM imaging. A total of 92 uRBC-derived and 62 iRBC-derived EVs were analysed, from two independent experiments. The violin plots indicate the median (values indicated), the 25$^{\text{th}}$ and the 75$^{\text{th}}$ quartiles.p=0.0205 using a Kolmogorov-Smirnov test.

EVs from uRBCs and iRBCs were imaged using negative staining Transmission Electron Microscopy (TEM), and Figure 7.6 shows such EVs from a single experiment. In this experiment, EVs from uRBCs ranged from 50nm to 262nm, while those from iRBCs ranged from 30nm to 105nm. It was striking that iRBC-derived EVs were more homogenous in size and shapes than uRBCs-derived EVs, an interesting observation given that uRBCs are also present, in a vast majority, in *P. falciparum* cultures.

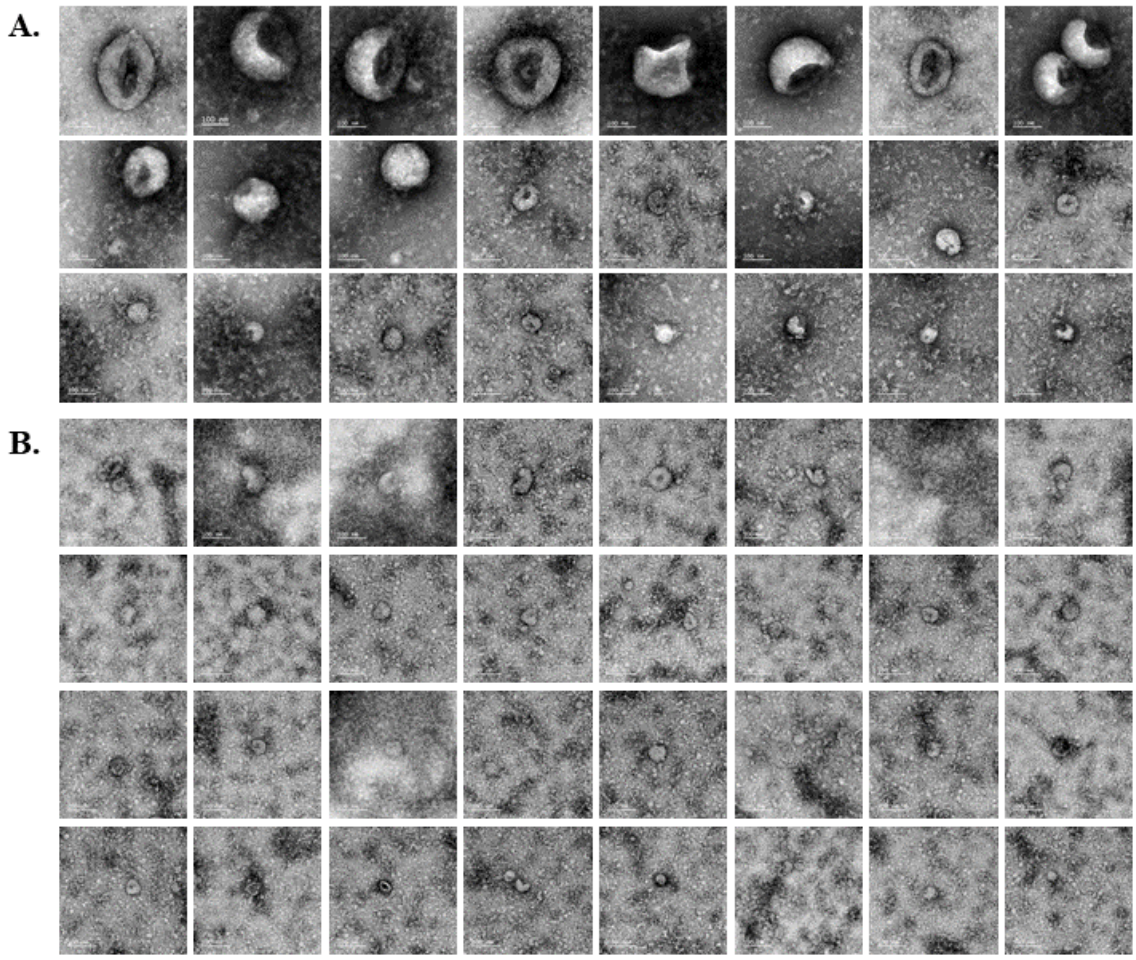

Figure 7.6: TEM images of uRBC- and iRBC-derived EVs. EVs enriched from **(A)** uRBCs or from **(B)** *P. falciparum* cultures were imaged by negative staining transmission electron microscopy (TEM). Images from a single experiment are shown. Panel (A) shows 24 uRBCs-EVs (50-262nm); Panel (B) shows 32 iRBCs-EVs (30-105nm).

Impact of iRBC-derived EVs on eryptosis of uRBCs

To test the role of iRBC-derived EVs on the increased levels of PS exposure on bystander RBCs, a controlled number of iRBC-derived EVs were added to fresh RBCs, and as a control, a similar number of uRBC-derived EVs were also added to fresh RBCs. 10^5 to 10^8 EVs were added per microliter of fresh RBC culture, *i.e.* ∼37 to ∼37,000 EVs per RBC. Following a 48h incubation, PS exposure was determined by flow cytometry. Data from three independent experiments, each performed in triplicate, are summarised in Figure 7.7. There was no significant difference in PS exposure levels of RBCs incubated with EVs derived from uRBCs or from iRBCs. Moreover, there did not seem to be increased PS exposure with increased number of EVs (larger points in Figure 7.7).

Overall, our data refutes our hypothesis: iRBC-derived EVs do not seem to be responsible for the increase in PS exposure of bystander RBCs observed earlier.

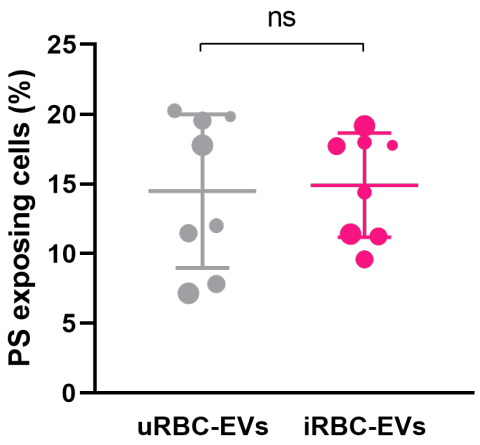

Figure 7.7: Effect of uRBC- and iRBC-derived EVs on eryptosis of fresh RBCs. A controlled number of EVs were added onto fresh RBCs. The size of each point is indicative of the numbers of EVs added in the cultures: 10^5, 10^6, 10^7 or 10^8 EVs per microliter of culture (in iRPMI, 4% hematocrit). Following a 48h incubation, PS exposure was determined by flow cytometry. Individual values, mean and SD of n=8 conditions from three independent experiments in triplicate are shown here.

7.2.5 Impact of *P. falciparum* conditioned media on eryptosis of uRBCs

Given that iRBC-derived EVs did not appear to have an impact on eryptosis of bystander RBCs, we investigated the contribution of other factors, namely, soluble factors secreted by iRBCs (by either ring stages, trophozoite stages, schizont stages or factors released upon schizont egress). Following a 48h incubation of naïve RBCs or *P. falciparum* asynchronous cultures, the conditioned media were collected, and residual cells were eliminated by centrifugation. The conditioned media were then filtered with a 0.45µm membrane filter, to exclude all cell debris and merozoites, or with a 0.22µm membrane filter to also exclude larger EVs. Fresh RBCs were incubated for 48h with these four types of conditioned media (uRBC 0.22µm and 0.45µm filtrate, iRBC 0.22µm and 0.45µm filtrate), or with complete RPMI (cRPMI) as a negative control, and eryptosis hallmarks were determined by flow cytometry as described above. Two independent experiments, each performed in triplicate, are summarised in Figure 7.8. Additional replicates of this experiment were prevented by laboratory access restrictions due to the COVID-19 pandemic. We nevertheless were able to provide statistical tests based on only two replicates, but these should be considered with caution in view of the small sample number.

While there was no significant increase of the PS exposure of fresh RBCs incubated with uRBC-derived conditioned media (when compared to the cRPMI control), conditioned medium from iRBCs (0.22µm filtrate) significantly increased PS exposure of RBCs when compared to the cRPMI control (p=0.0121). A trend of increased PS exposure was also observed in the cells incubated in iRBC-medium (0.45µm filtrate), although it was not statistically significant.

Fresh RBCs incubated with uRBC-derived conditioned media tended to be slightly smaller

than those incubated with iRBC-derived conditioned media, although this was not significant. Intracellular calcium levels remained unchanged across all conditions tested. Our preliminary data indicates that conditioned medium from *P. falciparum* culture induces PS exposure of fresh RBCs. Our findings suggest that increased eryptosis of bystander RBCs observed in *P. falciparum in vitro* cultures can be attributed to parasite secreted factors.

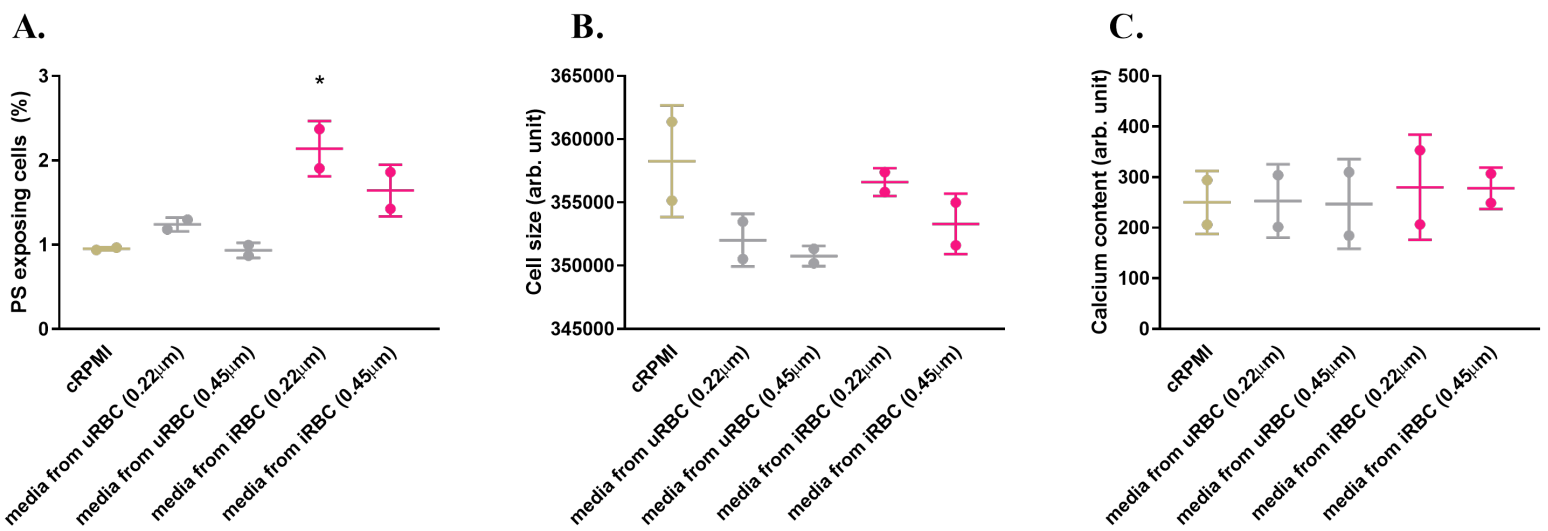

Figure 7.8: Conditioned medium from *P. falciparum* culture induces an increase in PS exposure of fresh RBCs. Conditioned media from uRBCs or asynchronous *P. falciparum*-iRBC cultures were filtered with 0.22µm or 0.45µm filters and added onto fresh RBCs. Following 48h incubation, PS exposure, cell size and intracellular calcium content were assessed by flow cytometry. Individual values, mean (SD) of two independent experiments (each performed in triplicate) are shown. An ordinary one-way ANOVA was performed. *: compare to cRPMI control.

7.2.6 Impact of glucose depletion by *P. falciparum* on eryptosis of uRBCs

P. falciparum relies mainly on glycolysis as an energy source for its intraerythrocytic development [236], leading to iRBCs consuming 20-times more glucose than uRBCs [237]. Sexton *et al.* recently discovered that RBCs cultured in presence of iRBCs displayed increased glycolysis rates [238]. Given that energy depletion can induce eryptosis [111], we decided to investigate whether the depletion of glucose in the medium by the parasite could be responsible for the increase in eryptosis of bystander RBCs.

To test the hypothesis that glucose depletion in parasite-derived conditioned medium induces eryptosis of uRBCs, we supplemented conditioned medium with 11mM glucose before adding it onto fresh RBCs. 11mM concentration was chosen because it corresponds to the glucose concentration found in complete RPMI (cRPMI). In addition, to precisely investigate the contribution of glucose levels, we excluded rupturing schizonts from this experiment, since free haemoglobin components can contribute to inducing eryptosis [233, 234].

The iRBC-derived conditioned medium originated from a 24h synchronised culture (ring to trophozoite transition) at high parasitemia (6-8%). As a control, conditioned medium from uRBCs was also collected after a 24h incubation in identical conditions. The pH of both these conditioned media was measured (Figure 7.9). The conditioned media were filter-sterilised (0.22µm filter), and supplemented (or not) with glucose, before being added to fresh RBCs. Fresh RBCs were therefore incubated in uRBC-derived conditioned medium (+/- glucose), iRBC-derived conditioned medium (+/- glucose) or cRPMI as a negative control. Moreover, based on preliminary data from Nathaniel Pywell (Creek Laboratory, Melbourne Institute of Pharmaceutical Sciences), we also decided to investigate the levels of PS exposure over time: we analysed these cultures 2, 4 and 7 days post initial incubation with the various conditioned media. Eryptosis hallmarks were measured by flow cytometry and hemolysis by absorbance of the cell free media. The results of three independent experiments performed in triplicate are presented in Figure 7.10. First, the pH of conditioned medium from *Plasmodium* culture was significantly lower than that from uRBCs: pH of 7.07 vs 7.52 respectively ($p<0.0001$).

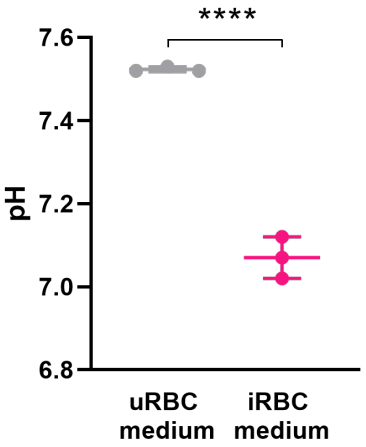

Figure 7.9: pH of uRBC- and iRBC-derived conditioned media. Conditioned media from uRBCs and a synchronised culture of *P. falciparum* were collected after 24h incubation (corresponding to the development from ring to trophozoite parasites) and their pH was measured. Individual values, mean (SD) of three independent experiments are shown. ****: $p<0.0001$ using a t-test.

At all timepoints, PS exposure was similar in uRBC-derived conditioned media with glucose, without glucose and the cRPMI control. PS exposure increased significantly over time in all conditions compared to the first timepoint: at day 7 for cRPMI (p=0.0012), uRBC media with and without glucose (p=0.0016 and 0.002 respectively), iRBC medium with glucose (p=0.0034); at day 4 for iRBC medium without glucose (p=0.0294). Compared to uRBC-derived conditioned media, media from iRBCs induced PS exposure of fresh RBCs: at day 7, PS exposure in both iRBC media conditions (+/- glucose) was significantly higher than cPRMI, uRBC (+/- glucose) (p<0.0232). However, addition of glucose to iRBC conditioned medium significantly blunted the increase of PS exposure. Indeed, at day 7, 87.40% of RBCs incubated in iRBC-derived conditioned medium (without glucose) exposed PS, against only 38.91% of cells when glucose was added (p<0.0001).

No significant changes in cell size were observed over time, although RBCs incubated in iRBC-derived conditioned medium without glucose supplementation tended to be smaller at day 4 and days 7, when compared to day 2.

When iRBC-derived conditioned medium (without glucose) was added to fresh RBCs, intracellular calcium levels measured at day 7 were lower than those measured at day 4 (p=0.03). At day 7, addition of glucose to iRBC-derived conditioned medium significantly increased calcium levels of fresh RBCs (p=0.0228).

No significant change in hemolysis was observed in any of the conditions. However, there was a clear trend for an increased hemolysis at day 7 when RBCs were incubated with iRBC-derived conditioned medium (without glucose addition) compared to all the other conditions.

In summary, we have found that *P. falciparum* induces PS exposure of bystander RBCs *in vitro*, an effect that is promoted by parasite derived soluble factors secreted to the extracellular milieu. Our data suggests this phenomenon is unlikely to be due to iRBC-derived EVs, partly attributed to the glucose depletion by the parasite, and of (an) as yet unidentified parasite specific factor(s).

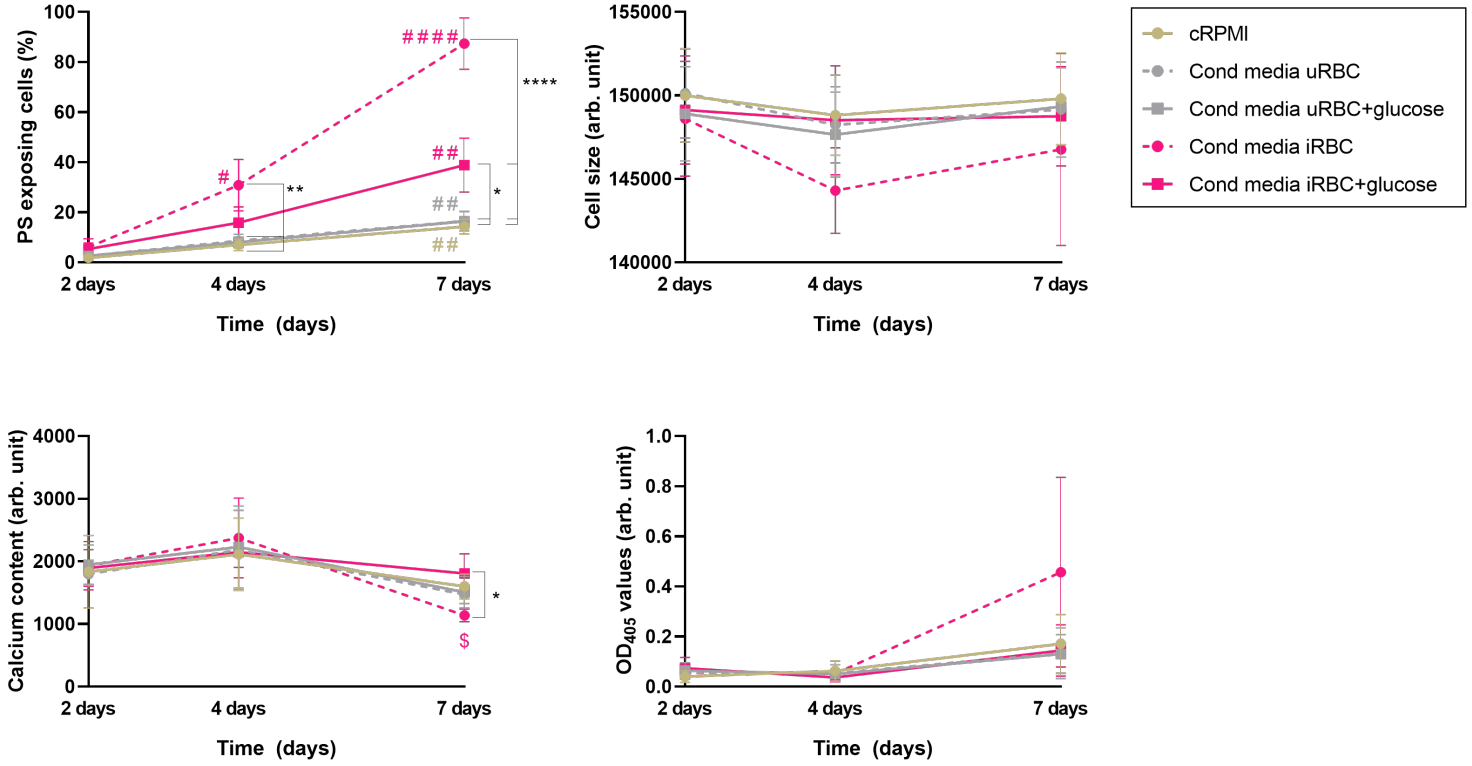

Figure 7.10: Conditioned medium from *P. falciparum* cultures induces exposure of PS on naïve uRBCs, an effect only partially due to glucose depletion. Conditioned media from uRBCs and a synchronised culture of *P. falciparum* were collected after 24h incubation (corresponding to the development from ring to trophozoite parasites), filtered (0.22µm), supplemented or not with 11mM glucose, and added onto fresh RBCs. RBC death levels were measured after incubations of 2, 4 and 7 days. Flow cytometry was used to estimate PS exposure, cell size and intracellular calcium levels. 405nm absorbance of the cell-free media was used as a proxy for hemolysis. Mean and SD of N=3 independent experiments in technical triplicate are shown. A one-way ANOVA with multiple Tukey tests was performed. *: compare conditions within one time point. #: compare day 4 and day 7 to day 2 within one condition. $: compare day 7 to day 4.

7.3 Discussion

Malarial anaemia is a common and severe symptom of malaria, and is driven mainly by the loss of uRBCs [50], partly due to their increased eryptosis levels [49]. In this chapter, we hypothesised that iRBC-derived EVs and/or other soluble factors are responsible for the death of bystander RBCs.

7.3.1 Mature stages of *P. falciparum* induce PS exposure of bystander RBCs

We have demonstrated that bystander non-infected erythrocytes within a *P. falciparum in vitro* culture expose increased levels of PS when compared to naïve RBCs (Figure 7.1). Specifically, our data indicates that trophozoite parasite stages induce significantly higher PS exposure on bystander RBCs, when compared to ring parasite stages (Figure 7.2). Further, we have demonstrated that parasitemia positively correlated with PS exposure of bystander RBCs (Figure 7.4).

Interestingly, we have previously demonstrated that parasite maturation induces eryptosis of its host cell (see Chapter 5), indicating that trophozoites (and perhaps schizont stages) are responsible for the increase of PS levels both of iRBCs and of non-infected neighbouring cells.

Possible mechanisms for this phenomenon include secretion of parasite factors in the extracellular milieu, release of RBC cytosolic content upon schizont egress, and 'collateral damage' due to alterations in the media (such as depletion of nutrient and alteration in pH). Regarding 'collateral damage', it is important to note that, in the time-course experiment, culture media was renewed at every time point. Therefore, bystander RBCs were only exposed to the same extracellular milieu for up to 12h, and severe depletion of essential nutrients in this short amount of time is unlikely.

Direct cell-to-cell contact could also be a contributing factor to bystander RBC death and will be briefly discussed here. However, malarial anaemia can be observed when parasitemia is low [50]; it therefore appeared to us more interesting to study the extracellular milieu (which affects a greater number of RBCs) than direct contact of iRBCs with bystander RBCs.

(1) Direct cell-to-cell contact. It is well established that *P. falciparum* exports many proteins to the host cell's surface during the trophozoite stage. These proteins (such as PfEMP1) are known to induce 'rosetting', whereby the non-infected cells stick to infected cells [40, 239]. The same mechanism allows iRBCs to cytoadhere to the endothelium of blood vessels, thereby avoiding splenic passage. Interestingly, sequestering iRBCs are known to induce changes in the endothelial cells they bind to, including transcription changes [240] as well as inducing apoptosis [232]. Although, to

my knowledge, it has not been studied yet, rosetting iRBCs could also be influencing bystander cell membrane's physiology. This could explain why trophozoites seem to induce more PS exposure on bystander cells compared to rings.

(2) EVs secreted by trophozoites but not rings. Ring- and trophozoite-iRBCs secrete extracellular vesicles (EVs) with different contents [86] and at different intensities (more EVs are secreted as the parasite matures [88]). We also know that iRBC-derived EVs can be uptaken by RBCs [89] and can modify them [92]. It is therefore possible that these differences in the content of EVs produced between ring- and trophozoite-iRBCs lead to differences in PS exposure. However, this hypothesis does not seem to be verified by our preliminary data (discussed below).

(3) Soluble factors secreted by trophozoites but not by rings. It is also possible that parasite-secreted factors responsible for increased PS exposure of bystander RBCs are soluble molecules, such as proteins or metabolites. For instance, *Plasmodium* kinases were shown to be secreted during the trophozoite stage [241, 242]. Besides, the increased digestion of haemoglobin by trophozoites lead to secretion of amino acids outside of the host cell [208]. This increase in extracellular amino acid concentration could also impact bystander RBCs. We therefore tested the impact of filtered conditioned media from cultures of parasites on eryptosis levels of fresh RBCs.

(4) "Collateral damage". A change in pH, waste accumulation and nutrient depletion (such as glucose) may lead to a stress response that could be partly responsible for the observed PS exposure levels on bystander cells. Glucose depletion, as well as pH changes, were therefore investigated, and discussed below.

Overall, trophozoites seemed to induce more PS exposure in bystander RBCs than rings. At all parasite stages, the induction of PS exposure in bystander RBCs positively correlates with parasitemia. However, no conclusion could be drawn with respect to the effect of schizonts-iRBCs, as the timepoints containing the most schizonts also contained newly formed rings and intracellular content of lysed iRBCs.

7.3.2 Rupturing schizonts might induce PS exposure of bystander RBCs

It was striking to see that within each timepoint (*i.e.* when similar stages of different cycles were not combined together), the only correlation observed between parasitemia and PS exposure of bystander RBCs was at times where schizonts were rupturing (Figure 7.3). Experimental replicates where parasitemia was high at 48h were replicates where many schizonts had ruptured and new rings had formed. Between 48h of cycle 1 and 12h of cycle 2, the rest of the schizonts had time to rupture, which might explain the significant correlation observed at 12h of cycle 2 as well. It is therefore possible that the release of RBC cytosolic contents and/or parasites factors induced this PS exposure. In particular, several haemoglobin by-products are known to adversely affect RBCs viability, including heme [233], hemin (oxidised heme) [234] and methaemoglobin (oxidised haemoglobin) [84].

In addition, other intracellular factors might be important players. For instance, erythrocyte lysate was shown to induce intracellular calcium elevation in fibroblasts, a process not induced by oxyhaemoglobin [243]. Finally, parasite factors released in the media during lysis of the host cell could also play a role, such as fragments of the parasitophorous vacuole, which was shown to induce complement deposition and phagocytosis on bystander RBCs [65], or such as the PfHRP2 protein which, when released upon schizont's rupture, activates inflammation pathways in endothelial cells [244].

To better investigate the contribution of schizont stages on PS exposure of bystander RBCs, we could use the protease inhibitor E64 to prevent schizont egress [245]. This would allow to discriminate between cytosolic factors released upon egress and factors secreted by intact schizonts.

In summary, rupture of schizonts seems to induce PS exposure in bystander RBCs, in a way that is proportional to the parasitemia.

7.3.3 iRBC-derived EVs are smaller than uRBC-derived EVs

EVs isolated from *P. falciparum* parasite cultures correspond to a mixture of EVs produced by iRBCs harbouring parasites at the ring and trophozoite stages and bystander RBCs. When iRBC-derived EVs were compared to uRBC-derived EVs, we observed that the latter were larger and more heterogenous (in size and shape) than the former (Figure 7.5 and 7.6).

At first, it might appear counterintuitive that uRBC-derived EVs would be larger than iRBC-derived EVs. Indeed, *P. falciparum* packs considerable cargo in iRBC-derived EVs: iRBC-derived EVs contain more proteins than uRBC-derived EVs [246]; they include over 150 parasitic proteins [247], and are enriched in kinases and proteasome subunits from both the parasite and the red blood cell [92]. We could assume that the parasite, packing more cargo than uRBCs, would produce larger EVs. However, uRBC-derived EVs necessarily originate from the plasma membrane and are therefore called 'microvesicles'. In addition to budding from the iRBC cell surface, iRBCs-derived EVs can also stem from *P. falciparum* intracellular compartments, which tend to be smaller in size [85] and are referred to as exosomes. Further, it has been shown that iRBCs secrete more EVs than uRBCs [87], and more precisely, that iRBCs secrete more small size EVs compared to uRBCs [246]. Overall, this could explain why iRBC-derived EVs are smaller on average.

Although our findings relating to the size of EVs are in accordance with other recent studies [248, 249], the reason for these differences is yet to be investigated. In particular, the largest EVs (160-260nm) have only been detected in uRBCs cultures, and not in parasite cultures (Figure 7.5 and 7.6). Considering that *P. falciparum* cultures contain a majority of uRBCs, this is particularly intriguing. It is possible that *P. falciparum* modulates the

EVs production by bystander RBCs, although this remains to be investigated.

7.3.4 iRBC-derived EVs are not the cause for the increased PS exposure of bystander RBCs

To investigate the loss of uRBCs during malarial anemia, we hypothesized that iRBC-derived EVs were responsible for increased eryptosis of bystander RBCs. However, our data seems to refute our hypothesis, as both iRBC- and uRBC-derived EVs lead to similar levels of PS exposure on fresh RBC (Figure 7.7). Moreover, the differences in number of EVs added to fresh RBCs did not seem to impact the PS exposure outcome. Precisely, 10^5 to 10^8 EVs were added per microliter of culture (*i.e.* ∼37 to ∼37,000 EVs per RBC): this covers a range of three orders of magnitude. Although more work would be required to confirm this, it did not appear that incubation with more EVs translated to more PS exposure (both with iRBC- or uRBC-derived EVs).

In a way, this may be beneficial for the parasite. Indeed, invasion is less efficient when RBCs expose PS [159]. Therefore, it would not be optimal for the parasite to induce eryptosis of bystander RBCs through EVs. In line with this, it was found that iRBC-derived EVs actually "prepare" RBCs for successful invasion, by reducing the RBC membrane stiffness, through phosphorylation and degradation of cytoskeletal proteins [92].

7.3.5 *P. falciparum*-secreted small molecule(s) are the likely cause for the PS exposure of bystander RBCs

Since iRBC-derived EVs did not induce PS exposure of naïve RBCs, we investigated whether other soluble extracellular factors (from rings, trophozoites, schizonts, and rupturing iRBCs) would induce RBC death. To do so, we exposed fresh RBCs to conditioned media from mix parasite cultures and from uRBCs, which were either filtered with a 0.45µm filter (to eliminate cell debris and merozoites) or with a 0.22µm filter (to eliminate larger EVs) (Figure 7.8).

In this experiment, it was interesting to note that cells incubated in 0.22µm-filtered iRBC-medium exposed more PS. This condition supposedly excluded the larger EVs. It is therefore possible that the subset of EVs that are larger (cf. TEM images in Figure 7.6) have a protecting effect against eryptosis. It would be very interesting to further investigate the role of different EVs subpopulations on eryptosis of RBCs. Another possible explanation for the observed difference between 0.22µm and 0.45µm filtrates is that we are filtering out other components, such as hemozoin. Hemozoin, also called the "malaria pigment", is a by-product of haemoglobin digestion, and a way for the parasite to circumvent the toxicity of heme alone (average length of 300-500nm [250]). However, this is unlikely to be the case. Indeed, previous studies suggest that hemozoin actually induces apoptosis of erythroid precursor [82], as well as impair macrophages function once engulfed [251]. Therefore, we would expect to observe more PS exposure when hemozoin is included in the media (*i.e.*

in the 0.45µm filtrate condition).

The conclusions from this experiment should be taken with precaution, considering that there were only two independent replicates. Overall, this experiment seems to confirm that PS exposure induced in bystander RBCs are due, at least in part, to soluble factors and not only to cell-to-cell contact.

7.3.6 Glucose depletion is only partly responsible for increased PS exposure of bystander RBCs

To eliminate the potential effect of schizont rupture and subsequent release of cytosolic content in the medium, a conditioned medium experiment was performed using tightly synchronised cultures that were only allowed to mature from ring to trophozoite stages (Figure 7.10). Further, to investigate the role of glucose depletion by the parasite, conditioned media from parasite and from uRBCs were supplemented (or not) with 11mM of glucose. Of note, this represents a surplus compared to *in vivo* conditions (up to 8mM in non-diabetic adults [252]). Eryptosis hallmarks were measured at 2, 4 and 7 days of incubation.

Our results confirmed that *P. falciparum*-conditioned medium induced PS exposure of naïve RBCs: this effect was observed after four days of incubation without glucose supplementation and after seven days in the presence of extra glucose. Further, and although no significant difference was observed, a clear trend indicated that hemolysis appears to be induced by parasite-derived conditioned medium (without glucose).

It has been described that glucose depletion induces eryptosis [111], at least in "erythrocyte culture conditions" (see Chapter 4A). It is also well established that *P. falciparum* consumes considerable amounts of glucose. Indeed, iRBCs consume approximately 20-times more glucose than uRBCs [237]. In addition, trophozoite-iRBCs consume around 6-times more glucose than ring-iRBC [237], linking nicely to the observation made earlier, whereby mature parasites seemed to induce more PS exposure of bystander cell than rings. It is therefore not surprising that depletion of glucose by the parasite would induce eryptosis of bystander RBCs.

In addition to glucose being depleted by the parasites, glucose might partially be depleted by RBCs exposed to conditioned media from parasites. Indeed, it has been shown that RBCs incubated with media from *P. falciparum* display increased glycolytic fluxes [238] (Boulet *et al.*, in preparation). We can therefore not exclude that the increase in PS exposure in RBCs exposed to medium from parasites is due to depletion of glucose by these uRBCs in high energy state. However this is unlikely to be the sole contributor since 11mM glucose already represents an excess compared to in vivo conditions, but also the recent studies did not identify a depletion of glucose in the extracellular milieu [238] (Boulet *et*

al., in preparation).

Although *in vitro* conditions are very different to *in vivo* environment (including different cell density, types of cells, fluxes, etc.), we discuss below some considerations linking malaria infections and (1) dysglycaemia, (2) diabetes and (3) malnutrition.

(1) Malaria and glucose levels. During severe *falciparum* malaria, patients may develop hypoglycaemia, especially in children [253, 254]. Hypoglycaemia is defined as a blood glucose concentration below 4mM. It would be interesting to measure glucose concentration in our *in vitro* experiment to check whether this threshold is reached. Hypoglycaemia during a malaria infection is associated with poor prognosis. The mechanisms behind this complication are not fully understood yet, but increased consumption of glucose seemed to be an important player [253]. Indeed, in murine models of malaria, hypoglycaemia correlates with hyperparasitemia [255] and glucose turnover increases in severe malaria [256].

(2) Malaria and diabetes. Kalra and colleagues (2017) comprehensively reviewed the interplay between malaria and diabetes [257]. Strikingly, type 2 diabetes increased the risks of malaria infection. Indeed, each mM increase in blood glucose increased the risk of *falciparum* infection by 5% [258]. Although the reasons behind this increased susceptibility to malaria are unclear, explanations include impaired immunity [259], increased mosquito feeding [260, 261] as well as enhanced parasite proliferation due to abundance of glucose [262]. Additionally, fever, hypoglycaemia and black fever water (a condition where urines are black due to the presence of haemoglobin, caused by excessive hemolysis) were less frequent in diabetic patients [263]. Hematocrit is also significantly higher than in non-diabetic patients [263]. Of note, albumin levels are higher in diabetic patients [263]: since we observed a protective role of Albumax (a lipid-rich bovine serum albumin used for cell culture) against eryptosis (see Chapter 4A), we could speculate that the higher albumin levels could be a contributing factor in these observations. Although many factors could play a role, it is possible that the increased glucose content in diabetic patients protects erythrocytes from lysis and splenic clearance. However, this is not to say that diabetic patients were protected from severe malaria: on the contrary, multi-organ failure and mortality were higher in diabetic patients [263].

(3) Malaria and malnutrition. Das and colleagues (2018) evaluated the effect of malnutrition on malaria risk in a systematic review [264]. A major consistency among the literature is that chronic malnutrition is associated with severity of malaria, including high parasitemia and anaemia. Authors suggested that this association is exacerbated by cofounding factors, in particular HIV co-infection and socio-economic factors. Further, Thien and colleagues (2006) argue that fasting may be a risk factor that has not been investigated and taken into account sufficiently [265].

Another consideration for follow-up experiments is to control for pH. Indeed, the use of glucose through glycolysis produces lactate, which decreases the media pH [262]. In particular, in *in vitro* culture, iRBCs produce about 18-times more lactate than uRBCs [262] and lactic acidosis is a common complication observed in severe malaria [266]. Concordantly we noticed that the pH was significantly lower in conditioned medium from parasites (Figure 7.9). Adjusting to the same pH in all conditions could give us insights whether this is also a "collateral damage" factor contributing to bystander cell death.

Overall, glucose supplementation only partially "rescued" eryptosis phenotypes of RBCs incubated in iRBC conditioned medium. Other soluble factors secreted by the parasite are responsible of bystander RBC death; such factors remain to be identified.

7.4 Conclusion

In this chapter, we report that *Plasmodium falciparum* induces PS exposure of bystander RBCs. This bystander effect tends to be stronger with trophozoite stages than with ring stages. Rupturing schizonts also seemed to affect bystander RBCs viability. Parasitemia positively correlated with PS exposure of bystander cells at all parasite stages. While investigating the factors responsible for the increased PS exposure in bystander RBCs, we demonstrated that iRBC-derived EVs do not appear to play a role. However, we have shown that although glucose depletion from the culture medium contributes to bystander RBC eryptosis, iRBC-secreted small molecules are key factors in eryptosis of bystander RBCs. Such parasite-derived secreted factors remain to be identified. Taken together, these findings provide novel insights in malarial anaemia, one of the most common complications of malaria.

Chapter 8

Concluding remarks: towards broad-spectrum anti-infectives?

Currently, all antimalarial drugs directly target *Plasmodium falciparum* and drug-resistance has emerged against all these drugs. In humans, malaria symptoms arise during the blood stages of *P. falciparum*, during which the parasite resides inside red blood cells (RBCs). Therefore, the opportunity to target factors from the host cell to eliminate the parasite is particularly attractive to circumvent drug resistance. This thesis aimed to identify erythrocyte factors targetable for novel antimalarial treatments, with a special focus on eryptosis (the "erythrocyte apoptosis") and the potential to repurpose clinically available drugs.

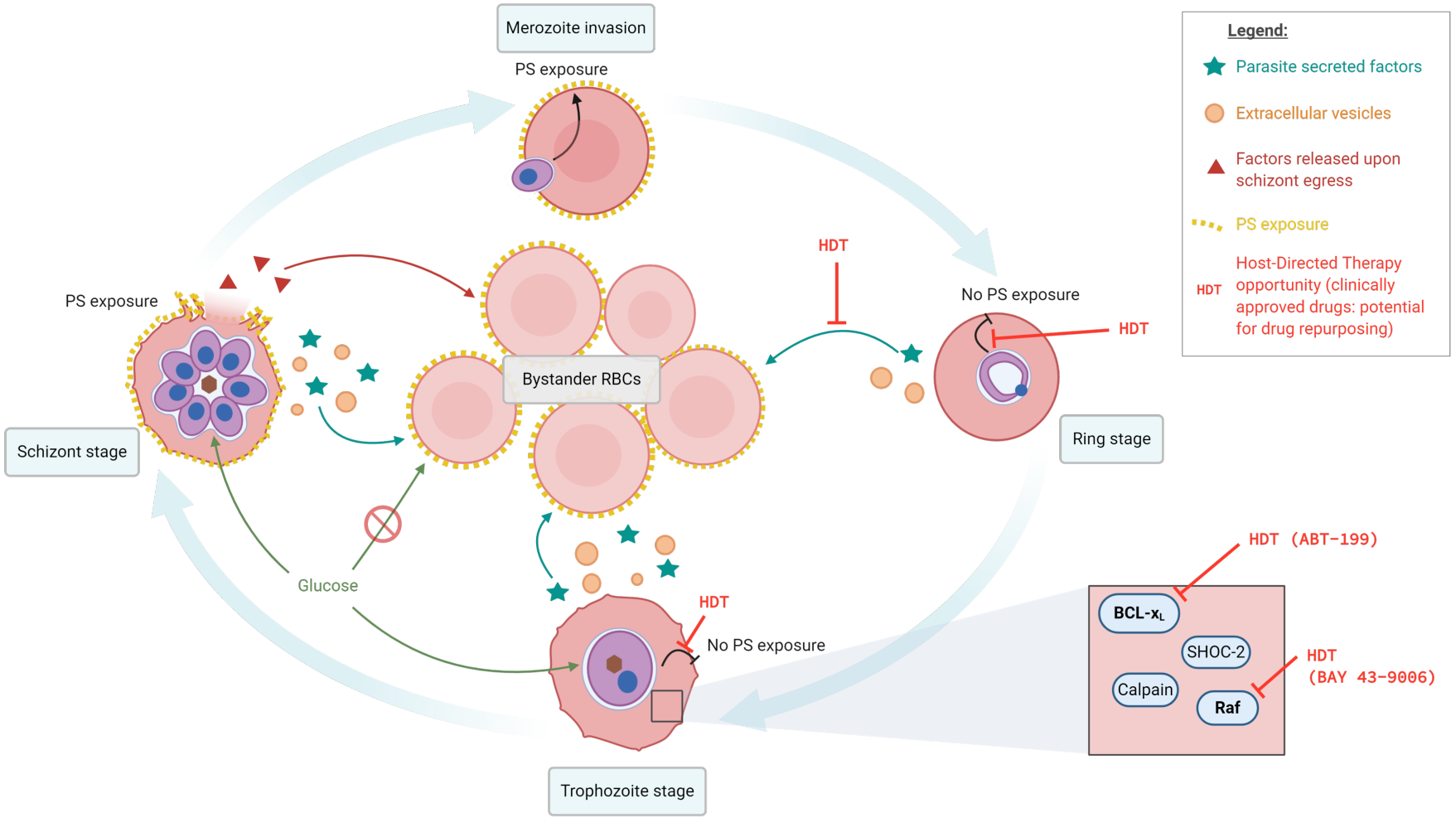

Figure 8.1: Summary of the findings reported in this thesis - A proposed model of interactions between *P. falciparum* and host red blood cells: host-directed opportunities.

Figure 8.1: Summary of the findings reported in this thesis - A proposed model of interactions between *P. falciparum* and host red blood cells: host-directed opportunities.
Phosphatidylserine (PS) exposure of the infected red blood cell (iRBC): Upon invasion, merozoites induce an increase in PS exposure of their host cells observed during young ring stages (Chapter 5). During the mid/late ring and trophozoite stages, PS exposure levels drop down to baselines levels (*i.e.* uRBC levels), and increase again during the schizont stage (Chapter 5). The variation of PS exposure levels suggests that the parasite actively represses PS exposure and represents an opportunity for host-directed therapy (HDT).
Host proteins important for *P. falciparum* development and drug repurposing opportunities: We propose that erythrocytic BCL-x_L and Raf kinase play an important role in the development of the parasite. Indeed, the use of inhibitors ABT-199 and BAY 43-9006 respectively impairs *P. falciparum* growth *in vitro* (Chapter 6 and 4 respectively). In addition, SHOC-2 and calpain were identified as potential binding partners of BCL-x_L and represent interesting targets to be explored for HDT (Chapter 6).
Mechanisms of bystander RBC death: Bystander non-infected RBCs display increased levels of PS exposure in the presence of infected RBCs, increasing with the parasite's maturation (Chapter 7). Parasite-derived extracellular vesicles (EVs) do not appear to play a role in the bystander effect (Chapter 7). However, depletion of glucose by the parasite (especially by trophozoites and schizonts), factors released upon schizont egress and factors secreted by intracellular stages of the parasite do play a role in the death of bystander RBCs (Chapter 7). Importantly, parasite-secreted soluble factors, yet to be identified, could represent interesting HDT opportunities.

8.1 Is eryptosis a true programmed cell death?

At the heart of this work is the hypothesis that *P. falciparum* needs to inhibit eryptosis of its host cell in order to survive during its intraerythrocytic development. However, I have identified significant issues with the assays that have been used to investigate eryptosis in earlier studies (Chapter 2 and 4A), which leads to reflections on eryptosis itself.

First, although cell-surface exposure of phosphatidylserine (PS) appears as a reliable marker for RBC death, other previously described hallmarks of eryptosis, namely cell shrinkage, intracellular calcium levels and membrane blebbing, were not consistently observed, both in the literature and in this work. Moreover, apart from ionomycin treatment, which induced rapid exposure of PS (similar to the rapid induction of apoptosis in nucleated cells), induction of RBC death with other compounds previously described as eryptosis inducers, and with conditioned medium from parasites, only became apparent after extended periods of time (Chapter 4, 5 and 6). In addition, hemolysis was frequently observed in conjunction to PS exposure. In nucleated cells, apoptosis does not induce cell lysis: it is a "silent death" [267], with apoptotic bodies ultimately cleared by macrophages. Taken together, this indicates that eryptosis might not be extensively comparable to apoptosis, but perhaps resembles more necrosis (passive cell death) or necroptosis (a regulated form of necrosis) [268]. Importantly, we demonstrated that the experimental set-up has a key impact on eryptosis hallmarks read-outs, highlighting a crucial need to re-assess eryptosis mechanisms within more physiological conditions (Chapter 4A).

Whether eryptosis is a "programmed cell death" of RBCs or not, I argue that the exposure of PS on the surface of erythrocytes remains profoundly relevant in the context of a malaria infection. PS exposure of bystander uRBCs plays a role in the pathogenesis of severe malaria, where the clearance of these bystander cells by macrophages can lead to severe

anaemia. Moreover, as we will now discuss, PS exposure on iRBCs can be considered as a potential target for host-directed therapies.

8.2 *P. falciparum* inhibits PS exposure of its own host cell

In Chapter 5, I have investigated the impact of the parasite's intraerythrocytic development on eryptotic hallmarks of the host RBC: in particular, I measured PS exposure of iRBCs over time (over two complete erythrocytic cycles). One of the most exciting discoveries of this chapter is the peak in PS exposure of the host RBC observed after merozoite invasion, after which PS exposure decreases back to baseline levels (*i.e.* uRBCs levels; see Figure 8.1). This indicates that the parasite could actively be reversing the exposure of PS on its host cell, supposedly to avoid splenic clearance. Gaining a better understanding of the molecular mechanisms leading to manipulation of PS exposure could lead to preventing these iRBCs from "appearing healthy". Importantly, preventing the parasite from inhibiting PS exposure of its host cell would allow the elimination of iRBCs during the early stages of the parasite, before they sequester, therefore alleviating the most severe clinical manifestations (*e.g.* blood flow impairment, cerebral and placental malaria). Excitingly, identifying pathways that are only present and active in iRBCs would allow to target specifically infected erythrocytes, therefore reducing undesirable side effects.

8.3 Mechanisms of *P. falciparum*-induced bystander erythrocyte death

Building on previous work, we found that, not only does *P. falciparum* affects its host RBC physiology, but the parasite also impacts bystander non-infected RBCs (Figure 8.1). To investigate the mechanisms responsible for the enhanced levels of PS exposure of bystander RBCs, we decided to focus on factors secreted by the parasite. Indeed, considering the systemic effect observed in circulating blood cells, factors present in the extracellular milieu appeared as more likely candidates than direct cell-to-cell contact. In addition, parasite-secreted factors could explain that malarial anaemia, driven by the loss of uRBCs, is also observed when parasitemia is low and can still be observed once parasites have been eliminated [50].

Among the factors I have investigated, iRBC-derived extracellular vesicles (EVs) did not induce PS exposure of fresh RBCs (Chapter 7; Figure 8.1). Although EVs are involved in malarial pathogenesis, in particular cerebral malaria [86], they do not appear to play a role in malarial anaemia.

The analysis of eryptotic hallmarks in bystander uRBCs over time revealed that factors released upon schizont egress induce PS exposure of RBCs (Figure 8.1). Moreover, to investigate the contribution of other parasite-secreted factors, I exposed fresh RBCs to

conditioned media from parasite cultures (excluding schizont egress). Further, to assess the impact of glucose depletion by *P. falciparum* on the bystander effect, conditioned medium was complemented, or not, with glucose. This work indicates that (i) conditioned medium from parasites increases PS exposure of fresh RBCs, (ii) this is partly due to the depletion of glucose by the parasite (*i.e.* glucose supplementation only partially "rescues" the increase in PS exposure), and therefore, (iii) other factor(s) secreted by intracellular parasites also contribute to this bystander effect (Figure 8.1). Identifying this/these factor(s) will lead to two major outcomes: (i) use such factors as biomarkers of malarial anaemia, (ii) target them to prevent the increase of bystander RBC PS exposure and therefore anemia.

8.4 Repurposing Drugs for Host-Directed Therapies

In the course of this work, I have identified several compounds, including clinically approved drugs used in cancer and cardiac dysfunction treatments, that also display a strong antiparasitic activity (Chapter 4A and 6).

The identification of the antimalarial effect of these compounds opens exciting perspectives, not only in host-directed therapy, but also in drug-repurposing.

Accelerating the development pipeline for antimalarial drugs is pressing, as novel treatments are urgently needed before the efficacy of artemisinin and derivatives severely fail due to resistant parasites. Further, reducing drug development costs is particularly relevant in the context of infectious diseases that primarily affect low-income countries. Indeed, the private for-profit sector does not have incentives to develop novel treatments for infectious diseases (which can be quickly resolved upon clearance of the pathogen), when the potential clients mainly have low-income [269]. Academia, on the other hand, often lacks the capacity, infrastructure and funds to develop a drug to its final delivery [270]. Repurposing already approved, or nearly approved, clinical drugs has the potential to shorten the development timelines and to reduce drug development costs [271].

Moreover, drug repurposing, in addition to lowering the drug development price, has another cost-related advantage. Tiered pricing is a price discrimination system whereby drugs are sold for profit in richer countries and sold at a much lower price in developing countries; it is currently used for HIV treatments and several childhood vaccines [272]. It is argued that, in the case of malaria, tiered pricing could not be relied on, since the market is very small outside of endemic regions [273]. Moreover, the already limited market of antimalarial prophylaxis used by higher-income travellers into endemic countries might further dwindle because of the COVID-19 pandemic and the subsequent travel restrictions. Therefore, repurposing drugs that are used in richer countries to treat other conditions could provide an incentive to pharmaceutical companies to sell them for a lower price for malaria afflicted regions.

In this thesis I have identified five compounds displaying antimalarial activity: three clinically approved drugs (amiodarone, BAY 43-9006 and ABT-199), one compound undergoing clinical trials (ABT-263) and one compound with a close derivative currently undergoing clinical trials (oridonin).

Oridonin is an active compound extracted from *Isodon rubescens*, a traditional Chinese herbal medicine, and was found to possess anticancer activity [170]. One of its derivatives, HAO472, is currently in Phase I clinical trials [170]. I demonstrated that oridonin displayed activity against *P. falciparum*, with an IC_{50} of 2µM (Chapter 4A). Testing the effect of HAO472 on *P. falciparum* parasites would be an exciting next step.

Amiodarone (Cordarone) is an antiarrhythmic drug. I demonstrated that amiodarone inhibits *P. falciparum in vitro* proliferation with an IC_{50} of 2.10µM (Chapter 4A). Encouraging activity against *P. berghei* was previously observed in a mouse model [156]. Moreover, the typical maximal drug concentration found in the blood in adults treated with amiodarone is of the same order of magnitude as the IC_{50} value I measured *in vitro* [185]. However, amiodarone can have serious side effects, including lung and liver complications, and the FDA recommends this drug only in cases of life-threatening arrythmia [274]. More investigation is therefore required before amiodarone can be suggested as an interesting antimalarial candidate.

BAY 43-9006 (Sorafenib or Nexavar) is a human Raf kinase inhibitor, used to treat hepatocellular carcinoma and advanced renal cell carcinoma [174]. I measured its *in vitro* IC_{50} against *P. falciparum* at 7.48µM (Chapter 4A). This appears to be nearly two orders of magnitude higher than the peak plasma concentrations in patients treated with this drug [275]. Interestingly, the more potent B-Raf inhibitor, SB-590885, was also found to inhibit *P. falciparum* growth *in vitro*, with a lower IC_{50} of 490nM [191], demonstrating that inhibitors of Raf are good antimalarial candidates.

Finally, the two most interesting candidates in this study are ABT-199 and ABT-263. ABT-199 (Venclexta, Venclyxto or Venetoclax) is a BCL-2 inhibitor used to treat chronic lymphocytic leukemia (CLL) or small lymphocytic lymphoma (SLL) [135]. In addition to being clinically available, the IC_{50} of ABT-199 measured for *P. falciparum* (4.6µM) is of the same order of magnitude as the peak plasma concentration (∼3.45µM) (Chapter 6). ABT-263 (Navitoclax), a BCL-x_L and BCL-2 inhibitor, is undergoing clinical trials for small cell lung cancer treatment (phase I/II [130, 276]). ABT-263's IC_{50} for *P. falciparum* was one of the lowest in this work (0.74µM), nearly 8-fold lower than the highest peak plasma concentrations measured in an escalation study in humans [130].

Although ABT-199 did not impair the growth of *Plasmodium* liver stages *in vitro* [277],

another ABT compound (ABT-737) was found to impair *Plasmodium* liver stages, both *in vitro* and in murine models [106]. If ABT-263 was also revealed to be effective against the parasite's liver stages, this would further increase the interest for this drug. Moreover, compared to amiodarone, for which the mechanism of action against *Plasmodium* is unknown, ABTs target proteins within the BCL-2 family. Excitingly, no BCL-2 or BCL-x_L orthologs have been identified in any *Plasmodium* species so far [193], suggesting that ABT-199 and ABT-263 impair *P. falciparum* growth through inhibition of host molecules, therefore representing a novel host-directed therapy opportunity.

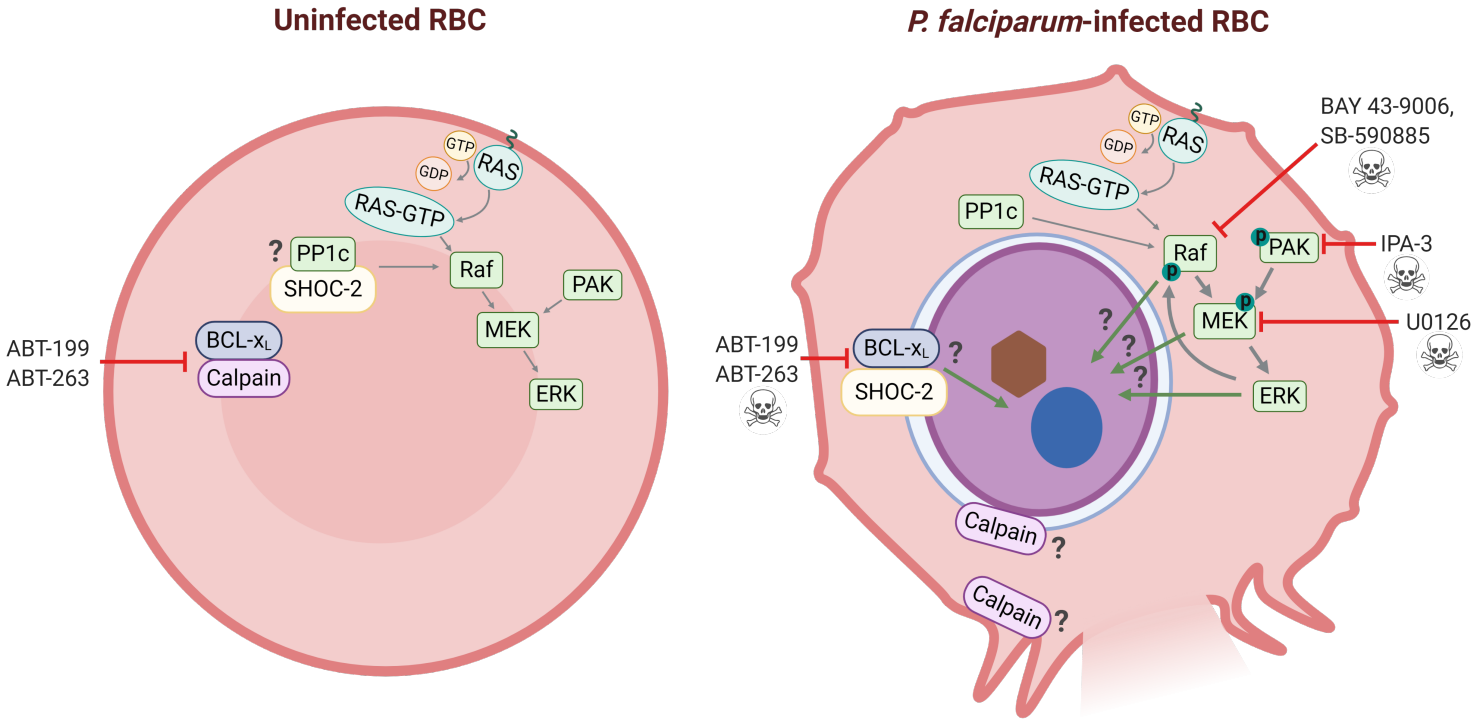

Figure 8.2: Summary of the findings reported in this thesis - Proposed model of erythrocyte pathways hijacked by *P. falciparum*.
BCL-x_L, SHOC-2 and Calpain. In this thesis, I have demonstrated that in uRBCs, BCL-x_L binds to calpain within the cytosol for an unknown function (Chapter 6). This interaction could potentially be disrupted with BCL-x_L-inhibitors, for instance ABT-199 (an approved drug, although more specific of BCL-2 than BCL-x_L) and ABT-263 (undergoing clinical trials). In iRBCs however, BCL-x_L is localised around the parasite (at the parasitophorous vacuole, at the parasite membrane or within the parasite), and interacts with the SHOC-2 protein, here again, performing an unknown role (Chapter 6). This interaction could be disrupted BCL-x_L-inhibitors. Moreover, BCL-x_L-inhibitors kill the parasite, supposedly via the inhibition of BCL-x_L (Chapter 6). This suggests that BCL-x_L carries out an important role for the parasite survival. In iRBCs, calpain shifts its localisation to the "membrane fraction", *i.e.* either to the parasite and/or to the RBC membrane. Since calpain is known to be co-opted by the parasite to facilitate its egress [204], I hypothesise that it localises (at least partly) to the RBC membrane. The typical function of SHOC-2 is to act with Phosphatase Protein 1c (PP1c) subunit: together, they activate Raf kinase by dephosphorylating an inhibitory residue.
The Raf/MEK/ERK cascade. In nucleated cells, this mitogen-activated protein kinase (MAPK) cascade typically starts with the activation of Ras, from its inactive GDP-bound form, to the active GTP-bound form. Active Ras then activates Raf kinase, which phosphorylates/activates MEK kinase, which phosphorylates/activates ERK kinase. In nucleated cells, ERK has over 150 downstream targets, including many in the nucleus, and including an inhibitory phosphorylation of Raf (as part of a negative feedback-loop). It was shown in previous work that this pathway is hyperactivated in iRBCs compared to uRBCs [195, 191]. In particular, Raf, MEK and PAK (a kinase which can also phosphorylate MEK) were more phosphorylated in iRBCs than in uRBCs. Interestingly, the Raf inhibitors BAY 43-9006 and SB-590885 (Chapter 4, [191]), the PAK inhibitor IPA-3 [195], and the MEK inhibitor U0126 [195], all showed antiparasitic effect against *P. falciparum*. This suggests that all these kinases play a crucial role in the parasite intraerythrocytic development.

8.5 Erythrocyte pathways hijacked by *P. falciparum*

In this thesis, I also investigated host-parasite interactions at the molecular level. Here, I discuss the role of erythrocyte proteins BCL-x_L, calpain, SHOC-2 and Raf kinase, in the development of *P. falciparum*.

- **BCL-x_L**

Since the molecular pathways leading to PS exposure in RBCs remain elusive, we investigated the role of an obvious potential candidate: the anti-apoptotic protein, BCL-x_L. BCL-x_L inhibitors have previously been shown to induce PS exposure of RBCs [125] and to have antiparasitic activity on *Plasmodium* liver stages [106].

In Chapter 6, I demonstrated that BCL-x_L inhibitors impair *P. falciparum* growth *in vitro* (albeit to various extents) via an eryptosis-independent mechanism. At the molecular level, we found that, while BCL-x_L is cytosolic in uRBCs, it is recruited towards the parasite in iRBCs (Figure 8.2). Surprisingly, an immunoprecipitation experiment did not identify any known binding partners of BCL-x_L. Instead, human protein µ-calpain appeared as a potential partner of BCL-x_L in uRBCs, while the human SHOC-2 protein was a potential partner of BCL-x_L in iRBCs (Figure 8.2). Importantly, all the interactions identified in this work will need to be further validated (*e.g.* through reciprocal immunoprecipitation assays).

While it was expected that BCL-x_L would have an unusual function (if any) in erythrocytes, it was surprising to identify binding partners that have not previously been shown to form complexes with BCL-x_L.

In nucleated cells, in addition to its role in sequestering BAX and BAK, BCL-x_L can also regulate Ca^{2+} levels at the endoplasmic reticulum (ER) by activating inositol 1,4,5-trisphosphate receptor (IP3R) [278]. The absence of ER in mature erythrocytes, together with the recruitment of BCL-x_L to the parasite, could hint towards a role of BCL-x_L in calcium regulation at the parasitophorous vacuole or parasite membranes. In *Toxoplasma gondii*, evidence suggests that Ca^{2+} release from stores sensitive to IP3 is important for invasion [279]. However, we did not identify IP3R in our BCL-x_L pull-down experiment, and no IP3R orthologs have been described in *Plasmodium spp.* so far [193]. Instead, our pull-down experiments identified human proteins µ-calpain and SHOC-2.

- **µ-Calpain**

We identified the human µ-calpain (or calpain-1) as a potential binding partner of BCL-x_L exclusively in uRBCs (Chapter 6; Figure 8.2). In nucleated cells, µ-calpain-cleavage of the N-terminus of BCL-x_L reduces its anti-apoptotic activity [280, 281]. However, we did not detect cleaved BCL-x_L at the expected size by Western Blot, suggesting that µ-calpain does not cleave BCL-x_L in uRBCs under normal culture conditions. Besides, I demonstrated

that µ-calpain subcellular localisation shifts upon infection with *P. falciparum* (Figure 8.2): similar to BCL-x_L, µ-calpain is cytosolic in uRBCs, and membrane-associated in iRBCs. Because µ-calpain (i) was not pulled-down with BCL-x_L in iRBCs, (ii) is co-opted by the parasite to assist in egress [204], and (iii) is a protease involved in the breakdown of cytoskeletal proteins of RBCs [282], I hypothesise that µ-calpain is recruited to the RBC membrane during the trophozoite stage (stage used for my Western Blots). The role of a potential complex between µ-calpain and BCL-x_L in uRBCs remains to be investigated.

- **SHOC-2**

We identified the human leucine-rich repeat SHOC-2 protein as a potential binding partner of BCL-x_L exclusively in iRBCs (Chapter 6; Figure 8.2)). The fact that SHOC-2 was not pulled-down with BCL-x_L in uRBCs indicates that their interaction is induced by the parasite's presence. However, the induction of this molecular complex did not seem to involve a parasite protein. The shift in SHOC-2-BCL-x_L binding might be induced by changes in post-translational modifications of either one or both these proteins: *e.g.* both proteins can be phosphorylated on multiple sites, which could play a role in their binding affinity.

Importantly, SHOC-2 has never been shown to interact with BCL-x_L in nucleated cells (UniProt information on SHOC-2 & BCL-xL). SHOC-2 has mainly been described as a regulatory subunit of protein phosphatase 1 (PP1c): once activated by Ras, SHOC-2-PP1c stimulates Raf-1 (or C-Raf) by dephosphorylating the inhibitory site Ser-259 [230]. This suggests an importance of the Ras/Raf/MEK/ ERK pathway in iRBCs.

- **Raf/MEK/ERK pathway**

Previous work identified the importance of the Raf/MEK/ERK pathway in iRBCs. Indeed, this pathway is hyperactivated in iRBCs compared to uRBCs, with more phosphorylation sites on Raf, MEK and PAK (a kinase phosphorylating MEK) present in iRBCs than uRBCs [195, 191] (see Figure 8.2). Chapter 4 and these previous publications demonstrate together that inhibition of Raf (with BAY 43-9006 and SB-590885), inhibition of MEK (with U0126) and inhibition of PAK (with IPA-3) all impaired *P. falciparum* growth *in vitro* (Figure 8.2). MEK inhibition also impaired the development of the liver stage of *P. berghei* [195]. Since no orthologs of these proteins have been identified in *Plasmodium spp.* [193], it is a solid indication that the parasite relies on this host pathway for survival. The exact mechanism of action remains to be elucidated. This pathway inhibition seemed particularly important in trophozoite stages, with MEK inhibition [195] and Raf inhibition (Chapter 4) leading to decreased DNA and RNA levels.

Taken together, this shows that the Raf/MEK/ERK and PAK/MEK/ERK pathways are activated specifically in iRBCs; inhibition of these pathways may therefore represent excellent targets for a host-directed therapy approach, with no (or minimal) effect on uRBCs.

8.6 Host-directed therapies: towards broad-spectrum anti-infectives?

The host ERK pathway, along with other MAPK pathways, are manipulated by other apicomplexan parasites (*e.g. Leishmania spp.* and *Trypanosoma cruzi* [283]), as well as by bacteria [284] and by viruses (*e.g.* Influenza A virus [285]). This brings me to the next exciting perspective of my research: host-directed therapies as broad-spectrum anti-infectives.

All intracellular pathogens need to interfere with their host cell pathways for their own survival. In particular, manipulation of host cell pathways is observed in infections by intracellular parasites [198], bacteria [97] and viruses [98]. Overall, this observation led researchers to propose the development of host-directed therapy against all these pathogens [286, 287, 288].

Excitingly, host-directed therapies are already applied clinically: maraviroc (Selzentry) prevents entry of the HIV virus by inhibiting a key human receptor [289, 290]. Clinical trials are assessing the efficacy of Celgosivir (inhibitor of the host enzyme endoplasmatic reticulum glucosidase) against Hepatitis C [291] and Dengue virus [292].

By going one step further, we can even propose to develop broad-spectrum host-directed therapies. Indeed, although the exact mechanisms behind the host cell manipulations are different depending of the pathogen and the host cell type, common targets exist. Such commonly hijacked molecules include NF-$\varkappa$B, PI3K, JAK-STAT, p53, JNK, p38 MAPK, ERK, BCL-2 proteins and PAK [198, 293, 294]. Many intracellular pathogens also finely control Ca^{2+} fluxes, which is often crucial for both invasion and for further intracellular development [198, 287].

In summary, host-directed therapy approach could lead to the development of broad-spectrum anti-infective treatments, while reducing the risk of antimicrobial resistance emergence and repurposing existing drugs [293].

Bibliography

[1] World Health Organization. World malaria report 2019, 2019. Library Catalog: www.who.int.

[2] Jeffrey Sachs and Pia Malaney. The economic and social burden of malaria. *Nature*, 415(6872):680–685, 2002.

[3] S. Bhatt, D. J. Weiss, E. Cameron, D. Bisanzio, B. Mappin, U. Dalrymple, K. E. Battle, C. L. Moyes, A. Henry, P. A. Eckhoff, E. A. Wenger, O. Briët, M. A. Penny, T. A. Smith, A. Bennett, J. Yukich, T. P. Eisele, J. T. Griffin, C. A. Fergus, M. Lynch, F. Lindgren, J. M. Cohen, C. L. J. Murray, D. L. Smith, S. I. Hay, R. E. Cibulskis, and P. W. Gething. The effect of malaria control on plasmodium falciparum in africa between 2000 and 2015. *Nature*, 526(7572):207–211, 2015. Number: 7572 Publisher: Nature Publishing Group.

[4] D. F. Clyde. Immunization of man against falciparum and vivax malaria by use of attenuated sporozoites. *Am J Trop Med Hyg*, 24(3):397–401, 1975.

[5] Machteld van den Berg, Bernhards Ogutu, Nelson K. Sewankambo, Nikola Biller-Andorno, and Marcel Tanner. RTS,s malaria vaccine pilot studies: addressing the human realities in large-scale clinical trials. *Trials*, 20(1):316, 2019.

[6] S Clinical Trials Partnership RTS. Efficacy and safety of RTS,s/AS01 malaria vaccine with or without a booster dose in infants and children in africa: final results of a phase 3, individually randomised, controlled trial. *The Lancet*, 386(9988):31–45, 2015.

[7] Elke Hertig. Distribution of anopheles vectors and potential malaria transmission stability in europe and the mediterranean area under future climate change. *Parasites & Vectors*, 12(1):18, 2019.

[8] E. T. Ngarakana-Gwasira, C. P. Bhunu, M. Masocha, and E. Mashonjowa. Assessing the role of climate change in malaria transmission in africa. *Malar Res Treat*, 2016, 2016.

[9] IPCC — Intergovernmental Panel on Climate Change. IPCC — intergovernmental panel on climate change report - global warming of 1.5 ^{o}c, 2018.

[10] TDR. Global report for research on infectious diseases of poverty, 2012.

[11] UNICEF. Nearly 15,000 cases of malaria reported in areas of mozambique affected by cyclone idai – UNICEF, 2019.

[12] Kanta Kumari Rigaud, Alex de Sherbinin, Bryan Jones, Jonas Bergmann, Viviane Clement, Kayly Ober, Jacob Schewe, Susana Adamo, Brent McCusker, Silke Heuser, and Amelia Midgley. Groundswell : Preparing for internal climate migration, 2018.

[13] Harald Noedl, Youry Se, Kurt Schaecher, Bryan L. Smith, Duong Socheat, Mark M. Fukuda, and Artemisinin Resistance in Cambodia 1 (ARC1) Study Consortium. Evidence of artemisinin-resistant malaria in western cambodia. *N. Engl. J. Med.*, 359(24):2619–2620, 2008.

[14] R. L. Miller, S. Ikram, G. J. Armelagos, R. Walker, W. B. Harer, C. J. Shiff, D. Baggett, M. Carrigan, and S. M. Maret. Diagnosis of plasmodium falciparum infections in mummies using the rapid manual ParaSight-f test. *Trans. R. Soc. Trop. Med. Hyg.*, 88(1):31–32, 1994.

[15] Kenneth J. Arrow, Claire Panosian, and Hellen Gelband. *A Brief History of Malaria*. National Academies Press (US), 2004. Publication Title: Saving Lives, Buying Time: Economics of Malaria Drugs in an Age of Resistance.

[16] T. Harinasuta, P. Suntharasamai, and C. Viravan. Chloroquine-resistant falciparum malaria in thailand. *Lancet*, 2(7414):657–660, 1965.

[17] D. V. Moore and J. E. Lanier. Observations on two plasmodium falciparum infections with an abnormal response to chloroquine. *Am. J. Trop. Med. Hyg.*, 10:5–9, 1961.

[18] Terry Grimmond, K Donovan, and Ian Riley. Chloroquine resistant malaria in papua new guinea. *Papua and New Guinea medical journal*, 19:184–5, 10 1976.

[19] Ambrose O. Talisuna, Peter Bloland, and Umberto D'Alessandro. History, dynamics, and public health importance of malaria parasite resistance. *Clin. Microbiol. Rev.*, 17(1):235–254, 2004.

[20] Natalie Slivinski. Are we headed for a new era of malaria drug resistance?, 2019. Library Catalog: www.the-scientist.com.

[21] D. L. Klayman. Qinghaosu (artemisinin): an antimalarial drug from china. *Science*, 228(4703):1049–1055, 1985.

[22] Xin-zhuan Su and Louis H. Miller. The discovery of artemisinin and nobel prize in physiology or medicine. *Sci China Life Sci*, 58(11):1175–1179, 2015.

[23] WHO. Guidelines for the treatment of malaria. third edition, 2015. ISBN: 9789241549127 Publisher: World Health Organization.

[24] Aline Uwimana, Eric Legrand, Barbara H. Stokes, Jean-Louis Mangala Ndikumana, Marian Warsame, Noella Umulisa, Daniel Ngamije, Tharcisse Munyaneza, Jean-Baptiste Mazarati, Kaendi Munguti, Pascal Campagne, Alexis Criscuolo, Frédéric Ariey, Monique Murindahabi, Pascal Ringwald, David A. Fidock, Aimable Mbituyumuremyi, and Didier Menard. Emergence and clonal expansion of in vitro artemisinin-resistant plasmodium falciparum kelch13 r561h mutant parasites in rwanda. *Nature Medicine*, pages 1–7, 2020. Publisher: Nature Publishing Group.

[25] Friedrich Frischknecht, Patricia Baldacci, Béatrice Martin, Christophe Zimmer, Sabine Thiberge, Jean-Christophe Olivo-Marin, Spencer L. Shorte, and Robert Ménard. Imaging movement of malaria parasites during transmission by anopheles mosquitoes. *Cellular Microbiology*, 6(7):687–694, 2004. _eprint: https://onlinelibrary.wiley.com/doi/pdf/10.1111/j.1462-5822.2004.00395.x.

[26] Miguel Prudêncio, Ana Rodriguez, and Maria M. Mota. The silent path to thousands of merozoites: the plasmodium liver stage. *Nat. Rev. Microbiol.*, 4(11):849–856, 2006.

[27] Greta E. Weiss, Paul R. Gilson, Tana Taechalertpaisarn, Wai-Hong Tham, Nienke W. M. de Jong, Katherine L. Harvey, Freya J. I. Fowkes, Paul N. Barlow, Julian C. Rayner, Gavin J. Wright, Alan F. Cowman, and Brendan S. Crabb. Revealing the sequence and resulting cellular morphology of receptor-ligand interactions during plasmodium falciparum invasion of erythrocytes. *PLOS Pathogens*, 11(2):e1004670, 2015.

[28] Joachim M. Matz, Josh R. Beck, and Michael J. Blackman. The parasitophorous vacuole of the blood-stage malaria parasite. *Nat. Rev. Microbiol.*, 18(7):379–391, 2020.

[29] L. H. Bannister, J. M. Hopkins, R. E. Fowler, S. Krishna, and G. H. Mitchell. A brief illustrated guide to the ultrastructure of plasmodium falciparum asexual blood stages. *Parasitol. Today (Regul. Ed.)*, 16(10):427–433, 2000.

[30] Justin A. Boddey and Alan F. Cowman. Plasmodium nesting: remaking the erythrocyte from the inside out. *Annu. Rev. Microbiol.*, 67:243–269, 2013.

[31] K. Kirk. Membrane transport in the malaria-infected erythrocyte. *Physiol. Rev.*, 81(2):495–537, 2001.

[32] Lorena M. Coronado, Christopher T. Nadovich, and Carmenza Spadafora. Malarial hemozoin: from target to tool. *Biochim. Biophys. Acta*, 1840(6):2032–2041, 2014.

[33] Rachel M. Rudlaff, Stephan Kraemer, Jeffrey Marshman, and Jeffrey D. Dvorin. Three-dimensional ultrastructure of plasmodium falciparum throughout cytokinesis. *PLOS Pathogens*, 16(6):e1008587, 2020. Publisher: Public Library of Science.

[34] Noëlie Béré Henry, Samuel Sindié Sermé, Giulia Siciliano, Salif Sombié, Amidou Diarra, N'fale Sagnon, Alfred S. Traoré, Sodiomon Bienvenu Sirima, Issiaka Soulama,

and Pietro Alano. Biology of plasmodium falciparum gametocyte sex ratio and implications in malaria parasite transmission. *Malar J*, 18(1):70, 2019.

[35] Alan F. Cowman, Julie Healer, Danushka Marapana, and Kevin Marsh. Malaria: Biology and disease. *Cell*, 167(3):610–624, 2016.

[36] Walter R. J. Taylor, Josh Hanson, Gareth D. H. Turner, Nicholas J. White, and Arjen M. Dondorp. Respiratory manifestations of malaria. *Chest*, 142(2):492–505, 2012.

[37] Ramesh Subramani, Katharina Quadt, Anine E. Jeppesen, Casper Hempel, Jens Emil Vang Petersen, Tue Hassenkam, Lars Hviid, and Lea Barfod. Plasmodium falciparum-infected erythrocyte knob density is linked to the PfEMP1 variant expressed. *mBio*, 6(5), 2015.

[38] Joseph D. Smith, J. Alexandra Rowe, Matthew K. Higgins, and Thomas Lavstsen. Malaria's deadly grip: cytoadhesion of plasmodium falciparum-infected erythrocytes. *Cell. Microbiol.*, 15(12):1976–1983, 2013.

[39] P H David, M Hommel, L H Miller, I J Udeinya, and L D Oligino. Parasite sequestration in plasmodium falciparum malaria: spleen and antibody modulation of cytoadherence of infected erythrocytes. *Proc Natl Acad Sci U S A*, 80(16):5075–5079, 1983.

[40] Xue Yan Yam, Makhtar Niang, Kripa Gopal Madnani, and Peter R. Preiser. Three is a crowd – new insights into rosetting in plasmodium falciparum. *Trends in Parasitology*, 33(4):309–320, 2017.

[41] Beatrice Autino, Yolanda Corbett, Francesco Castelli, and Donatella Taramelli. Pathogenesis of malaria in tissues and blood. *Mediterr J Hematol Infect Dis*, 4(1), 2012.

[42] Laurent Rénia, Shanshan Wu Howland, Carla Claser, Anne Charlotte Gruner, Rossarin Suwanarusk, Teck Hui Teo, Bruce Russell, and Lisa F. P. Ng. Cerebral malaria: mysteries at the blood-brain barrier. *Virulence*, 3(2):193–201, 2012.

[43] Nicholas J. White. Anaemia and malaria. *Malaria Journal*, 17(1):371, 2018.

[44] WHO. Haemoglobin concentrations for the diagnosis of anaemia and assessment of severity, 2011. Library Catalog: www.who.int Publisher: World Health Organization.

[45] Nicholas M. Douglas, Daniel A. Lampah, Enny Kenangalem, Julie A. Simpson, Jeanne R. Poespoprodjo, Paulus Sugiarto, Nicholas M. Anstey, and Ric N. Price. Major burden of severe anemia from non-falciparum malaria species in southern papua: A hospital-based surveillance study. *PLoS Med*, 10(12), 2013.

[46] R. E. Phillips, S. Looareesuwan, D. A. Warrell, S. H. Lee, J. Karbwang, M. J. Warrell, N. J. White, C. Swasdichai, and D. J. Weatherall. The importance of anaemia in cerebral and uncomplicated falciparum malaria: role of complications, dyserythropoiesis and iron sequestration. *Q. J. Med.*, 58(227):305–323, 1986.

[47] Vrushali A. Pathak and Kanjaksha Ghosh. Erythropoiesis in malaria infections and factors modifying the erythropoietic response. *Anemia*, 2016:e9310905, 2016.

[48] G. N. Jakeman, A. Saul, W. L. Hogarth, and W. E. Collins. Anaemia of acute malaria infections in non-immune patients primarily results from destruction of uninfected erythrocytes. *Parasitology*, 119 (Pt 2):127–133, 1999.

[49] Paulo R. R. Totino, Cláudio T. Daniel-Ribeiro, and Maria de Fátima Ferreira-da Cruz. Evidencing the role of erythrocytic apoptosis in malarial anemia. *Front Cell Infect Microbiol*, 6, 2016.

[50] Krystal J. Evans, Diana S. Hansen, Nico van Rooijen, Lynn A. Buckingham, and Louis Schofield. Severe malarial anemia of low parasite burden in rodent models results from accelerated clearance of uninfected erythrocytes. *Blood*, 107(3):1192–1199, 2006.

[51] Luis L. Fonseca, Harnel S. Alezi, Alberto Moreno, John W. Barnwell, Mary R. Galinski, and Eberhard O. Voit. Quantifying the removal of red blood cells in macaca mulatta during a plasmodium coatneyi infection. *Malaria Journal*, 15(1):410, 2016.

[52] Igor V. Pivkin, Zhangli Peng, George E. Karniadakis, Pierre A. Buffet, Ming Dao, and Subra Suresh. Biomechanics of red blood cells in human spleen and consequences for physiology and disease. *PNAS*, 113(28):7804–7809, 2016. Publisher: National Academy of Sciences Section: Biological Sciences.

[53] Hernando A. del Portillo, Mireia Ferrer, Thibaut Brugat, Lorena Martin-Jaular, Jean Langhorne, and Marcus V. G. Lacerda. The role of the spleen in malaria. *Cellular Microbiology*, 14(3):343–355, 2012. _eprint: https://onlinelibrary.wiley.com/doi/pdf/10.1111/j.1462-5822.2011.01741.x.

[54] Pierre A. Buffet, Innocent Safeukui, Guillaume Deplaine, Valentine Brousse, Virginie Prendki, Marc Thellier, Gareth D. Turner, and Odile Mercereau-Puijalon. The pathogenesis of plasmodium falciparum malaria in humans: insights from splenic physiology. *Blood*, 117(2):381–392, 2011.

[55] S. Looareesuwan, M. Ho, Y. Wattanagoon, N. J. White, D. A. Warrell, D. Bunnag, T. Harinasuta, and D. J. Wyler. Dynamic alteration in splenic function during acute falciparum malaria. *N. Engl. J. Med.*, 317(11):675–679, 1987.

[56] Sornchai Looareesuwan, Timothy M. E. Davis, Sasithon Pukrittayakamee, Wichai Supanaranond, Varunee Desakorn, Kamolrat Silamut, Sanjeev Krishna, Sanga Boonamrung, and Nicholas J. White. Erythrocyte survival in severe falciparum malaria. *Acta Tropica*, 48(4):263–270, 1991.

[57] Simon Kotlyar, Julius Nteziyaremye, Peter Olupot-Olupot, Samuel O. Akech, Christopher L. Moore, and Kathryn Maitland. Spleen volume and clinical disease manifestations of severe plasmodium falciparum malaria in african children. *Trans R Soc Trop Med Hyg*, 108(5):283–289, 2014.

[58] S. Majid Hosseini and James J. Feng. How malaria parasites reduce the deformability of infected red blood cells. *Biophys J*, 103(1):1–10, 2012.

[59] Arjen M. Dondorp, Brian Angus, Kesinee Chotivanich, Kamolrat Silamut, Ronnatrai Ruangveerayuth, Max R. Hardeman, Piet A. Kager, J. Vreeken, and Nicholas J. White. Red blood cell deformability as a predictor of anemia in severe falciparum malaria. *The American journal of tropical medicine and hygiene*, 1999.

[60] Sha Huang, Anburaj Amaladoss, Min Liu, Huichao Chen, Rou Zhang, Peter R. Preiser, Ming Dao, and Jongyoon Han. In vivo splenic clearance correlates with in vitro deformability of red blood cells from plasmodium yoelii-infected mice. *Infect Immun*, 82(6):2532–2541, 2014.

[61] Apurba Paul, Rani Pallavi, Utpal S. Tatu, and Vasant Natarajan. The bystander effect in optically trapped red blood cells due to plasmodium falciparum infection. *Trans. R. Soc. Trop. Med. Hyg.*, 107(4):220–223, 2013.

[62] Apurba Paul, Ghania Ramdani, Utpal Tatu, Gordon Langsley, and Vasant Natarajan. Studying the rigidity of red blood cells induced by plasmodium falciparum infection. *Sci Rep*, 9(1):1–4, 2019. Number: 1 Publisher: Nature Publishing Group.

[63] Fausta Omodeo-Salè, Anna Motti, Arjen Dondorp, Nicholas J. White, and Donatella Taramelli. Destabilisation and subsequent lysis of human erythrocytes induced by plasmodium falciparum haem products. *Eur. J. Haematol.*, 74(4):324–332, 2005.

[64] Corinne Layez, Paulo Nogueira, Valery Combes, Fabio T. M. Costa, Irène Juhan-Vague, Luiz H. Pereira da Silva, and Jürg Gysin. Plasmodium falciparum rhoptry protein RSP2 triggers destruction of the erythroid lineage. *Blood*, 106(10):3632–3638, 2005.

[65] Prasad Dasari, Anja Fries, Sophia D. Heber, Abdulgabar Salama, Igor-Wolfgang Blau, Klaus Lingelbach, Sebastian Chakrit Bhakdi, Rachanee Udomsangpetch, Michael Torzewski, Karina Reiss, and Sucharit Bhakdi. Malarial anemia: digestive vacuole of plasmodium falciparum mediates complement deposition on bystander cells to provoke hemophagocytosis. *Med Microbiol Immunol*, 203(6):383–393, 2014.

[66] Antonella Pantaleo, Giuliana Giribaldi, Franca Mannu, Paolo Arese, and Franco Turrini. Naturally occurring anti-band 3 antibodies and red blood cell removal under physiological and pathological conditions. *Autoimmunity Reviews*, 7(6):457–462, 2008.

[67] John N. Waitumbi, Malachi O. Opollo, Richard O. Muga, Ambrose O. Misore, and José A. Stoute. Red cell surface changes and erythrophagocytosis in children with severe plasmodium falciparum anemia. *Blood*, 95(4):1481–1486, 2000. Publisher: American Society of Hematology.

[68] Luiza Carvalho Mourão, Rodrigo de Paula Baptista, Zélia Barbosa de Almeida, Priscila Grynberg, Maíra Mazzoni Pucci, Thiago Castro-Gomes, Cor Jesus Fernandes Fontes, Sumit Rathore, Yagya D. Sharma, Rosiane A. da Silva-Pereira, Marcelo Porto Bemquerer, and Érika Martins Braga. Anti-band 3 and anti-spectrin antibodies are increased in plasmodium vivax infection and are associated with anemia. *Scientific Reports*, 8(1):8762, 2018. Number: 1 Publisher: Nature Publishing Group.

[69] Cristina Fernandez-Arias, Juan Rivera-Correa, Julio Gallego-Delgado, Rachel Rudlaff, Clemente Fernandez, Camille Roussel, Anton Götz, Sandra Gonzalez, Akshaya Mohanty, Sanjib Mohanty, Samuel Wassmer, Pierre Buffet, Papa Alioune Ndour, and Ana Rodriguez. Anti-self phosphatidylserine antibodies recognize uninfected erythrocytes promoting malarial anemia. *Cell Host Microbe*, 19(2):194–203, 2016.

[70] Bridget E. Barber, Matthew J. Grigg, Kim Piera, Fiona H. Amante, Timothy William, Michelle J. Boyle, Gabriela Minigo, Arjen M. Dondorp, James S. McCarthy, and Nicholas M. Anstey. Antiphosphatidylserine immunoglobulin m and immunoglobulin g antibodies are higher in vivax than falciparum malaria, and associated with early anemia in both species. *J. Infect. Dis.*, 220(9):1435–1443, 2019.

[71] Coralie Boulet, Christian D. Doerig, and Teresa G. Carvalho. Manipulating eryptosis of human red blood cells: A novel antimalarial strategy? *Front Cell Infect Microbiol*, 8, 2018.

[72] Elisabeth Lang and Florian Lang. Mechanisms and pathophysiological significance of eryptosis, the suicidal erythrocyte death. *Semin. Cell Dev. Biol.*, 39:35–42, 2015.

[73] Katsumori Segawa and Shigekazu Nagata. An apoptotic 'eat me' signal: Phosphatidylserine exposure. *Trends in Cell Biology*, 25(11):639–650, 2015.

[74] R. S. Schwartz, J. A. Olson, C. Raventos-Suarez, M. Yee, R. H. Heath, B. Lubin, and R. L. Nagel. Altered plasma membrane phospholipid organization in plasmodium falciparum-infected human erythrocytes. *Blood*, 69(2):401–407, 1987.

[75] Ioana Alesutan, Diwakar Bobbala, Syed M. Qadri, Adriana Estremera, Michael Föller, and Florian Lang. Beneficial effect of aurothiomalate on murine malaria. *Malar. J.*, 9:118, 2010.

[76] Saisudha Koka, Camelia Lang, Olivier M. Niemoeller, Krishna M. Boini, Jan P. Nicolay, Stephan M. Huber, and Florian Lang. Influence of NO synthase inhibitor l-NAME on parasitemia and survival of plasmodium berghei infected mice. *Cell. Physiol. Biochem.*, 21(5):481–488, 2008.

[77] Paulo Renato Rivas Totino, Raquel Alves Pinna, Ana Cecilia Amado Xavier De-Oliveira, Dalma Maria Banic, Cláudio Tadeu Daniel-Ribeiro, and Maria de Fátima Ferreira-da Cruz. Apoptosis of non-parasitised red blood cells in plasmodium yoelii malaria. *Mem Inst Oswaldo Cruz*, 108(6):686–690, 2013.

[78] Paulo Renato Rivas Totino, Aline das Dores Magalhães, Eliana Brasil Alves, Monica Regina Farias Costa, Marcus Vinícius Guimarães de Lacerda, Cláudio Tadeu Daniel-Ribeiro, and Maria de Fátima Ferreira-da Cruz. Plasmodium falciparum, but not p. vivax, can induce erythrocytic apoptosis. *Parasites & Vectors*, 7:484, 2014.

[79] Saisudha Koka, Stephan M. Huber, Krishna M. Boini, Camelia Lang, Michael Föller, and Florian Lang. Lead decreases parasitemia and enhances survival of plasmodium berghei-infected mice. *Biochem. Biophys. Res. Commun.*, 363(3):484–489, 2007.

[80] Kovit Pattanapanyasat, Panudda Sratongno, Pattamawan Chimma, Supapart Chitjamnongchai, Korakot Polsrila, and Kesinee Chotivanich. Febrile temperature but not proinflammatory cytokines promotes phosphatidylserine expression on plasmodium falciparum malaria-infected red blood cells during parasite maturation. *Cytometry Part A*, 77A(6):515–523, 2010. _eprint: https://onlinelibrary.wiley.com/doi/pdf/10.1002/cyto.a.20879.

[81] Kathrin Wennicke, Françoise Debierre-Grockiego, Dominic Wichmann, Norbert W. Brattig, Sabine Pankuweit, Bernhard Maisch, Ralph T. Schwarz, and Volker Ruppert. Glycosylphosphatidylinositol-induced cardiac myocyte death might contribute to the fatal outcome of plasmodium falciparum malaria. *Apoptosis*, 13(7):857–866, 2008.

[82] Abigail A. Lamikanra, Michel Theron, Taco W. A. Kooij, and David J. Roberts. Hemozoin (malarial pigment) directly promotes apoptosis of erythroid precursors. *PLOS ONE*, 4(12):e8446, 2009. Publisher: Public Library of Science.

[83] Nana O. Wilson, Ming-Bo Huang, Winston Anderson, Vincent Bond, Michael Powell, Winston E. Thompson, Henry B. Armah, Andrew A. Adjei, Richard Gyasi, Yao Tettey, and Jonathan K. Stiles. Soluble factors from plasmodium falciparum-infected erythrocytes induce apoptosis in human brain vascular endothelial and neuroglia cells. *Mol Biochem Parasitol*, 162(2):172–176, 2008.

[84] S. N. Balaji and Vishal Trivedi. Extracellular methemoglobin primes red blood cell aggregation in malaria: an in vitro mechanistic study. *FEBS Lett.*, 587(4):350–357, 2013.

[85] Clotilde Théry, Kenneth W. Witwer, Elena Aikawa, Maria Jose Alcaraz, Johnathon D. Anderson, Ramaroson Andriantsitohaina, Anna Antoniou, Tanina Arab, Fabienne Archer, Georgia K. Atkin-Smith, D. Craig Ayre, Jean-Marie Bach, Daniel Bachurski, Hossein Baharvand, Leonora Balaj, Shawn Baldacchino, Natalie N. Bauer, Amy A. Baxter, Mary Bebawy, Carla Beckham, Apolonija Bedina Zavec, Abderrahim Benmoussa, Anna C. Berardi, Paolo Bergese, Ewa Bielska, Cherie Blenkiron, Sylwia

Bobis-Wozowicz, Eric Boilard, Wilfrid Boireau, Antonella Bongiovanni, Francesc E. Borràs, Steffi Bosch, Chantal M. Boulanger, Xandra Breakefield, Andrew M. Breglio, Meadhbh Á Brennan, David R. Brigstock, Alain Brisson, Marike LD Broekman, Jacqueline F. Bromberg, Paulina Bryl-Górecka, Shilpa Buch, Amy H. Buck, Dylan Burger, Sara Busatto, Dominik Buschmann, Benedetta Bussolati, Edit I. Buzás, James Bryan Byrd, Giovanni Camussi, David RF Carter, Sarah Caruso, Lawrence W. Chamley, Yu-Ting Chang, Chihchen Chen, Shuai Chen, Lesley Cheng, Andrew R. Chin, Aled Clayton, Stefano P. Clerici, Alex Cocks, Emanuele Cocucci, Robert J. Coffey, Anabela Cordeiro-da Silva, Yvonne Couch, Frank AW Coumans, Beth Coyle, Rossella Crescitelli, Miria Ferreira Criado, Crislyn D'Souza-Schorey, Saumya Das, Amrita Datta Chaudhuri, Paola de Candia, Eliezer F. De Santana Junior, Olivier De Wever, Hernando A. del Portillo, Tanguy Demaret, Sarah Deville, Andrew Devitt, Bert Dhondt, Dolores Di Vizio, Lothar C. Dieterich, Vincenza Dolo, Ana Paula Dominguez Rubio, Massimo Dominici, Mauricio R. Dourado, Tom AP Driedonks, Filipe V. Duarte, Heather M. Duncan, Ramon M. Eichenberger, Karin Ekström, Samir EL Andaloussi, Celine Elie-Caille, Uta Erdbrügger, Juan M. Falcón-Pérez, Farah Fatima, Jason E. Fish, Miguel Flores-Bellver, András Försönits, Annie Frelet-Barrand, Fabia Fricke, Gregor Fuhrmann, Susanne Gabrielsson, Ana Gámez-Valero, Chris Gardiner, Kathrin Gärtner, Raphael Gaudin, Yong Song Gho, Bernd Giebel, Caroline Gilbert, Mario Gimona, Ilaria Giusti, Deborah CI Goberdhan, André Görgens, Sharon M. Gorski, David W. Greening, Julia Christina Gross, Alice Gualerzi, Gopal N. Gupta, Dakota Gustafson, Aase Handberg, Reka A. Haraszti, Paul Harrison, Hargita Hegyesi, An Hendrix, Andrew F. Hill, Fred H. Hochberg, Karl F. Hoffmann, Beth Holder, Harry Holthofer, Baharak Hosseinkhani, Guoku Hu, Yiyao Huang, Veronica Huber, Stuart Hunt, Ahmed Gamal-Eldin Ibrahim, Tsuneya Ikezu, Jameel M. Inal, Mustafa Isin, Alena Ivanova, Hannah K. Jackson, Soren Jacobsen, Steven M. Jay, Muthuvel Jayachandran, Guido Jenster, Lanzhou Jiang, Suzanne M. Johnson, Jennifer C. Jones, Ambrose Jong, Tijana Jovanovic-Talisman, Stephanie Jung, Raghu Kalluri, Shin-ichi Kano, Sukhbir Kaur, Yumi Kawamura, Evan T. Keller, Delaram Khamari, Elena Khomyakova, Anastasia Khvorova, Peter Kierulf, Kwang Pyo Kim, Thomas Kislinger, Mikael Klingeborn, David J. Klinke II, Miroslaw Kornek, Maja M. Kosanović, Árpád Ferenc Kovács, Eva-Maria Krämer-Albers, Susanne Krasemann, Mirja Krause, Igor V. Kurochkin, Gina D. Kusuma, Sören Kuypers, Saara Laitinen, Scott M. Langevin, Lucia R. Languino, Joanne Lannigan, Cecilia Lässer, Louise C. Laurent, Gregory Lavieu, Elisa Lázaro-Ibáñez, Soazig Le Lay, Myung-Shin Lee, Yi Xin Fiona Lee, Debora S. Lemos, Metka Lenassi, Aleksandra Leszczynska, Isaac TS Li, Ke Liao, Sten F. Libregts, Erzsebet Ligeti, Rebecca Lim, Sai Kiang Lim, Aija Linē, Karen Linnemannstöns, Alicia Llorente, Catherine A. Lombard, Magdalena J. Lorenowicz, Ákos M. Lörincz, Jan Lötvall, Jason Lovett, Michelle C. Lowry, Xavier Loyer, Quan Lu, Barbara Lukomska, Taral R. Lunavat, Sybren LN Maas, Harmeet Malhi, Antonio Marcilla, Jacopo Mariani, Javier

Mariscal, Elena S. Martens-Uzunova, Lorena Martin-Jaular, M. Carmen Martinez, Vilma Regina Martins, Mathilde Mathieu, Suresh Mathivanan, Marco Maugeri, Lynda K. McGinnis, Mark J. McVey, David G. Meckes Jr, Katie L. Meehan, Inge Mertens, Valentina R. Minciacchi, Andreas Möller, Malene Møller Jørgensen, Aizea Morales-Kastresana, Jess Morhayim, François Mullier, Maurizio Muraca, Luca Musante, Veronika Mussack, Dillon C. Muth, Kathryn H. Myburgh, Tanbir Najrana, Muhammad Nawaz, Irina Nazarenko, Peter Nejsum, Christian Neri, Tommaso Neri, Rienk Nieuwland, Leonardo Nimrichter, John P. Nolan, Esther NM Nolte-'t Hoen, Nicole Noren Hooten, Lorraine O'Driscoll, Tina O'Grady, Ana O'Loghlen, Takahiro Ochiya, Martin Olivier, Alberto Ortiz, Luis A. Ortiz, Xabier Osteikoetxea, Ole Østergaard, Matias Ostrowski, Jaesung Park, D. Michiel Pegtel, Hector Peinado, Francesca Perut, Michael W. Pfaffl, Donald G. Phinney, Bartijn CH Pieters, Ryan C. Pink, David S. Pisetsky, Elke Pogge von Strandmann, Iva Polakovicova, Ivan KH Poon, Bonita H. Powell, Ilaria Prada, Lynn Pulliam, Peter Quesenberry, Annalisa Radeghieri, Robert L. Raffai, Stefania Raimondo, Janusz Rak, Marcel I. Ramirez, Graça Raposo, Morsi S. Rayyan, Neta Regev-Rudzki, Franz L. Ricklefs, Paul D. Robbins, David D. Roberts, Silvia C. Rodrigues, Eva Rohde, Sophie Rome, Kasper MA Rouschop, Aurelia Rughetti, Ashley E. Russell, Paula Saá, Susmita Sahoo, Edison Salas-Huenuleo, Catherine Sánchez, Julie A. Saugstad, Meike J. Saul, Raymond M. Schiffelers, Raphael Schneider, Tine Hiorth Schøyen, Aaron Scott, Eriomina Shahaj, Shivani Sharma, Olga Shatnyeva, Faezeh Shekari, Ganesh Vilas Shelke, Ashok K. Shetty, Kiyotaka Shiba, Pia R.-M. Siljander, Andreia M. Silva, Agata Skowronek, Orman L. Snyder II, Rodrigo Pedro Soares, Barbara W. Sódar, Carolina Soekmadji, Javier Sotillo, Philip D. Stahl, Willem Stoorvogel, Shannon L. Stott, Erwin F. Strasser, Simon Swift, Hidetoshi Tahara, Muneesh Tewari, Kate Timms, Swasti Tiwari, Rochelle Tixeira, Mercedes Tkach, Wei Seong Toh, Richard Tomasini, Ana Claudia Torrecilhas, Juan Pablo Tosar, Vasilis Toxavidis, Lorena Urbanelli, Pieter Vader, Bas WM van Balkom, Susanne G. van der Grein, Jan Van Deun, Martijn JC van Herwijnen, Kendall Van Keuren-Jensen, Guillaume van Niel, Martin E. van Royen, Andre J. van Wijnen, M. Helena Vasconcelos, Ivan J. Vechetti Jr, Tiago D. Veit, Laura J. Vella, Émilie Velot, Frederik J. Verweij, Beate Vestad, Jose L. Viñas, Tamás Visnovitz, Krisztina V. Vukman, Jessica Wahlgren, Dionysios C. Watson, Marca HM Wauben, Alissa Weaver, Jason P. Webber, Viktoria Weber, Ann M. Wehman, Daniel J. Weiss, Joshua A. Welsh, Sebastian Wendt, Asa M. Wheelock, Zoltán Wiener, Leonie Witte, Joy Wolfram, Angeliki Xagorari, Patricia Xander, Jing Xu, Xiaomei Yan, María Yáñez-Mó, Hang Yin, Yuana Yuana, Valentina Zappulli, Jana Zarubova, Vytautas Žėkas, Jian-ye Zhang, Zezhou Zhao, Lei Zheng, Alexander R. Zheutlin, Antje M. Zickler, Pascale Zimmermann, Angela M. Zivkovic, Davide Zocco, and Ewa K. Zuba-Surma. Minimal information for studies of extracellular vesicles 2018 (MISEV2018): a position statement of the international society for extracellular vesicles and update of the MISEV2014 guidelines. *Journal*

of Extracellular Vesicles, 7(1):1535750, 2018. Publisher: Taylor & Francis _eprint: https://doi.org/10.1080/20013078.2018.1535750.

[86] Natalia Guimaraes Sampaio, Lesley Cheng, and Emily M. Eriksson. The role of extracellular vesicles in malaria biology and pathogenesis. *Malar J*, 16, 2017.

[87] Duangdao Nantakomol, Arjen M. Dondorp, Srivicha Krudsood, Rachanee Udomsangpetch, Kovit Pattanapanyasat, Valery Combes, Georges E. Grau, Nicholas J. White, Parnpen Viriyavejakul, Nicholas P. J. Day, and Kesinee Chotivanich. Circulating red cell–derived microparticles in human malaria. *J Infect Dis*, 203(5):700–706, 2011. Publisher: Oxford Academic.

[88] Pierre-Yves Mantel, Anh N. Hoang, Ilana Goldowitz, Daria Potashnikova, Bashar Hamza, Ivan Vorobjev, Ionita Ghiran, Mehmet Toner, Daniel Irimia, Alexander R. Ivanov, Natasha Barteneva, and Matthias Marti. Malaria infected erythrocyte-derived microvesicles mediate cellular communication within the parasite population and with the host immune system. *Cell Host Microbe*, 13(5):521–534, 2013.

[89] Neta Regev-Rudzki, Danny W. Wilson, Teresa G. Carvalho, Xavier Sisquella, Bradley M. Coleman, Melanie Rug, Dejan Bursac, Fiona Angrisano, Michelle Gee, Andrew F. Hill, Jake Baum, and Alan F. Cowman. Cell-cell communication between malaria-infected red blood cells via exosome-like vesicles. *Cell*, 153(5):1120–1133, 2013.

[90] Pierre-Yves Mantel, Daisy Hjelmqvist, Michael Walch, Solange Kharoubi-Hess, Sandra Nilsson, Deepali Ravel, Marina Ribeiro, Christof Grüring, Siyuan Ma, Prasad Padmanabhan, Alexander Trachtenberg, Johan Ankarklev, Nicolas M. Brancucci, Curtis Huttenhower, Manoj T. Duraisingh, Ionita Ghiran, Winston P. Kuo, Luis Filgueira, Roberta Martinelli, and Matthias Marti. Infected erythrocyte-derived extracellular vesicles alter vascular function via regulatory ago2-miRNA complexes in malaria. *Nature Communications*, 7:12727, 2016.

[91] Livia Neves Borgheti-Cardoso, Sander A. A. Kooijmans, Lucía Gutiérrez Chamorro, Arnau Biosca, Elena Lantero, Miriam Ramírez, Yunuen Avalos-Padilla, Isabel Crespo, Irene Fernández, Carmen Fernandez-Becerra, Hernando A. del Portillo, and Xavier Fernàndez-Busquets. Extracellular vesicles derived from plasmodium-infected and non-infected red blood cells as targeted drug delivery vehicles. *International Journal of Pharmaceutics*, 587:119627, 2020.

[92] Elya Dekel, Dana Yaffe, Irit Rosenhek-Goldian, Tamar Ziv, Xavier Sisquella, Matthew A. Pimentel, Thomas Nebl, Eugene Kapp, Yael Ohana-Daniel, Paula Abou-Karam, Shimrit Malihi, Tal Block Temin, Debakshi Mullick, Or-Yam Revach, Ariel Rudik, Nir Gov, Ido Azuri, Ziv Porat, Teresa Carvalho, Gili Ben-Nissan, Sidney R. Cohen, Michal Sharon, and Neta Regev-Rudzki. [under review] 20s proteasomes exported by the malaria parasite promote its growth. 2020.

[93] Evelyn J Strauss. Intracellular pathogens: A virus joins the movement. *Current Biology*, 6(5):504–507, 1996.

[94] Pascale Cossart and Craig R. Roy. Manipulation of host membrane machinery by bacterial pathogens. *Curr Opin Cell Biol*, 22(4):547–554, 2010.

[95] Debopam Ghosh and Jason S. Stumhofer. Do you see what i see: Recognition of protozoan parasites by toll-like receptors. *Curr Immunol Rev*, 9(3):129–140, 2013.

[96] D. Channe Gowda and Xianzhu Wu. Parasite recognition and signaling mechanisms in innate immune responses to malaria. *Front Immunol*, 9, 2018.

[97] Hiroshi Ashida, Hitomi Mimuro, Michinaga Ogawa, Taira Kobayashi, Takahito Sanada, Minsoo Kim, and Chihiro Sasakawa. Cell death and infection: A double-edged sword for host and pathogen survival. *J Cell Biol*, 195(6):931–942, 2011.

[98] Stewart Hay and George Kannourakis. A time to kill: viral manipulation of the cell death program. *J. Gen. Virol.*, 83:1547–1564, 2002.

[99] Eric R. James and Douglas R. Green. Manipulation of apoptosis in the host–parasite interaction. *Trends in Parasitology*, 20(6):280–287, 2004.

[100] Antje Flieger, Freddy Frischknecht, Georg Häcker, Mathias W. Hornef, and Gabriele Pradel. Pathways of host cell exit by intracellular pathogens. *Microb Cell*, 5(12):525–544.

[101] Peter E. Czabotar, Guillaume Lessene, Andreas Strasser, and Jerry M. Adams. Control of apoptosis by the BCL-2 protein family: implications for physiology and therapy. *Nature Reviews Molecular Cell Biology*, 15(1):49–63, 2014.

[102] Dana Westphal, Grant Dewson, Marie Menard, Paul Frederick, Sweta Iyer, Ray Bartolo, Leonie Gibson, Peter E. Czabotar, Brian J. Smith, Jerry M. Adams, and Ruth M. Kluck. Apoptotic pore formation is associated with in-plane insertion of bak or bax central helices into the mitochondrial outer membrane. *PNAS*, 111(39):E4076–E4085, 2014. Publisher: National Academy of Sciences Section: PNAS Plus.

[103] M. Enari, H. Sakahira, H. Yokoyama, K. Okawa, A. Iwamatsu, and S. Nagata. A caspase-activated DNase that degrades DNA during apoptosis, and its inhibitor ICAD. *Nature*, 391(6662):43–50, 1998.

[104] Debabrata Mandal, Veronique Baudin-Creuza, Asima Bhattacharyya, Shresh Pathak, Jean Delaunay, Manikuntala Kundu, and Joyoti Basu. Caspase 3-mediated proteolysis of the n-terminal cytoplasmic domain of the human erythroid anion exchanger 1 (band 3). *J. Biol. Chem.*, 278(52):52551–52558, 2003.

[105] Faraaz B. Chekeni, Michael R. Elliott, Joanna K. Sandilos, Scott F. Walk, Jason M. Kinchen, Eduardo R. Lazarowski, Allison J. Armstrong, Silvia Penuela, Dale W.

Laird, Guy S. Salvesen, Brant E. Isakson, Douglas A. Bayliss, and Kodi S. Ravichandran. Pannexin 1 channels mediate 'find-me' signal release and membrane permeability during apoptosis. *Nature*, 467(7317):863–867, 2010.

[106] A Kaushansky, P G Metzger, A N Douglass, S A Mikolajczak, V Lakshmanan, H S Kain, and S HI Kappe. Malaria parasite liver stages render host hepatocytes susceptible to mitochondria-initiated apoptosis. *Cell Death Dis*, 4(8):e762, 2013.

[107] Claudia van de Sand, Sebastian Horstmann, Anja Schmidt, Angelika Sturm, Stefanie Bolte, Andreas Krueger, Marc Lütgehetmann, Jörg-Matthias Pollok, Claude Libert, and Volker T. Heussler. The liver stage of plasmodium berghei inhibits host cell apoptosis. *Mol. Microbiol.*, 58(3):731–742, 2005.

[108] J.W. Baynes. Oxygen and life. *Medical Biochemistry*, pages 497–506, 2005.

[109] Shilpa M. Hattangadi and Harvey F. Lodish. Regulation of erythrocyte lifespan: do reactive oxygen species set the clock? *J. Clin. Invest.*, 117(8):2075–2077, 2007.

[110] Florian Lang, Majed Abed, Elisabeth Lang, and Michael Föller. Oxidative stress and suicidal erythrocyte death. *Antioxid. Redox Signal.*, 21(1):138–153, 2014.

[111] Barbara A. Klarl, Philipp A. Lang, Daniela S. Kempe, Olivier M. Niemoeller, Ahmad Akel, Malgorzata Sobiesiak, Kerstin Eisele, Marlis Podolski, Stephan M. Huber, Thomas Wieder, and Florian Lang. Protein kinase c mediates erythrocyte "programmed cell death" following glucose depletion. *American Journal of Physiology-Cell Physiology*, 290(1):C244–C253, 2006.

[112] D. Bratosin, J. Estaquier, F. Petit, D. Arnoult, B. Quatannens, J.-P. Tissier, C. Slomianny, C. Sartiaux, C. Alonso, J.-J. Huart, J. Montreuil, and J. C. Ameisen. Programmed cell death in mature erythrocytes: a model for investigating death effector pathways operating in the absence of mitochondria. *Cell Death and Differentiation*, 8(12):1143, 2001.

[113] Etheresia Pretorius, Jeanette N. du Plooy, and Janette Bester. A comprehensive review on eryptosis. *CPB*, 39(5):1977–2000, 2016.

[114] Elizabeth K. K. Glennon, Selasi Dankwa, Joseph D. Smith, and Alexis Kaushansky. Opportunities for host-targeted therapies for malaria. *Trends Parasitol*, 34(10):843–860, 2018.

[115] Benedito A. Carneiro and Wafik S. El-Deiry. Targeting apoptosis in cancer therapy. *Nature Reviews Clinical Oncology*, 17(7):395–417, 2020. Number: 7 Publisher: Nature Publishing Group.

[116] Rehmat Jan and Gul-e-Saba Chaudhry. Understanding apoptosis and apoptotic pathways targeted cancer therapeutics. *Adv Pharm Bull*, 9(2):205–218, 2019.

[117] Claire M. Pfeffer and Amareshwar T. K. Singh. Apoptosis: A target for anticancer therapy. *Int J Mol Sci*, 19(2), 2018.

[118] Natalie M. Niemi and Jeffrey P. MacKeigan. Mitochondrial phosphorylation in apoptosis: Flipping the death switch. *Antioxid Redox Signal*, 19(6):572–582, 2013.

[119] P. A. Gregoli and M. C. Bondurant. The roles of bcl-x(l) and apopain in the control of erythropoiesis by erythropoietin. *Blood*, 90(2):630–640, 1997.

[120] N. Motoyama, F. Wang, K. A. Roth, H. Sawa, K. Nakayama, K. Nakayama, I. Negishi, S. Senju, Q. Zhang, and S. Fujii. Massive cell death of immature hematopoietic cells and neurons in bcl-x-deficient mice. *Science*, 267(5203):1506–1510, 1995.

[121] Alex RD Delbridge, Brandon J. Aubrey, Craig Hyland, Jonathan P. Bernardini, Ladina Di Rago, Jean-Marc Garnier, Guillaume Lessene, Andreas Strasser, Warren S. Alexander, and Stephanie Grabow. The BH3-only proteins BIM and PUMA are not critical for the reticulocyte apoptosis caused by loss of the pro-survival protein BCL-XL. *Cell Death & Disease*, 8(7):e2914, 2017.

[122] Sehar Afreen, Sheila Bohler, Alexandra Müller, Eva-Maria Demmerath, Julia Miriam Weiss, Jonas Samuel Jutzi, Kristina Schachtrup, Mirjam Kunze, and Miriam Erlacher. BCL-XL expression is essential for human erythropoiesis and engraftment of hematopoietic stem cells. *Cell Death & Disease*, 11(1):1–15, 2020. Number: 1 Publisher: Nature Publishing Group.

[123] Kylie D. Mason, Marina R. Carpinelli, Jamie I. Fletcher, Janelle E. Collinge, Adrienne A. Hilton, Sarah Ellis, Priscilla N. Kelly, Paul G. Ekert, Donald Metcalf, Andrew W. Roberts, David C. S. Huang, and Benjamin T. Kile. Programmed anuclear cell death delimits platelet life span. *Cell*, 128(6):1173–1186, 2007.

[124] Florence Roux-Dalvai, Anne Gonzalez de Peredo, Carolina Simó, Luc Guerrier, David Bouyssié, Alberto Zanella, Attilio Citterio, Odile Burlet-Schiltz, Egisto Boschetti, Pier Giorgio Righetti, and Bernard Monsarrat. Extensive analysis of the cytoplasmic proteome of human erythrocytes using the peptide ligand library technology and advanced mass spectrometry. *Mol. Cell Proteomics*, 7(11):2254–2269, 2008.

[125] Melanie Walsh, Robert J. Lutz, Thomas G. Cotter, and Rosemary O'Connor. Erythrocyte survival is promoted by plasma and suppressed by a bak-derived BH3 peptide that interacts with membrane-associated bcl-XL. *Blood*, 99(9):3439–3448, 2002.

[126] Brenda Rocamonde, Auriane Carcone, Renaud Mahieux, and Hélène Dutartre. HTLV-1 infection of myeloid cells: from transmission to immune alterations. *Retrovirology*, 16(1):45, 2019.

[127] Kirsteen J. Campbell and Stephen W. G. Tait. Targeting BCL-2 regulated apoptosis in cancer. *Open Biol*, 8(5), 2018.

[128] Tilman Oltersdorf, Steven W. Elmore, Alexander R. Shoemaker, Robert C. Armstrong, David J. Augeri, Barbara A. Belli, Milan Bruncko, Thomas L. Deckwerth, Jurgen Dinges, Philip J. Hajduk, Mary K. Joseph, Shinichi Kitada, Stanley J. Korsmeyer, Aaron R. Kunzer, Anthony Letai, Chi Li, Michael J. Mitten, David G. Nettesheim, ShiChung Ng, Paul M. Nimmer, Jacqueline M. O'Connor, Anatol Oleksijew, Andrew M. Petros, John C. Reed, Wang Shen, Stephen K. Tahir, Craig B. Thompson, Kevin J. Tomaselli, Baole Wang, Michael D. Wendt, Haichao Zhang, Stephen W. Fesik, and Saul H. Rosenberg. An inhibitor of bcl-2 family proteins induces regression of solid tumours. *Nature*, 435(7042):677–681, 2005.

[129] Cheol-Min Park, Milan Bruncko, Jessica Adickes, Joy Bauch, Hong Ding, Aaron Kunzer, Kennan C. Marsh, Paul Nimmer, Alexander R. Shoemaker, Xiaohong Song, Stephen K. Tahir, Christin Tse, Xilu Wang, Michael D. Wendt, Xiufen Yang, Haichao Zhang, Stephen W. Fesik, Saul H. Rosenberg, and Steven W. Elmore. Discovery of an orally bioavailable small molecule inhibitor of prosurvival b-cell lymphoma 2 proteins. *J. Med. Chem.*, 51(21):6902–6915, 2008. Publisher: American Chemical Society.

[130] Leena Gandhi, D. Ross Camidge, Moacyr Ribeiro de Oliveira, Philip Bonomi, David Gandara, Divis Khaira, Christine L. Hann, Evelyn M. McKeegan, Elizabeth Litvinovich, Philip M. Hemken, Caroline Dive, Sari H. Enschede, Cathy Nolan, Yi-Lin Chiu, Todd Busman, Hao Xiong, Andrew P. Krivoshik, Rod Humerickhouse, Geoffrey I. Shapiro, and Charles M. Rudin. Phase i study of navitoclax (ABT-263), a novel bcl-2 family inhibitor, in patients with small-cell lung cancer and other solid tumors. *J. Clin. Oncol.*, 29(7):909–916, 2011.

[131] National Cancer Institute (NCI). An open label, two-part, phase ib/II study to investigate the safety, pharmacokinetics, pharmacodynamics, and clinical activity of the MEK inhibitor trametinib and the BCL2-family inhibitor navitoclax (ABT-263) in combination in subjects with KRAS or NRAS mutation-positive advanced solid tumors, 2020. submitted: March 4, 2014.

[132] Aksana Kaefer, Jianning Yang, Peter Noertersheuser, Sven Mensing, Rod Humerickhouse, Walid Awni, and Hao Xiong. Mechanism-based pharmacokinetic/pharmacodynamic meta-analysis of navitoclax (ABT-263) induced thrombocytopenia. *Cancer Chemother. Pharmacol.*, 74(3):593–602, 2014.

[133] Andrew J. Souers, Joel D. Leverson, Erwin R. Boghaert, Scott L. Ackler, Nathaniel D. Catron, Jun Chen, Brian D. Dayton, Hong Ding, Sari H. Enschede, Wayne J. Fairbrother, David C. S. Huang, Sarah G. Hymowitz, Sha Jin, Seong Lin Khaw, Peter J. Kovar, Lloyd T. Lam, Jackie Lee, Heather L. Maecker, Kennan C. Marsh, Kylie D. Mason, Michael J. Mitten, Paul M. Nimmer, Anatol Oleksijew, Chang H. Park, Cheol-Min Park, Darren C. Phillips, Andrew W. Roberts, Deepak Sampath, John F. Seymour, Morey L. Smith, Gerard M. Sullivan, Stephen K. Tahir, Chris Tse, Michael D. Wendt, Yu Xiao, John C. Xue, Haichao Zhang, Rod A. Humerickhouse,

Saul H. Rosenberg, and Steven W. Elmore. ABT-199, a potent and selective BCL-2 inhibitor, achieves antitumor activity while sparing platelets. *Nat Med*, 19(2):202–208, 2013.

[134] Andrew W. Roberts, Matthew S. Davids, John M. Pagel, Brad S. Kahl, Soham D. Puvvada, John F. Gerecitano, Thomas J. Kipps, Mary Ann Anderson, Jennifer R. Brown, Lori Gressick, Shekman Wong, Martin Dunbar, Ming Zhu, Monali B. Desai, Elisa Cerri, Sari Heitner Enschede, Rod A. Humerickhouse, William G. Wierda, and John F. Seymour. Targeting BCL2 with venetoclax in relapsed chronic lymphocytic leukemia. *N. Engl. J. Med.*, 374(4):311–322, 2016.

[135] Center for Drug Evaluation {and} Research. Venetoclax (venclexta) tablets. *FDA*, 2016. Publisher: FDA.

[136] Guillaume Lessene, Peter E. Czabotar, Brad E. Sleebs, Kerry Zobel, Kym N. Lowes, Jerry M. Adams, Jonathan B. Baell, Peter M. Colman, Kurt Deshayes, Wayne J. Fairbrother, John A. Flygare, Paul Gibbons, Wilhelmus J. A. Kersten, Sanji Kulasegaram, Rebecca M. Moss, John P. Parisot, Brian J. Smith, Ian P. Street, Hong Yang, David C. S. Huang, and Keith G. Watson. Structure-guided design of a selective BCL-x(l) inhibitor. *Nat. Chem. Biol.*, 9(6):390–397, 2013.

[137] Zhi-Fu Tao, Lisa Hasvold, Le Wang, Xilu Wang, Andrew M. Petros, Chang H. Park, Erwin R. Boghaert, Nathaniel D. Catron, Jun Chen, Peter M. Colman, Peter E. Czabotar, Kurt Deshayes, Wayne J. Fairbrother, John A. Flygare, Sarah G. Hymowitz, Sha Jin, Russell A. Judge, Michael F. T. Koehler, Peter J. Kovar, Guillaume Lessene, Michael J. Mitten, Chudi O. Ndubaku, Paul Nimmer, Hans E. Purkey, Anatol Oleksijew, Darren C. Phillips, Brad E. Sleebs, Brian J. Smith, Morey L. Smith, Stephen K. Tahir, Keith G. Watson, Yu Xiao, John Xue, Haichao Zhang, Kerry Zobel, Saul H. Rosenberg, Chris Tse, Joel D. Leverson, Steven W. Elmore, and Andrew J. Souers. Discovery of a potent and selective BCL-XL inhibitor with in vivo activity. *ACS Med Chem Lett*, 5(10):1088–1093, 2014.

[138] Joel D. Leverson, Darren C. Phillips, Michael J. Mitten, Erwin R. Boghaert, Dolores Diaz, Stephen K. Tahir, Lisa D. Belmont, Paul Nimmer, Yu Xiao, Xiaoju Max Ma, Kym N. Lowes, Peter Kovar, Jun Chen, Sha Jin, Morey Smith, John Xue, Haichao Zhang, Anatol Oleksijew, Terrance J. Magoc, Kedar S. Vaidya, Daniel H. Albert, Jacqueline M. Tarrant, Nghi La, Le Wang, Zhi-Fu Tao, Michael D. Wendt, Deepak Sampath, Saul H. Rosenberg, Chris Tse, David C. S. Huang, Wayne J. Fairbrother, Steven W. Elmore, and Andrew J. Souers. Exploiting selective BCL-2 family inhibitors to dissect cell survival dependencies and define improved strategies for cancer therapy. *Sci Transl Med*, 7(279):279ra40, 2015.

[139] Michael Föller, Stephan M. Huber, and Florian Lang. Erythrocyte programmed cell death. *IUBMB Life*, 60(10):661–668, 2008.

[140] W. Trager and J. B. Jensen. Human malaria parasites in continuous culture. *Science*, 193(4254):673–675, 1976.

[141] C. Lambros and J. P. Vanderberg. Synchronization of plasmodium falciparum erythrocytic stages in culture. *J. Parasitol.*, 65(3):418–420, 1979.

[142] Clotilde Ribaut, Antoine Berry, Séverine Chevalley, Karine Reybier, Isabelle Morlais, Daniel Parzy, Françoise Nepveu, Françoise Benoit-Vical, and Alexis Valentin. Concentration and purification by magnetic separation of the erythrocytic stages of all human plasmodium species. *Malaria Journal*, 7(1):45, 2008.

[143] Brian T. Grimberg. Methodology and application of flow cytometry for investigation of human malaria parasites. *J. Immunol. Methods*, 367(1):1–16, 2011.

[144] Katherine E. Jackson, Tobias Spielmann, Eric Hanssen, Akinola Adisa, Frances Separovic, Matthew W. A. Dixon, Katharine R. Trenholme, Paula L. Hawthorne, Don L. Gardiner, Tim Gilberger, and Leann Tilley. Selective permeabilization of the host cell membrane of plasmodium falciparum-infected red blood cells with streptolysin o and equinatoxin II. *Biochem J*, 403:167–175, 2007.

[145] Jeffrey H. Ringrose, Wouter W. van Solinge, Shabaz Mohammed, Martina C. O'Flaherty, Richard van Wijk, Albert J. R. Heck, and Monique Slijper. Highly efficient depletion strategy for the two most abundant erythrocyte soluble proteins improves proteome coverage dramatically. *J. Proteome Res.*, 7(7):3060–3063, 2008.

[146] Geoffrey W. Birrell, Matthew P. Challis, Amanda De Paoli, Dovile Anderson, Shane M. Devine, Gavin D. Heffernan, David P. Jacobus, Michael D. Edstein, Ghizal Siddiqui, and Darren J. Creek. Multi-omic characterisation of the mode of action of a potent new antimalarial compound, JPC-3210, against plasmodium falciparum. *Molecular & Cellular Proteomics*, 2019-01-01. Publisher: American Society for Biochemistry and Molecular Biology Section: Research.

[147] Sean J. Humphrey, Ozge Karayel, David E. James, and Matthias Mann. High-throughput and high-sensitivity phosphoproteomics with the EasyPhos platform. *Nat Protoc*, 13(9):1897–1916, 2018.

[148] Juri Rappsilber, Yasushi Ishihama, and Matthias Mann. Stop and go extraction tips for matrix-assisted laser desorption/ionization, nanoelectrospray, and LC/MS sample pretreatment in proteomics. *Anal. Chem.*, 75(3):663–670, 2003.

[149] Ghizal Siddiqui, Anubhav Srivastava, Adrian S. Russell, and Darren J. Creek. Multi-omics based identification of specific biochemical changes associated with PfKelch13-mutant artemisinin-resistant plasmodium falciparum. *J Infect Dis*, 215(9):1435–1444, 2017. Publisher: Oxford Academic.

[150] Jürgen Cox and Matthias Mann. MaxQuant enables high peptide identification rates, individualized p.p.b.-range mass accuracies and proteome-wide protein quantification.

Nature Biotechnology, 26(12):1367–1372, 2008. Number: 12 Publisher: Nature Publishing Group.

[151] Miaoyi Wang, Ghizal Siddiqui, Ove J. R. Gustafsson, Aleksandr Käkinen, Ibrahim Javed, Nicolas H. Voelcker, Darren J. Creek, Pu Chun Ke, and Thomas P. Davis. Plasma proteome association and catalytic activity of stealth polymer-grafted iron oxide nanoparticles. *Small*, 13(36), 2017.

[152] World Health Organization. Test procedures for insecticide resistance monitoring in malaria vector mosquitoes. 2016. ISBN: 9241511575 Publisher: World Health Organization.

[153] Nicholas J. White. The role of anti-malarial drugs in eliminating malaria. *Malaria Journal*, 7(1):S8, 2008.

[154] Mohamed Lamkanfi and Vishva M. Dixit. Manipulation of host cell death pathways during microbial infections. *Cell Host & Microbe*, 8(1):44–54, 2010.

[155] Karl Lang, Philipp Lang, Christian Bauer, Christophe Duranton, Thomas Wieder, Stephan Huber, and Florian Lang. Mechanisms of suicidal erythrocyte death. *CPB*, 15(5):195–202, 2005.

[156] Diwakar Bobbala, Ioana Alesutan, Michael Föller, Serena Tschan, Stephan M. Huber, and Florian Lang. Protective effect of amiodarone in malaria. *Acta Trop.*, 116(1):39–44, 2010.

[157] Ohud Fallatah and Elias Georges. Apigenin-induced ABCC1-mediated efflux of glutathione from mature erythrocytes inhibits the proliferation of plasmodium falciparum. *Int. J. Antimicrob. Agents*, 2017.

[158] Elisabeth Lang, Kashif Jilani, Christine Zelenak, Venkanna Pasham, Diwakar Bobbala, Syed M. Qadri, and Florian Lang. Stimulation of suicidal erythrocyte death by benzethonium. *CPB*, 28(2):347–354, 2011.

[159] Paulo Renato Rivas Totino, Cláudio Tadeu Daniel-Ribeiro, and Maria de Fátima Ferreira-da Cruz. Refractoriness of eryptotic red blood cells to plasmodium falciparum infection: A putative host defense mechanism limiting parasitaemia. *PLOS ONE*, 6(10):e26575, 2011.

[160] Adrian Lupescu, Nazneen Shaik, Kashif Jilani, Christine Zelenak, Elisabeth Lang, Venkanna Pasham, Mohanad Zbidah, Ansgar Plate, Michael Bitzer, Michael Föller, Syed M. Qadri, and Florian Lang. Enhanced erythrocyte membrane exposure of phosphatidylserine following sorafenib treatment: An in vivo and in vitro study. *CPB*, 30(4):876–888, 2012.

[161] National Center for Biotechnology Information. PubChem database. amiodarone, CID=2157. https://pubchem.ncbi.nlm.nih.gov/compound/Amiodarone.

[162] Zimetbaum Peter. Antiarrhythmic drug therapy for atrial fibrillation. *Circulation*, 125(2):381–389, 2012.

[163] Jan P. Nicolay, Peter J. Bentzen, Mehrdad Ghashghaeinia, Thomas Wieder, and Florian Lang. Stimulation of erythrocyte cell membrane scrambling by amiodarone. *Cell. Physiol. Biochem.*, 20(6):1043–1050, 2007.

[164] Raymond Ng and Eric X. Chen. Sorafenib (BAY 43-9006): review of clinical development. *Curr Clin Pharmacol*, 1(3):223–228, 2006.

[165] Ziwen Wang, Zelin Chen, Zhongyong Jiang, Peng Luo, Lang Liu, Yu Huang, Huilan Wang, Yu Wang, Lei Long, Xu Tan, Dengqun Liu, Taotao Jin, Yawei Wang, Yang Wang, Fengying Liao, Chi Zhang, Long Chen, Yibo Gan, Yunsheng Liu, Fan Yang, Chunji Huang, Hongming Miao, Jieping Chen, Tianmin Cheng, Xiaobing Fu, and Chunmeng Shi. Cordycepin prevents radiation ulcer by inhibiting cell senescence via NRF2 and AMPK in rodents. *Nat Commun*, 10(1):1–16, 2019. Number: 1 Publisher: Nature Publishing Group.

[166] Julian C. K. Lui, Judy W. Y. Wong, Y. K. Suen, T. T. Kwok, K. P. Fung, and S. K. Kong. Cordycepin induced eryptosis in mouse erythrocytes through a ca2+-dependent pathway without caspase-3 activation. *Arch. Toxicol.*, 81(12):859–865, 2007.

[167] National Center for Biotechnology Information. Apigenin. Library Catalog: pubchem.ncbi.nlm.nih.gov.

[168] Mohanad Zbidah, Adrian Lupescu, Kashif Jilani, Abul Fajol, Diana Michael, Syed M. Qadri, and Florian Lang. Apigenin-induced suicidal erythrocyte death. *J. Agric. Food Chem.*, 60(1):533–538, 2012.

[169] Mahdi Amiri, Abbasali Nourian, Maryam Khoshkam, and Ali Ramazani. Apigenin inhibits growth of the plasmodium berghei and disrupts some metabolic pathways in mice. *Phytotherapy Research*, 32(9):1795–1802, 2018. _eprint: https://onlinelibrary.wiley.com/doi/pdf/10.1002/ptr.6113.

[170] Ye Ding, Chunyong Ding, Na Ye, Zhiqing Liu, Eric A. Wold, Haiying Chen, Christopher Wild, Qiang Shen, and Jia Zhou. Discovery and development of natural product oridonin-inspired anticancer agents. *Eur J Med Chem*, 122:102–117, 2016.

[171] Jimin Xu, Eric A. Wold, Ye Ding, Qiang Shen, and Jia Zhou. Therapeutic potential of oridonin and its analogs: From anticancer and antiinflammation to neuroprotection. *Molecules*, 23(2), 2018.

[172] Kashif Jilani, Syed M. Qadri, Christine Zelenak, and Florian Lang. Stimulation of suicidal erythrocyte death by oridonin. *Archives of Biochemistry and Biophysics*, 511(1):14–20, 2011.

[173] David A. Geier, Sarah K. Jordan, and Mark R. Geier. The relative toxicity of compounds used as preservatives in vaccines and biologics. *Med. Sci. Monit.*, 16(5):SR21–27, 2010.

[174] National Center for Biotechnology Information. PubChem database. benzethonium. CID=2335. Library Catalog: www.pubchem.ncbi.nlm.gov.

[175] Kenneth W. Yip, Xinliang Mao, P. Y. Billie Au, David W. Hedley, Sue Chow, Shadi Dalili, Joseph D. Mocanu, Carlo Bastianutto, Aaron Schimmer, and Fei-Fei Liu. Benzethonium chloride: A novel anticancer agent identified by using a cell-based small-molecule screen. *Clin Cancer Res*, 12(18):5557–5569, 2006.

[176] Qiangzhong Ma, Yawen Wang, Agnes Shuk-Yee Lo, Erica M. Gomes, and Richard P. Junghans. Cell density plays a critical role in ex vivo expansion of t cells for adoptive immunotherapy, 2010. ISSN: 2314-6133 Library Catalog: www.hindawi.com Pages: e386545 Publisher: Hindawi Volume: 2010.

[177] Qi Wei, Venkatesh Hariharan, and Hayden Huang. Cell-cell contact preserves cell viability via plakoglobin. *PLoS One*, 6(10), 2011.

[178] Feng Yang, Yao Zhang, and Hong Liang. Interactive association of drugs binding to human serum albumin. *Int J Mol Sci*, 15(3):3580–3595, 2014.

[179] Francesc R. Garcia-Gonzalo and Juan Carlos Izpisúa Belmonte. Albumin-associated lipids regulate human embryonic stem cell self-renewal. *PLoS One*, 3(1), 2008.

[180] Toni Petan, Eva Jarc, and Maida Jusović. Lipid droplets in cancer: Guardians of fat in a stressful world. *Molecules*, 23(8), 2018.

[181] Luisa Diomede, Bianca Piovani, Edward J. Modest, and Mario Salmona. The effect of culture medium composition on ether lipid cytotoxic activity. *Lipids*, 28(3):189–192, 1993. _eprint: https://aocs.onlinelibrary.wiley.com/doi/pdf/10.1007/BF02536638.

[182] Minghui Gao, Prashant Monian, Nosirudeen Quadri, Ravichandran Ramasamy, and Xuejun Jiang. Glutaminolysis and transferrin regulate ferroptosis. *Molecular cell*, 59(2):298, 2015. Publisher: NIH Public Access.

[183] Edouard M. Bevers, Paul Comfurius, and Robert F. A. Zwaal. Changes in membrane phospholipid distribution during platelet activation. *Biochimica et Biophysica Acta (BBA) - Biomembranes*, 736(1):57–66, 1983.

[184] Virinchipuram S. Sreevidya, Kade A. Lenz, Kurt R. Svoboda, and Hongbo Ma. Benzalkonium chloride, benzethonium chloride, and chloroxylenol - three replacement antimicrobials are more toxic than triclosan and triclocarban in two model organisms. *Environ. Pollut.*, 235:814–824, 2018.

[185] Nora Goldschlager, Andrew E. Epstein, Gerald Naccarelli, Brian Olshansky, Braman Singh, and North American Society of Pacing {and} Electrophysiology for the Practice Guidelines Subcommittee. Practical guidelines for clinicians who treat patients with amiodarone. 160(12):1741–1748. Publisher: American Medical Association.

[186] Rou Zhang, Rajesh Chandramohanadas, Chwee Teck Lim, and Ming Dao. Febrile temperature elevates the expression of phosphatidylserine on plasmodium falciparum (FCR3csa) infected red blood cell surface leading to increased cytoadhesion. *Sci Rep*, 8, 2018.

[187] Paulo Renato Totino and Stefanie Costa Lopes. Insights into the cytoadherence phenomenon of plasmodium vivax: The putative role of phosphatidylserine. *Front Immunol*, 8:1148, 2017.

[188] Paulo RR Totino, Aline D. Magalhaes, Luciene A. Silva, Dalma M. Banic, Cláudio T. Daniel-Ribeiro, and Maria de Fátima Ferreira-da Cruz. Apoptosis of non-parasitized red blood cells in malaria: a putative mechanism involved in the pathogenesis of anaemia. *Malaria Journal*, 9:350, 2010.

[189] Nicole Lawrence, Adelaide S. M. Dennis, Adele M. Lehane, Anna Ehmann, Peta J. Harvey, Aurélie H. Benfield, Olivier Cheneval, Sónia Troeira Henriques, David J. Craik, and Brendan J. McMorran. Defense peptides engineered from human platelet factor 4 kill plasmodium by selective membrane disruption. *Cell Chemical Biology*, 25(9):1140–1150.e5, 2018. Publisher: Elsevier.

[190] Tatsuaki Tagami, Hiroshi Yanai, Yuka Terada, and Tetsuya Ozeki. Evaluation of phosphatidylserine-specific peptide-conjugated liposomes using a model system of malaria-infected erythrocytes. *Biol. Pharm. Bull.*, 38(10):1649–1651, 2015.

[191] Jack D. Adderley, Simona John von Freyend, Sarah A. Jackson, Megan J. Bird, Amy L. Burns, Burcu Anar, Tom Metcalf, Jean-Philippe Semblat, Oliver Billker, Danny W. Wilson, and Christian Doerig. Analysis of erythrocyte signalling pathways during plasmodium falciparum infection identifies targets for host-directed antimalarial intervention. *Nature Communications*, 11(1):4015, 2020. Number: 1 Publisher: Nature Publishing Group.

[192] David Matallanas, Marc Birtwistle, David Romano, Armin Zebisch, Jens Rauch, Alexander von Kriegsheim, and Walter Kolch. Raf family kinases. *Genes Cancer*, 2(3):232–260, 2011.

[193] Plasmodb. https://plasmodb.org/plasmo/app, accessed 2020-09-10.

[194] Roman Aranda, Shauna M. Dineen, Rhonda L. Craig, Richard A. Guerrieri, and James M. Robertson. Comparison and evaluation of RNA quantification methods using viral, prokaryotic, and eukaryotic RNA over a 104 concentration range. *Analytical Biochemistry*, 387(1):122–127, 2009.

[195] Audrey Sicard, Jean-Philippe Semblat, Caroline Doerig, Romain Hamelin, Marc Moniatte, Dominique Dorin-Semblat, Julie A Spicer, Anubhav Srivastava, Silke Retzlaff, Volker Heussler, Andrew P Waters, and Christian Doerig. Activation of a PAK-MEK signalling pathway in malaria parasite-infected erythrocytes. *Cell Microbiol*, 13(6):836–845, 2011.

[196] A. Caulier, L. Guyonneau Harmand, and L. Garçon. Immortalisation érythrocytaire pour production de globules rouges in vitro. *Transfusion Clinique et Biologique*, 24(3):263–267, 2017.

[197] Gergana Galabova-Kovacs, Dana Matzen, Daniela Piazzolla, Katrin Meissl, Tatiana Plyushch, Adele P. Chen, Alcino Silva, and Manuela Baccarini. Essential role of b-raf in ERK activation during extraembryonic development. *PNAS*, 103(5):1325–1330, 2006. Publisher: National Academy of Sciences Section: Biological Sciences.

[198] Shalini Chakraborty, Sonti Roy, Hiral Uday Mistry, Shweta Murthy, Neena George, Vasundhra Bhandari, and Paresh Sharma. Potential sabotage of host cell physiology by apicomplexan parasites for their survival benefits. *Front Immunol*, 8:1261, 2017.

[199] Alexander G. Maier, Manoj T. Duraisingh, John C. Reeder, Sheral S. Patel, James W. Kazura, Peter A. Zimmerman, and Alan F. Cowman. Plasmodium falciparum erythrocyte invasion through glycophorin c and selection for gerbich negativity in human populations. *Nat Med*, 9(1):87–92, 2003.

[200] David J. Head, Zoe E. Lee, Joyce Poole, and Neil D. Avent. Expression of phosphatidylserine (PS) on wild-type and gerbich variant erythrocytes following glycophorin-c (GPC) ligation. *Br. J. Haematol.*, 129(1):130–137, 2005.

[201] Jakob M. A. Mauritz, Alessandro Esposito, Hagai Ginsburg, Clemens F. Kaminski, Teresa Tiffert, and Virgilio L. Lew. The homeostasis of plasmodium falciparum-infected red blood cells. *PLOS Computational Biology*, 5(4):e1000339, 2009. Publisher: Public Library of Science.

[202] H. M. Staines, J. C. Ellory, and K. Kirk. Perturbation of the pump-leak balance for na(+) and k(+) in malaria-infected erythrocytes. *Am. J. Physiol., Cell Physiol.*, 280(6):C1576–1587, 2001.

[203] James A. Thomas, Michele S. Y. Tan, Claudine Bisson, Aaron Borg, Trishant R. Umrekar, Fiona Hackett, Victoria L. Hale, Gema Vizcay-Barrena, Roland A. Fleck, Ambrosius P. Snijders, Helen R. Saibil, and Michael J. Blackman. A protease cascade regulates release of the human malaria parasite plasmodium falciparum from host red blood cells. *Nat Microbiol*, 3(4):447–455, 2018.

[204] Rajesh Chandramohanadas, Paul H. Davis, Daniel P. Beiting, Michael B. Harbut, Claire Darling, Geetha Velmourougane, Ming Yeh Lee, Peter A. Greer, David S.

Roos, and Doron C. Greenbaum. Apicomplexan parasites co-opt host calpains to facilitate their escape from infected cells. *Science*, 324(5928):794–797, 2009.

[205] C. P. Berg, I. H. Engels, A. Rothbart, K. Lauber, A. Renz, S. F. Schlosser, K. Schulze-Osthoff, and S. Wesselborg. Human mature red blood cells express caspase-3 and caspase-8, but are devoid of mitochondrial regulators of apoptosis. *Cell Death and Differentiation*, 8(12):1197, 2001.

[206] Mathieu Brochet and Oliver Billker. Calcium signalling in malaria parasites. *Molecular Microbiology*, 100(3):397–408, 2016. _eprint: https://onlinelibrary.wiley.com/doi/pdf/10.1111/mmi.13324.

[207] Thomas R. L. Klei, Sanne M. Meinderts, Timo K. van den Berg, and Robin van Bruggen. From the cradle to the grave: The role of macrophages in erythropoiesis and erythrophagocytosis. *Front Immunol*, 8, 2017.

[208] Virgilio L. Lew, Teresa Tiffert, and Hagai Ginsburg. Excess hemoglobin digestion and the osmotic stability of plasmodium falciparum-infected red blood cells. *Blood*, 101(10):4189–4194, 2003.

[209] H. Atamna and H. Ginsburg. Origin of reactive oxygen species in erythrocytes infected with plasmodium falciparum. *Mol. Biochem. Parasitol.*, 61(2):231–241, 1993.

[210] Alessandro Esposito, Jean-Baptiste Choimet, Jeremy N. Skepper, Jakob M.A. Mauritz, Virgilio L. Lew, Clemens F. Kaminski, and Teresa Tiffert. Quantitative imaging of human red blood cells infected with plasmodium falciparum. *Biophys J*, 99(3):953–960, 2010.

[211] J. Adovelande, B. Bastide, J. Délèze, and J. Schrével. Cytosolic free calcium in plasmodium falciparum-infected erythrocytes and the effect of verapamil: a cytofluorimetric study. *Exp. Parasitol.*, 76(3):247–258, 1993.

[212] Guillaume Bouyer, Luc Reininger, Ghania Ramdani, Lee D Phillips, Vikram Sharma, Stephane Egee, Gordon Langsley, and Edwin Lasonder. Plasmodiumfalciparum infection induces dynamic changes in the erythrocyte phospho-proteome. *Blood Cells Mol. Dis.*, 58:35–44, 2016.

[213] Christiaan van Ooij, Pamela Tamez, Souvik Bhattacharjee, N. Luisa Hiller, Travis Harrison, Konstantinos Liolios, Taco Kooij, Jai Ramesar, Bharath Balu, John Adams, Andy Waters, Chris Janse, and Kasturi Haldar. The malaria secretome: From algorithms to essential function in blood stage infection. *PLOS Pathogens*, 4(6):e1000084, 2008. Publisher: Public Library of Science.

[214] Y. Takakuwa. Protein 4.1, a multifunctional protein of the erythrocyte membrane skeleton: structure and functions in erythrocytes and nonerythroid cells. *Int. J. Hematol.*, 72(3):298–309, 2000.

[215] Eva-Rachele Pesce, Pragyan Acharya, Utpal Tatu, William S. Nicoll, Addmore Shonhai, Heinrich C. Hoppe, and Gregory L. Blatch. The plasmodium falciparum heat shock protein 40, pfj4, associates with heat shock protein 70 and shows similar heat induction and localisation patterns. *Int. J. Biochem. Cell Biol.*, 40(12):2914–2926, 2008.

[216] UniProt ConsortiumEuropean Bioinformatics InstituteProtein Information Resource-SIB Swiss Institute of Bioinformatics. Bcl-2-like protein 1, Aug 2020.

[217] Sasa Koncarevic, Petra Rohrbach, Marcel Deponte, Georg Krohne, Judith Helena Prieto, John Yates, Stefan Rahlfs, and Katja Becker. The malarial parasite plasmodium falciparum imports the human protein peroxiredoxin 2 for peroxide detoxification. *Proc. Natl. Acad. Sci. U.S.A.*, 106(32):13323–13328, 2009.

[218] Bernardo Javier Foth, Neng Zhang, Balbir Kaur Chaal, Siu Kwan Sze, Peter Rainer Preiser, and Zbynek Bozdech. Quantitative time-course profiling of parasite and host cell proteins in the human malaria parasite plasmodium falciparum. *Mol. Cell Proteomics*, 10(8):M110.006411, 2011.

[219] Thierry Blisnick, Laetitia Vincensini, Jean Christophe Barale, Abdelkader Namane, and Catherine Braun Breton. LANCL1, an erythrocyte protein recruited to the maurer's clefts during plasmodium falciparum development. *Mol. Biochem. Parasitol.*, 141(1):39–47, 2005.

[220] Jianfang Wang, Myriam Beauchemin, and Richard Bertrand. Bcl-xL phosphorylation at ser49 by polo kinase 3 during cell cycle progression and checkpoints. *Cell. Signal.*, 23(12):2030–2038, 2011.

[221] David T. Terrano, Meenakshi Upreti, and Timothy C. Chambers. Cyclin-dependent kinase 1-mediated bcl-xL/bcl-2 phosphorylation acts as a functional link coupling mitotic arrest and apoptosis. *Mol Cell Biol*, 30(3):640–656, 2010.

[222] J. Megyesi, A. Tarcsafalvi, Nshl Seng, R. Hodeify, and P. M. Price. Cdk2 phosphorylation of bcl-xL after stress converts it to a pro-apoptotic protein mimicking bax/bak. *Cell Death Discov*, 2, 2016.

[223] Meenakshi Upreti, Elena N. Galitovskaya, Rong Chu, Alan J. Tackett, David T. Terrano, Susana Granell, and Timothy C. Chambers. Identification of the major phosphorylation site in bcl-xL induced by microtubule inhibitors and analysis of its functional significance. *J. Biol. Chem.*, 283(51):35517–35525, 2008.

[224] Aruna Basu and Subrata Haldar. Identification of a novel bcl-xL phosphorylation site regulating the sensitivity of taxol- or 2-methoxyestradiol-induced apoptosis. *FEBS Letters*, 538(1):41–47, 2003.

[225] Senthil Raja Jayapal, Chelsia Qiuxia Wang, Xavier Bisteau, Matias J. Caldez, Shuhui Lim, Vinay Tergaonkar, Motomi Osato, and Philipp Kaldis. Hematopoiesis specific

loss of cdk2 and cdk4 results in increased erythrocyte size and delayed platelet recovery following stress. *Haematologica*, 100(4):431–438, 2015.

[226] Kristen M. Bullard, Carolyn Broccardo, and Susan M. Keenan. Effects of cyclin-dependent kinase inhibitor purvalanol b application on protein expression and developmental progression in intra-erythrocytic plasmodium falciparum parasites. *Malaria Journal*, 14(1):147, 2015.

[227] K. Nakamura, N. Yokoyama, and I. Igarashi. Cyclin-dependent kinase inhibitors block erythrocyte invasion and intraerythrocytic development of babesia bovis in vitro. *Parasitology*, 134:1347–1353, 2007.

[228] B. J. Perrin and A. Huttenlocher. Calpain. *Int. J. Biochem. Cell Biol.*, 34(7):722–725, 2002.

[229] Eun Ryoung Jang and Emilia Galperin. The function of shoc2: A scaffold and beyond. *Commun Integr Biol*, 9(4), 2016.

[230] Pablo Rodriguez-Viciana, Juan Oses-Prieto, Alma Burlingame, Mike Fried, and Frank McCormick. A phosphatase holoenzyme comprised of shoc2/sur8 and the catalytic subunit of PP1 functions as an m-ras effector to modulate raf activity. *Mol. Cell*, 22(2):217–230, 2006.

[231] HyeIn Jang, Erin Oakley, Marie Forbes-Osborne, Melissa V Kesler, Rebecca Norcross, Ann C Morris, and Emilia Galperin. Hematopoietic and neural crest defects in zebrafish shoc2 mutants: a novel vertebrate model for noonan-like syndrome. *Hum Mol Genet*, 28(3):501–514, 2019.

[232] Nadine N'Dilimabaka, Zacharie Taoufiq, Sergine Zougbédé, Serge Bonnefoy, Audrey Lorthiois, Pierre Oliver Couraud, Angelita Rebollo, Georges Snounou, Dominique Mazier, and Alicia Moreno Sabater. P. falciparum isolate-specific distinct patterns of induced apoptosis in pulmonary and brain endothelial cells. *PLoS One*, 9(3), 2014.

[233] Forradee Nuchsongsin, Kesinee Chotivanich, Prakaykaew Charunwatthana, Fausta Omodeo-Salè, Omodeo-Salè Fausta, Donatella Taramelli, Nicholas P. Day, Nicholas J. White, and Arjen M. Dondorp. Effects of malaria heme products on red blood cell deformability. *Am. J. Trop. Med. Hyg.*, 77(4):617–622, 2007.

[234] Sergios Gatidis, Michael Föller, and Florian Lang. Hemin-induced suicidal erythrocyte death. *Ann. Hematol.*, 88(8):721–726, 2009.

[235] Guillaume van Niel, Gisela D'Angelo, and Graça Raposo. Shedding light on the cell biology of extracellular vesicles. *Nature Reviews Molecular Cell Biology*, 19(4):213–228, 2018. Number: 4 Publisher: Nature Publishing Group.

[236] Kellen L. Olszewski and Manuel Llinás. Central carbon metabolism of plasmodium parasites. *Mol Biochem Parasitol*, 175(2):95–103, 2011.

[237] Rupali Shivapurkar, Tejashri Hingamire, Akshay S. Kulkarni, P. R. Rajamohanan, D. Srinivasa Reddy, and Dhanasekaran Shanmugam. Evaluating antimalarial efficacy by tracking glycolysis in plasmodium falciparum using NMR spectroscopy. *Sci Rep*, 8, 2018.

[238] Anna Sexton. *Characterising novel aspects of Plasmodium falciparum phosphorylation and pathogenesis*. PhD thesis, 2020.

[239] Shiroma M. Handunnetti, Peter H. David, K. L. R. L. Perera, and Kamini N. Mendis. Uninfected erythrocytes form "rosettes" around plasmodium falciparum infected erythrocytes. *The American Journal of Tropical Medicine and Hygiene*, 40(2):115–118, 1989. Publisher: The American Society of Tropical Medicine and Hygiene.

[240] Abhai K. Tripathi, Wei Sha, Vladimir Shulaev, Monique F. Stins, and David J. Sullivan. Plasmodium falciparum–infected erythrocytes induce NF-ϰb regulated inflammatory pathways in human cerebral endothelium. *Blood*, 114(19):4243–4252, 2009. Publisher: American Society of Hematology.

[241] Dominique Dorin-Semblat, Claudia Demarta-Gatsi, Romain Hamelin, Florence Armand, Teresa Gil Carvalho, Marc Moniatte, and Christian Doerig. Malaria parasite-infected erythrocytes secrete PfCK1, the plasmodium homologue of the pleiotropic protein kinase casein kinase 1. *PLoS ONE*, 10(12):e0139591, 2015.

[242] Abdirahman I. Abdi, Teresa G. Carvalho, Jonathan M. Wilkes, and Christian Doerig. A secreted plasmodium falciparum kinase reveals a signature motif for classification of tyrosine kinase-like kinases. *Microbiology (Reading)*, 159:2533–2547, 2013.

[243] Kazuya Aoki, Rex Williams, and John H. Zhang. Mechanism of hemolysate-induced [ca2+]i elevation in cultured fibroblasts. *Neurological Research*, 23(4):367–373, 2001. Publisher: Taylor & Francis _eprint: https://doi.org/10.1179/016164101101198578.

[244] Priya Pal, Brian P. Daniels, Anna Oskman, Michael S. Diamond, Robyn S. Klein, and Daniel E. Goldberg. Plasmodium falciparum histidine-rich protein II compromises brain endothelial barriers and may promote cerebral malaria pathogenesis. *mBio*, 7(3), 2016. Publisher: American Society for Microbiology Section: Research Article.

[245] B. L. Salmon, A. Oksman, and D. E. Goldberg. Malaria parasite exit from the host erythrocyte: a two-step process requiring extraerythrocytic proteolysis. *Proc. Natl. Acad. Sci. U.S.A.*, 98(1):271–276, 2001.

[246] Shaban J. Mwangi, Agnes Gwela, Kioko Mwikali, Joel L. Bargul, Eunice W. Nduati, Francis M. Ndungu, Philip Bejon, Julian C. Rayner, and Abdirahman I. Abdi. Impact of plasmodium falciparum small-sized extracellular vesicles on host peripheral blood mononuclear cells. *Wellcome Open Research*, 5:197, 2020.

[247] Abdirahman Abdi, Lu Yu, David Goulding, Martin K. Rono, Philip Bejon, Jyoti Choudhary, and Julian Rayner. Proteomic analysis of extracellular vesicles from

a plasmodium falciparum kenyan clinical isolate defines a core parasite secretome. *Wellcome Open Res*, 2, 2017.

[248] Xavier Sisquella, Yifat Ofir-Birin, Matthew A. Pimentel, Lesley Cheng, Paula Abou Karam, Natália G. Sampaio, Jocelyn Sietsma Penington, Dympna Connolly, Tal Giladi, Benjamin J. Scicluna, Robyn A. Sharples, Andreea Waltmann, Dror Avni, Eli Schwartz, Louis Schofield, Ziv Porat, Diana S. Hansen, Anthony T. Papenfuss, Emily M. Eriksson, Motti Gerlic, Andrew F. Hill, Andrew G. Bowie, and Neta Regev-Rudzki. Malaria parasite DNA-harbouring vesicles activate cytosolic immune sensors. *Nature Communications*, 8(1):1985, 2017. Number: 1 Publisher: Nature Publishing Group.

[249] Raya Sorkin, Rick Huisjes, Filip Bošković, Daan Vorselen, Silvia Pignatelli, Yifat Ofir-Birin, Joames K. Freitas Leal, Jürgen Schiller, Debakshi Mullick, Wouter H. Roos, Giel Bosman, Neta Regev-Rudzki, Raymond M. Schiffelers, and Gijs J. L. Wuite. Nanomechanics of extracellular vesicles reveals vesiculation pathways. *Small*, 14(39):1801650, 2018. _eprint: https://onlinelibrary.wiley.com/doi/pdf/10.1002/smll.201801650.

[250] Gregory S Noland, Noelle Briones, and David J Sullivan. The shape and size of hemozoin crystals distinguishes diverse plasmodium species. *Molecular and Biochemical Parasitology*, 130(2):91–99, 2003.

[251] E. Schwarzer, F. Turrini, D. Ulliers, G. Giribaldi, H. Ginsburg, and P. Arese. Impairment of macrophage functions after ingestion of plasmodium falciparum-infected erythrocytes or isolated malarial pigment. *J. Exp. Med.*, 176(4):1033–1041, 1992.

[252] Written by Editor Updated on 15th January 2019 and Editor. Normal blood sugar ranges and blood sugar ranges for adults and children with type 1 diabetes, type 2 diabetes and blood sugar ranges to determine people with diabetes., Apr 2020.

[253] N. J. White, D. A. Warrell, P. Chanthavanich, S. Looareesuwan, M. J. Warrell, S. Krishna, D. H. Williamson, and R. C. Turner. Severe hypoglycemia and hyperinsulinemia in falciparum malaria. *N. Engl. J. Med.*, 309(2):61–66, 1983.

[254] T. E. Taylor, M. E. Molyneux, J. J. Wirima, K. A. Fletcher, and K. Morris. Blood glucose levels in malawian children before and during the administration of intravenous quinine for severe falciparum malaria. *N. Engl. J. Med.*, 319(16):1040–1047, 1988.

[255] K Elased and J H Playfair. Hypoglycemia and hyperinsulinemia in rodent models of severe malaria infection. *Infect Immun*, 62(11):5157–5160, 1994.

[256] T. M. E. Davis, S. Looareesuwan, S. Pukrittayakamee, J. C. Levy, B. Nagachinta, and N. J. White. Glucose turnover in severe falciparum malaria. *Metabolism*, 42(3):334–340, 1993.

[257] Sanjay Kalra, Deepak Khandelwal, Rajiv Singla, Sameer Aggarwal, and Deep Dutta. Malaria and diabetes. *J Pak Med Assoc*, 67(5):810–813, 2017.

[258] Ina Danquah, George Bedu-Addo, and Frank P. Mockenhaupt. Type 2 diabetes mellitus and increased risk for malaria infection. *Emerg Infect Dis*, 16(10):1601–1604, 2010.

[259] H. M. Calvet and T. T. Yoshikawa. Infections in diabetes. *Infect. Dis. Clin. North Am.*, 15(2):407–421, viii, 2001.

[260] W. Takken and B. G. Knols. Odor-mediated behavior of afrotropical malaria mosquitoes. *Annu. Rev. Entomol.*, 44:131–157, 1999.

[261] Pamela Dalton, Alan Gelperin, and George Preti. Volatile metabolic monitoring of glycemic status in diabetes using electronic olfaction. *Diabetes Technology & Therapeutics*, 6(4):534–544, 2004. Publisher: Mary Ann Liebert, Inc., publishers.

[262] Mona D. Jensen, Margaret Conley, and Lucy Dale Helstowski. Culture of plasmodium falciparum: The role of pH, glucose, and lactate. *The Journal of Parasitology*, 69(6):1060–1067, 1983. Publisher: [The American Society of Parasitologists, Allen Press].

[263] Manoj Kumar Mohapatra. Profile of severe falciparum malaria in diabetics. 21:6, 2001.

[264] D Das, R F Grais, E A Okiro, K Stepniewska, R Mansoor, S van der Kam, D J Terlouw, J Tarning, K I Barnes, and P J Guerin. Complex interactions between malaria and malnutrition: a systematic literature review. *BMC Med*, 16, 2018.

[265] Huynh V. Thien, Piet A. Kager, and Hans P. Sauerwein. Hypoglycemia in falciparum malaria: is fasting an unrecognized and insufficiently emphasized risk factor? *Trends Parasitol.*, 22(9):410–415, 2006.

[266] Tsiri Agbenyega, Brian J Angus, George Bedu-Addo, Benjamin Baffoe-Bonnie, Tom Guyton, Peter W Stacpoole, and Sanjeev Krishna. Glucose and lactate kinetics in children with severe malaria. 85(4):8, 2000.

[267] Ingrid Böhm and Hans Schild. Apoptosis: the complex scenario for a silent cell death. *Mol Imaging Biol*, 5(1):2–14, 2003.

[268] Mark S. D'Arcy. Cell death: a review of the major forms of apoptosis, necrosis and autophagy. *Cell Biol. Int.*, 43(6):582–592, 2019.

[269] Julie Frearson and Paul Wyatt. Drug discovery in academia- the third way? *Expert Opin Drug Discov*, 5(10):909–19, 2010.

[270] Jeffrey S. Flier. Academia and industry: allocating credit for discovery and development of new therapies. *J Clin Invest*, 129(6):2172–2174, 2019. Publisher: American Society for Clinical Investigation.

[271] Sudeep Pushpakom, Francesco Iorio, Patrick A. Eyers, K. Jane Escott, Shirley Hopper, Andrew Wells, Andrew Doig, Tim Guilliams, Joanna Latimer, Christine McNamee, Alan Norris, Philippe Sanseau, David Cavalla, and Munir Pirmohamed. Drug repurposing: progress, challenges and recommendations. *Nature Reviews Drug Discovery*, 18(1):41–58, 2019. Number: 1 Publisher: Nature Publishing Group.

[272] Suerie Moon, Elodie Jambert, Michelle Childs, and Tido von Schoen-Angerer. A win-win solution?: A critical analysis of tiered pricing to improve access to medicines in developing countries. *Globalization and Health*, 7(1):39, 2011.

[273] Kenneth J. Arrow, Claire Panosian, Hellen Gelband, and Institute of Medicine (US) Committee on the Economics of Antimalarial Drugs. *The Cost and Cost-Effectiveness of Antimalarial Drugs*. National Academies Press (US), 2004. Publication Title: Saving Lives, Buying Time: Economics of Malaria Drugs in an Age of Resistance.

[274] Center for Drug Evaluation and Research. Amiodarone hydrochloride (marketed as cordarone and pacerone) information. *FDA*, 2019. Publisher: FDA.

[275] Lokesh Jain, Sukyung Woo, Erin R Gardner, William L Dahut, Elise C Kohn, Shivaani Kummar, Diane R Mould, Giuseppe Giaccone, Robert Yarchoan, Jürgen Venitz, and William D Figg. Population pharmacokinetic analysis of sorafenib in patients with solid tumours. *Br J Clin Pharmacol*, 72(2):294–305, 2011.

[276] Charles M. Rudin, Christine L. Hann, Edward B. Garon, Moacyr Ribeiro de Oliveira, Philip D. Bonomi, D. Ross Camidge, Quincy Chu, Giuseppe Giaccone, Divis Khaira, Suresh S. Ramalingam, Malcolm R. Ranson, Caroline Dive, Evelyn M. McKeegan, Brenda J. Chyla, Barry L. Dowell, Arunava Chakravartty, Cathy E. Nolan, Niki Rudersdorf, Todd A. Busman, Mack H. Mabry, Andrew P. Krivoshik, Rod A. Humerickhouse, Geoffrey I. Shapiro, and Leena Gandhi. Phase II study of single-agent navitoclax (ABT-263) and biomarker correlates in patients with relapsed small cell lung cancer. *Clin Cancer Res*, 18(11):3163–3169, 2012.

[277] Alyse N Douglass, Heather S Kain, Marian Abdullahi, Nadia Arang, Laura S Austin, Sebastian A Mikolajczak, Zachary P Billman, Jen C C Hume, Sean C Murphy, Stefan H I Kappe, and Alexis Kaushansky. Host-based prophylaxis successfully targets liver stage malaria parasites. *Molecular Therapy*, 23(5):857–865, 2015.

[278] Carl White, Chi Li, Jun Yang, Nataliya B. Petrenko, Muniswamy Madesh, Craig B. Thompson, and J. Kevin Foskett. The endoplasmic reticulum gateway to apoptosis by bcl-x l modulation of the InsP 3 r. *Nature Cell Biology*, 7(10):1021–1028, 2005. Number: 10 Publisher: Nature Publishing Group.

[279] Jennie L. Lovett, Norma Marchesini, Silvia N. J. Moreno, and L. David Sibley. Toxoplasma gondii microneme secretion involves intracellular ca(2+) release from inositol 1,4,5-triphosphate (IP(3))/ryanodine-sensitive stores. *J. Biol. Chem.*, 277(29):25870–25876, 2002.

[280] Shirley Gil-Parrado, Amaury Fernández-Montalván, Irmgard Assfalg-Machleidt, Oliver Popp, Felix Bestvater, Andreas Holloschi, Tobias A. Knoch, Ennes A. Auerswald, Katherine Welsh, John C. Reed, Hans Fritz, Pablo Fuentes-Prior, Eberhard Spiess, Guy S. Salvesen, and Werner Machleidt. Ionomycin-activated calpain triggers apoptosis: A PROBABLE ROLE FOR bcl-2 FAMILY MEMBERS. *Journal of Biological Chemistry*, 277(30):27217–27226, 2002.

[281] Toshiyuki Nakagawa and Junying Yuan. Cross-talk between two cysteine protease families. *J Cell Biol*, 150(4):887–894, 2000.

[282] Adam Wieschhaus, Anwar Khan, Asma Zaidi, Henry Rogalin, Toshihiko Hanada, Fei Liu, Lucia De Franceschi, Carlo Brugnara, Alicia Rivera, and Athar H. Chishti. Calpain-1 knockout reveals broad effects on erythrocyte deformability and physiology. *Biochem J*, 448(1):141–152, 2012.

[283] Mercedes Soares-Silva, Flavia F. Diniz, Gabriela N. Gomes, and Diana Bahia. The mitogen-activated protein kinase (MAPK) pathway: Role in immune evasion by trypanosomatids. *Front Microbiol*, 7, 2016.

[284] Anne Marie Krachler, Andrew R. Woolery, and Kim Orth. Manipulation of kinase signaling by bacterial pathogens. *J Cell Biol*, 195(7):1083–1092, 2011.

[285] Stephan Pleschka, Thorsten Wolff, Christina Ehrhardt, Gerd Hobom, Oliver Planz, Ulf R. Rapp, and Stephan Ludwig. Influenza virus propagation is impaired by inhibition of the raf/MEK/ERK signalling cascade. *Nature Cell Biology*, 3(3):301–305, 2001. Number: 3 Publisher: Nature Publishing Group.

[286] Sanjay Varikuti, Bijay Kumar Jha, Greta Volpedo, Nathan M. Ryan, Gregory Halsey, Omar M. Hamza, Bradford S. McGwire, and Abhay R. Satoskar. Host-directed drug therapies for neglected tropical diseases caused by protozoan parasites. *Front Microbiol*, 9, 2018.

[287] Daniel M. Czyż, Lakshmi-Prasad Potluri, Neeta Jain-Gupta, Sean P. Riley, Juan J. Martinez, Theodore L. Steck, Sean Crosson, Howard A. Shuman, and Joëlle E. Gabay. Host-directed antimicrobial drugs with broad-spectrum efficacy against intracellular bacterial pathogens. *mBio*, 5(4), 2014. Publisher: American Society for Microbiology Section: Research Article.

[288] Stefan H. E. Kaufmann, Anca Dorhoi, Richard S. Hotchkiss, and Ralf Bartenschlager. Host-directed therapies for bacterial and viral infections. *Nat Rev Drug Discov*, 17(1):35–56, 2018.

[289] FDA. Drug approval package: Selzentry (maraviroc) NDA #022128.

[290] Alisa Opar. New HIV drug classes on the horizon. *Nature Reviews Drug Discovery*, 6(4):258–259, 2007. Number: 4 Publisher: Nature Publishing Group.

[291] David Durantel. Celgosivir, an alpha-glucosidase i inhibitor for the potential treatment of HCV infection. *Curr Opin Investig Drugs*, 10(8):860–870, 2009.

[292] Jenny G Low, Cynthia Sung, Limin Wijaya, Yuan Wei, Abhay P S Rathore, Satoru Watanabe, Boon Hian Tan, Liying Toh, Lian Tee Chua, Yan'an Hou, Angelia Chow, Shiqin Howe, Wing Ki Chan, Kah Hin Tan, Jasmine S Chung, Benjamin P Cherng, David C Lye, Paul A Tambayah, Lee Ching Ng, John Connolly, Martin L Hibberd, Yee Sin Leo, Yin Bun Cheung, Eng Eong Ooi, and Subhash G Vasudevan. Efficacy and safety of celgosivir in patients with dengue fever (CELADEN): a phase 1b, randomised, double-blind, placebo-controlled, proof-of-concept trial. *The Lancet Infectious Diseases*, 14(8):706–715, 2014.

[293] Anita Schwegmann and Frank Brombacher. Host-directed drug targeting of factors hijacked by pathogens. *Sci. Signal.*, 1(29):re8–re8, 2008. Publisher: American Association for the Advancement of Science Section: Review.

[294] Simona John von Freyend, Terry Kwok-Schuelein, Hans J. Netter, Gholamreza Haqshenas, Jean-Philippe Semblat, and Christian Doerig. Subverting host cell p21-activated kinase: A case of convergent evolution across pathogens. *Pathogens*, 6(2), 2017.